

**WAVELET BASED FAULT TOLERANT CONTROL OF
INDUCTION MOTOR**

KHALAF SALLOUM GAEID

**THESIS SUBMITTED IN FULFILMENT OF THE
REQUIREMENTS FOR THE DEGREE OF PHILOSOPHY
DOCTORATE IN ELECTRICAL ENGINEERING /
CONTROL**

FACULTY OF ENGINEERING

UNIVERSITY OF MALAYA

KUALA LUMPUR

2012

UNIVERSITY MALAYA

ORIGINAL LITERARY WORK DECLARATION

Name of Candidate: **Khalaf Salloum Gaeid** (I.C/Passport No: **G 1547748**)

Registration/Matric No: **KHA080002**

Name of Degree: **Ph.D of Engineering Science**

Title of Thesis: **Wavelet based Fault Tolerant Control of Induction Motor**

Field of study: **Electrical Machines and Control**

I do solemnly and sincerely declare that:

- 1) I am the sole author/writer of this work;
- 2) This work is original;
- 3) Any use of any work in which copyright exists was done by way of fair dealing and for permitted purposes and any excerpt or extract from, or reference to or reproduction of any copyright work has been disclosed expressly and sufficiently and the title of the Work and its authorship have been acknowledged in this work;
- 4) I do not have any actual knowledge nor ought I reasonably to know that the making of this work constitutes an infringement of any copyright work;
- 5) I hereby assign all and every rights in the copyright to this Work to the University of Malaya ("UM"), who henceforth shall be owner of the copyright to this Work and that any reproduction or use in any form or by any means whatsoever is prohibited without the written consent of UM having been first had and obtained;
- 6) I am fully aware that if in the course of making this Work I have infringed any copyright whether intentionally or otherwise, I may be subjected to legal action or any other action as may be determined by UM.

Candidate's Signature

Date

Subscribed and solemnly declared before,

Witness's Signature

Date

Name:

Designation:

ABSTRACT

IMs are an important part of the industry as they provide convenience through their simple construction and a minimum maintenance. In addition they are highly rigid and reliable. They are mostly used in compressors, fans and pumps, but their usage has progressed to a much advanced level such as, aircrafts, space shuttles and military applications. These operations are crucial and cannot tolerate compromise in reliability and safety.

This thesis aims at exploring the fault tolerant control of the IMs. This involves sensor based closed loop vector control for a healthy IM, Variable frequency with constant flux(V/F) closed loop for both stator open winding and stator short winding faults, V/F open loop to control the drive in case of minimum voltage fault and using the sensorless vector control in case of encoder faults.

The model that has been suggested for the fault tolerant control has been verified through a 0.5 hp IM with the inclusion of condition monitoring and protection against the above faults. A platform of more than 13 trips has been included in this work. The faults will be classified according to the location, severity and the time. The speed for the sensorless vector control and closed loop V/F controllers is evaluated through the model reference adaptive control estimator. There are two steps in the fault tolerant control process; in the first step the fault is identified with the feature extraction module, a fault decision module and a feature cluster module. After that the controller is redesigned accordingly. In this work however, the fault protection is an additional feature of the control system, where the wavelet based fault tolerant system has been tested and simulated using a 1kW IM, which has a short stator winding and sensor faults, while the primary faults are open stator winding. The additional fault presented to the system is under voltage.

The wavelet packed decomposition covers the transient and steady state regions of the IM operations with respect to both time and frequency domain. The motor features are extracted through the proposed Discrete Wavelet Transform (DWT) based analysis method, while the wavelet inlet acts as an expert tool to adapt the right controller in accordance with the fault type. The fault detection algorithm identifies the time and location of each fault. The optimal levels of decomposition of the stator current error signal and mother wavelet function are selected with the help of the maximum entropy and description length data. The effect of faults and the effectiveness of the fault tolerant algorithm is demonstrated by observing the speed response of the induction machine, which is the strategy adopted by the majority of researchers in this area.

The reliability and the effectiveness of the proposed DWT based fault tolerant controller will be confirmed by the simulation and experimental results on the 1kW IM. This will further ascertain the effectiveness of the controller for high performance motor drive applications in the industry.

ABSTRAK

Motor induksi merupakan sebahagian penting bagi industri ini kerana mereka menyediakan kemudahan melalui pembinaan mudah dan penyelenggaraan minimum. Di samping itu mereka adalah sangat tegar dan boleh dipercayai. Mereka kebanyakannya digunakan dalam pemampat, kipas dan pam, tetapi penggunaan mereka telah berkembang kepada tahap yang lebih maju seperti, pesawat, kapal angkasa dan aplikasi tentera. Operasi-operasi ini adalah penting dan tidak boleh bertolak ansur dengan sifat tolak ansur dalam kebolehpercayaan dan keselamatan.

Tesis ini bertujuan untuk meneroka kawalan bersalah toleran motor induksi. Ini melibatkan langkah-langkah seperti menggunakan sensor kawalan vektor untuk motor aruhan yang sihat, motor aruhan berlebihan, V / F gelung tertutup bagi kedua-dua penggulungan pemegun terbuka dan kerosakan penggulungan pendek pemegun, V / F gelung terbuka untuk mengawal memandu dalam kes daripada kesalahan minimum dan menggunakan kawalan vektor sensorless dalam kes kerosakan pengekod.

Model yang telah dicadangkan untuk mengawal kerosakan yang toleran telah disahkan melalui motor 0.5 induksi Hp dengan kemasukan pemantauan keadaan dan perlindungan terhadap kerosakan di atas. Sebuah platform lebih daripada 13 perjalanan telah dimasukkan ke dalam kerja-kerja ini. Kebatilan akan dikelaskan mengikut keterukan lokasi dan masa. Kelajuan kawalan vektor sensorless dan gelung tertutup V / F pengawal dinilai melalui penganggar model kawalan rujukan penyesuaian. Terdapat dua langkah-langkah dalam proses kawalan toleran bersalah; dalam langkah pertama bersalah dikenalpasti dengan modul penyarian sifat, modul bersalah keputusan dan modul ciri kelompok. Selepas itu, pengawal direkabentuk semula dengan sewajarnya. Dalam kerja-kerja ini bagaimanapun, perlindungan bersalah merupakan ciri tambahan sistem kawalan, di mana salah sistem berasaskan wavelet toleran telah diuji dan

simulasi menggunakan motor induksi 1Kw, yang mempunyai litar pintas untuk penggulangan pemegun dan kerosakan sensor, manakala sekolah rendah kerosakan adalah terbuka. Salah tambahan yang dibentangkan kepada sistem voltan yang minimum.

Penguraian wavelet yang dibungkus meliputi kawasan negeri yang fana dan mantap operasi motor aruhan berkenaan ke semasa dan domain frekuensi. Ciri-ciri motor diekstrak melalui Diskret Api Tanah yang dicadangkan Transform (DWT) kaedah analisis berasaskan, manakala masuk wavelet bertindak sebagai alat pakar untuk menyesuaikan diri pengawal yang betul mengikut jenis kesalahan. Algoritma pengesanan kesilapan mengenal pasti masa dan lokasi setiap daripada kesalahan. Tahap optimum penguraian isyarat ralat pemegun semasa dan ibu fungsi wavelet dipilih dengan bantuan entropi maksimum dan data panjang description. Kesan kerosakan dan keberkesanan algoritma kesalahan toleransi yang ditunjukkan oleh memerhatikan sambutan kelajuan mesin aruhan, yang merupakan strategi yang diterima pakai oleh majoriti penyelidik dalam bidang ini.

Kebolehpercayaan dan keberkesanan pengawal salah toleransi yang dicadangkan akan disahkan oleh simulasi dan keputusan eksperimen motor aruhan 1Kw. Ini akan terus memastikan keberkesanan pengawal dari segi aplikasi berprestasi tinggi dalam sistem pemacu motor.

In the name of Allah, the Beneficent, the Merciful (1).

Say: "Verily, my Lord hath guided me to a way that is straight, - a religion of right, - the path (trod) by Abraham the true in Faith, and he (certainly) joined not gods with Allah." ((161)). Say: "Truly, my prayer and my service of sacrifice, my life and my death, are (all) for Allah, the Cherisher of the Worlds: ((162)). No partner hath He: this am I commanded, and I am the first of those who bow to His will ((163)). Say: "Shall I seek for (my) Cherisher other than Allah, when He is the Cherisher of all things (that exist)? Every soul draws the meed of its acts on none but itself: no bearer of burdens can bear the burden of another. Your goal in the end is towards Allah. He will tell you the truth of the things wherein ye disputed." ((164)).

The Holy Quran, chapter 6, verse 161-164.

ACKNOWLEDGMENT

First and foremost, all praise is for Allah, the Almighty, the creator of heavens and earth and may his peace and blessings be on the last prophet Muhammad, on his family and companions.

The author would like to acknowledge and extend his heartfelt gratitude to his supervisor, Prof. Dr. Hew Wooi Ping, for his vital advice and encouragement, without his guidance, this research would not have been possible.

The author wishes to thank the Institute of research management and consultancy, University of Malaya for providing the research fund (IPPP Fund under the research grant No.PS131/2008c) to cover part of the research materials and equipments.

The author is very grateful to his companions and best friends, Moatasem, Samer, Omar, Ahmed, Baraa, Amjed, Ammar, Mustafa, Haji Mohammed and all friends. They have been always ready to help and provide advice; each one has a unique contribution in this thesis. The author is deeply thankful to all technicians, secretaries and staff of the department of electrical engineering, University of Malaya, without them this work would not be possible.

Special thanks to professor Barry Williams from Scotland, for his advices and approval of the algorithm as an effective one in the field of control of induction machines.

To my wife and children Salim, Meha, Hassen, Hazim, Muna, Ali^{1,2}

**In recognition and love of their sacrifices, patience and affection that are beyond
description**

Table of Contents

Abstract	iii
Abstrak	v
Acknowledgement	viii
Table of Contents	x
List of Figures	xiv
List of Tables and List of graphical user interface.....	xxii
List of Symbols and Abbreviations	xxiv
List of appendix	xxvii
Chapter1 Introduction	1
1.1 Background	1
1.2 Basic fault tolerant control terminology	3
1.3 Objectives of the Study	4
1.4 Contributions	5
1.5 Thesis Organization	6
Chapter 2 Literature Review	7
2.1 Introduction.....	7
2.2 IM Faults	11
2.2.1 IM faults without wavelet	11
2.2.1.1 Air Gap Eccentricity	11
2.2.1.2 Gear Box and Bearing Faults	13
2.2.1.3 Stator Opening, Shorting Phase Winding	14
2.2.1.4 Shorted Rotor Field Winding	15

2.2.1.5 Broken rotor Bar and Cracked Ring	16
2.2.1.6 Shaft Bent	17
2.2.2 wavelet based fault diagnosis	17
2.2.2.1 Introduction	17
2.2.2.2 Air Gap Eccentricity	18
2.2.2.3 Gear Box and Bearing Faults	20
2.2.2.4 Stator Opening, Shorting Phase Winding	21
2.2.2.5 Shorted Rotor Field Winding	22
2.2.2.6 Broken rotor Bar and Cracked Ring	22
2.3 Fault Tolerant Control Survey	24
2.3.1 Stator Winding Fault Tolerant	27
2.3.2 Speed Sensor Fault Tolerant Operating Strategy	33
2.3.3 Design methodologies	34
2.4 Inverter faults	37
2.5 AC drive	41
2.5.1 Space vector modulation	42
2.6 Application	46
Chapter 3 Control Techniques of IM	48
3.1 Introduction.....	48
3.2 Modeling of IM	48
3.2.1 State Space Modeling of IM	49
3.2.2 T Model of IM	51
3.2.3 Inverse Γ model of IM	52
3.3 Control techniques of IM	53
3.3.1 Vector Control with Encoder	57

3.3.2 Vector Control without Encoder	61
3.3.3 Closed Loop Voltage /Frequency Control	67
3.3.4 Open Loop Voltage /Frequency Control	71
Chapter 4 Wavelet Techniques of IM Detection	76
4.1 Introduction.....	76
4.2 Wavelet Definition	77
4.3 Structure of the Wavelet	81
4.4 Decomposition Levels of the Wavelet	91
4.5 Multiresolution Analysis	93
4.6 Wavelet Choosing	95
4.7 Wavelet Index Construction.....	96
Chapter 5 Fault Tolerant Control OF IM	98
5.1 Introduction.....	98
5.2 Definitions	98
5.3 Features and Limitations of Fault Tolerant Types	99
5.3.1 Passive Fault Tolerant Control.....	99
5.3.2 Active Fault Tolerant Control.....	100
5.3.3 Fault Detection.....	101
5.3.4 Fault Isolation	101
5.3.5 Reconfiguration.....	102
5.3.6 Fault Tolerant Control System.....	102
5.4 Switching Between the Controllers.....	104
5.5 Computer Simulation	110
5.5.1 Speed Sensor Fault.....	110

5.5.2 Stator Shorted Winding Fault	111
5.5.3 Stator Opened Winding Fault	113
Chapter 6 Condition Monitoring of IM	117
6.1 Introduction.....	117
6.2 Condition monitoring.....	118
6.2.1 Stator Current	118
6.2.2 Stator Voltage	120
6.2.3 DC Voltage	122
6.2.4 Speed Monitoring	123
6.3 Proposed Methodology	124
6.4 Protection	125
6.5 Case studies	126
6.5.1 Healthy case	126
6.5.2 Faulty case	129
6.5.2.1 Voltage and Speed Monitoring	129
6.6 Summary	133
Chapter 7 Experimental Results	134
7.1 Introduction	134
7.2 Serial Communication Interface	135
7.3 Experimental Work	136
7.4 Prognostic unit	136
7.5 Healthy case	142
7.6 Faulty case	143
7.6.1 Shorted stator winding fault.....	144
7.6.2 Opened stator winding fault.....	152

7.6.3 Speed sensor fault	160
Chapter 8 Conclusions and Suggestions for Future Work	167
8.1 Introduction	167
8.2 Conclusions	170
8.3 Suggestions for future work	171
8.4 The publications.....	172
References	174
Appendix A: Designs and Specifications of Hardware Prototype	
A1. Introduction	194
A2. Description of the system	194
A2.1 Digital Photo of the System Topology	194
A2.2 DSP Controller Board	196
A2.3 Signal Conditioning Circuit	197

List of Figures

Figure 2.1.IM components	7
Figure 2.2.Cross section IM	7
Figure 2.3.Faults modes in the fault tolerant motor drive.....	8
Figure 2.4.Types of faults in the IM	8
Figure 2.5.IM faults percentages according to IEEE	18
Figure2.6 .Possible failure modes in delta connected stator winding	28
Figure2.7.Stator resistance configuration during short winding	29
Figure2.8. Stator resistance configuration during open winding	30
Figure2.9.Generator with fault simulating resistance	30
Figure2.10.Stator winding configuration with an inter turn short (delta)	31

Figure2.11.Basic block diagram of FTC scheme	34
Figure2.12.Block diagram of the proposed FTC	34
Figure2.13.FTC structure used in (M.Benbouzid, 2007)	35
Figure2.14. FTC structure used in (M.A.Rodriquez, 2008)	35
Figure2.15.Structure of the conventional FTC	36
Figure2.16. Block diagram of the proposed FTC algorithm	37
Figure2.17.Basic power circuit to obtain 3-phase variable supply	38
Figure2.18.Percentage of components failure in ASD	39
Figure2.19. Percentage of components failure in switch mode power supply	39
Figure2.20.Experimental DC level in the healthy inverter	40
Figure2.21. Experimental DC level in the faulty inverter	40
Figure2.22.AC drive	42
Figure2.23.Phase A voltage	43
Figure2.24. Phase B voltage	43
Figure2.25. Phase C voltage	43
Figure2.26.SVM switching times	44
Figure2.27.Six sectors control strategy of SVM	44
Figure2.28.Voltage space vector and its (d,q) components	45
Figure2.29.Space vector PWM switches pattern at each sector	46
Figure 3.1.Types of electric motors	48
Figure 3.2.Modeling of IM in q-axis	49
Figure 3.3.Modeling of IM in d-axis	50
Figure 3.4.Approximate equivalent circuit of IM	51
Figure 3.5.Dynamic inverse Γ modeling of IM	53
Figure 3.6. Block diagram FBTC base IM drive system	55

Figure 3.7. Block diagram of the passivity based method	56
Figure 3.8. Block diagram of classical DTC	56
Figure 3.9. Park transformation principle	57
Figure 3.10. Vector control principle	58
Figure 3.11. Vector control implementation	59
Figure 3.12. Phase angle relation for different components	60
Figure 3.13. Vector control SVM generation using DMC blocks	61
Figure 3.14. DMC simulink implementation of sensorless control	62
Figure 3.15. Conventional BMRAS used for speed estimation	62
Figure 3.16. Simulink implementation of proposed BMRAS	62
Figure 3.17. Booster actual, simulated reference speed with speed error	65
Figure 3.18. Simulated speed response of the proposed BMRAS estimated and variable reference speed.....	65
Figure 3.19. Simulated speed response of the proposed BMRAS estimated and constant reference speed	65
Figure 3.20. Experimental BMRAS based estimated speed and constant reference speed	66
Figure 3.21. Experimental error between of BMRAS and reference speeds.....	66
Figure 3.22. PI controllers for I_d and I_q with vector control	67
Figure 3.23. Torque controller in the vector control scheme.....	67
Figure 3.24. Voltage / Frequency control principle.....	68
Figure 3.25. Simulink implementation V / F control circuit	68

Figure 3.26.Inverse park transformation principle.....	69
Figure 3.27.Stator voltage vs. frequency in V / F control.....	70
Figure 3.28.Simulink implementation V / F control in details	71
Figure 3.29.Open loop V / F voltage generation	72
Figure 3.30.Simulink implementation of open and closed loop V / F control	73
Figure 3.31.Types of control techniques for IM	74
Figure 3.32Simulink based implementation for the proposed FTC based IM drive.....	75
Figure 4.1.Tree of wavelet decomposition	78
Figure 4.2 .Percentage of energy corresponding to the terminal nodes of the tree	78
Figure 4.3.db10 wavelet dec. into high pass and low pass with transfer modulus	80
Figure 4.4.Mother wavelet function(db10) and scaling function	80
Figure 4.5.Two levels simulink signal decomposition through side band filters	81
Figure 4.6.Complete 1D-DWT simulink signal decomposition	82
Figure 4.7.Magnitude and phase response of (0-10)Khz low pass filter	82
Figure 4.8.Magnitude and phase response of (10-20)Khz high pass filter	83
Figure 4.9.Magnitude and phase response of (0-5)Khz low pass filter	83
Figure 4.10.Magnitude and phase response of (5-10)Khz high pass filter	83
Figure 4.11.Magnitude and phase response of (0-2.5)Khz low pass filter	84
Figure 4.12.Magnitude and phase response of (2.5-5)Khz high pass filter	84
Figure 4.13.Magnitude and phase response of (0-1.25)Khz low pass filter	85
Figure 4.14.Magnitude and phase response of (1.25-2.5)Khz high pass filter	85
Figure 4.15.Magnitude and phase response of (0-625)Hz low pass filter	85

Figure 4.16.Magnitude and phase response of (625-1250)Hz high pass filter	86
Figure 4.17.Magnitude and phase response of (0-312.5)Hz low pass filter	86
Figure 4.18.Magnitude and phase response of (312.5-625-10)Hz high pass filter	87
Figure 4.19.Magnitude and phase response of (0-156.25)Hz low pass filter	87
Figure 4.20.Magnitude and phase response of (156.25-312.5)Hz high pass filter	87
Figure 4.21.Magnitude and phase response of (0-78.125)Hz low pass filter	88
Figure 4.22.Magnitude and phase response of (78.125-156.25)Hz high pass filter	88
Figure 4.23.Magnitude and phase response of (0-39.06) Hz low pass filter	89
Figure 4.24.Magnitude and phase response of (39.06-78.125)Hz high pass filter	89
Figure 4.25.Magnitude and phase response of (0-19.5)Hz low pass filter	89
Figure 4.26.Magnitude and phase response of (19.5-39.06)Hz high pass filter	90
Figure 4.27.Magnitude and phase response of (0-9.76)Hz low pass filter	90
Figure 4.28.Magnitude and phase response of (9.76-19.53)Hz high pass filter	91
Figure 4.29.Wavelet tree with(11,1601) node response	92
Figure 4.30.Wavelet tree with(8,22) node response	92
Figure 4.31.Filtering process performed by DWT	94
Figure 4.32.Simulink wavelet index implementation	96
Figure 4.33.Fault detection according to the wavelet index	97
Figure 5.1.Main components of the fault tolerant control	98
Figure 5.2.Methods of fault detection and isolation part of FTCS	99
Figure 5.3.Passive fault tolerant control	99
Figure 5.4.Active fault tolerant control	100

Figure 5.5.Active fault tolerant control methods	101
Figure 5.6.Simulink implementation of fault detection and isolation unit	103
Figure 5.7.Simulink implementation of trip data for different controllers	104
Figure 5.8.Switching mechanism block diagram	106
Figure 5.9.Simulink implementation of scaling unit	107
Figure 5.10.Simulink implementation of first block of Figure 5.8	108
Figure 5.11.Fault tolerant controller with switching mechanism	108
Figure 5.12.Simulink implementation of fault tolerant control proposed circuit	109
Figure 5.13.Simulink implementation of speed sensor checking	110
Figure 5.14.Speed error (blue) and error status(red)	111
Figure 5.15.Stator currents I_{abc} during the operation	112
Figure 5.16.Wavelet decomposition for the healthy case	112
Figure 5.17.Speed response after applying fault tolerant algorithm	113
Figure 5.18.Stator currents I_{abc} during the operation	113
Figure 5.19.Wavelet decomposition for the I_a healthy case	114
Figure 5.20.Speed response after applying fault tolerant algorithm	114
Figure 5.21. I_{abc} response with applying fault tolerant algorithm to test flexibility	115
Figure 5.22.SVM inverter signal of the flexibility algorithm test	115
Figure 5.23 I_{abc} response with applying fault tolerant control to test stator faults	116
Figure 6.1.Condition monitoring procedure	118
Figure 6.2.Motor current monitoring circuit	120
Figure 6.3.Motor voltage monitoring	121

Figure 6.4.DC voltage monitoring circuit	122
Figure 6.5.Speed monitoring	123
Figure 6.6.Block diagram of proposed monitoring and protection circuit	125
Figure 6.7.Simulink implementation of internal connections of monitoring unit	125
Figure 6.8.Protection unit mechanism	126
Figure 6.9.SVPWM duty cycle with trip in healthy case	127
Figure 6.10.Actual and reference speeds in healthy case	127
Figure 6.11.Stator currents I_{abc} in healthy case	127
Figure 6.12.Wavelet decomposition of stator currents I_a in healthy case	128
Figure 6.13.Monitoring outputs for the healthy case	128
Figure 6.14.Speed response of actual and reference speeds in the under speed	129
Figure 6.15.Binary decision of fault occurrence	130
Figure 6.16.Monitoring outputs for the first case study.....	130
Figure 6.17.Monitoring outputs for the three faults case	131
Figure 6.18.SVM(red) with trip binary decision	132
Figure 6.19.SVM signal for different control strategies	132
Figure 7.1.Serial communication interface to show the experimental output	135
Figure 7.2Structure of the proposed work	136
Figure 7.3.Simulink representation of prognostic scheme	137
Figure 7.4.Simulink representation of fault recognition and action unit.....	137
Figure 7.5.Simulink representation of inside prognostic unit of each fault.....	138
Figure 7.6.Simulink representation of details prognostic unit in healthy case	138

Figure 7.7.Experimental wavelet index for prognostic in open stator winding	139
Figure 7.8.Experimental wavelet index for prognostic in short stator winding	140
Figure 7.9.Experimental and simulation wavelet index for the healthy IM	142
Figure 7.10.ARX modeling of healthy IM wavelet index	143
Figure 7.11.Wavelet decomposition in healthy IM	143
Figure 7.12.Wavelet decomposition of stator current in the short winding fault	144
Figure 7.13.Experimental IM operation at 450RPM	145
Figure 7.14.Simulation and experimental wavelet index for shunt at 450RPM	145
Figure 7.15.Experimental IM operation at 900RPM	146
Figure 7.16.Simulation and experimental wavelet index for shunt at 900RPM	147
Figure 7.17.Experimental IM operation at 1600RPM	147
Figure 7.18.Simulation and experimental wavelet index for shunt at 1600RPM	148
Figure 7.19.Experimental wavelet indices for different speeds in short winding	149
Figure 7.20.Experimental speed transition for different controller at 1200RPM	151
Figure 7.21.Experimental setup to measure wavelet index in the short winding	151
Figure 7.22.Wavelet decomposition of stator current in the open winding fault	152
Figure 7.23.Simulation and experimental wavelet index for shunt at 450RPM	153
Figure 7.24.Simulation and experimental wavelet index for shunt at 900RPM	154
Figure 7.25.Simulation and experimental wavelet index for shunt at 1600RPM	155
Figure 7.26.Experimental wavelet indices for different speeds in open winding	155
Figure 7.27.Experimental speed transition for different controller with filtering	157
Figure 7.28.Experimental logical sensorless and sensor VC activation.....	157

Figure 7.29.Speed sensor fault recovery due to activation of sensorless V. C.....	158
Figure 7.30.Experimental logical closed loop V/F control activation	158
Figure 7.31.Stator open fault recovery due to activation of closed loop V/F	159
Figure 7.32.Experimental logical protection stage activation during the operation	159
Figure 7.33.Experimental setup for stator open winding fault wavelet index	160
Figure 7.34.Exp. output of BMRAS estimated and encoder failure rotor position	160
Figure 7.35.Exp. output of BMRAS estimated and fault of encoder rotor position	161
Figure 7.36.Experimental speed transition for different controller for flexibility test	162
Figure 7.37.Stator short fault recovery due to activation of closed loop V/F	162
Figure 7.38.Minimum voltage fault recovery due to activation of open loop V/F	163
Figure 7.39.Speed transitions at 1450RPM	163
Figure 7.40.Block diagram of multisensory control system	164
Figure 7.41.Flow chart of the work done in this thesis	165

Graphical user interface

GUI7.1.The stator open winding fault reaches 50% of its complete value	139
GUI7.2.The stator open winding fault reaches 90% of its complete value	139
GUI7.3.The stator short winding fault reaches 50% of its complete value	140
GUI7.4.The stator short winding fault reaches 90% of its complete value	141

List of Tables

Table 2.1.Fault diagnosis methods properties	10
Table 2.2.IM Frequency Characteristics formulas	24
Table 3.1.PI gain for different control techniques in Sim and Experiment	73
Table 4.1.Frequency bands of levels of wavelet signals	93

Table 4.2.The property parameters of the wavelet bases	96
Table 5.1.IM parameters used in the simulation	109
Table 6.1.Observation of IM according to IEEE standard	122
Table 6.2.SIEBER LS71 IM parameters	122
Table 7.1.Wavelet index due to the variable shunt resis. with 20Ω at 450RPM	146
Table 7.2.Wavelet index due to the variable shunt resis. with 20Ω at 900RPM	147
Table 7.3.Wavelet index due to the variable shunt resis. with 20Ω at 1600RPM	148
Table 7.4.Wavelet index due to the variable series resis. with 20Ω at 450RPM	153
Table 7.5.Wavelet index due to the variable series resis. with 20Ω at 900RPM	154
Table 7.6.Wavelet index due to the variable series resis. with 20Ω at 1600RPM	155
Table A2.2a.TMS320F28335DSP performance specification	197

List of Symbols and abbreviations

AC	Aternating Current
ADC	Analaogue to Digital Converter
AR	Autoregressive
ASD	djustable Speed Drive
AFTCS	Active Fault Tolerant Control System
AF	Axial Flow
AGC	Automatic Gain Control
ANN	Artificial Neural Network
ANFIS	Adaptive Network Based Fuzzy Inference System
ARR	Analytical Redundancy Relation
BD	Ball Diameter
BMARS	Boosted Model Adaptive Reference System
BPA	Bandpass Absorbe
CPV	Complex Park Vector
CWT	Continuous Wavelet Transforms
DC	Direct Current
DWT	Discrete Wavelet Transform
DLPF	Digital Low Pass Filtering
DTFT	discrete-timeFourier transforms
DRNN	Diagonal Recurrent Neural Network
DFIM	Doubly Fed Induction Machine
DSP	Digital Signal processing
E	Energy

EMAM	Experiment Modal Analysis Method
EMD	Empirical Mode Decomposition
FDI	Fault Detection and Isolation
FDD	Fault Detection and Diagnosis
FTCS	Fault Tolerant Control System
FTC	Fault Tolerant Control
FPGA	Field Programmable Gate Array
FFT	Fast Fourier Transform
FEM	Finite Element Method
GMFs	Gear Mesh Frequencies
GTO	Gate Turn-Off
GUI	Graphical User Interface
HPF	High Pass Filter
IMASD	Induction Machine Adjustable Speed Drives
IM	Induction Motor
IGBT	Insulated Gate Bipolar Transistor
IPMSM	Interior Permanent Magnet Synchronous Motor
LED	Light Emitting Diode
LPF	Low Pass Filter
MARS	Model Adaptive Reference System
MRA	Multiresolution Analysis
MCSA	Motor Current Signature Analysis
MPC	Model Predictive Control
N	Number of Bearing Balls
<i>P</i>	No. of pole pair

PDD.....	Power Detail Density
PD	Ball Pitch Diameter
PI	Proportional Intergral
PID	Proportional Intergral Derivative
PMSM	Permenant Magnet Synchronous Motor
PWM-VSI.....	Pulse Width Modulation-Voltage Source Inverter
RBF.....	Radial Basis Function
RSH.....	Rotor Slot Harmonics
SCM.....	Stator Current Monitoring
SCA.....	Stator Current Analysis
RPM	Revolutions per minute
s	slip
SNR.....	Signal to noise ratio
SVM.....	Space Vector Modulation
svm.....	Support Vector Machine
SVD.....	Singular Value Decomposition
TSCFE-SS.....	Time Step Coupled Finite Element-State space
TSDM	Time Series Data Mining
U_{dc}	DC supply voltage
V/F	Voltage /Frequency
WEKA.....	Waikato Environment for Knowledge Analysis
WTMRA	Wavelet Transforms Multi Resolution Analysis
WPD.....	Wavelet Package Decomposition
f_b	Damage Frequency
f_i	Inner Bearing Race Frequency

$f_{r,m}$	Rotational Frequency of the Mechanical Coupling Equipment
β	Contact angle of the ball with the races
f_o	Outer Bearing Race Frequency
I_a, I_b, I_c	Currents of the phases A, B, and C of the stator
R_d	The faulty branch resistance is connected with the original stator resistance
$\psi(\omega)$	Fourier Transform of the Wavelet Function
$\psi(t)$	Wavelet Function

List of Appendices

Appendix A

Specifications and design of hardware

A1. Introduction	185
A2. Description of the system	185
A2.1. Digital photo of overall system topology.....	186
A2.2. DSP controller board	186
A2.3. Signal conditioning circuits	186

Chapter 1: Introduction

1.1 Background

The literature review has revealed many control techniques for the IM drives. The vector control is the most frequently used technique for a high performance IM drive system. This is applicable over a wide speed range. The rotor position feedback and the motor current feedback have been incorporated in the controllers. The need for position feedback is eliminated through the use of sensorless vector control, but its efficiency is compromised at low speeds. In case of non maintenance of the rotor flux, the scalar or V/F control methods are used. The decoupled torque and flux control are not permitted through these methods.

In the recent times demand for high performance variable speed drive has been increasing rapidly. As a result more sophisticated control methods have been designed. This thesis has also chosen to focus on the IM due to its benefits in terms of cost, size, efficiency and low maintenance.

The fault is identified under two categories; model based or physical based. The mathematical models are effectively used in the model based diagnosis. There are various methods applied with respect to the various faults identified. The least used is the model based on the time series prediction for the detection of faults in the IMs. Sometimes the models are not at all used, but instead the fault is detected through limit checking or classification. Majority of the papers may seem to favor the use of a physical model as it offers an additional benefit of containing physical variables. But at times accuracy is compromised in gaining physical relevance. For instance, inaccurate results may be obtained when the converter fed voltages are induced in the physical based models. Therefore, the physical based models may not provide accurate results when identifying a fault from the stator current and applied to the rotor and stator faults.

Another system, known for its sophisticated control functions and high standards of system integrity through a unified framework, is the Fault Tolerant Control (FTC). This system automatically accommodates the system failure parameters. The fault tolerant control is vital to functions such as, power plants, machines, refineries, flight control and computer networks (Ahmad Akrad M. H., 2011). Designing a fault sensitive controller which is also robust at the same time is the greatest challenge in a fault tolerant control system (Zhang Ren, 2011).

The FTC systems can be of two types; passive or active (Liang Tang, 2008). The active type will act in accordance with the fault detected and the isolation unit to perform the correct functions. On the other hand, the passive type will function independently, irrespective of any fault data and will use the controller's robustness.

Although many types of the methods are available to deal with the active FTC such as, linearization feedback, control law rescheduling, linear quadrature method, Eigen structure assignment method, Pseudo inverse method, neural network, model predictive control MPC, norm optimization and four parameter controller, this work will focus on the switching between the redundant controllers to achieve the fault tolerant control with high efficiency.

To achieve high performance of the IM drives, the close loop vector control technique is used. By controlling the torque and the flux component separately, the torque control of the IM is achieved. In the V/F control there is no need of any current or speed measurements. Thus, the V/F controlled drives are made more robust by restricting to low dynamic performance.

The wavelet principles are now efficiently utilized in the IM fault diagnosis and protection, all owing to the advancements in the signal processing technology. All the data is easily extracted in the time and frequency domains, through the wavelet technique. In addition, it also provides a more sensitive method of detection as

compared to other signal processing methods available such as Fourier Transform. The wavelet technique is attracting the scientist's attention owing to its dynamic property of multi resolution analysis and good time localization. Features such as extraction module, fault decision module and feature cluster module are present in the wavelet based fault diagnosis technique.

The active fault tolerant control is based on the fault detection and isolation unit as the key component. An analyzer of the machine parameters should be part of a good FDI unit. Besides the wavelet index, the negative sequence current and impedance are also good fault indicators for many methods of the fault diagnosis of induction.

1.2 Basic Fault Tolerant Terminology

The following important terms will be used frequently in this thesis:

Fault: A fault is a deviation of at least one characteristic property or parameter of the system from the usual or the standard condition that is not tolerable (Inseok Hwang, 2010).

Failure: A failure occurs when a system's ability to perform a function is compromised or interrupted permanently (Isermann, 2011).

Disturbance: A disturbance is said to occur when the system is subjected to an unknown input which causes the system to deviate from the current state.

Symptom: Symptom is a change in the quantity from the normal behaviour as observed that is an effect of a fault that is observable.

Reliability: Reliability is the ability of a system to function under the stated conditions.

Availability: The probability of a system to operate efficiently at any time is termed as availability.

Safety: A system is safe when it has the ability to function without causing harm to the people or the environment or the equipment.

Fault identification: To evaluate the fault's type.

Maintainability: A system's requirement to repair and the ease with which these repairs can be made is termed as maintainability.

Fault detection: To detect a malfunction as soon as possible with surety.

Fault isolation: In fault isolation, by isolating the system components operating at nominal mode the root cause is identified.

Prognostic: To predict the development of the IM status and the gradual development in the motor is known as prognostic.

Diagnostic: To determine the size, type, location and time of a fault.

Fault tolerant control: The ability of a system to continue with its normal operations in the presence of hardware or a software fault is termed as fault tolerant control. Some extent of redundancy is also included in it.

Monitoring: It is a continuous real time task, which records the data recognizing and indicating the anomalies of the behaviour, to determine the conditions of a physical system.

Protection: It is a way to prevent the system from being effected by a potentially dangerous behavior of the system. It also prevents the effects of a dangerous behavior.

1.3 Objectives of the Study

The objective of this thesis is to design a fault tolerant control with the following features:

1. Reconfigurable fault tolerant controller algorithm based on the discrete wavelet transformation, which is efficient
2. Fault detection and isolation of the IM and sensor faults.
3. Switching mechanism to allow smooth transition between the controllers.
4. To prevent motor damage through a protection circuit.

The following considerations should be included in the fault tolerant control system,

1. To ensure safety, the integrity of the system should be considered.
2. Performance or the design specifications.
3. Redundancy, which includes the physical and financial constraints.

1.4 Contributions

The following contributions have been made:

1. Low cost fault tolerant approach that is able to deal with any sort of the IM faults.
2. Closed form of the analytical solution for the voltage to frequency controller has been used to improve the speed performance.
3. Boosted Model Adaptive Reference System (BMARS) has been developed to evaluate the motor speed for sensorless vector control and V/F control.
4. Wavelet based fault prognosis to be early stage of alarm of stator open winding and stator short winding faults when its reach 50% and 90% of its intensity.
5. The smooth transition between the controllers has been achieved by the novel switching techniques from sensor vector control to sensorless vector control, then to V/F closed loop and open loop V/F and back to the sensor vector control at any time with fault free IM and finally to the protection stage.
6. The exact time to change the controller is determined through the WI.
7. When the IM performance degradation is at a fast pace, the protection mechanism is employed to stop the operations.
8. A new fault tolerant control algorithm. In this work, a protection circuit is incorporated in the design to the previously existent fault diagnostics and redesigning.
9. New mathematical relationship between the wavelet index and the phase resistance has been found. These relationships will support the effectiveness of this algorithm as well as for further studies in the future.

1.5 Thesis Organization

The thesis is divided into 8 chapters, which are as follows:

Chapter 1: the study objectives, research background and an overview of the study are included in this chapter.

Chapter 2: the literature review associated with the utilization of wavelet as an expert system to determine the exact time for switching the controller, will be discussed in this chapter. It will also include, vector control of IM, V/F controllers and the model reference adaptive controls used to predict speed.

Chapter 3: the control techniques of the IM used in this experiment will be discussed. An in depth explanation of the vector control and the V/F control techniques will also be discussed.

Chapter 4: the wavelet techniques used in the fault diagnosis and detection will be discussed. In this chapter the theory behind the wavelet will be outlined with the other relevant data.

Chapter 5: the fault tolerant control of the IM will be discussed. The types of fault tolerant control, with the conditions of each type and the manner of their implementation in accordance with the system requirements will be discussed.

Chapter 6: the conditional monitoring process of the IM, parameters behind it and the circuit conditions for the implementation of the protection circuit will be discussed.

Chapter 7: the experimental setup with the hardware implementation will be discussed. In addition, the TMS320F28335 DSP controller circuits and the results will also be discussed.

Chapter 8: the conclusions obtained from the study and the recommendations for future work will be presented in this chapter.

Chapter 2: Literature review

2.1 Introduction

The IM is a much preferred option in the industrial processes as it provides rigidity, is strong, needs low cost maintenance, is reliable, relatively simple and is easy to use. But still to prevent any damages or losses, it is better to run a fault diagnosis procedure to reduce the faults that may occur due to the motor.

The parts of an IM can be seen in Figure 2.1.

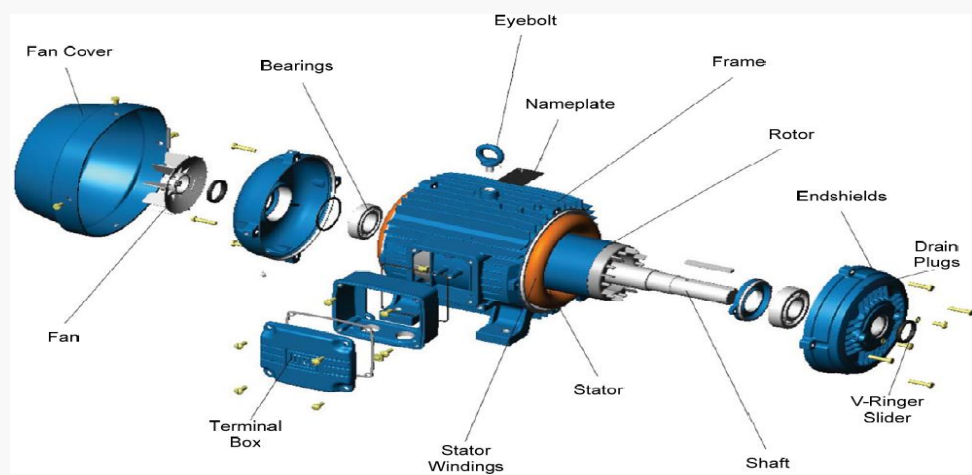


Figure 2.1.IM components

The IM magnetic fields, air gap, bars of the rotor are illustrated in Figure 2.2.

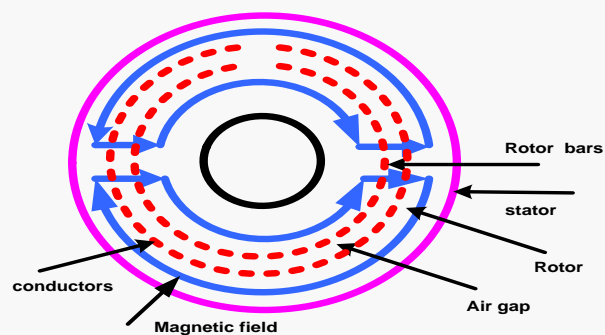


Figure 2.2.Cross section IM

The general fault modes in the system can be interpreted as in Figure 2.3.

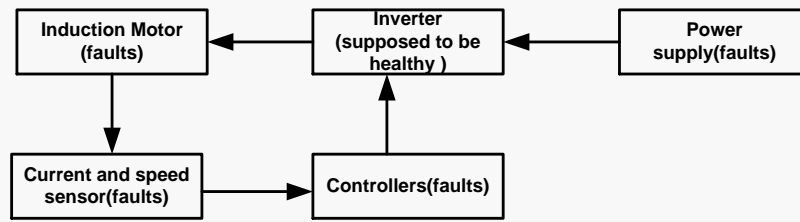


Figure 2.3. Faults modes in the fault tolerant motor drives (Zhu J. , 2008)

In this thesis, the inverter is supposed to be healthy. The faults of IMs can be divided into two main parts: electrical faults and mechanical fault as interpreted in Figure 2.4.

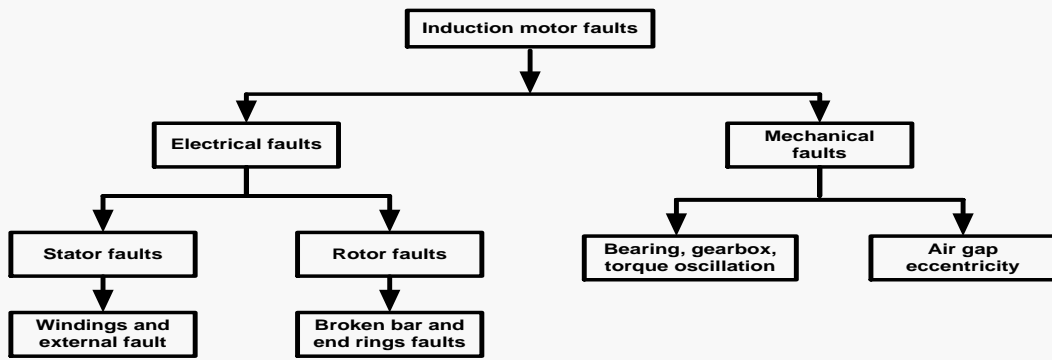


Figure 2.4. Types of faults in the IMs

The main methods used in the fault diagnosis are as follows:

1. Artificial Neural Networks (ANN): These types of fault diagnosis render a stable a speedy result enabling the parallel processing. But however these methods require a huge amount of data if applied to dynamic processing. Accuracy maintained in this system is more as compared to the conventional techniques. In addition the solution time required by the calculating machine circuit parameters through the neural network model has been reduced to a great extent.
2. Fast Fourier Transform (FFT): The sum of complex exponentials of varying magnitudes, phases and frequencies represent an image in this. It plays a significant role in various applications such as; broad range image processing like analysis, compressions, restoration and enhancements.

3. Time Stepping Coupled Finite Element State Space (TSCFE-SS): This is used to calculate the sampled data from the time domain waveforms and profiles of the input phase and the line currents, torques, voltages and power.
4. Finite Element Method (FEM): The FEM models are the mathematical idealization of the continuous systems, although they have been able to increase accuracy and induce better insights into a design. The results formed from the FEM are not closed formed solutions but are numerical approximations.
5. Motor Current Signature Analysis (MCSA): In this method, the signal spectral is used to detect the faults according to the position of sidebands frequency harmonies. This method has interested many owing to the ease of use and also as it does not require access to the IM parameters. But the main issue is that the amplitude of the current components is dependent on the loads that are linked to the motor which restricts its use to some operations owing to the variable system loads.
6. Wavelet: In this system the data can be split into two stages of low pass filters and the high pass filters to obtain all the signal data with respect to both time domain and frequency domain. This technique is applicable to any sort of signaling such as; engine vibration, human speech, medical images, financial data and many other sorts of signals.
7. Complex Park Vector (CPV): The variables of the three phase machines are indicated through the park transformation, through a system of two quadrature (I_d & I_q) shafts. Table 2.1 lists the properties of this method.

$$I_d = \sqrt{3/2}I_a - \sqrt{1/6}I_b - \sqrt{1/6}I_c \quad (2.1)$$

$$I_q = \sqrt{1/2}I_b - \sqrt{1/2}I_c \quad (2.2)$$

8. Axial Flow (AF): an alternating magnetic field with the relevant harmonics is included in the axial flow IM. It consists of a stator with a winding around the slot and a rotatable supported laminated rotor, which is spaced away from the stator by an air gap. A remotely positioned magnetically conductive layer with a closely spaced electrical layer is included in the rotor.
9. Impedances of Inverse Sequence (IIS): two stator currents and voltages are required in this method. In addition great precision is required in all the measurements.

There are two types of fault diagnosis which are; cause effect diagnosis and effect cause diagnosis. The cause effect diagnosis is also termed as the dictionary based diagnosis as it stores all the pre-evaluated failing responses of all the designs in a dictionary. The main drawback is that a large amount of memory is required to store the data (Huaxing Tang, 2007). Table 2.1 shows the properties of the fault diagnosis methods of the IM.

Table 2.1. Fault diagnosis methods properties

Techniques	Measurement required	Applications	Advantages	Drawbacks
MCSA	One stator current	Broken rotor bar, Stator winding turn, Air gap eccentricity	Low cost, Non invasive	Vary in Frequency Liked to some states
CPV	Two stator currents	Broken rotor bar, Stator winding turn, Air gap eccentricity	Non invasive simple	Mismatch faults
AF	Axial flux	Broken rotor bar, Stator winding turn, Air gap eccentricity	Low cost	invasive
THA	Two stator currents and voltages	Broken rotor bar, Stator winding turn, Air gap eccentricity	Non invasive Mechanical fault detection	Not effect in short circuit faults
IIS	Two stator currents and voltages	Stator winding turn	Non invasive Incipient fault detection	Required great measurements precision
ANN	Two stator currents and voltages	Stator winding turn	Non invasive Incipient fault detection, Easy to adapt to each motor	Required training time, Not effected with motor changes states

2.2 IM faults

The squirrel cage type is used in more than 97% of the IMs (Poyhonen, 2004), while 3% of the IMs are wound rotor type. As explained ahead, there are various types of faults that may occur during the operation of the IM. In this work, the survey will be divided in three sections:

- 1 IM faults detection without the wavelet,
- 2 IM faults detection with the wavelet and
- 3 Fault tolerant control survey.

Some of the inverter faults are listed after that.

2.2.1 IM Faults Detection without Wavelet

In this section most of the IM faults are discussed, such as air gap eccentricity, gear box and bearing faults, stator opening or shorting phase winding, shorted rotor field winding, broken rotor bar and shaft bent. The methods of faults detection and diagnosis will not contain wavelet in this part.

2.2.1.1 Air Gap Eccentricity

There are many reasons behind the mechanical faults such as machine manufacturing and assembly, unbalanced loads, bent shaft and bearing wear. For unequal air gap distance between the rotor and stator, a vibration in the induction machines is introduced a frequency of $2*f_{supply}$ (Intesar Ahmed, 2011). There are three classes of air gap eccentricity; static, dynamic and mixed.

The following expression represents the static air gap eccentricity frequency:

$$f_{secc} = [kQ_r \frac{1-s}{p} \pm n]f \quad (2.3)$$

kQ_r is the number of rotor slots

f is the supply frequency

$k=1, 2, 3\dots$

$n=1, 3, 5$ order is used for the power supply being fed to the motor.

The following expression represents the dynamic air gap eccentricity frequency:

$$f_{decc} = [(kQ_r + n_d) \frac{1-s}{p} \pm n]f \quad (2.4)$$

f is the supply frequency

$K=1, 2, 3\dots$

n_d is the dynamic eccentric order ($n_d=1, 2, 3,$).

$n=1, 2, 3,$

The following expression represents the mixed air gap eccentricity frequency:

$$f_{mixecc} = [1 \pm k \frac{1-s}{p}]f \quad (2.5)$$

f is the supply frequency

This fault is investigated at various instances, in which the air gap eccentricity is identified by the inclined static eccentricity analysis (Li, Wu, & Nandi, 2007).

At varying rotor positions, the offline monitoring of the variations of the surge waveforms was used by (Huang X. H., 2007), to identify the eccentricity occurring owing to the axial non uniform air gap. (Sulowicz, 2007) identified the faults of eccentricity through the ANFIS technique. A new concept based on the signature analysis of the complex apparent power was presented by (Drif M. M., 2008) to identify the occurrence of air gap eccentricity in the three phases of an IM. By using the TSFE, (Faiz J. E., 2008), studied the mixed eccentricity at the initial period. The voltage was applied as an input to the FE calculations. The severity of the static eccentricity was studied through the RSH and LSH side bands of both the line currents and the vibrations. The motor static eccentricity has been studied on the basis of the evidence theory using the BPA for each sensor by observing the magnitudes features (Grieger J. S., 2006). The most significant methods applied to the air gap eccentricity were

reviewed by (Wolbank, 2007) such as; digital camera or the laser sensors for the detection of faults. The instantaneous power was used by (Drif M. M., 2006) to study the squirrel cage IM eccentricity mixed faults. By using the neural networks, the drive of the IM as a closed loop was studied by (Huang X. H., 2007) to detect the rotor eccentricity associated harmonics in the stator voltage and current space vectors. A new approach was invented by (Drif M. M., 2008) to detect the air gap eccentricity through the usage of instantaneous power signature analysis. The pre-published pulse sequence application in the inverter can help in the detection of the air gap eccentricity effect on the zero sequence voltage. The diagnostic results obtained through this procedure were quite obvious (Bossio, 2006).

2.2.1.2 Gear Box and Bearing Faults

These mechanical faults can arise due to many reasons such as improper installation of the bearing, inadequate balancing of the loads and improper lubrication.

The mechanical faults need the following frequencies to be investigated:

$$f_{mech} = |f \pm mf_{r,m}| \quad (2.6)$$

$$m=1, 2, 3, ..$$

The damage frequency in the outer bearing race is:

$$f_o = \left(\frac{N}{2}\right)f \left[1 - \frac{BD}{PD} \cos(\beta)\right] \quad (2.7)$$

The damage frequency in the inner bearing race is:

$$f_i = \left(\frac{N}{2}\right)f \left[1 - \frac{BD}{PD} \cos(\beta)\right] \quad (2.8)$$

The frequency of the damaged ball is:

$$f_b = \left(\frac{BD}{PD}\right)f \left\{1 - \left[\frac{BD}{PD} \cos(\beta)\right]^2\right\} \quad (2.9)$$

β is the load angle based on the ratio of axial to radial load, PD is the bearing pitch diameter, N number of bearing balls and BD is the ball diameter.

The approximate characteristic race frequencies for most bearings can be found between 6 to 12 balls. The bearing of the outer race defect of the ball faults was detected by using the RBF neural network through the MCSA techniques (Izzet, 2006). The gear box faults can be identified for the three shafts and their respective GMFs, through the demodulation of the motor current waveform (Mohanty A., 2006). In the process of detection of inter turn insulation of main winding and bearing wear of a single phase IM, (Makarand S. Ballal, 2007), demonstrated the feasibility of the ANFIS approach. In the field of monitoring the IM bearing faults, (Zarei, 2006), studied the Park's vector by observing the thickness of Lissajou's curves. The incipient faults in the bearing were explained by (Zhou, 2009). The noise was cancelled through the stator current as a gear fault diagnosis tools. The rolling element of the bearing faults for a 0.75 kW IM was detected through the stator current monitoring circuit (Blodt, 2009). This led (Onel, 2008) to the conclusion that the diagnosis properties of Park transformation were better than the Concordia in the diagnosis of the bearing fault.

2.2.1.3 Stator Opening, Shorting Phase Winding

The following are the frequencies of the stator faults:

$$f_{st} = f \left[n \left(\frac{1-s}{p} \right) \pm k \right] \quad (2.10)$$

f is the supply frequency

$$n = 1, 2, 3 \dots$$

$$k = 1, 3, 5, 7,$$

The fault diagnosis of the stator and the alternator inter turn in the electric machines was presented by (Leite, 2007). The detection of the stator winding inter-turn shorts was presented by (Guan, 2007). A unique diagnostic system was presented by (Abdesselam,

2007), which was based on the hidden Markov models to detect the short circuit fault of the IM. The fault diagnosis was studied by (El Menzhi, 2007), associated with the auxiliary winding using the spectral analysis. The short circuit faults of the IM were presented by (Nakamura, 2007), which was based on the hidden Markov model. By using the pendulum phenomenon, the inter turn and rotor broken bar faults in the IM were detected by (Mirafzal, 2006). A neural network for the detection of online stator and rotor resistance in the sensorless vector control was presented by (Karanayil, 2007). An analytical study of the negative effects on the stator winding faults was presented by (Babaa, 2007).

To detect the abnormal connection faults in the stator of the IM, the abilities of the signature graphical tools were demonstrated by (Youssef, 2007). The vibration faults were studied by (Ma, 2007) in the stator winding based EMAM. In addition, a model of dual stator winding of induction machines was presented by (Andriamalala, 2006) for the stator and rotor faults diagnosis. A diagnosis of the IMs was presented by (Claudio Bonivento, 2004) for the mechanical faults in the stator and rotor windings. The online stator faults were identified through the B-spline membership of a neuro-fuzzy system by (Xu hong, 2007). A method was invented by (Xuhong, 2007), in which the two DRNNs were used to detect the fault in the stator winding by evaluating the severity of the fault.

2.2.1.4 Shorted Rotor Winding

The best modeling techniques for the IM and pumps were presented by (Choi, 2006). This technique was used for the identification of shorted rotor winding faults. Various faults in the IM were identified by (Silva, 2006) such as shorted rotor winding, machine monitoring, etc.

2.2.1.5 Broken Rotor Bar and Crack End Ring

These faults are caused by various factors such as vibrations and electromagnetic distortions created by the mechanical or magnetic effects. These may vary from thermal effects in some parts to fatigue (Masoud Hajiaghajan, 2004). In the asymmetrical condition, the rotor broken bar frequency is as:

$$f_{br} = \left[\left(\frac{k}{p} \right) (1-s) \pm s \right] f \quad k/p = 1, 5, 7, 11, 13, \quad (2.11)$$

f is the supply frequency

(Eltabach, 2004), conducted a comparative study between the internal diagnosis method derived from the analytical studies and the external studies of the IM model such as, spectral analysis of stator current with a broken rotor bar fault. The impacts of the inter bars current were studied by (Meshgin Kelk, 2004), as it is the contributing factor behind the broken rotor bar faults. Various cases of the process monitoring were studied by (Yang Q. S., 2004), while a global fault index was used by (Gaetan Didier, 2006) to do the fault diagnosis of the broken bars. The inter turn stator faults and the broken bars of the poly phase IM, was detected by (Chia Chou, 2007). The broken bar diagnosis was presented by (Supangat R. N., 2006) by using the starting current analysis. The voltage analysis modulation was used by (Nemec, 2010) to detect the fault in the rotor bar. A new approach of using the svm for the broken bar was adopted by (Gordi Armaki, 2010) in accordance with the side band frequency and FFT application. While (Ying, 2009), used the time stepping with finite element characteristics for the identification of the broken rotor bar of 1.1kW squirrel cage IM. Hilbert transform was used by (Oumar amar, 2007) for the same. The stator current envelope effect was used by (Da Silva, 2008) to detect the faults in the broken bar and stator short circuit. A lower sampling rate with the DTFT and AR with the motor current signature analysis was used by

(Ayhan, 2008) for the same fault. The effects of position and the number of broken bar in the stator current spectrum were investigated by (Menacer A. M., 2006).

2.2.1.6 Shaft Bent

IM tests for 1.5 kW IM was presented by (Mohamadi, 2008) through the shaft misalignment and damage bearing. There were a variety of faults considered by (Jose M . Machorro Lopeza, 2009) such as, imbalance, transverse cracks, bent shafts, misalignment and combination of these faults. On the other hand, a flexural vibration of the induction rotor system with the transverse or slant crack analysis was undertaken by (Chua, 2009) under the torsion excitation.

2.2.2 Wavelet Base Faults Diagnosis

In this section the methods of faults detection and diagnosis of the IM with wavelet will be discussed. The different faults including, air gap eccentricity, gear box and bearing faults, stator opening or shorting phase winding, shorted rotor field winding, broken rotor bar and shaft bent are considered.

2.2.2.1 Introduction

The fault diagnosis using the wavelet technique is relatively new in this field. These techniques allow the extraction of data within the time and frequency domain. A review of the machine diagnosis with conditions based on the maintenance approach was presented by (Andrew K.S. Jardine, 2006). There are two main levels in the fault diagnosis:

1. Traditional control based fault diagnosis.
2. Knowledge based fault diagnosis.

Figure 2.5 shows the percentages of different faults in an IM such as bearing, stator winding, miscellaneous, rotor faults respectively. The wavelet based fault diagnosis

consists of; wavelet feature extraction module, fault decision module and feature cluster module. Faults are best indicated by a negative sequence current and impedance. The stator short circuit faults were detected through the Park's vector and MCSA.

The wavelet however, has emerged as an attractive option through its multi resolution analysis and good time localization, which is able to counter the drawbacks such as; the assumption undertaken that the values of load, motor speed and stator fundamental frequency are constant, as done in the FFT technique.

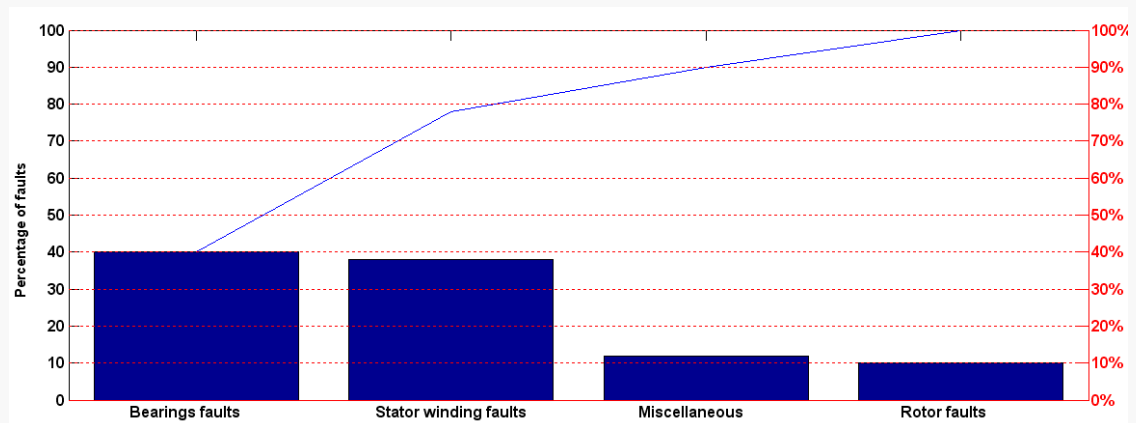


Figure 2.5. IM faults percentages according to IEEE

Among different wavelet technique, the discrete wavelet transform is a favorable option, in which the mother wavelet is scaled to the power of 2 (R. Salehi Arashloo, 2010). The resolution issue apparent in this method were attempted to be solved by (Lorand SZABO, 2005) through the CWT.

2.2.2.2 Air gap Eccentricity

The broken rotor bar and air gap eccentricity faults frequencies were detected through the wavelet of current space vector by (Tsoumas, 2005).

$$f_{ecc} = f_s \left(1 \pm k \cdot \frac{1-s}{p} \right) \quad (2.12)$$

f_s is the supply frequency

$$f_{brk} = f_s (1 \pm 2ks) \quad (2.13)$$

f_s is the supply frequency

The MCSA method and wavelet were used by (Cusido J. R., 2007) to detect the air gap eccentricity fault as it only requires a single line current. The following classification was obtained of the fault frequencies:

Eccentricity fault frequency is:

$$f_{ecc} = f_1 \left[1 \pm m \left(\frac{1-s}{p} \right) \right] \quad (2.14)$$

f_1 is the supply frequency

$m=1, 2, 3, \dots$ is the ordinal number

$$f_{ecc} = f_1 \left[\frac{n}{p} \cdot (1-s) \pm k \right] \quad (2.15)$$

f_1 is the supply frequency

The broken rotor bar fault frequency is:

$$f_{brb} = f_1 \left[m \left(\frac{1-s}{p/2} \right) \pm s \right] \quad (2.16)$$

The air gap fault frequency is:

$$f_{airgap} = \left| f_1 \pm m f_{i,o} \right| \quad (2.17)$$

f_1 is the supply frequency

The WPD with the modified winding function was used by (Hamidi, 2004) to detect the mixed eccentricity fault. The diagnosis of mixed eccentricity and rotor asymmetries was demonstrated by (Antonino-Daviu, 2006) using varying sizes and conditions and under varying effects of the oscillations due to load torque and voltage. By using the DWT at start up current of induction machines in accordance with the stator parallel branches, (Antonino, 2005) showed a variety of fault diagnoses such as; inter-turn, mixed eccentricity, broken rotor and inter coil stator short circuits. The Hilbert Huang

Transform with the DWT was used by (J. Antonino Daviu P. J., 2009) for the detection of the mixed eccentricity faults in the IM. The air gap eccentricity and broken rotor bar was simultaneously detected through the WPD by (Ye, 2001), after a brief explanation of the wavelet and feature extraction. The most significant indexes were reviewed by (Jawad Faiz, 2009) in the various types of eccentricities faults of the IM.

2.2.2.3 Gear Box and Bearing Faults

The lean model was used by (Yixiang Huang, 2010) to evaluate the machine performance by using the DWT for the vibration and bearing IM faults. The broken rotor bar, eccentricity and the bearing IM faults were detected through the lean model by utilizing the DWT for the vibrations and bearing IM faults. The bearing faults in the IM were detected due to current, voltage and instantaneous power through the wavelet by (Lu, 2008). The bearing defect was detected through the Meyer wavelet in the WP structure using the fault index of SCA and energy comparison (Jafar Zarei, 2007). The test results of the fault diagnosis of the rolling bearings conducted by (Qiao Hua, 2007) showed that the support vector machines can separate and distinguish between the faults according to their intensity and conditions. In addition it provided a better classification performance as compared to the single svm. Through the wavelet technique, the bearing fault of 5hp IM was demonstrated by (Serhat Seker, 2003).

Three line to line voltages, two vibration signals, one speed dial, three currents and four temperatures were obtained from the wavelet monitoring and were then analyzed and treated through the detection of the bearing fault of IM by (G.K. Singh a, 2009).

To use the MCSA, (Chinmaya Kar, 2006), studied the multistage transmission gearbox in the place of conventional vibration monitoring done with DWR and FFT to study the sideband frequencies.

The svm was introduced by (S. Abbasiona, 2007) as a classifier to evaluate the optimum wavelet decomposition. This was used in the diagnosis of the rolling element bearing

fault in the IMs. A novel technique based on the combination of the wavelet and power spectral density techniques was introduced by (Cusido J. J., 2006) for the detection of the bearing defect through the PDD as a fault factor. The mechanical equipment fault diagnosis based on the vibration signal was done by (Rui Zhou, 2010) through the wavelet technique. The algorithms in the WEKA were used to apply the logarithm. The WPD was used in the application of the MCSA by (Teotrakool, 2009) for the detection of the bearing faults in the adjustable speed drives. The bearing damages were detected by (Ayaz, 2006) through six accelerometers to measure the vibration data of 5 kW that were placed in various locations around the motor. The bearing fault was detected by (Yang D. , 2007) with the intelligent diagnosis techniques using the methods of wave transform and SVD.

2.2.2.4 Stator Open and Short Winding Faults

The time stepping approach was used by (Mohammed, 2006) to solve the model system equation in the FE modeling of the IM internal faults. He solved the equations by time stepping approach of the broken bar and stator shorted turns. In this method he used the db10 for both the sinusoidal and non-sinusoidal faults.

(Ponci, 2007) conducted the software diagnosis of the short inter turn and the open circuit of the stator winding as a sort of an initial fault. This was specifically used in the case of varying stator resistances ($R_s = 0.001, 0.1, 0.7, 1, 4, 8$) Ω to prevent any inconvenience in using the wavelet decomposition or hardware costs. The MCSA was used by (Cusido J. R., 2006) in the detection of stator faults with wavelet. The dq components were used in this paper for the stator teeth harmonics. The MCSA was used by (S. Radhika, 2010) for the fault diagnosis of the IM, where the stator faults were classified with WT using the svm. A fault detection in the vector controlled IMs was presented by (Chen, 1998), to detect the fault index in the stator windings.

2.2.2.5 Shorted Rotor Field Winding

Two DWTs were used by (Khan M., 2006) for the detection and classification of faults in the IM's rotor. A new technique was presented by (Saleh S. K., 2005), based on the WTMRA in the detection and diagnosis of the stator and rotor winding faults of a wound rotor IM.

2.2.2.6 Broken Rotor Bar and Crack Ring

The EMD, which is based on the nonlinear systems, was used by (Zhang Jian-wen, 2007) in the detection of the broken rotor bar using the WDT. The multi resolution wavelet was used by (Cao Zhitong, 2001) for the detection of the broken rotor bars with respect to the stator current analysis. He explained that the signal is entered into the wavelet after filtering and then differentiating it (Daubechies with 5 levels). The wavelet was used by (Faiz J. E., 2007) for the detection of a broken bar in case of load variations in the IM.

A rotor's broken bar was detected by (Yang C. C., 2007) using the Ridge wavelet, in which the characteristic frequency components of the broken bar were easily extracted using only one phase of the stator current. The broken bar in the transient region using the TMCSA via frequency B-Splines and wavelet was effectively detected by (Pons-Llinares, 2009). The WPT decomposition was used by (Eren, 2004) in the detection of the bearing fault of the IM. As an indicator of faults, the test of current spectral frequency for both the healthy and faulty bearings of a 1hp IM was used. The status of the broken bar of the IM using the mean square of discrete wavelet function has been measured by (Ordaz Moreno A., 2008). There were many faults detected in the squirrel cage IM by (Cabal Yopez, 2009) using the FPGA such as, faulty bearings, imbalance, broken bars with the parallel combination of fused FFT and wavelets. Various other new techniques were used for the broken bar fault detection by (J.Antonino Daviu,

2009). These techniques were based on the high discrete wavelet, db40, which were compared with the classical methods like the Fourier transform.

Many researchers have studied the drawbacks that accompany the FFT when used for the detection of the broken rotor bars through the db40 as a mother function. This prevented the low overlapping with the adjacent bands. The instantaneous power FFT was used as a medium and the wavelets to detect the faults by (Douglas, 2003). The fault detection was presented in the transient region for the broken rotor bars. This was used to decompose the residual stator current after filtering the noise using the notch filter. The broken rotor faults detection was done through the wavelet indicator by calculating the absolute values of the summed coefficients in the third pattern (Supangat R. E., 2006). This test uses the summation of the wavelet coefficient, the number of scales and the number of samples. The detection of the broken rotor bar in the transient region was done by (Riera Guasp, 2008), using the DWT with the fault component depending on the slip according to the energy ration of the current signal and the wavelet signal.

The optimized DWT and FFT in the steady state function, was used by (J. Antonino Daviu M. R., 2006) to detect the broken rotor bar fault. A DWT was also used by (Kia, 2009) for the broken bar detection. The various broken bar fault severities and load levels were attained by the application of the energy tests of bandwidth with time domain and analysis to the stator current space vector. The discrete and continuous wavelet were used by the (Cusido J. R., 2007) to study the broken bar faults. A new method was presented by (Jose A. Antonino Daviu, 2006) for the fault detection in the IMs, in which the faults were found by using wavelet transform. Table 2.2 shows the frequency characteristics for a healthy and faulty IM.

Table 2.2.IM frequency characteristics formulas

Air gap eccentricity fault	$f_{ecc} = f_s (1 \pm k(1-s)/p)$
Broken bar	$f_{brk} = f_s (1 \pm 2ks) \& f_{brk} = k/p (1-s) \pm s) f_s$
Healthy machine harmonic	$f_{psh} = [kR/p(1-s) \pm v] f_s$
Inter turns short circuit of stator winding	$f_{st1} = (3-2s)f_s \& f_{st2} = (5-4s)f_s$
Fault frequency component of bearing inner ring	$f_{bri} = N/2 f_r (1 + D_b/D_c \cos(\alpha))$

2.3 Fault Tolerant Control (FTC) Survey

The FTC systems have been studied by many researchers in the control community. In depth studies were done by (Patton, 1997) on the types of the fault tolerant systems, areas applied to, the control systems that detect the incipient faults in sensors, the architectures, actuators, the adaptation of the control laws in a way that protects and preserves the pre-specified performances with respect to production quality and safety. Hardware redundancies have inflicted the FTC in most of the real industrial systems. The redundant sensors are used in majority of the voting schemes to deal with the sensor faults. Since the last two decades, limitations such as hardware redundancies, high cost and occupying large spaces, solutions based on analytical redundancies have been studied.

The analytical redundancies are applied through two various approaches:

1. Passive approaches as a type of classical control
2. Active approaches as a type of adaptive control

The passive approach was applied through various design methods such as, linear matrix inequality (LMI) method, which was used for the synthesis of a reliable controller (J. Chen, 1999). In this paper he considered the uncertainty and robustness of the system performances. The main disadvantages of the passive approach are:

1. This method is not capable of controlling the nonlinear process, as it is based on the accurate linear state space model. The linear processes require accurate analytical models that are seldom available.
2. The amplitudes of the faults that are tolerable are small and cannot fulfill the practice requirements as the passive approach considers the fault tolerance in only the stage of the controller design and doesn't take adaptive measures in case of a fault.

The FTC systems only deal with the major faults that therefore do not test the full potential of the system and thus its robustness is not challenged. If it were to incorporate small faults that are hard to detect, then the case would have been different and the system would be put against a realistic challenge. The fault tolerant controls are often used with the remote diagnosis. Another FTC classification is as:

1. There is unlimited computing power in the off board component but it still has to deal with the limited and biased measurement data.
2. Restricted computing power is granted to the on board components, which limits the algorithm complexity of the task to be performed.

A fault tolerant design consisting of two parts was presented by (Mohamed, 2008). The system was based on performance controller and fault detection element that provided the fault compensating signals to the feedback loop. According to the design specifications the nominal controller can be adjusted to any structure. The detection element can function in parallel with the system until the point when the fault is detected.

A method was proposed by (Dongmo, 2007) for switching control and the analysis of the achievable performance for the motor drives for the maintenance of the system operations. (Paoli, 2003), gives the collection of the results associated with the unified framework for fault tolerant control in the distributed control system.

The issue of loss of one phase in a field oriented controlled three phase IM was solved through the fault tolerant strategy proposed by (Saleh A. S., 2007). The solution proposed was a control strategy in the single phase mode of the operation of the IM. An original strategy was proposed by (El Khil, 2006), associated with the fault tolerant operation linked with the DFM.

The issue of designing the fault tolerant system for the IPM synchronous motor drive was considered by (Nademi, 2008), in the case when these are subjected to current sensor fault. Two control design strategies were proposed to address this, the first was based on the field oriented control and an adaptive back stepping observer used at the same time for the fault free case. The second approach was based on the observer for the faulty conditions. An online sliding mode control allocation scheme was also proposed by (Halim Alwi, 2008) for the fault tolerant control. An intelligent evaluative strategy for the nonlinear state was proposed by (Anjali P. Deshpandea, 2009) to diagnose the main reasons behind the plant model mismatch. This was done by the isolation of the subset of active faults after which the model was corrected automatically online with the incorporation of all the isolated faults and failures. A control system design was considered by (Matthew O.T. Cole, 2004) for the rotor magnetic bearing system that used a number of fault tolerant control methods. A plug in robust compensator was presented by (Gan, 2003) to enhance the speed and position control of an indirect field oriented control induction machine drive.

A bibliographical review was presented by (Y. Zhang, 2008) on the reconfigurable AFTCS. While the rest of the approaches of fault detection and FTC diagnosis and FDD techniques have been classified according to the various criteria in a general framework. An adaptive FTC of system based on nonlinear parameters was presented by (Liu, 2008). This system progressed on the basis of the innovative feedback technique, based on the homogenous feedback stabilization, called the addition of the power integrator. It

was proposed initially to stabilize the nonlinear systems with uncontrollable linearization globally. A multisensory switching was proposed by (Romero, 2010) for the fault tolerant controls on the basis of direct torque and flux control of the IM. The most dominating methods used in the fault tolerant controls were proposed by (Kanev, 2004) and (M. Blanke, 2006). (A. S. Ahmed, 2011) introduced the fault tolerant technique for both the open loop and vector control motor drive systems. In this method a delta connected circuit is used in stator winding. The function of the three phase motor still continued in case of a failure in one of its phase and no detection algorithm was required. The torque pulsation created by the open delta configuration in the stator windings was eliminated by this technique.

The reliability and the availability characteristic will define a fault tolerance of any system. By reliability we refer to the system's ability to continue its operation under damaging conditions. Availability refers to the system's readiness to attempt a correct action. The addition or a spare available in a system to replace the unit that fails to perform in a manner that the system is able to continue with its operation in spite of the failure, is referred to as the redundancy of a system. An asymmetry is created between the three phases due to the faults in the stator winding of an induction machine, which results in a negative sequence component in the line currents (Habetler, 2002). A combination of various stresses acting on the stator is the reason behind the majority of the faults. These stresses can be thermal, mechanical, electrical and environmental (Siddique, 2005).

2.3.1 Stator Winding Fault Tolerant

The failure of the motor windings is almost 38% of all the motor faults. The stator winding faults can be classified as (Lee Y. , 2007).

1. Open circuit faults
2. Short between any turns in the winding

3. Short circuit between line to ground
4. Short circuit fault between coil to coil
5. Short circuit between line to line

The above mentioned faults are explained in Figure 2.6

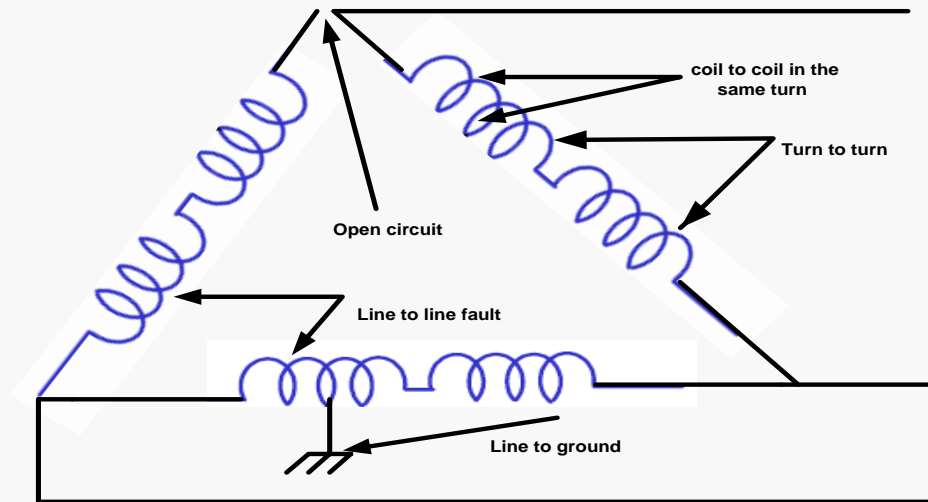


Figure 2.6. Possible failure modes in delta-connected stator windings

There are various fault diagnosis methods for the detection of stator winding faults mentioned in the literature. Developments are still required in the detection methods of delay times between two turn faults and its intensity. Dangerous affects can be prevented if the stator winding faults are detected as early as possible and will give enough time to plan an action to maintain the required performance.

During the short turn fault, a large circulating current will be induced which creates excessive heat. Majority of the stator winding fault detection methods proposed are revolving around the perturbation in the motor parameters through the second order harmonic in the air gap torque (Hsu, 1995); zero sequence voltage (M. A. Cash, 1998); negative sequence current and impedance (G. B. Kliman, 1996); mismatches in the sequence impedance matrix (F. C. Trutt, 2002), the AI techniques, the wavelet, and negative sequence approaches (Okuda, 2009). The action of the controller does not influence these methods but they need the voltage sensors in the circuit.

The system's smooth operation in the presence of stator winding faults is very important for any fault tolerant control system. The critical operations of a system may be damaged severely by an unexpected shut down.

To maintain the operations in the presence of a stator winding fault, the redundancy action is one of the solutions considered. The main preference has been given to stopping the operations at the initial stage as it is sometimes difficult to maintain satisfactory functions in the presence of a fault (P. H. Mellor, 2003). (A. S.Ahmed, 2011), on the other hand applied the fault tolerant technique with the Δ -connected circuits in the stator windings with the faulty stator phase separated by a solid state switch.

The voltage of the faulty area is set at zero or to the minimum quantity to label the shorted stator winding. The parallel resistance is assumed to be at the lowest possible value and is varied between the original stator winding and the reduced value by ten times. This has been demonstrated in Figure 2.7

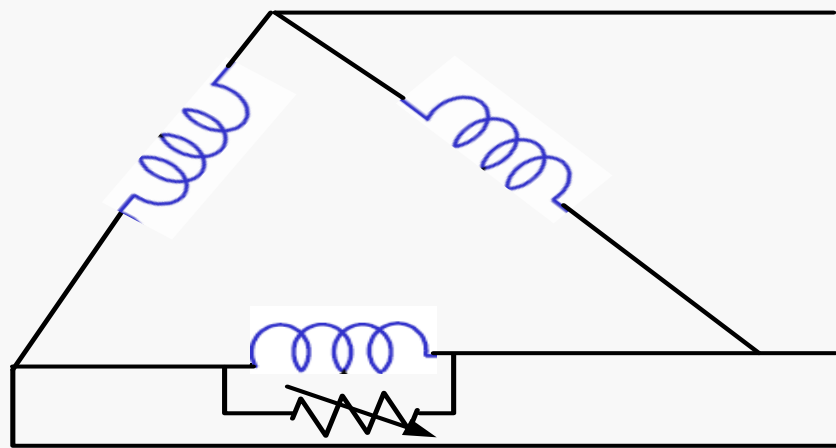


Figure 2.7. Stator resistance configuration during short winding test

A resistance of a greater value is introduced in the series with the original stator resistance to denote the open stator winding fault. The series resistance is considered to be high and variable. It is assumed to range between the original stator winding

resistance and up to a ten times increased value (Zanardelli, W.G., 2005). This is demonstrated in Figure 2.8.

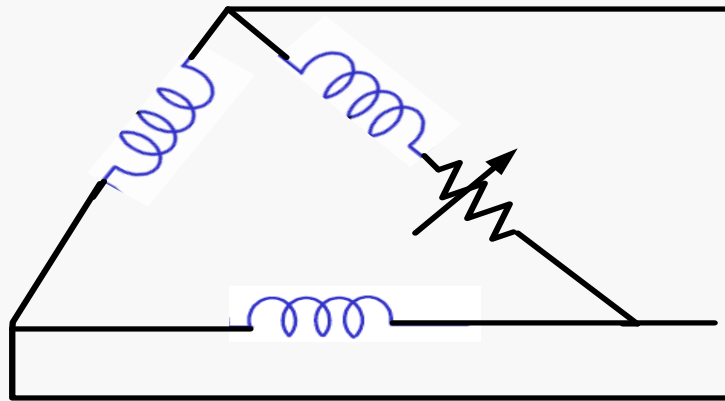


Figure 2.8. Stator resistance configuration during open winding test

There will be no change in the IM mathematical model, inductance, resistance and the corresponding magnetic field equation. Figure 2.9 shows the simulation circuit (Barakat, 2011).

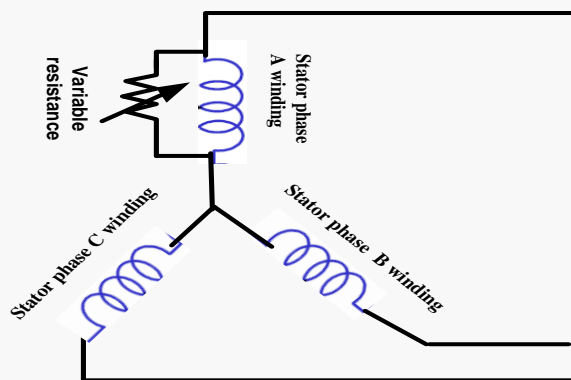


Figure 2.9. Generator with fault simulating resistor (R. Rajeswari, 2007)

According to the equation 2.8, IM equations can also be arranged for both the rotor and stator (G. M. Joksimovic, 2000).

$$\begin{bmatrix} v_s \\ v_r \end{bmatrix} = \begin{bmatrix} R_s & 0 \\ 0 & R_r \end{bmatrix} \begin{bmatrix} I_s \\ I_r \end{bmatrix} + \frac{d}{dt} \begin{bmatrix} \lambda_s \\ \lambda_r \end{bmatrix} \quad (2.8)$$

The supply voltage and the stator windings are symmetrical in the healthy IM, thus no change is required in the system parameters. The system parameters should be changed to make them applicable and matched with Kirchhoff's current rule in the case of a fault. The above stated equation can be expanded for both the stator short winding and stator open winding. The simulation of the stator delta connection can be expressed as a voltage drop in parallel for the stator winding, with a specific phase winding. The faulty phase is B in Figure 2.10

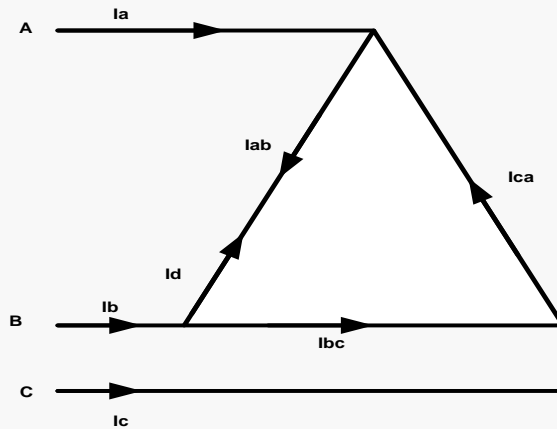


Figure 2.10. Stator winding configuration with an inter-turn short (delta connection)

The mathematical model of an IM can be represented as,

$$\begin{bmatrix} v_{sa} \\ v_{sb} \\ v_{sc} \\ v_d \end{bmatrix} = \begin{bmatrix} R_a & -R_b & R_c & R_d \\ R_a & R_b & -R_c & R_d \\ -R_a & R_b & R_c & R_d \\ R_a & R_b & R_c & R_d \end{bmatrix} \begin{bmatrix} i_a \\ i_b \\ i_c \\ i_d \end{bmatrix} + \frac{d}{dt} \begin{bmatrix} \lambda_{sa} \\ \lambda_{sb} \\ \lambda_{sc} \\ \lambda_d \end{bmatrix} \quad (2.9)$$

Where R_a, R_b, R_c is self resistance of phase A, B, C stator winding respectively, v_d is the voltage drop across the added resistance, i_d is the current flowing through the connected faulty connected resistance (R_d), i_a, i_b, i_c are the phase A, B, C stator current. $\lambda_{sa}, \lambda_{sb}, \lambda_{sc}, \lambda_d$ are phase A, B, C and the faulty connected branch fluxes respectively.

The magnetic field equation can be written in the form of the following matrix for the voltages with the stator LL voltages.

$$\begin{bmatrix} \lambda_{sa} \\ \lambda_{sb} \\ \lambda_{sc} \\ \lambda_{sd} \end{bmatrix} = \begin{bmatrix} L_{aa} & L_{ab} & L_{ac} & L_{ad} \\ L_{ba} & L_{bb} & L_{bc} & L_{bd} \\ L_{ca} & L_{cb} & L_{cc} & L_{cd} \\ L_{da} & L_{db} & L_{dc} & L_{dd} \end{bmatrix} \begin{bmatrix} i_a \\ i_b \\ i_c \\ i_d \end{bmatrix} + \begin{bmatrix} L_{ar} \\ L_{br} \\ L_{cr} \\ L_{dr} \end{bmatrix} [I_r] \quad (2.10)$$

Where L_{aa}, L_{bb}, L_{cc} is self inductance of phase A,B,C stator winding respectively, L_{bc}, L_{ab}, L_{ac} is the mutual inductances between phases of the stator windings, L_{dc}, L_{db}, L_{ad} is the mutual inductances between phases of the stator windings and added inductance.

The above equation is expressed for phase C in order for the current to satisfy the Kirchhoff's current rule:

$$\begin{bmatrix} v_{sa} \\ v_{sb} \\ v_{sc} \\ v_d \end{bmatrix} = \begin{bmatrix} R_a & -R_b & R_d \parallel R_c & R_d \parallel R_c \\ R_a & R_b & -R_d \parallel R_c & R_d \parallel R_c \\ -R_a & R_b & R_d \parallel R_c & R_d \parallel R_c \\ R_a & R_b & R_d \parallel R_c & R_d \parallel R_c \end{bmatrix} \begin{bmatrix} i_a \\ i_b \\ i_c \\ i_d \end{bmatrix} + \frac{d}{dt} \begin{bmatrix} \lambda_{sa} \\ \lambda_{sb} \\ \lambda_{sc} \\ \lambda_d \end{bmatrix} \quad (2.11)$$

The original stator resistance is connected with the faulty shunt voltage branch:

$$v_{sh} = i_{sh}(R_d \parallel R_c) \quad (2.12)$$

where v_{sh}, i_{sh} are the voltage and current of faulty branch respectively. Taking into consideration the magnetic flux, the stator short winding voltage can be described as follows (J. A. Farooq, 2008):

$$v_{sh} = -\frac{N_{sh}}{N_s} R_{sh} i_{sh} + \frac{d\lambda_{sh}}{dt} \quad (2.13)$$

The extra resistance for the stator open winding equation and the series combination of the phase C is described by the following expression:

$$\begin{bmatrix} v_{sa} \\ v_{sb} \\ v_{sc} \\ v_d \end{bmatrix} = \begin{bmatrix} R_a & -R_b & R_d + R_c & R_d + R_c \\ R_a & R_b & -R_d + R_c & R_d + R_c \\ -R_a & R_b & R_d + R_c & R_d + R_c \\ R_a & R_b & R_d + R_c & R_d + R_c \end{bmatrix} \begin{bmatrix} i_a \\ i_b \\ i_c \\ i_d \end{bmatrix} + \frac{d}{dt} \begin{bmatrix} \lambda_{sa} \\ \lambda_{sb} \\ \lambda_{sc} \\ \lambda_d \end{bmatrix} \quad (2.14)$$

Following formulas helps in calculating the value of the inductances of open and short stator winding, respectively (K. Kumar, 2010):

$$\frac{R_{Norstat}}{R_{series}} = \frac{L_{Norstat}}{L_{series}} \quad (2.15)$$

$$\frac{R_{Norstat}}{R_{sh}} = \frac{L_{Norstat}}{L_{sh}} \quad (2.16)$$

Where $R_{nor stat}$, $L_{nor stat}$, R_{series} , R_{sh} , L_{series} is the normal value of stator resistance, inductance, series added resistance, shunt added resistance and series inductance respectively.

The input to the DWT based fault diagnosis algorithm is the stator current. The open or short stator winding is the only thing which can alter the resistance of the any faulty branch as mentioned above.

2.3.2 Speed Sensor Fault Tolerant Operating Strategy

Two types of measurements are present in the IM such as; electrical and mechanical. The electrical is associated with the currents and voltages for the stator or rotor, while the mechanical is associated with the rotor position (D.U. Campos Delgado, 2008). The speed encoders mounted in the motor shaft are used to measure the angular shaft's position. The possibilities of faults arise from the presence of noise, drift, offset and disconnections (Bekheira Tabbache, 2011). The motor's performance will deteriorate due to the failure in the encoder. Therefore, (R.B. Sepe, 2003), introduced a fault control system with the controller reconfiguration to adapt the operations in accordance with the event of sensor loss or sensor recovery through speed observer. A fault detection process and isolation of the mechanical speed sensor in the IM was proposed by (Zidani, 2007) according to the fuzzy logic technique.

2.3.3 Design Methodologies

(Y. Zhang, 2008), presented the basic topology of fault tolerant control as shown in Figure 2.11. Actuator saturation is serious problem in this method which is needed to change the input/output controller parameters and structure of the controller.

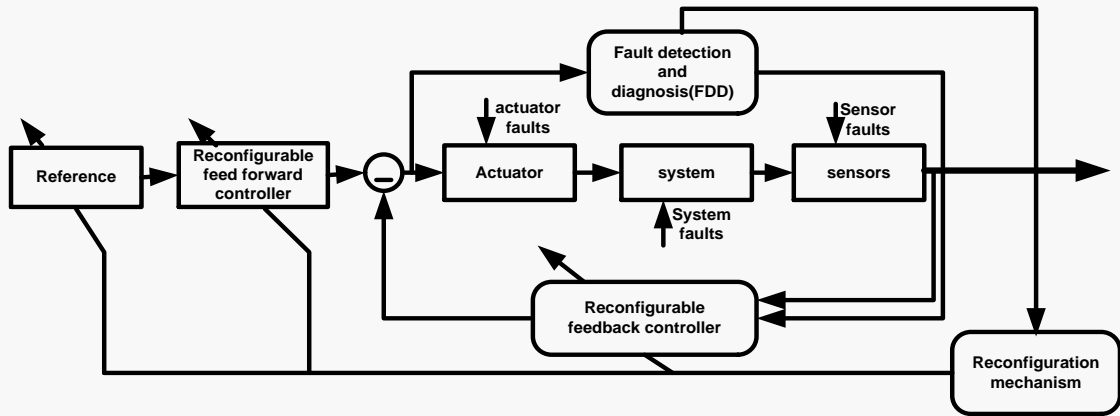


Figure 2.11. Basic block diagram of the FTC scheme

In the case of a nonlinear system being subjected to various faults, (Afef Fekih, 2006) introduced a fault tolerant controller. Temperature variations and sensor faults cause these faults. The internal and the external factors were dealt with the help of the passive FTC and active FTC strategies, as shown in Figure 2.12. The limitation of this algorithm is the availability of transient overshoot and the time limitation to replace the defected device.

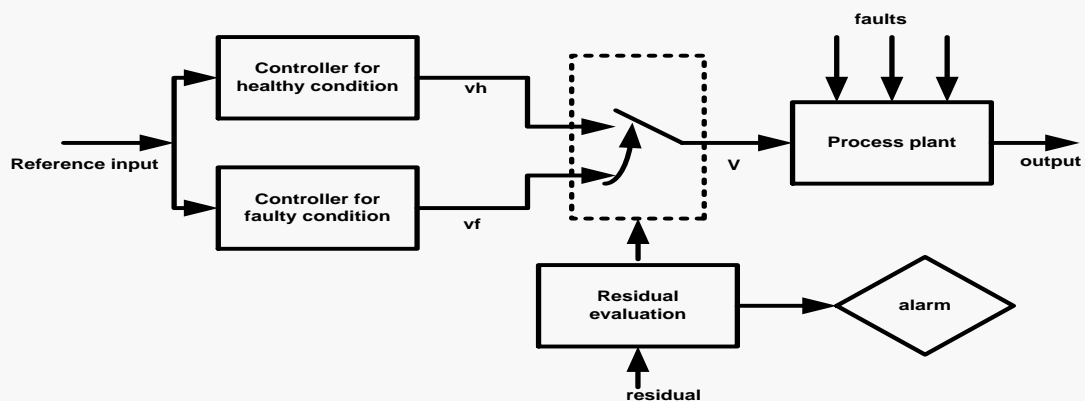


Figure 2.12. Block Diagram of the proposed FTC (Afef Fekih, 2006)

The multi controllers were introduced by (M. El Hachemi Benbouzid, 2007), as shown in Figure 2.13.

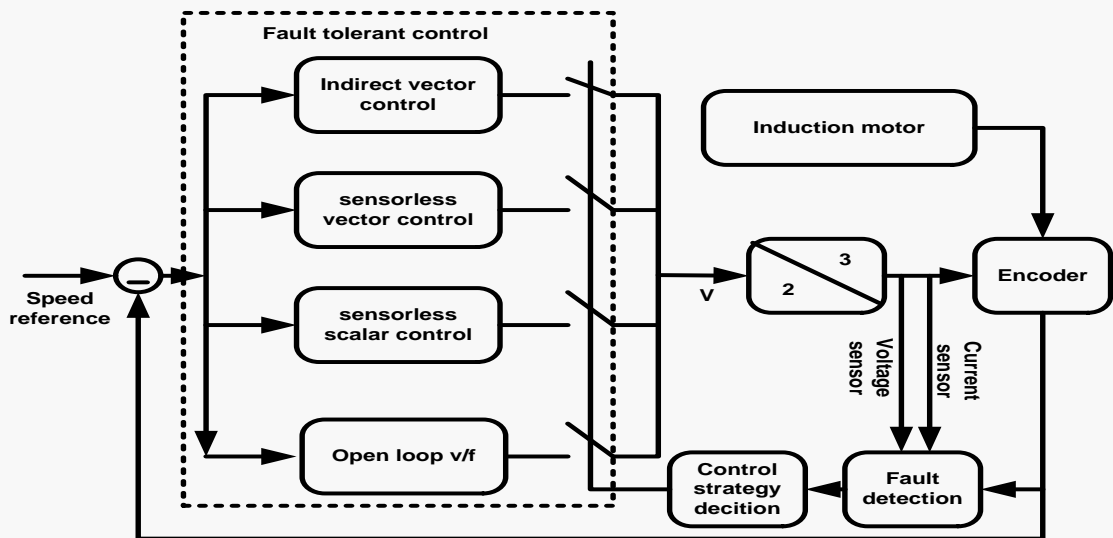


Figure 2.13.FTC structure used in (M. Benbouzid, 2007)

The performance specifications were maintained at the acceptable levels through the main IM controllers. As the transition between the controllers was smooth, therefore the algorithm was successful. This paper aims at the creation of a logical variable that allows the specific controller when ($\Delta\theta = 0$). Verifying this condition is a difficult process. The best time for the replacement of the damage components was determined through the fault tolerant IM algorithm of (M. A. Rodriguez, 2008). This dealt with the short circuit or the open circuit failure in the power device. The isolation of the damaged elements by the blown fuse was the basis of the algorithm, through which the damage was replaced at the best suited time. This is shown in Figure 2.14.

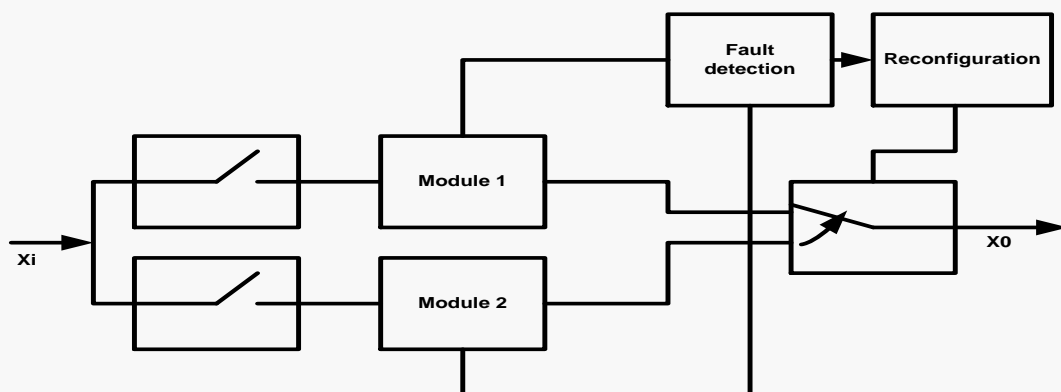


Figure 2.14.FTC structure used in (M. A. Rodriguez, 2008)

The FTC architecture was presented by (A. Arakad, 2011) as the FTC based PMSM drive was robust against the mechanical sensor failures shown in figure 2.15. Enhance the reliability was the main objective of this paper, as it is the main concern in the electric vehicles. Two virtual sensors and a maximum likelihood voting algorithm constitute the architecture. The drawback of this algorithm it is cannot handle large number of IM faults.

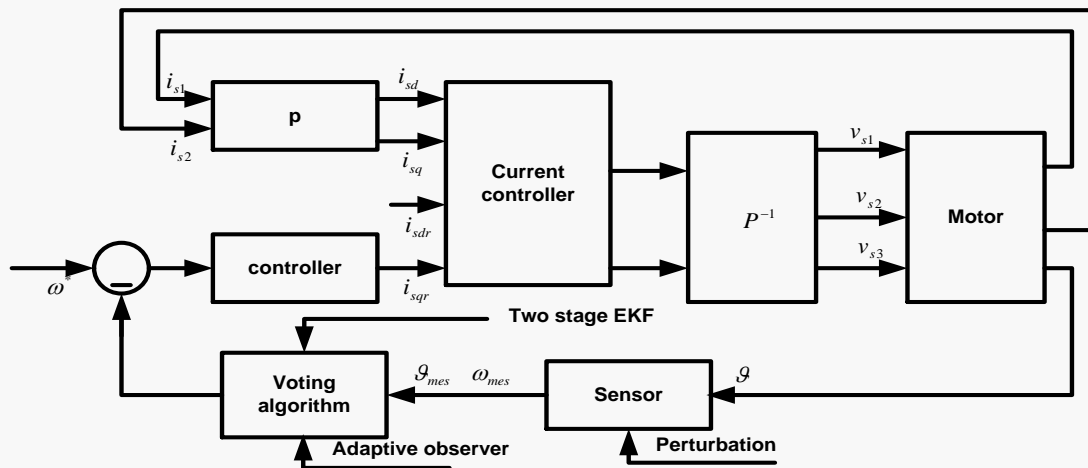


Figure 2.15. Structure of the conventional FTC

In all the above works, they either focus on accommodation of limited faults of IM or stop the motor directly to avoid the damage. In this thesis as well as a platform of more 13 faults are included, there are new circuit added to this algorithm to be as standard for fault tolerant control field such as combined both accommodation and protection in this work. Another important devolvement in this work, it contains a prognostic unit which is not included in any work previously.

Figure 2.16 shows the new fault tolerant algorithm used in this thesis.

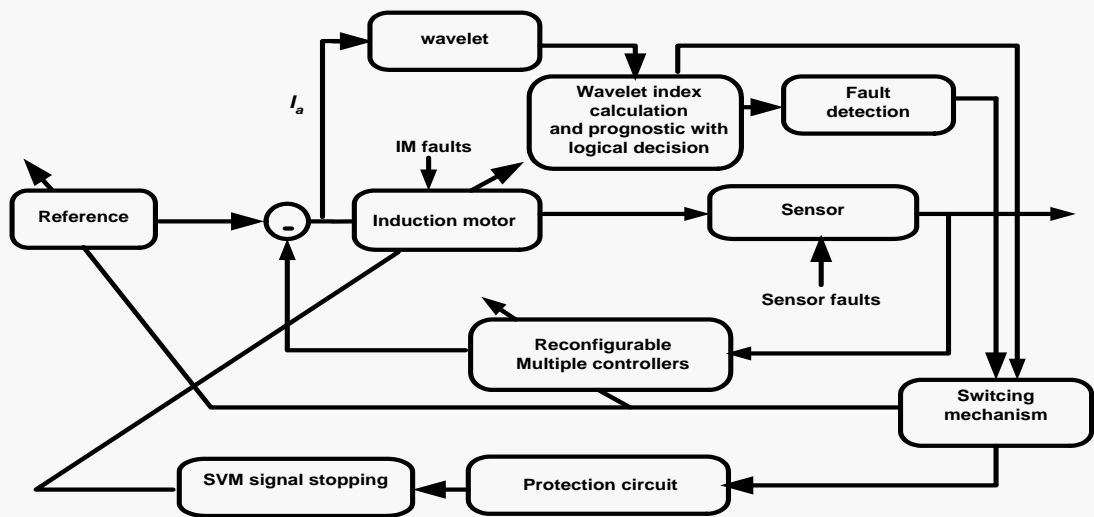


Figure 2.16. Block diagram of the proposed FTC algorithm

The key improvements introduced by this algorithm are:

1. The DWT input is stator current.
2. Four algorithms, namely sensor vector control, sensorless vector control, closed loop V/F and open loop V/F controls are implemented using Simulink.
3. The fault detection and diagnosis tracks the location, type and time of faults.
4. The control strategy is decided according to the wavelet index which is highly sensitive to signal changes.
5. Equations relating the wavelet index (and thus the faults) and the stator resistance after it is modified by a fault are found.

The chapter 5 gives the details of the proposed FTC based IM drive system.

2.4 Inverter Faults

As shown in Figure 2.17, the three phase inverter consists of three legs with two transistors in each leg. IGBT transistors in the normal power level or the GTO thyristors types with freewheeling diodes in the high power case have been used (K. Bose, 2006).

The inverter can provide the three phase voltage supplied to the IM, that is supplied by a voltage source comprising of a diode rectifier and a capacitor filter C to serve the dc-

link (Yeh C. C., 2008). To obtain low impedance for the AC component in the dc-link, the C value of 3300 μF is used in this thesis. Figure 2.17 shows the rectifier-inverter arrangements to obtain variable voltage and frequency supply.

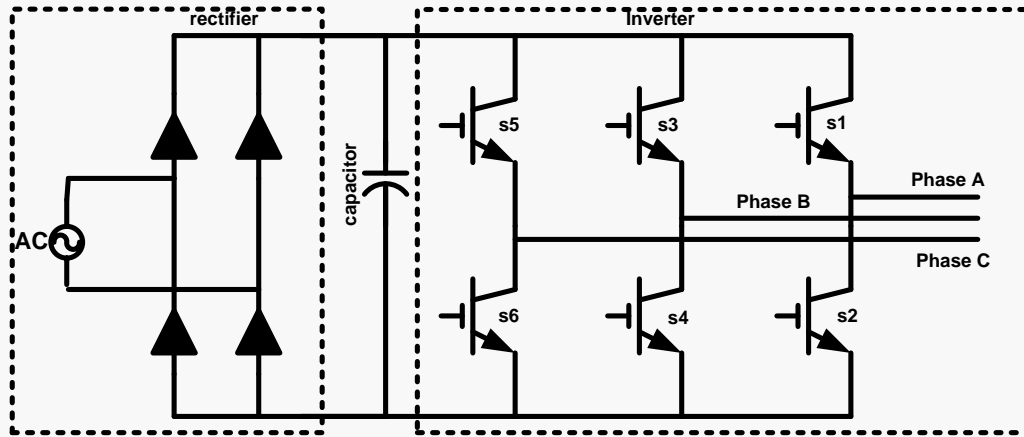


Figure 2.17. Basic power circuit to obtain 3-phase variable supply

The voltage source inverter (VSI) can provide high performance (Q.T. An, 2010). The inverter diagnostic methods are classified as current based and voltage based methods. Faults such as, short circuit in one or more transistor in the same or different leg can occur. These faults can be highly damaging specially in the case of the complementary IGBT being turned on and an open circuit in one or more leg. In some cases the drive may still manage to perform but with low efficiency owing to the pulsation torque and the freewheeling diodes. The stability of the system was maintained through the evaluation of the stator flux at zero voltage and the frequency at minimum through an ANN, by using a simple open loop inverter (PWM_VSI) fed IM (Yusof, 2003). The path linking the uncontrolled rectifier of a variable V/F control IM drive was studied by (Mahmoud, 2007). (Cui, 2007), detected the faults through the simulation of inverter as a switching technique. (Yeh C., 2007), presented the fault tolerant operations of soft starters and adjustable speed drives (ASDs) during the power switch open circuit or short circuit.

The motor operations are affected by these faults, therefore the fault diagnostic is an important step as it will allow early detection and control. This work will however assume that the inverter is healthy in all the operations, as we will not discuss the faults associated with the inverter. Figure 2.18 shows the percentage of component failures in the adjustable speed drives according Pareto chart. The control circuit faults are higher than the power electronics and external auxiliaries' faults.

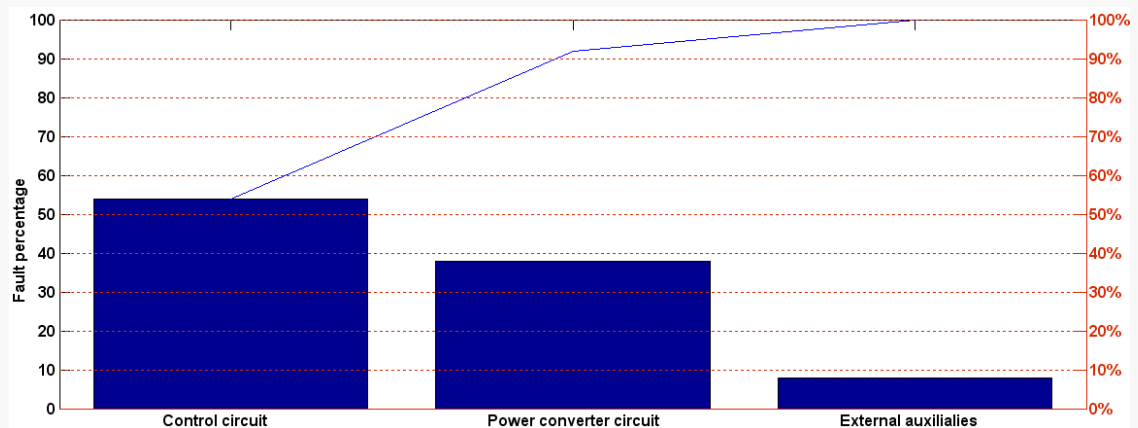


Figure 2.18. Percentage of component failures in ASD

Fig2.19 shows the percentage of component failures in the switch power supply. In this figure more than 60% of switch mode power supply faults are DC link capacitor, 32% is power transistor and 8% is diodes and other faults.

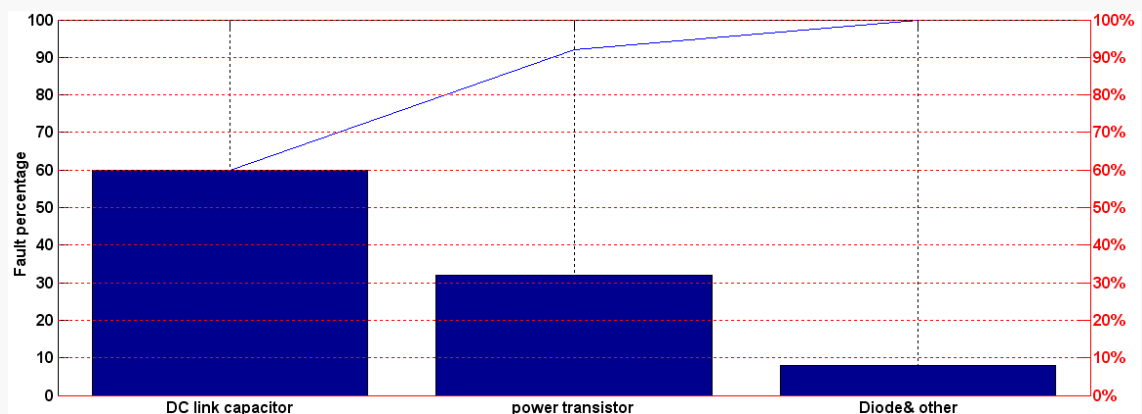


Figure 2.19. Percentage of component failures in switch mode power supply

(G. Mahmoud, 2007), introduced the VSI open circuit and short circuit faults with V/F control strategy.

As expressed by (Bech, 2000), the Fourier series of the phase voltage obtained from a 3- Φ inverter can be written as.

$$U_A = 2 / \pi U_{dc} \sum_{n=1}^{\infty} \frac{1}{n} \sin(n\omega t) = U_{m(n)} \sum_{n=1}^{\infty} \sin(n\omega t) \quad (2.26)$$

$$U_{m(n)} = \frac{2}{n\pi} U_{dc} \quad \text{Is the peak value of the nth harmonic,} \quad (2.27)$$

$$n = 1+6k, k = 0, \pm 1, \pm 2$$

The wavelet diagnosis of the inverter fed IM was presented by (Samsi R. R., 2006) where a DC voltage of 460V with a voltage source inverter is used to feed the IM. The DC voltage contains the ripple components as well as the power delivered to the inverter, which affects the inverter negatively. Several sources constitute the DC-link voltage pulsation such as, pulsation components in the diode rectifier circuit and asymmetrical AC voltage (Cross, 1999). There is an increase in the electric losses. A healthy operation of the IM and inverter are indicated by the DC link, as can be seen from Figure 2.20 and Figure 2.21 for healthy and faulty inverter respectively. In this thesis, the inverter will be considered as healthy and without faults after the replacement of the burn G4PH50UD IGBT transistor.

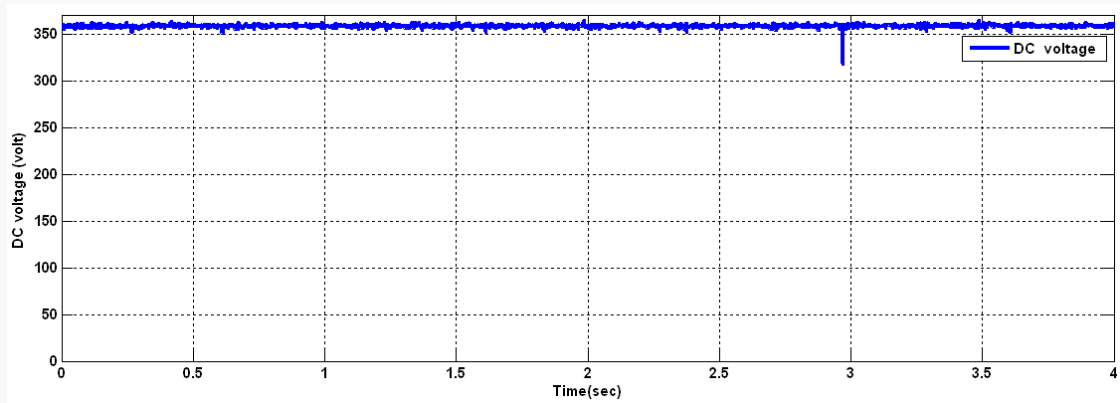


Figure 2.20. Experimental DC level in the healthy inverter

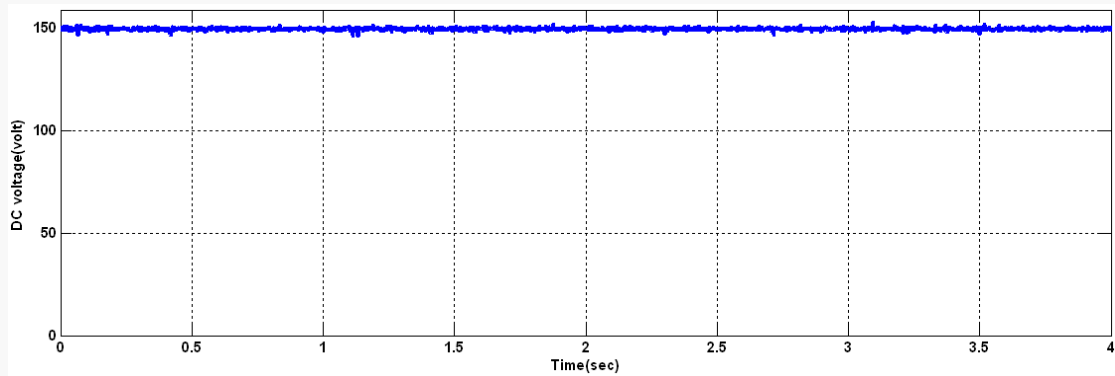


Figure 2.21.Experimental DC level in the faulty inverter

For the healthy inverter case, the DC voltage was 362 V and it reduced until 150V in the faulty inverter which is good observation of inverter fault.

2.5 AC Drive

AC drives have risen in prominence, not just because motors such as the squirrel cage type are exceptionally rugged and reliable, but also because the speed control methods with AC motors are direct and efficient. An AC drive requires power components that can provide it the desired voltage and current levels in a suitable form, which includes conversion from DC to AC. The drive also needs control components that create flexible and adjustable speed settings.

Figure 2.22 shows the configuration of an AC drive.

Key advantages of an AC motor drive are as follows:

- The motor requires very little maintenance.
- The cost is minimal and efficiency is substantial.
- Operation with multiple motors is simplified.
- Since the linear acceleration and deceleration is controlled, the motor starts and stops smoothly. Speed transitions are also smoothed.
- Torque control is rapid and accurate with the current limit

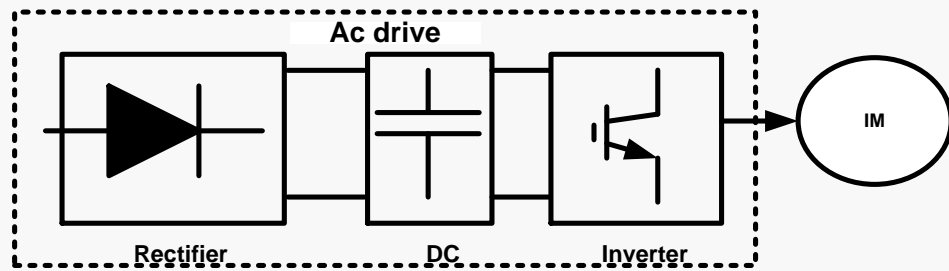


Figure 2.22.AC drive

2.5.1 Space Vector Modulation

The inverter pulse width modulations are controlled by the SVM, which is an algorithm. The AC waveforms are created in it from a DC source, specifically in the variable speed system. Performance is enhanced through the SVM as it also gives additional benefits such as, reduced switching losses and reduced total harmonic distortions. It can be easily applied through the digital processor (Reney, 2011).

All the stages in a three phase analysis are considered as one set instead of considering them as separate stages. The properties of vector rotation can therefore be used. The analysis in the DC components can be obtained by withdrawing the rotational effects when the rotation with t is used (Neacsu, 2001).

Various types of the SVM are present such as; basic bus clamping, asymmetrical zero changing and clamping (Parekh R. , 2005). A conventional type will be used in this work. The voltage across the legs in a common mode three phase bridge inverter is a bus direct current voltage U_{dc} which is assumed as a constant value. Therefore, the magnitude of the current switched and the switching frequency determine the losses. The number of commutations required for each modulation scheme and the current at the switching instant determines their evaluation. There are three main modulation techniques employed: high commutation pulse width modulation (PWM), low commutation simple six-step modulation and progressive space vector modulation SVM

(Egorov, 2011). Figure 2.23 shows the phase A voltage v_a according to the conventional space vector modulation.

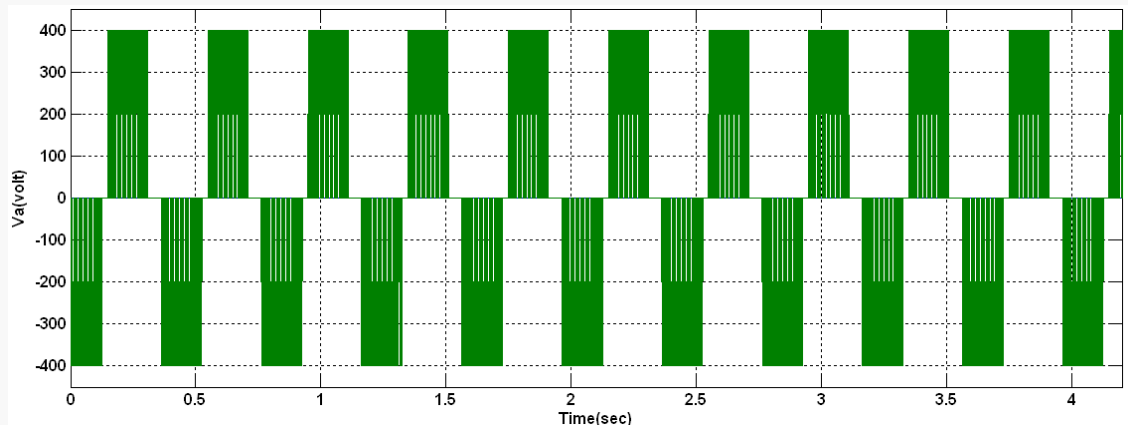


Figure 2.23. Phase A voltage

Figure 2.24 voltage generated in phase B

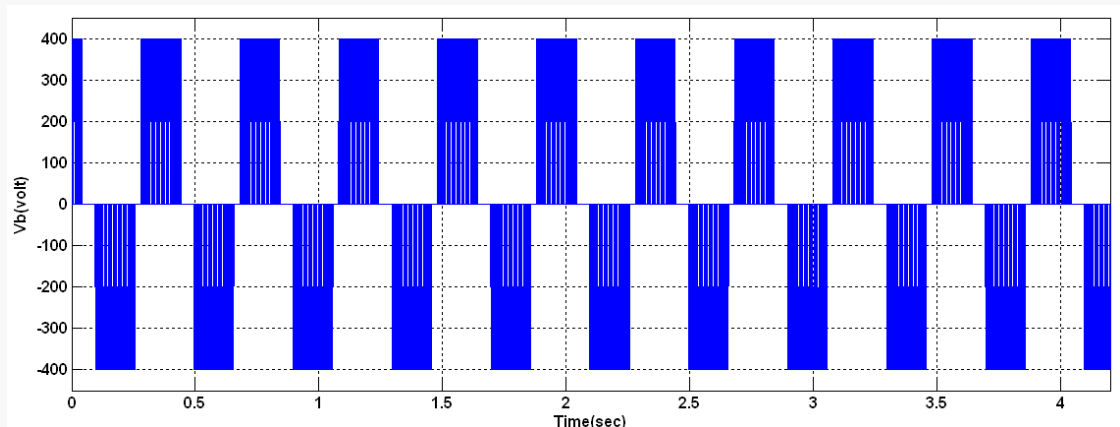


Figure 2.24. Phase B voltage

Figure 2.25 shows the voltage generated in phase C.

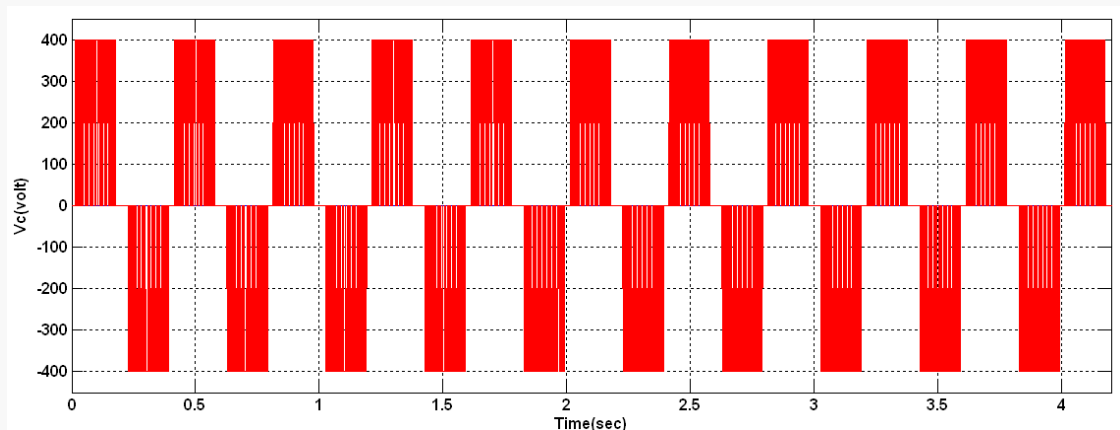


Figure2.25. phase C voltage

The voltage source inverter is said to be primarily based on the pulse width modulation and the instantaneous power theory. It is important to consider the vested voltage or the current in the PWM techniques. The utilization rate of the DC voltage, obtained after the selection of the proper switching mode to decrease the harmonic content, is 78.5% which is much less than the 100% of the six step wave. Thus, studies have been focused on the improvement of the DC voltage rate (Hengli Quan, 2011). Figure 2.26 shows the SVM switch time.

The SVM switch time (T_a , T_b , and T_c) are shown in Figure 2.26

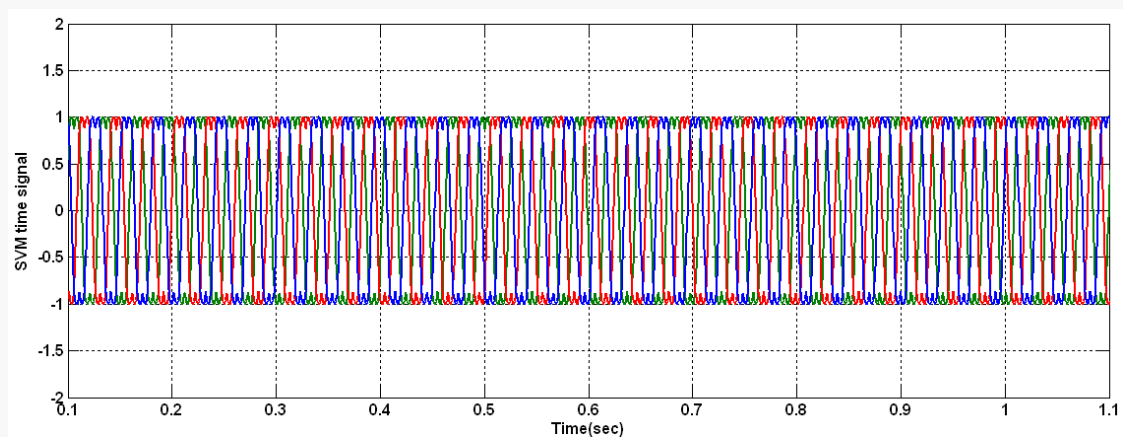


Figure 2.26.SVM switching times

Figure 2.27 shows the six sector control strategy of the space vector modulation.

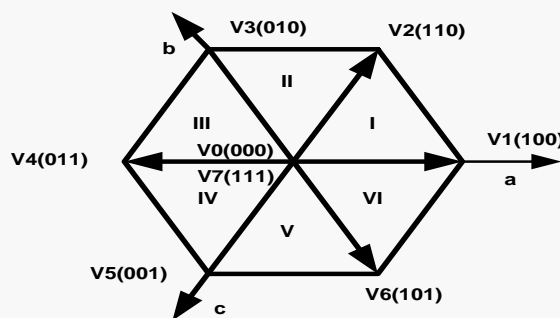


Figure 2.27.Six sectors control strategy of SVM

Therefore, space vector PWM can be implemented by the following steps (Keyhani, N/A):

Step1. Through the following equations the voltage and the angle can be determined:

$$\begin{bmatrix} v_d \\ v_q \end{bmatrix} = \begin{bmatrix} 1 & -0.5 & -0.5 \\ 0 & \sqrt{3}/2 & -\sqrt{3}/2 \end{bmatrix} \begin{bmatrix} v_{an} \\ v_{bn} \\ v_{cn} \end{bmatrix} \quad (2.18)$$

The voltage reference equation is:

$$v_{refer} = \sqrt{v_d^2 + v_q^2} \quad (2.19)$$

The angle can be obtained by the following equation:

$$\alpha = \tan^{-1}\left(\frac{v_q}{v_d}\right) \quad (2.20)$$

The phasor diagram is shown in Figure 2.28

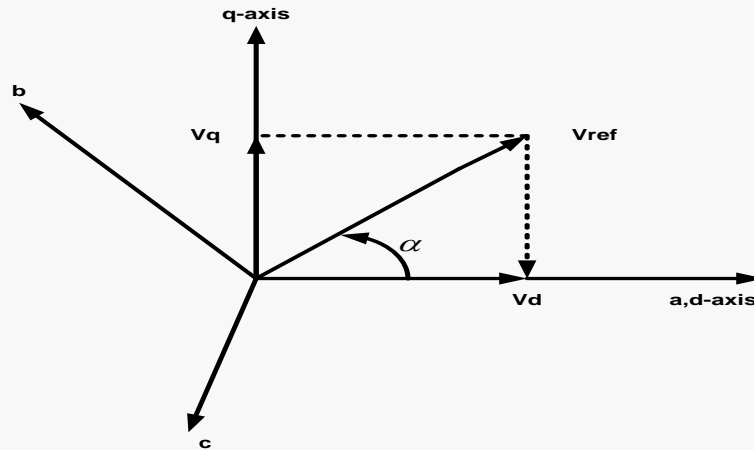


Figure 2.28. Voltage space vector and its (d, q) components

Step2. According to the following equation the time duration can be calculated.

$$T_1 = T_z a \frac{\sin(\pi/3 - \alpha)}{\sin(\pi/3)} \quad (2.21)$$

$$a = \frac{|v_{refe}|}{2/3v_{dc}} \quad (2.22)$$

$$T_z = \frac{1}{f_s} \quad (2.23)$$

$$T_2 = T_z a \frac{\sin(\alpha)}{\sin(\pi/3)} \quad (2.24)$$

$$T_0 = T_z - (T_1 + T_2) \tag{2.25}$$

Step3. As shown in Figure2.29, the switching time for all the six sectors can be evaluated.

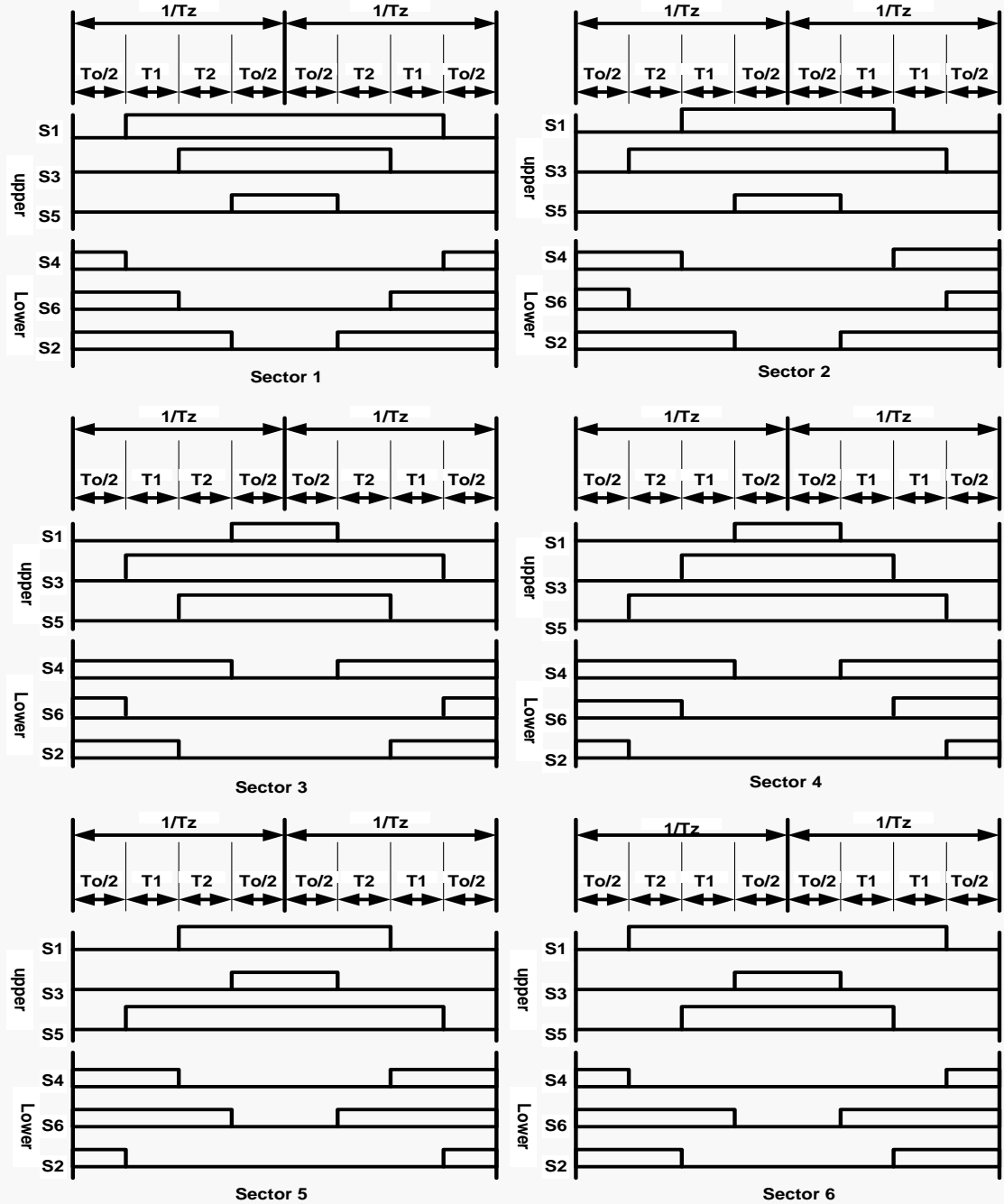


Figure 2.29.Space vector PWM switching patterns at each sector

2.6 Applications

The fault tolerant system is applicable in many situations such as:

1. Petrochemical
2. Military
3. Communication
4. Industrial and manufacturing
5. Air space shuttles
6. Air conditioning
7. Medical
8. Nuclear power system

The wide usage of the fault tolerant system shows its growing importance in the industrial and the academic communities owing to the enhanced safety and reliability demands beyond the extent of the conventional control system.

Chapter 3: Control Techniques of IM

3.1 Introduction

This chapter will present the details of the performance and application of the four control techniques such as, sensorless vector control, sensor vector control, closed loop and open loop V/F control schemes.

3.2 Modeling of IM

In many fields the rotating electrical machines have played a significant role, specifically in the industrial processes. This is owing to their low cost, rigidity, reliability, easy maintenance and robustness (Khalaf Salloum Gaeid, 2010).

Mechanical motions have been produced through various IMs and electrical machines are using almost 50% of the total electrical energy produced on the planet earth .thus it has led to developments in the control strategy of the IM systems (Kim, 2007). Figure 3.1 shows the types of electrical motors.

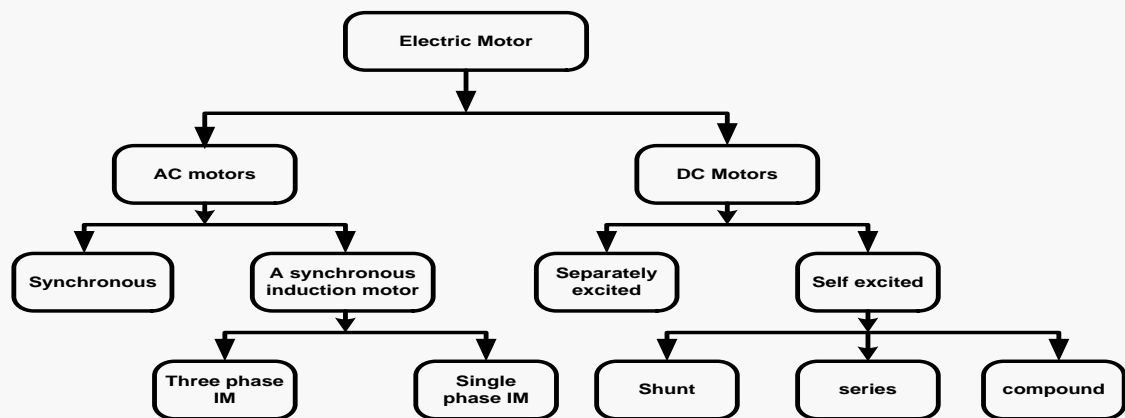


Figure 3.1.Types of electric motors

(Anjaneyulu, 2007), presented the dq dynamic model of a squirrel cage IM with respect to the frame fixed to the stator.

The system analysis and the system performance in both transient and steady state regions need a model for IM to diagnose a fault (Pedra, 2009). There are various IM

models such as voltage model, current model and the state space models developed by the researchers (Tze Fun Chan, 2011). The following sections will further explain these models.

3.2.1 State Space Modeling of IM

The electrical part was modeled by the fourth order state, while the mechanical part was modeled by the second order (P. C. Krause, 2002).

Three phase to two phase transformation constitutes the model of the IM, as in the equation 3.1:

$$\begin{bmatrix} i_{ds} \\ i_{qs} \end{bmatrix} = \begin{bmatrix} \cos(\theta) & \cos(\theta - 2\pi/3) & \cos(\theta + 2\pi/3) \\ \sin(\theta) & \sin(\theta - 2\pi/3) & \sin(\theta + 2\pi/3) \end{bmatrix} \begin{bmatrix} i_{sa} \\ i_{sb} \\ i_{sc} \end{bmatrix} \quad (3.1)$$

The following expression gives the stator and flux linkage equations, the IM electrical model according to the asynchronously rotating d-q coordinates:

1. Stator voltage in q -axis direction is:

$$V_{qs} = R_s i_{qs} + \frac{d\phi_{qs}}{dt} + \omega \phi_{ds} \quad (3.2)$$

R_s is the stator resistance

V_{qs} , i_{qs} are the q axis stator voltage and current

ϕ_{qs} , ϕ_{ds} are the stator q and d axis fluxes

The modeling of IM in q -axis is shown in Figure 3.2.

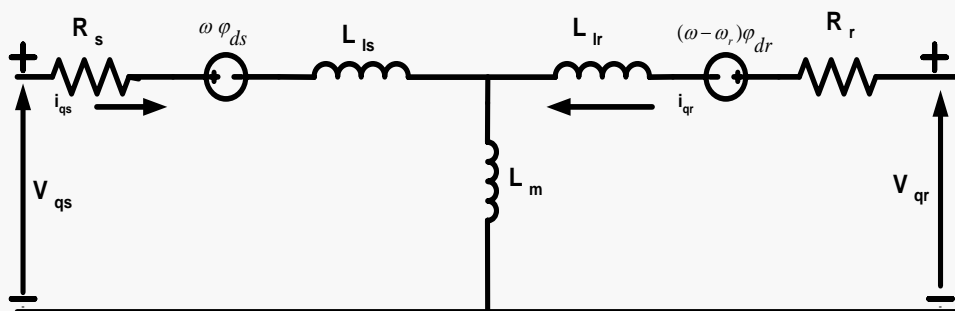


Figure 3.2. Modeling of IM in q -axis

where

$$\phi_{qs} = L_s i_{qs} + L_m i'_{qr} \quad (3.3)$$

$$\phi_{ds} = L_s i_{ds} + L_m i'_{dr} \quad (3.4)$$

$$L_s = L_{ls} + L_m \quad (3.5)$$

L_s , is the total stator inductances

L_m , is the magnetizing inductance

L_{ls} , is the stator leakage inductance

2. Stator voltage in d -axis direction is:

$$V_{ds} = R_s i_{ds} + \frac{d\phi_{ds}}{dt} + \omega \phi_{qs} \quad (3.6)$$

Figure 3.3 shows the modeling of IM in d -axis

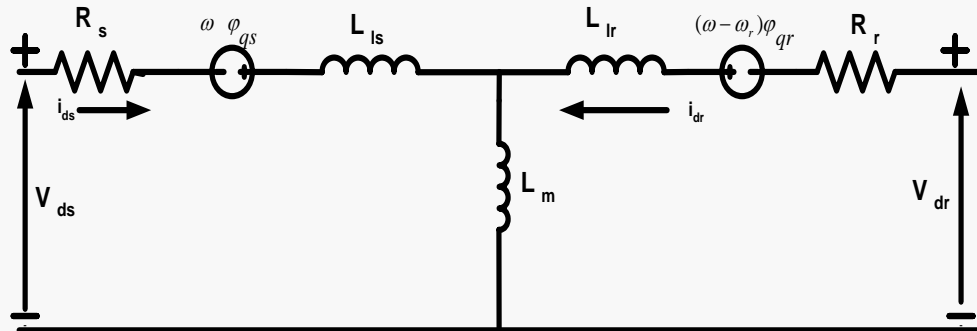


Figure 3.3. Modeling of IM in d -axis

3. Rotor voltage in q -axis direction referred to the stator is:

$$V'_{qr} = R'_r i_{qr} + \frac{d\phi'_{qr}}{dt} + (\omega - \omega_r) \phi'_{dr} \quad (3.7)$$

where

$$\phi'_{qr} = L'_r i'_{qr} + L_m i_{qs} \quad (3.8)$$

L'_r , is the total rotor inductances

$$\phi'_{dr} = L'_r i'_{dr} + L_m i_{ds} \quad (3.9)$$

$$L'_r = L'_{lr} + L_m \quad (3.10)$$

L'_{lr} is the rotor leakage inductance

4. Rotor voltage in d -axis direction referred to the stator is:

$$V'_{dr} = R'_r i'_{dr} + \frac{d\phi'_{dr}}{dt} + (\omega - \omega_r)\phi'_{qr} \quad (3.11)$$

5. The torque equation in stationary reference frame is expressed as:

$$T_e = 1.5p(\phi_{ds}i_{qs} - \phi_{qs}i_{ds}) \quad (3.12)$$

3.2.2 T Model of IM

There many aspects assumed when modeling the IM such as; linear magnetic field, uniform air gap, pure sine wave voltage source, perfect shaft alignment. The T modeling is used in the stationary reference frames of the vector modulation, after the abc - dq transformation and then to a $\alpha\beta$ system.

Figure 3.4 shows the dynamic T-modeling of the IM.

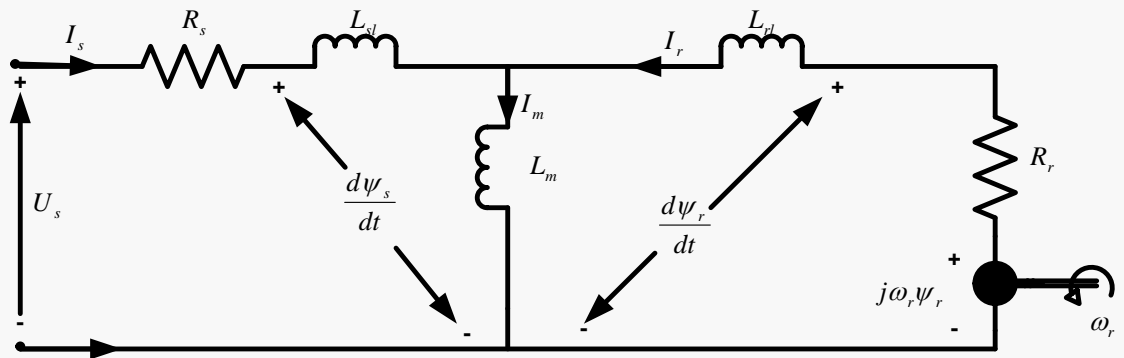


Figure 3.4. Approximate equivalent circuit of IM

The equations 3.14, 3.15 and 3.16 can be used to express the T-modeling of stator, rotor and the torque of the IM (Qian Cheng, 2011).

The following equations will express the stator voltage:

$$U_s = R_s I_s + \frac{d\psi_s}{dt} \quad (3.14)$$

And the rotor equation will be expressed as follows:

$$U_r = 0 = R_r I_r + \frac{d\psi_r}{dt} - j\omega_r \psi_r \quad (3.15)$$

The electromagnetic torque equation is:

$$T_e = 1.5p I_m \psi_s I_s = 1.5p(\psi_{s\alpha} i_{s\beta} - \psi_{s\beta} i_{s\alpha}) \quad (3.16)$$

These components are associated with the stationary reference frame.

This system however can't work efficiently with systems having variable parameters such as mutual inductance and rotor resistance owing to the complicated nonlinear behavior.

3.2.3 Inverse Γ Model of IM

The T-model is complicated and over-parameterized due to the three inductances used. This is not preferable for the dynamic analysis or the vector control design. There are two state variables for the IM; (ψ_r, i_s) the rotor inductance can be referred to the stator side that will negate the over parameterization. Thus the Γ Model parameters obtained are as follows (Pietilainen, 2005):

$$R_R = (L_m^2 / L_r) R_r \quad (3.17)$$

R_R is the rotor resistance in Γ model

$$L_M = (L_m^2 / L_r) \quad (3.18)$$

L_M is the mutual inductance in Γ model

$$\psi_R = (L_m / L_r) \psi_r \quad (3.19)$$

ψ_R is the stator flux in stationary coordinates

Figure 3.5 shows the dynamic inverse Γ modeling.

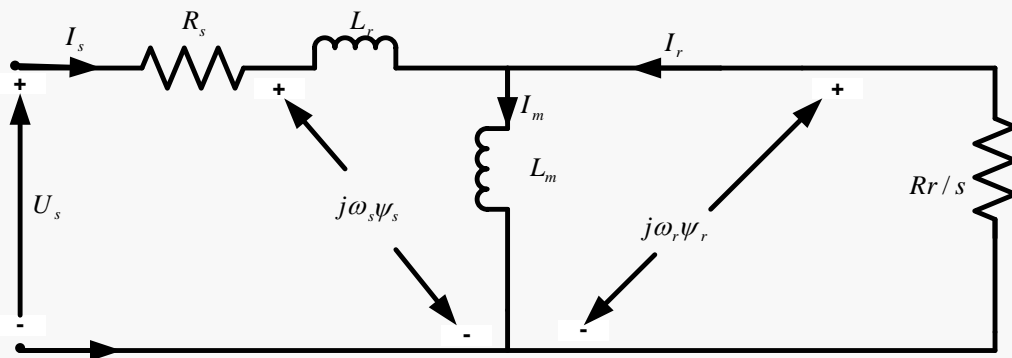


Figure 3.5. Dynamic Inverse Γ modeling of IM

3.3 Control Techniques of IM

The IMs have found their way through many applications such as robotics, fan, electrical vehicles, elevator pumps, ventilation and air conditioning (HVAC), heating and wind generation system (Bose, 2002). They are considered as a standard in the industry. Since three decades, much preference was given to the DC machines owing to their decoupling of the flux and torque. On the contrary they are notorious for their drawbacks such as high rotor inertia, difficulty in maintenance, high cost and inconvenience in commutations and brushes.

The AC motors were frequently used after the development of the IGBT and the Digital DSP technology. These technologies are able to copy the decoupling effect of the DC motor while eliminating the drawbacks that may be found in the DC machines.

The frequency converters usage characterizes the optimal operations of the IM speed control methods. The following components are present in the converters:

1. Rectifier circuit,
2. Space Vector Pulse Width Modulated (SVPWM) voltage source inverter
3. Gate drives for the inverter
4. DC filter

The following properties should be present in the inverter fed IM drive (Żelechowski, 2005):

1. Minimum torque and flux ripples.
2. A constant switching frequency.
3. A maximum output torque for all periods of operation.
4. Low parameter variations in aspects like the rotor resistance.
5. Fast torque and flux responses.
6. The main objectives of the control strategy should be to gain the best possible parameters of drive and simplicity.

The control methods can be classified in two groups of vector control and scalar control. The scalar control, which is the easiest way to apply, is further divided into the stator current control and the V/F control. The V/F control methods aim at maintaining a constant frequency ratio. It is frequently used in the industries owing to its simplicity and satisfactory performance. The scalar control is either open loop V/F or closed loop V/F.

The following are the characteristics of the vector control:

1. Voltage amplitude control(common with scalar control)
2. Frequency control(common with scalar control)
3. Control of both vectors of current and flux.

The overall performance of the drive improves according to the above specifications. Sophisticated methods are required for the nonlinear behavior of the IM and the coupling between torque and flux in the functions of the machine. The torque and the flux can be decoupled through a variety of methods, which differ in the main concept and analytical procedure of the decoupling.

There are four types of variable frequency control; field oriented control (FOC) which can be either direct field oriented control (DFOC) or the indirect field oriented control (IFOC). The IM equations are transformed from three phase coordinates (a, b, c) into two phase coordinate system due to the vector control ($d-q$). The flux produced component

forms the d -axis and the torque produced component forms the q -axis. There is a synchronous rotation of both of them. The vector control successfully decouples the flux and the torque. Feedback linearization control (FBLC) is the second method, which is a nonlinear control algorithm. The decoupling of the torque and the rotor flux are enabled through linearization control technique. Figure 3.6 shows block diagram of feedback linearization control (Chandorkar, 2010).

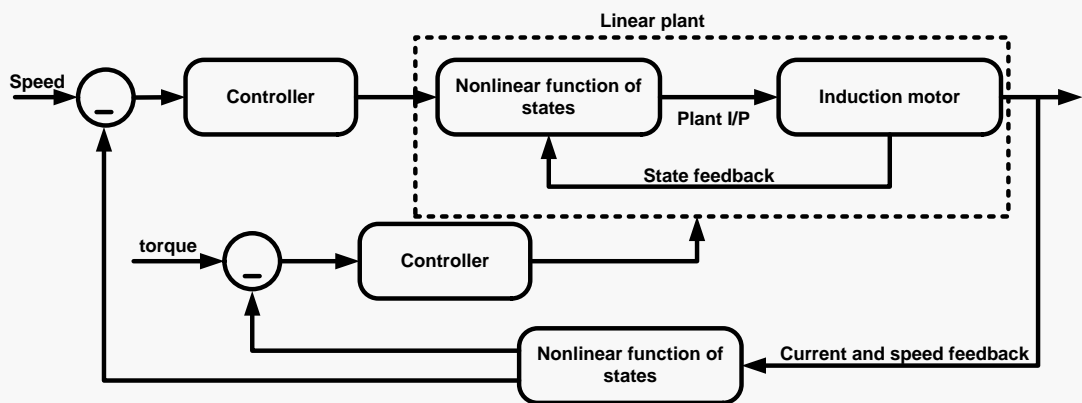


Figure 3.6. Block diagram of FBLC based IM drive system

The Passivity Based Control (PBC) is the third method, which is a controller design algorithm that stabilizes the system. It attempts to make the closed loop system passive through various methods such as Liapunov function. It also provides the required storage function. Figure 3.7 shows the passivity based control (C. BatlleA, 2006):

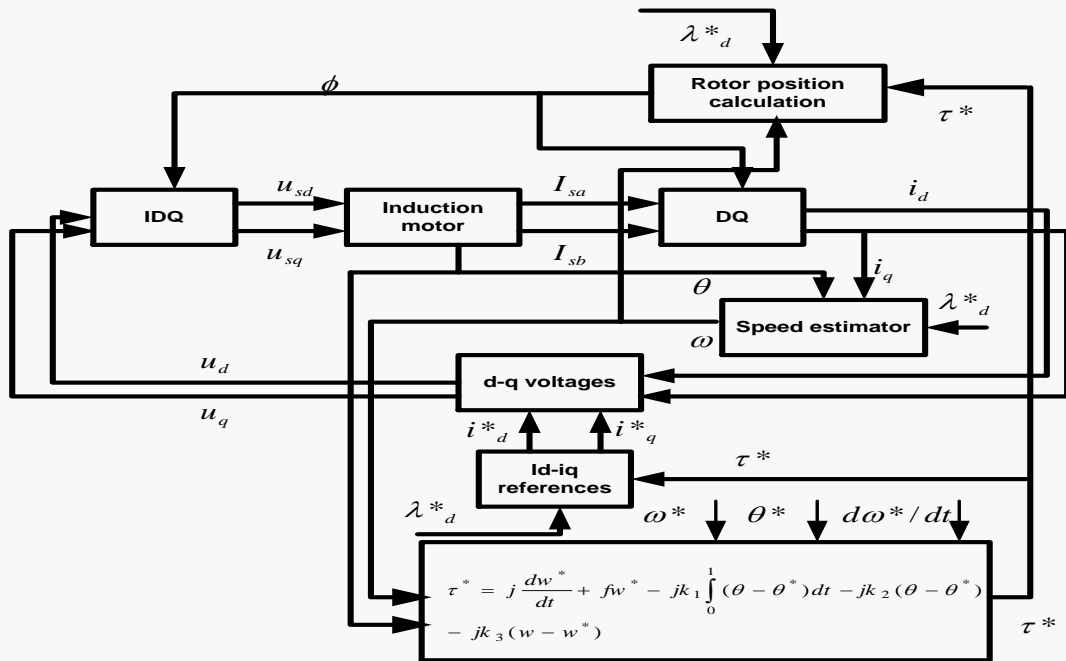


Figure 3.7. Block diagram for the passivity based method (Simaan, 1997)

The direct torque control (DTC) is the fourth method. The hysteresis controllers are used in this method to introduce the on-off functions of the inverter switches. Various DTC types are used such as classical DTC or Direct Torque Control space vector modulated (DTC-SVM). Figure 3.8 shows the classical direct torque control block diagram.

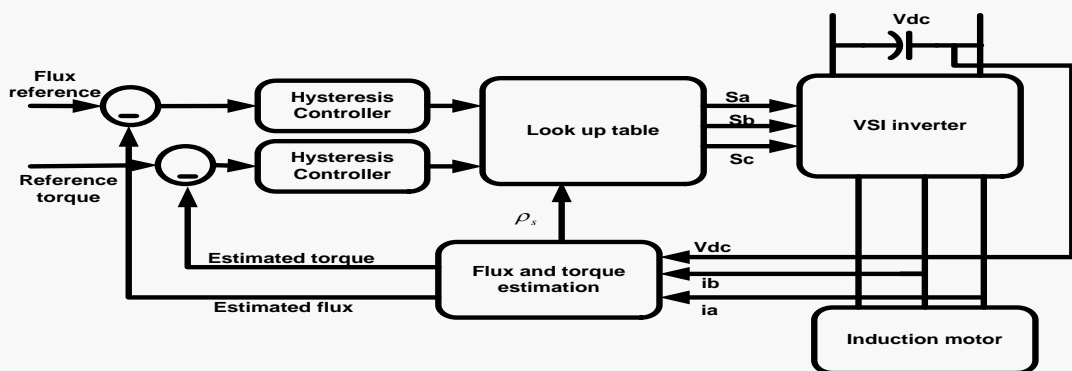


Figure 3.8. Block diagram of classical DTC (Yuttana Kumsuwan, 2008) based IM drive

Four controllers: Sensor based vector control (with encoder), sensorless vector control (without encoder), V/F closed loop and open loop controllers, are used for the proposed

FTC technique. The performance is maintained through these controllers at a satisfactory level during the faults occurrence in the steady and transient areas.

The algorithm is simulated through the digital motor control (DMC), as it is easy to compile via the Simulink/Matlab to C++ or C through F28335 DSP.

3.3.1 Vector Control with Encoder

To control the torque and the speed of the IMs, the vector control is the best control technique (Jannati, 2010). In the 1970s the vector control was invented that showed that the IM could be controlled as a separately excited DC motor. This was a revolutionary technique that was based on the orientation of the flux vector along the direct (d) axis:

$$\varphi_{qr} = 0 \quad (3.20)$$

$$\varphi_{dr} = \text{const ant} \quad (3.21)$$

The following calculations are carried out in the vector control according to the Park transformation:

$$\begin{bmatrix} i_q \\ i_d \end{bmatrix} = \begin{bmatrix} \cos \theta & \sin \theta \\ -\sin \theta & \cos \theta \end{bmatrix} \begin{bmatrix} i_Q \\ i_D \end{bmatrix} \quad (3.22)$$

This operation can be illustrated in Figure 3.9

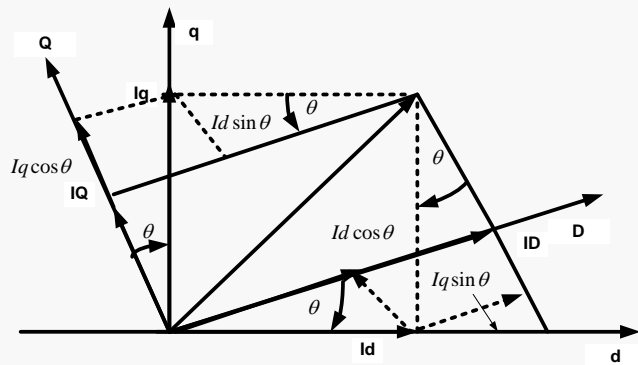


Figure 3.9. Park transformation principle

The dq to abc transformation can be written as,

$$\begin{bmatrix} i_{as} \\ i_{bs} \\ i_{cs} \end{bmatrix} = \begin{bmatrix} 1 & 0 \\ -0.5 & -\sqrt{3}/2 \\ -0.5 & -\sqrt{3}/2 \end{bmatrix} \begin{bmatrix} i_{ds} \\ i_{qs} \end{bmatrix} \quad (3.23)$$

Therefore, the rotor flux and the torque can be independently controlled to obtain a linear current/torque relationship through the stator current in the dq -axis.

An accurate performance can be obtained through accurate evaluation of the position of the flux space (Serna, 2006).

In the case of enhanced performance, industrialists are mainly looking for accuracy, speedy recovery, speedy responses and insensitiveness to the variations in the parameters (Uddin, 2000). High performance is obtained at variable speeds and frequency through the vector control of the squirrel cage IM. This is conducted as shown in Figure 3.10.

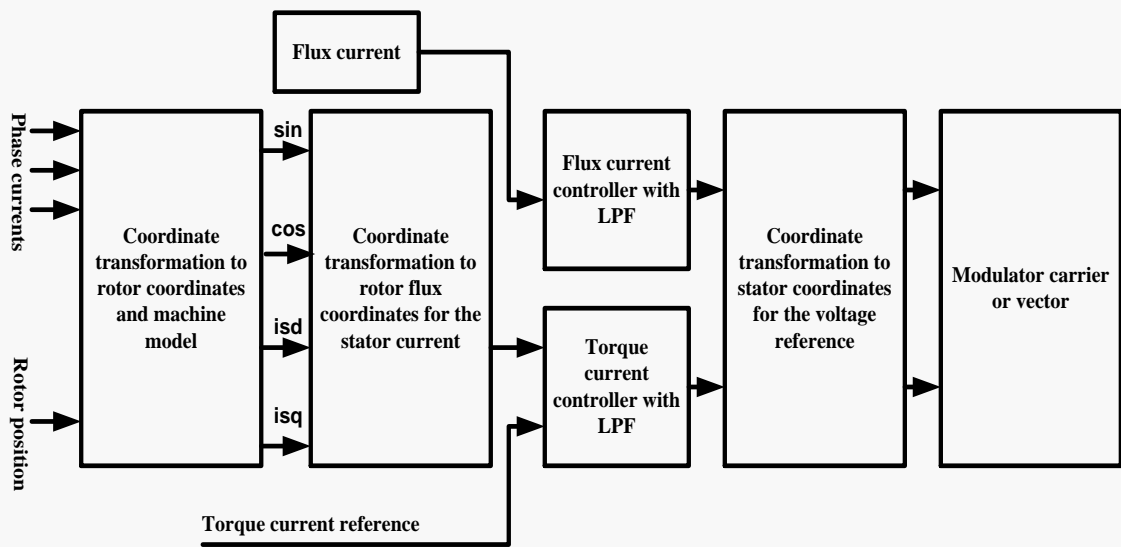


Figure 3.10. Vector control principle

Figure 3.11 shows the block diagram of a conventional vector control scheme. The speed control involves a number of loops but still it cannot completely reach the satisfactory levels (Kumar, 2007).

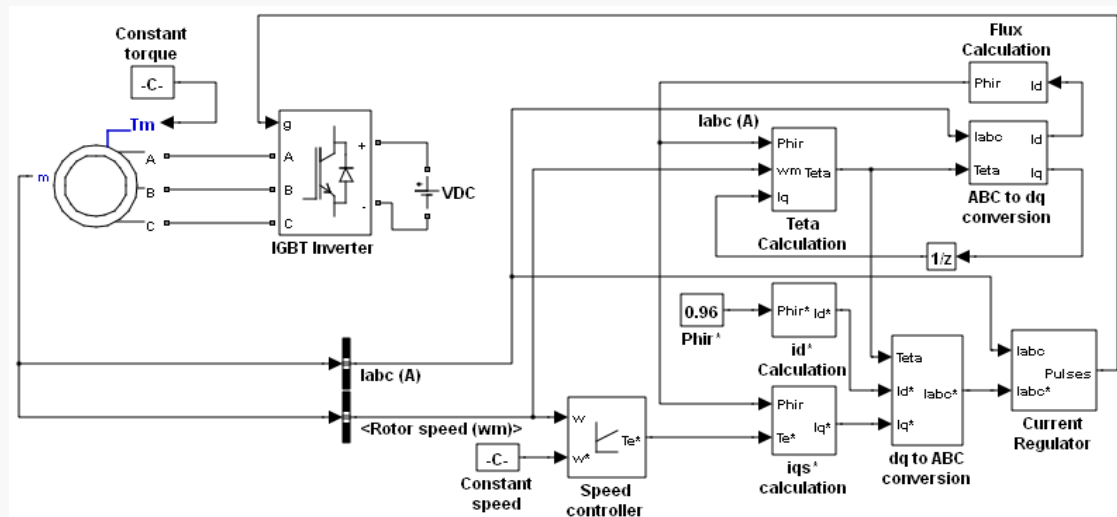


Figure 3.11. Vector control implementation

Two constants are used by the vector controlled machines as input references. These constants are the torque component aligned with the q -axis coordinate and the flux component aligned with the d -axis. The control system handles the instantaneous electrical quantities as the control is based on the projections. Accurate controls are produced through these behaviors in both steady and transient states, both independent of the bandwidth mathematical model of the IM. Figure 3.12 shows this.

The following ways are written to be explored as control problems, through this technique:

1. Easily accessible stator current and hence torque and flux components can be reached easily.
2. Removal of the difficulties that surface in direct torque control (Instrument, 1998).
3. A flux sensor is used to measure the rotor flux vector by positioning it over the air gap. It is also measured through the voltage equations with the electrical machine parameters. The direct rotor speed can be used to evaluate the rotor flux parameter.

Three PI controllers are used in the vector control. It becomes hard to tune all the controllers together. The sampling time required for the inner controller is ten times faster than needed for the outer controller. The controller's efficiency is tuned through the Ziegler-Nichols method, through which the K_p and K_i for both I_{sq} and I_{sd} are set accurately allowing to reach the constant references. The constants K_p and K_i for both I_{sq} and I_{sd} effect the sensibility and the steady state errors respectively. The optimum values for K_p and K_i are listed in table 3.1 after tuning. Figure3.13 shows the main block of the IM vector control to create the space vector modulation.

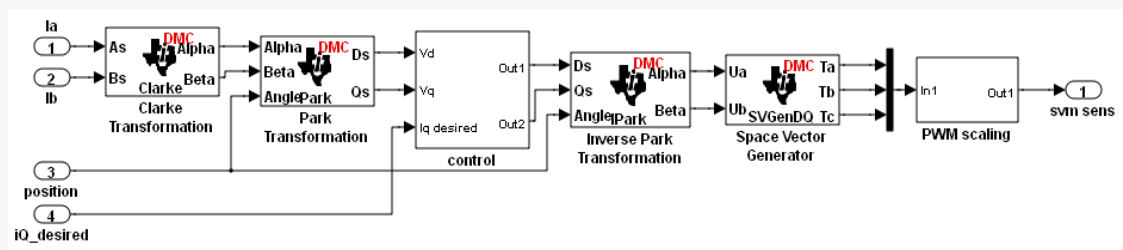


Figure 3.13. Vector control SVM generation using DMC blocks

3.3.2 Vector Control without Encoder

Recently the IM drives controlled without the speed sensors have been developed, but they have not been able to perform efficiently at low speeds. The variable parameters of sensitivity of the factors, limited parameter bandwidth and unbalance current sources are the reasons behind this low performance (Joachin Holtz, 2000). The Model Reference Adaptive System (MRAS) is a popular option for the speed estimation. The observer and the extended Kalman filter are also popular options. New MRAS has been developed in this thesis, known as the Boosted (BMRAS). This thesis will investigate the manner of its operation in case of a fault and how it can be used to evaluate the speed as main parameter in the all fault tolerant control works. Figure 3.14 shows the Simulink implementation of the sensorless vector control.

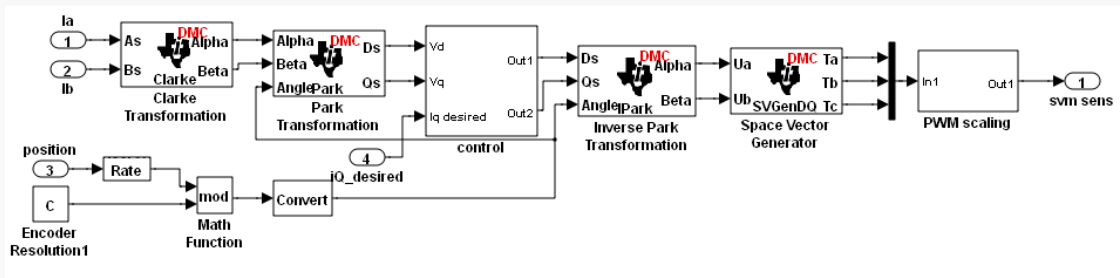


Figure 3.14. DMC Simulink implementation of sensorless controller

A reference model, an adaptive model and an adaptation mechanism makes up the classical MRAS. Figure 3.15 shows the estimated speed obtained through conventional MRAS. Estimated speed through MARS feed the sensorless in Figure 3.14 after integrate it.

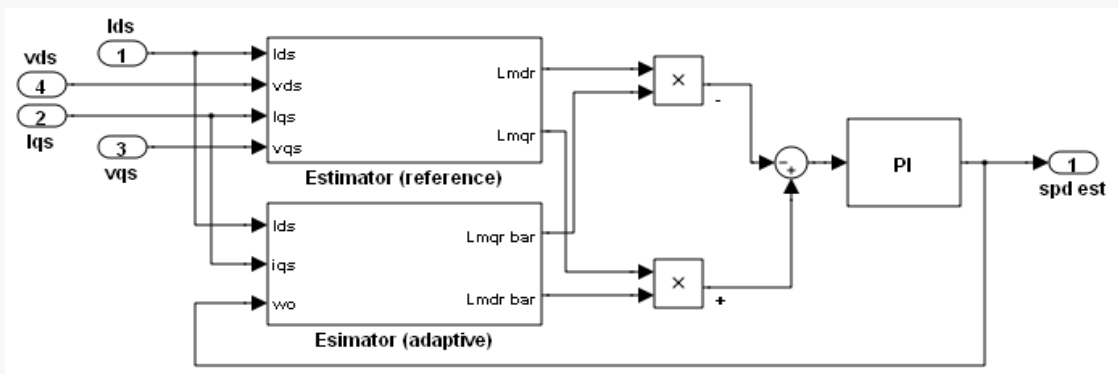


Figure 3.15. Conventional MRAS used for speed estimation

The PI controller is eliminated in the construction of the BMRAS, in order to save the tuning time. Figure 3.16 shows the block diagram of the BMRAS used in this thesis.

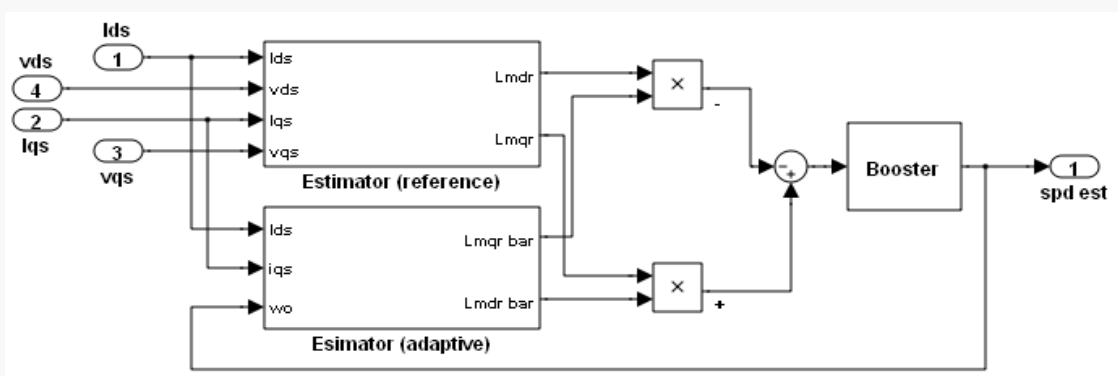


Figure 3.16. Simulink implementation of the proposed BMRAS

The following equations give the reference model according to the system shown in (Gadoue, 2010):

$$p\lambda_{dr} = L_r / L_m (v_{ds} - (R_s i_{ds} + \sigma L_s di_{ds} / dt)) \quad (3.24)$$

$$p\lambda_{qr} = L_r / L_m (v_{qs} - (R_s i_{qs} + \sigma L_s di_{qs} / dt)) \quad (3.25)$$

The adaptive model can be expressed in the following equations:

$$p\lambda'_{dr} = R_r L_m / L_r (i_{ds} - (R_r / L_r)\lambda'_{dr} - \omega_0 \lambda'_{qr}) \quad (3.26)$$

$$p\lambda'_{qr} = R_r L_m / L_r (i_{qs} - (R_r / L_r)\lambda'_{qr} - \omega_0 \lambda'_{dr}) \quad (3.27)$$

$$\varepsilon = \lambda_{qr} \lambda'_{dr} - \lambda_{dr} \lambda'_{qr} \quad (3.28)$$

A simple fixed gain linear PI controller is applied by the MRAS speed observer to create the evaluated rotor speed. Inaccurate flux estimations by the integration of the rotor voltages are obtained due to the poor performance of the classical MRAS especially at the synchronous speeds (Roberto Cardena, 2008).

The limit rate, zero order hold and initial conditions of the signals can apply the BMRAS, which contains the booster as a new part.

$$S = \frac{I_{in}(i) - O_{o/p}(i-1)}{t(i) - t(i-1)} \quad (3.29)$$

The current input and the time are given by: I_{in} , $t(i)$

While the previous time and the signal outputs are given by: $t(i-1)$, $O_{o/p}(i-1)$.

There are three conditions in the slope or the limit rate, that is the slew rate parameter (δ) should be more than rising, the rate between the values δ and γ and less than falling slew rate parameter (γ) as well as the initial condition =0.

The mathematical model of the first case is:

$$O_{o/p}(i) = \nabla t \cdot \delta + I(t-1) \quad (3.30)$$

t , indicates the current sample

$t-1$, indicates the past sample

The mathematical model of the second case is:

$$O_{o/p}(i) = \nabla t.\gamma + I(t-1) \quad (3.31)$$

The mathematical model of the third case is:

$$O_{o/p}(i) = I(i) \quad (3.32)$$

In the 2nd step, the zero order hold (ZOH) has to be defined to construct the booster. The zero order hold will generate a continuous time input by holding each sample value as a constant over one sample period. The ZOH can be considered as a hypothetical filter to obtain a piece wise signal as indicated by the following equation:

$$O_{ZOH\ o/p}(t) = \sum_{n=-\infty}^{\infty} I_{in}[n].rect\left(\frac{t-nT}{T} - \frac{1}{2}\right) \quad (3.33)$$

Time domain impulse response is as follows:

$$S_{ZOH\ o/p}(t) = \frac{1}{T} rect\left(\frac{t}{T} - \frac{1}{2}\right) = \begin{cases} \frac{1}{T} & \text{if } 0 \leq t < T \\ 0 & \text{elsewhere} \end{cases} \quad (3.34)$$

The application will determine the usage of the scaling time T , but in the case when the scaling time is omitted then the time of the measurement unit will determine the low pass filter. The transfer function of the booster block is:

$$T.f = \frac{-1.1659e-011z^2}{z^2 - 0.99819z - 0.0018641} \quad (3.35)$$

Predictable error measurement was used to calculate eq. (3.35).

Simulink was used to prove the effectiveness of this transfer function when the input is (ε) and the output is estimated speed as can be seen in Fig. 3.17. The simulation and experimental results are for 1kW IM with 2780RPM.

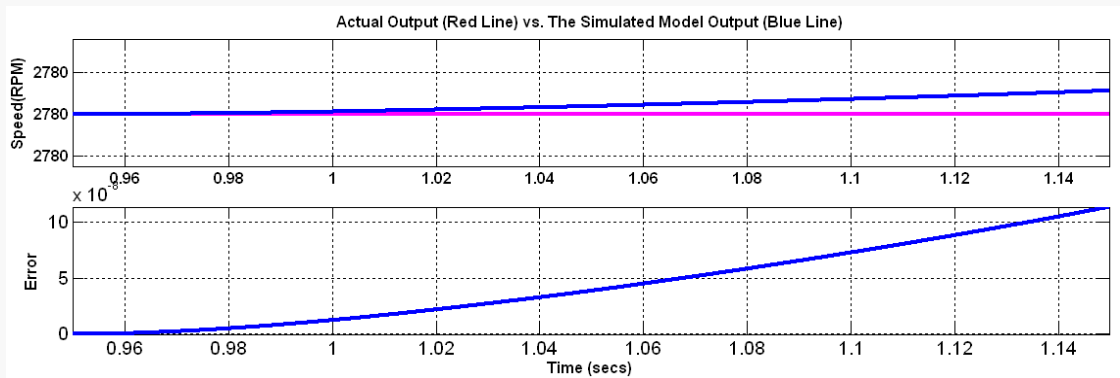


Figure 3.17. Booster actual, simulated reference speed with the speed error

The initial testing of the BMRAS speed estimator was in the simulation with the variable reference speed. Figure 3.18 and Figure 3.19 show the accurate responses of the BMRAS system with variable and constant reference speed respectively.

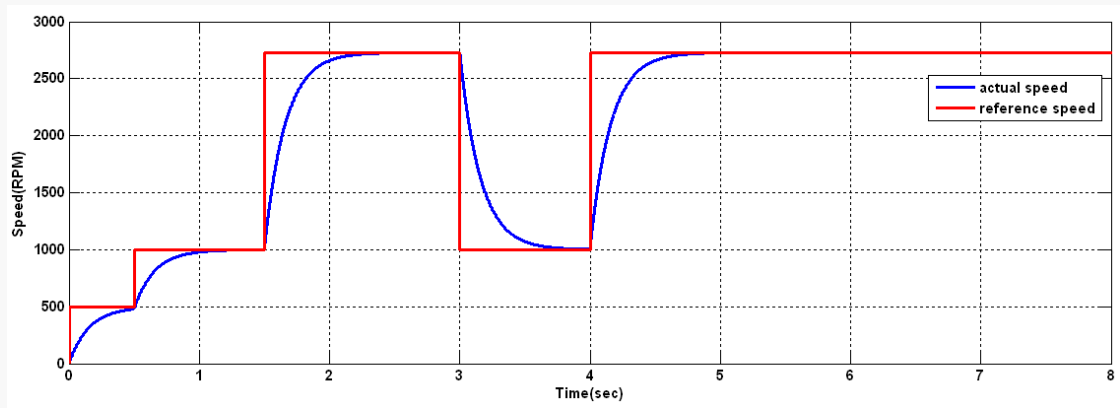


Figure 3.18. Simulated speed response of the proposed BMRAS based IM drive for step change in the reference speed

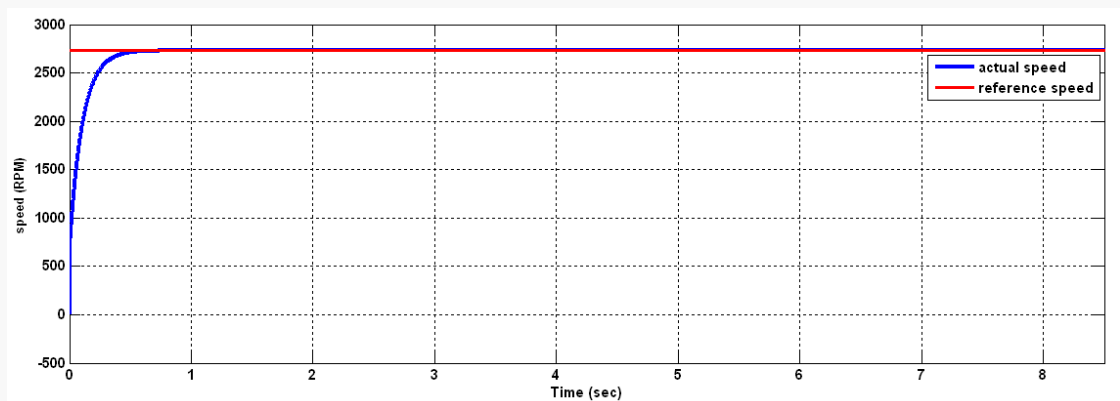


Figure 3.19. Simulated speed response of the proposed BMRAS based IM drive constant reference speed

Experimental test on the BMRAS was performed, which yielded results showing an error between the estimated speed and reference speeds less than 0.0187. Figure 3.20 and Figure 3.21 shows this.

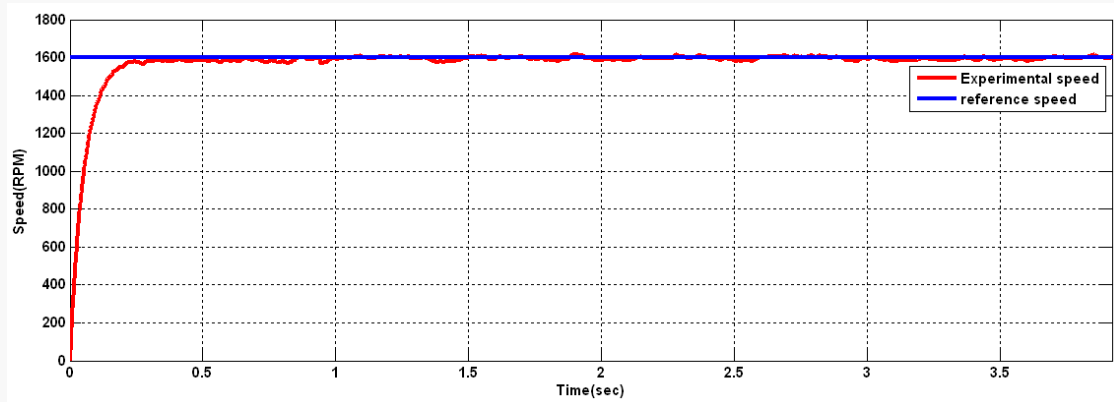


Figure 3.20. Experimental BMRAS based estimated speed and reference speed

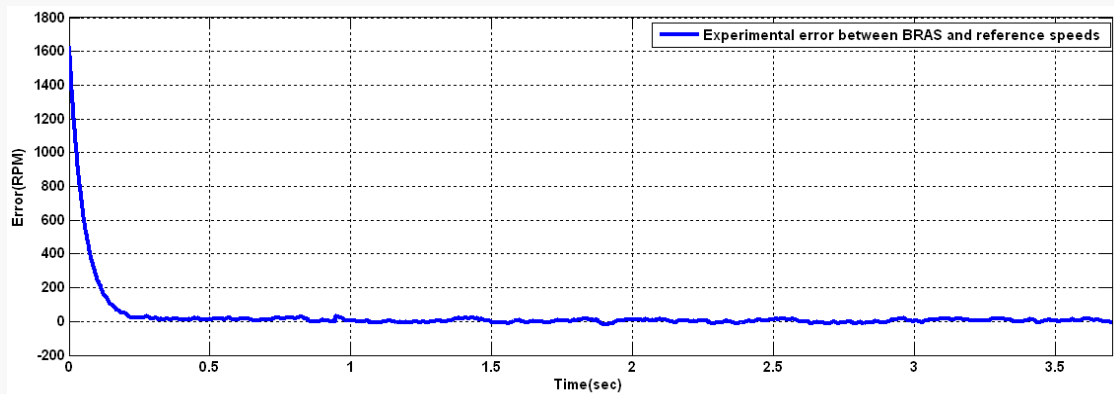


Figure 3.21. Experimental error between the BMRAS based estimated and reference speeds

The applied PI controller structure and parameter tuning will determine the performance of the IM control via the indirect vector control method (Matic, 2010). The PI controller is primarily used to process the error value as a difference between the reference value and the actual value. The error is reduced by adjusting the process control inputs to maintain the parameter values at the satisfactory levels. The integral and derivative values, denoted by K_p , K_i , K_d gains of the system, are included. The $u(t)$ denotes the control input and $e(t)$ denotes the error signal (Banerjee, 2010).

$$\hat{V} \approx j\omega\hat{\Lambda} \quad (3.38)$$

Where \hat{V} and $\hat{\Lambda}$ are the phasors of stator voltage and stator flux respectively

$$|\hat{V}| \approx |j\omega\hat{\Lambda}| \quad (3.39)$$

$$V \approx 2\pi f\Lambda \quad (3.40)$$

$$\Lambda = \frac{1}{2\pi f}V \text{ or } \Lambda = \frac{1}{2\pi} \frac{V}{f} \quad (3.41)$$

The stator flux remains constant if the ratio V/F remains constant despite the change in the frequency. As evidenced from Figure 3.24, the IM torque is not dependent upon the supply frequency (Figoli, 1998).

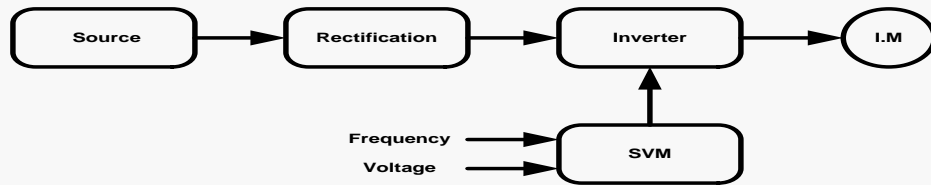


Figure 3.24. Voltage /frequency (v/f) control principle

For IM control systems, the V/F control algorithm is an independent parameter that can be implemented without any problems. Hence, it is employed on a large scale in general purpose inverters (Wei Chen, 2009).

Variable frequency supply can be generated for doing this. The two sinusoidal voltages, V_d and V_q are each 90 degrees out of phase. Figure 3.25 demonstrates the Simulink implementation of the V/F controller circuit.

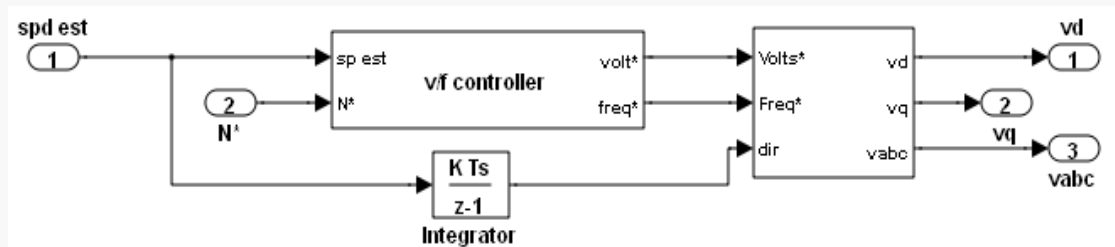


Figure 3.25. Simulink implementation of V/F controller circuit

$$\omega_r = \frac{R_r}{L_r} \quad (3.44)$$

The critical slip therefore is:

$$S_{critical} = \frac{1}{\tau \omega} \quad (3.45)$$

Generally, the torque is proportional to the speed and the IM operates efficiently below this slip for obtaining adequate outcomes. Figure 3.27 shows the relationship between stator voltage and frequency that is made use of in V/F control (Anderzej M., 2001).

The following formula is used for controlling the stator voltage in V/F:

$$V_s = (V_{srated} - V_{0freq}) \frac{f}{f_{supply}} + V_{0freq} \text{ For frequency } f < f_{supply} \quad (3.46)$$

Or

$$V_s = V_{srated} \text{ for } f \geq f_{supply} \quad (3.47)$$

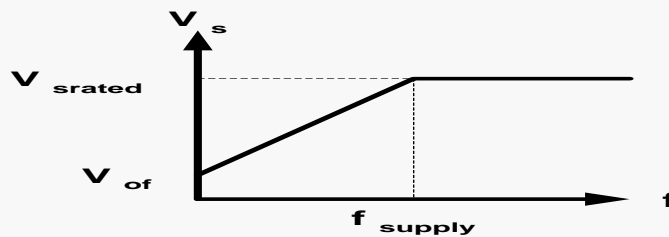


Figure 3.27. Stator voltage vs. frequency in V/F control

Due to slip change with the load of motor, it is not possible to obtain an accurate speed control in V/F. These drawbacks are avoided here as the V/F is not utilized in the beginning of the operation but in the steady state. Furthermore, as the stator or rotor winding faults result in alterations of the parameters of motor equivalent circuit, the used state variable estimators should be robust to motor parameter uncertainties in sensorless drives (Teresa Orłowska Kowalska, 2010). As done in this work, an observer can be used for estimating the speed of the IM or a quadrature encoder can be mounted to the rotor for a direct connection with the TMS320F28335 DSP for obtaining velocity

feedback from the rotor. By comparing the actual (estimated) speed with the reference speed, the speed error is calculated by the closed loop control. Figure 3.28 shows the Simulink implementation of V/F in detail.

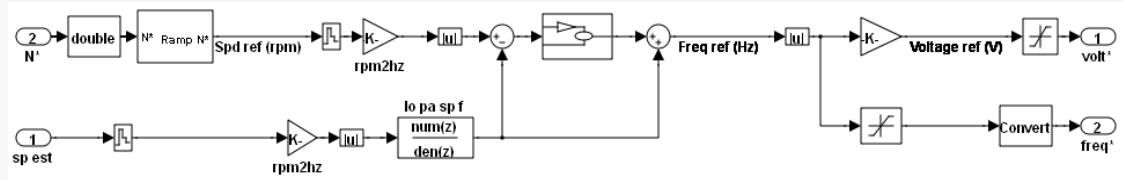


Figure 3.28. Simulink implementation of V/F control in details

A boost model reference adaptive system estimator is utilized for estimating the speed and compensating the voltage drop of the stator leakage impedance to realize an advanced V/F control. The speed performance is enhanced at the same time as well.

3.3.4 Open Loop V/ F Control

When accuracy in speed response is not of a grave concern like in fan or blower applications and in HVAC, open loop speed control is then preferred for use. In this situation, the desired speed is used for determining the supply frequency together with the assumption that the synchronous speed will be adhered to by the motor. It is acceptable for an error to occur in speed from the slip of the motor. By regulating the slip speed, a closed-loop speed control can be implemented with the constant Volt/Hz principle when accuracy in speed response is of significance. In this case, for keeping the speed of the motor at its set value, a PI controller is employed for regulating the motor's slip speed. V/F controlled drives are very strong due to the restriction to low dynamic performance and the absence of closed loop control (J. Amarnath, 2009). Figure 3.29 illustrates this

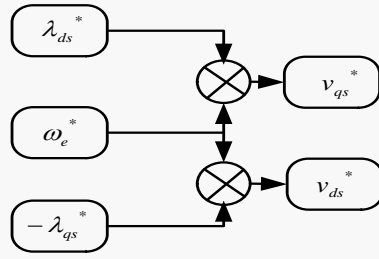


Figure 3.29. Open loop V/F voltage generation

The responsibility for acceleration and deceleration of the speed response can be attributed to the ramping generation block shown in Figure 3.28. The number of poles determines the conversion of the RPM to Hz by the speed to frequency block. The ratio is $(2 \times 1/120)$ in this work.

All the noise is suppressed by the low pass speed filters block. The following presents the transfer function of this filter:

$$TF = \frac{[1 - \exp(-2\pi * 75 * 5 * 10^{-6})]}{[1 - \exp(-2\pi * 75 * 5 * 10^{-6})]} \quad (3.48)$$

Where the sampling time of the filter is denoted by 5×10^{-6} sec and 75 Hz is the cut off frequency of the filter. The ratio of volt/frequency stands at 3.9 according to the degradation of the output voltage to 195V and the reference flux is 0.62 Wb.

The transfer function parameters in eq. (3.48) are of 0.5 hp IM.

When the air gap flux decreases, the voltage drops across the stator leakage impedance, resulting in the deterioration of the IM performance at low frequencies (Tsuji, 2008). Limited starting torque and low accuracy due to load variation is another problem with V/F in variable adjustable speed.

To keep the speed of the motor at its set value and to regulate its slip speed, a PID controller is employed (C.U. Ogbuka, 2009).

The constant Volt/Hz principle can be used as a basis for implementing both open and closed loop control of the speed of an AC. For performing suite speed maintenance, closed loop V/F can be utilized more efficiently in contrast to the open loop V/F. Large

transient behavior in the motor current and torque characterizes the performance of the open loop V/F (Sepe, 2001).

Figure 3.30 illustrates the complete Simulink based block diagram for the FTC based IM drive.

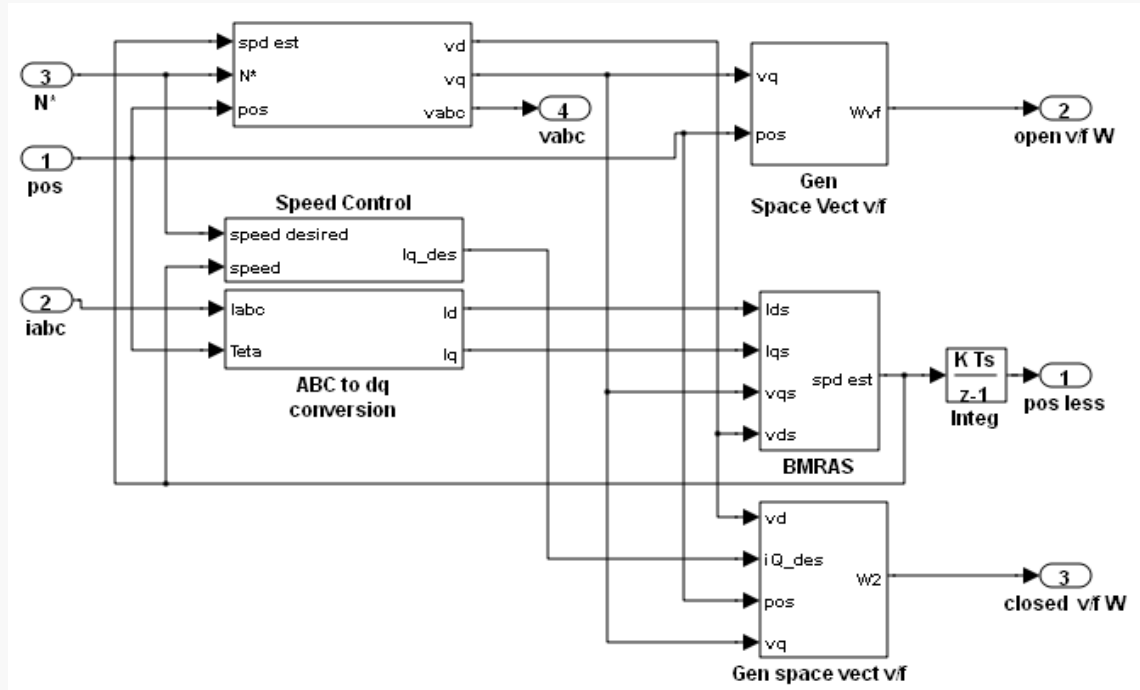


Figure 3.30. Simulink implementation of the open and closed loop V/F control

Table 3.1. PI gains for the different control techniques in simulation and experiment

Control technique	Simulation		Experiment	
	k_p	k_i	k_p	k_i
Sensor V.C.	32	1	0.001	0.11
Sensorless V.C	0.1	0.002	19	2.99
Closed loop V/F	1	0.0005	1	0.0005

In table 3.1, the k_p and k_i values are for 1 kW IM PI controllers in the various control techniques.

This work has expanded on the control techniques implemented in (Zelechowski, 2005) with more blocks. Figure 3.31 illustrates expanded control techniques of IM.

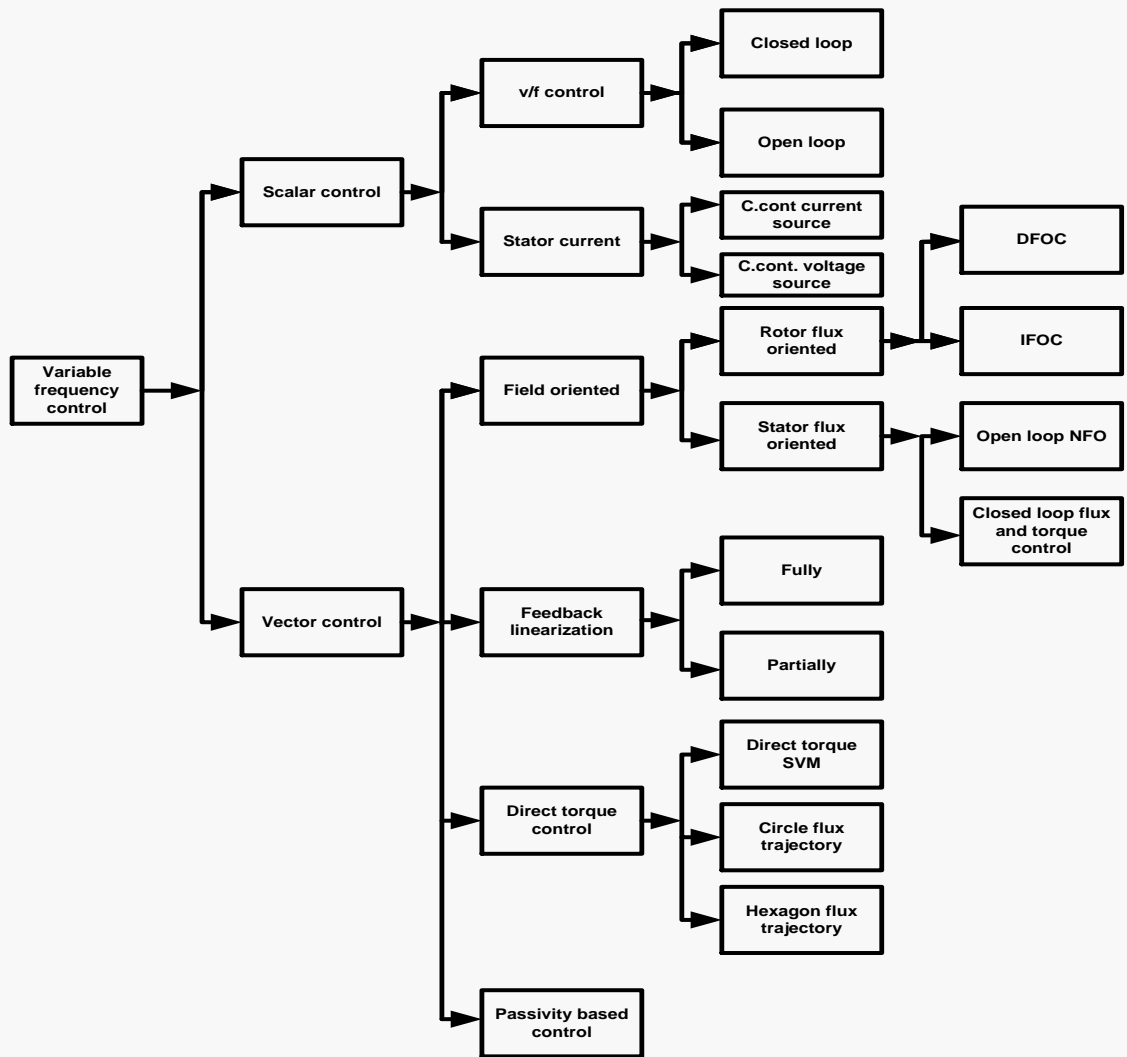


Figure 3.31.Types of control techniques for IM

Figure3.32 shows the complete circuit of all the control techniques employed in this thesis

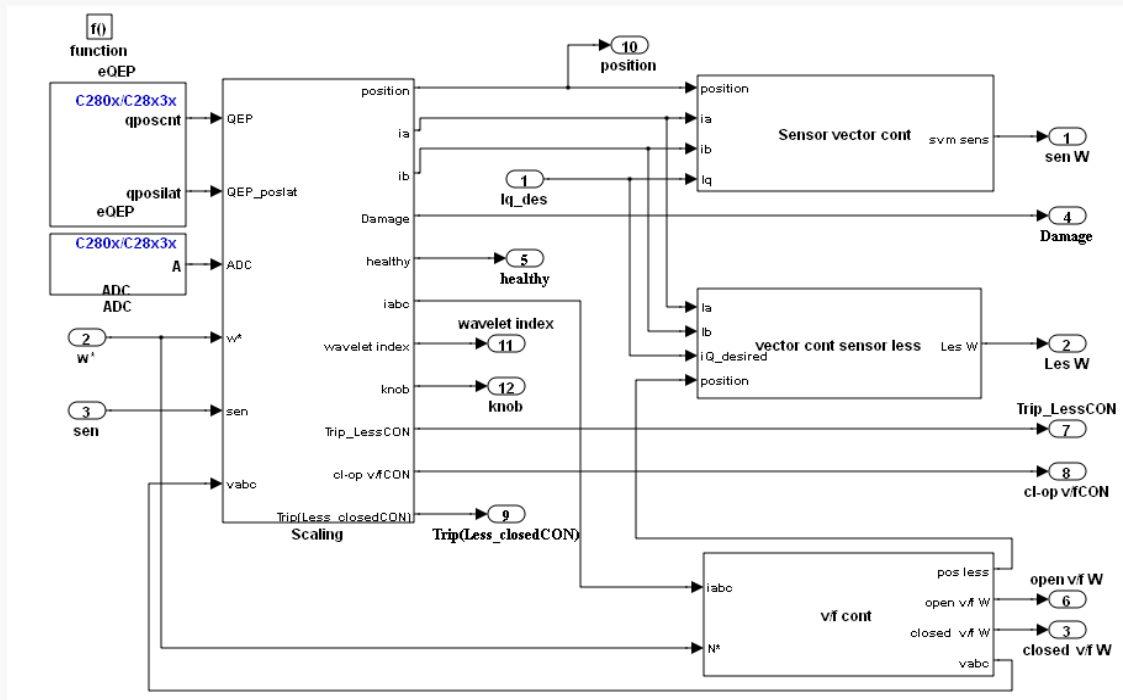


Figure 3.32. Simulink based implementation for the proposed FTC based IM drive.

Chapter 4: Wavelet Techniques for IM fault Detection

4.1 Introduction

Wavelets are mathematical functions that cut up data into different frequency components, and then study each component with a resolution matched to its scale.

This technology was introduced in 1807 and was explored and improved by a number of scientists and has fascinated them till today. It attracted scientists from different disciplines especially mathematicians were more interested in this technique due to its accuracy and practicality. The credit of introducing this technique goes to Joseph Fourier (1807) who presented his theories of frequency analysis. The work was further investigated in 1930 and the functional energy was obtained from the computation of conserve energy, it was carried out on scale varying basis functions. During two decades (1960-1980), the work was further accelerated by Guido Weiss and Ronald R. Coifman who worked on ‘atom’ and showed remarkable research in the reconstruction of functional elements. However, the quantum physics definition of wavelet was given by Grossman and Morlet. Within the short time period of five years, in 1985, Stephane Mallat, introduced digital signal processing which proved a milestone in the development of wavelet. Y. Meyer made a progression in the same direction and presented first most significant, continuously differentiable wavelets. Hence, the modern day wavelet application owes Ingrid Daubechies’s effort in the field who constructed a set of orthogonal basis functions which paved the way to the current applications (Nirmesh Yadav, 2007).

This chapter will discuss advantages/disadvantages of wavelet, construction of the wavelet, scaling factor, levels of decomposition, wavelet index in the fault detection, Simulink implementation of the wavelet and prognostics using wavelet.

4.2 Wavelets Definition

A wavelet is a wave like oscillation which is purposefully generated to have specific properties that make them useful for signal processing. It is a ripple created for a short time period. This chapter will discuss in detail how this technique is different and far better than other signal processing techniques (Khan A. , 2010). The wavelets are categorized into orthogonal and non orthogonal. These are some of the properties of the wavelet:

1. The Fourier transform can go to zero (see the equation 4.1), when provided with appropriate admissible condition.

$$|\psi(\omega)|^2 = 0 \quad (4.1)$$

2. The following equation will show the admissibility condition:

$$\int \frac{|\psi(\omega)|^2}{|\omega|} d\omega < +\infty \quad (4.2)$$

3. The concentration and the smoothness of the wavelet function are regularized in both time and frequency parameter in order to keep the squared relationship between the time bandwidth products of the wavelet transforms and the input signal intact.
4. Finite energy: Finite energy helps to reconstruct a signal without computing all values of its decomposition when a wavelet confirms an admissibility condition.

$$\psi_{m,n}(t) = 2^{-1/2} \psi(2^{-m}t - n) \quad (4.3)$$

m & n are the wavelet dilation and translation used to transform the original new one with smaller scales according to the high frequency components, $\psi(t)$ is a symbol that is used to investigate the signals and later on it reconstructs them without losing any information.

Figure 4.1 shows the tree decomposition of the stator current with 6 levels as a first checking of the wavelet index which did not satisfy the desired accuracy level.

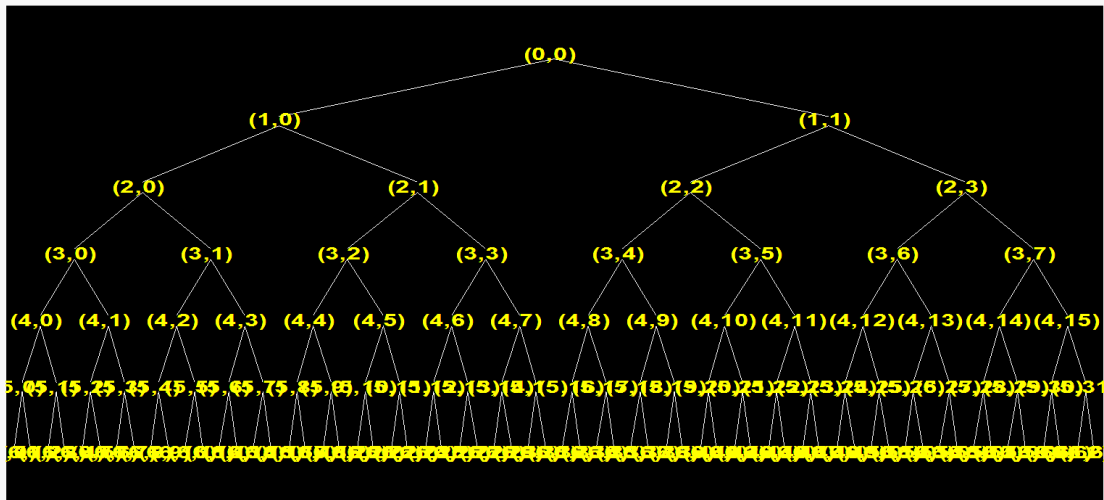


Figure 4.1. Tree of wavelet decomposition with 6 levels (63 nodes)

Figure 4.2 shows the illustration of the energy representation of the signal after 11 levels of decomposition

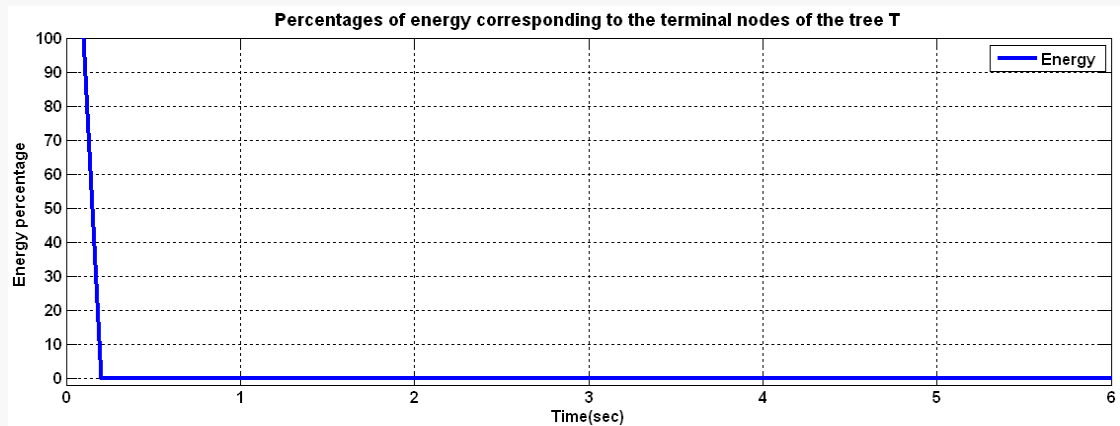


Figure 4.2. Percentage of the energy corresponding to the terminal nodes of the tree

Duplicated information cannot be stored in both frequency and time domains as per the definition of finite energy property. Equation 4.4 better expresses the wavelet energy:

$$E = \int_{-\infty}^{\infty} |\psi(t)|^2 dt < \infty \tag{4.4}$$

The Equation 4.5 expresses the energy of the details of any signal at level j . These are called the wavelet coefficients (M. Sabarimalai Manikandan, 2007):

$$E_j = \sum d_{j,k}^2 \quad (4.5)$$

where

$$d_{j,k} = \langle f(t), \psi_{j,k} \rangle = \frac{1}{\sqrt{2^j}} \int f(t) \psi(2^j t - k) dt \quad (4.6)$$

5. Decay quickly in time: when the wavelet's intervals $k+1$ moment equal to zero as in the following Equation:

$$M = \int_R t^j \psi(t) dt = 0, \text{ at } j = 0, 1, \dots, k \quad (4.7)$$

The zero wavelet coefficients are obtained through this equation which subsequently makes the possibility of getting signals suppression polynomials are $\leq k$.

6. The Equation (4.8) (Jian, 2009) indicates that the wavelet is an oscillating and a fragile function and its integrals equal to zero:

$$\int \psi(\omega) = 0 \quad (4.8)$$

The analysis in transient region relies upon this property; similarly it is quite significant for non stationary signals. The scaling function and the wavelet function comprise the orthogonal wavelet. The scaling function is signified by the symbol $\phi(t)$, it is basically used to produce the basis function when the original signal is being analysed or synthesized, and it also describes the LPF for the wavelet transform. Whereas, BPF is defined by the wavelet function for the transform. The Equation 4.9 expresses the scaling function:

$$\phi_{j,k}(t) = 2^{-j/2} \phi(2^{-j} t - k) \quad (4.9)$$

j = resolution levels number, and k = dimension at level j

The HPF determines the wavelet function and deals with the details of the wavelet decomposition as shown in Figure 4.3, whereas LPF determines the scaling function and deals with the approximations of the wavelet decomposition.

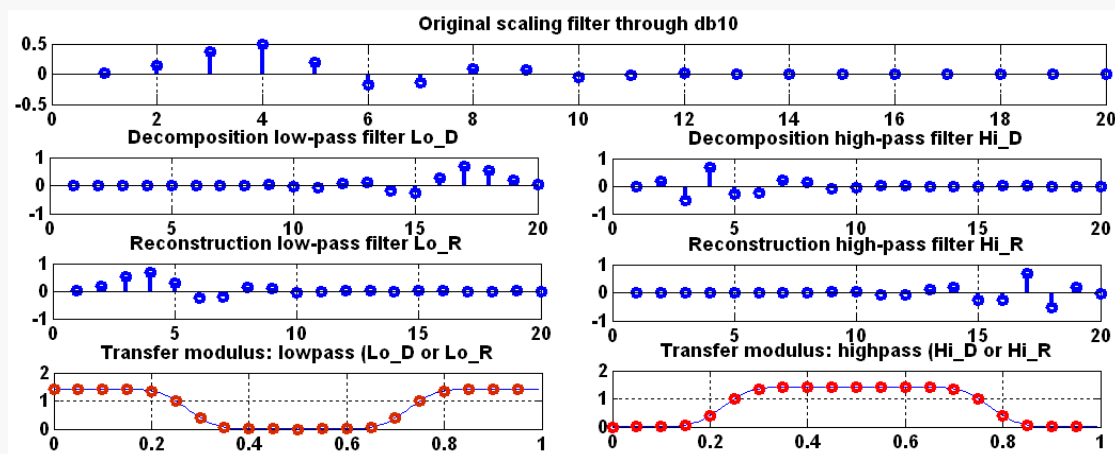


Figure 4.3.db10 wavelet decomposing into HP and LPF with transfer modulus

The following equation shows the discrete wavelet transform

$$DWT(m,k) = \frac{1}{\sqrt{a_0^m}} \sum f(n) g\left(\frac{k - nb_0 a_0^m}{a_0^m}\right) \quad (4.10)$$

$g(n), f(n)$ is the mother wavelet and input signal respectively. The scaling and translation parameters “ a & b ” are functions of the integer parameter m (M. Sushama, 2009). Daubechies wavelet (db10) in this thesis has been used as a base of wavelet index construction as well as a unit to analyze the stator current. Figure 4.4 shows its function

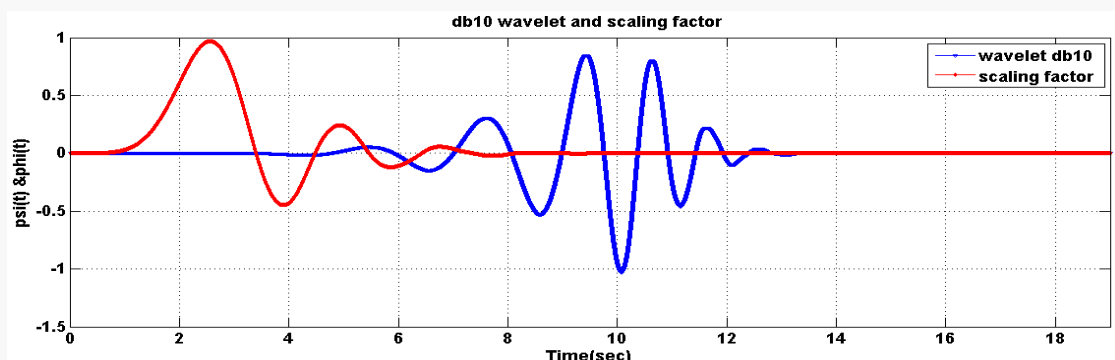


Figure 4.4.Mother Wavelet function (db10) and scaling factor (red)

The Fourier Transform has lost its significance over the years due to its very basic drawbacks both in the usage of a single window function for all frequency components and the procurement of linear resolution in the whole frequency domain. The wavelet technique on the other hand provides a better solution for the above mentioned deficiencies. Its performance has been found excellent in diagnosing fault as it can extract all the information in both time and frequency domain with equal dexterity. This quality has attracted the scientists to use it for fault diagnosis (M. Riera Guaspa, 2009). Three modules namely, feature extraction (wavelet), feature cluster and fault decision comprises the fault diagnosis technique.

Some of the other helpful characteristics of wavelets in terms of fault diagnosis include multi resolution analysis and good time localization.

4.3 Structure of the Wavelet

The structure of a one dimension DWT is based on filter bank for sub band decomposition (Longa, 2006) as can be shown in Figure 4.5.

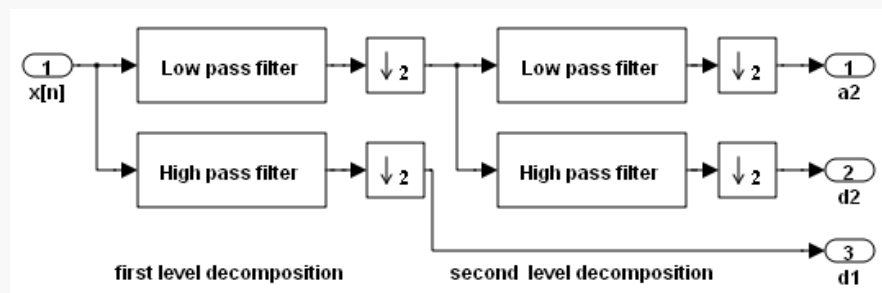


Figure 4.5. Two levels Simulink signal decomposition through sub band filters

Figure 4.5. shows two levels Simulink signal decomposition through sub band filters. The construction of both low and high pass filters depends upon the Finite Impulse Response (FIR), its transfer functions help to achieve the desired results. Figure 4.6 shows the complete functioning of the (db10) wavelet asymmetrical (one dimension).

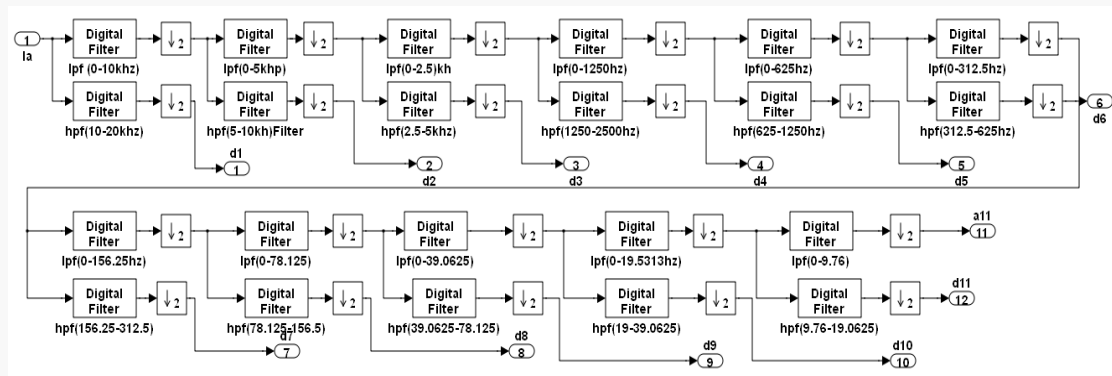


Figure 4.6. Complete 1D-DWT Simulink signal decomposition

The detailed information of the signal is dependent upon the high pass filters while approximate information of the signal relies upon the low pass filters. The sampling frequency is generated by the fusion of the magnitude and phase response with the impulse response at each level of 20 kHz.

The LPF gathers the approximate information at level 1(a_1) through (0-10) kHz FIR.

Figure 4.7 shows the magnitude and phase response of this filter.

The FIR is the best option in this construction as its response is easily adjustable to the zero in finite time and it is helpful for all high pass filters and low pass filters.

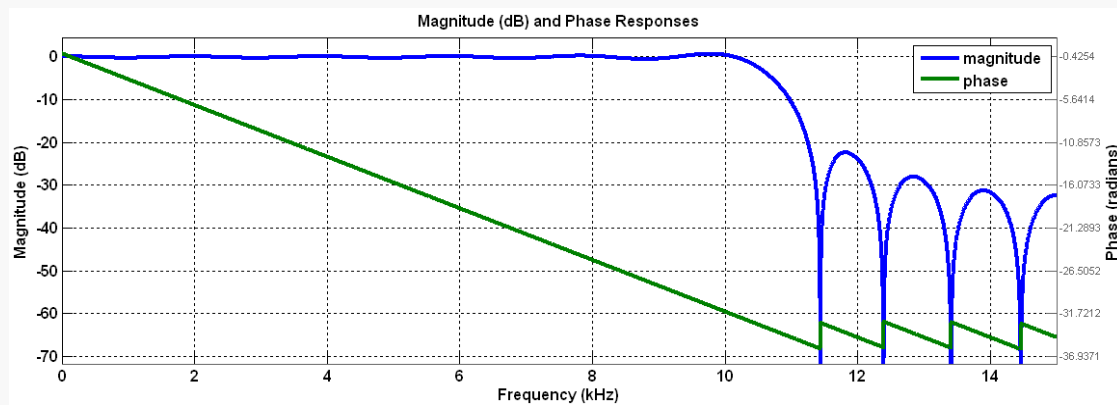


Figure 4.7. Magnitude and phase response of (0-10) kHz low pass filter

FIR high pass filter with frequency range (10-20) kHz helps to generate the detailed information at level 1 (d_1). Figure 4.8 shows the magnitude and phase response of this filter.

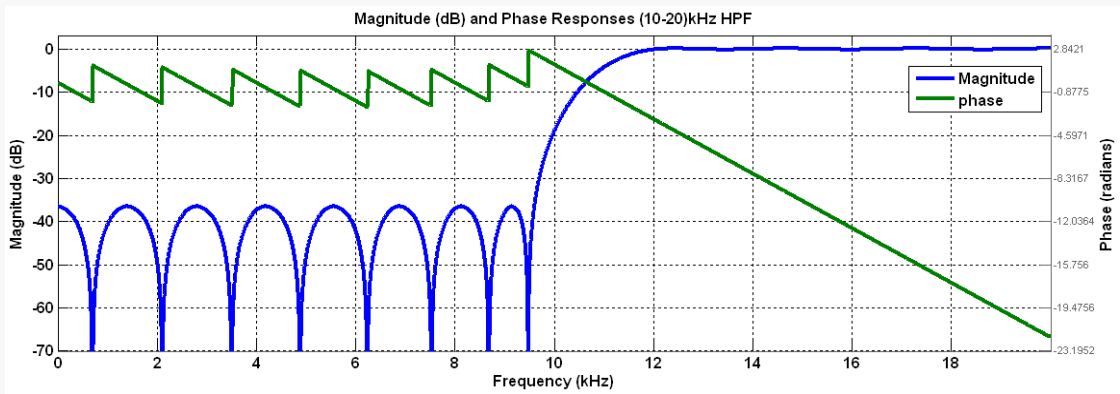


Figure 4.8. Magnitude and phase response of (10-20) kHz high pass filter

(0-5) kHz FIR low pass filter helps to produce the approximated information at level 2

(a₂). Figure 4.9 illustrates the magnitude and phase response of this filter

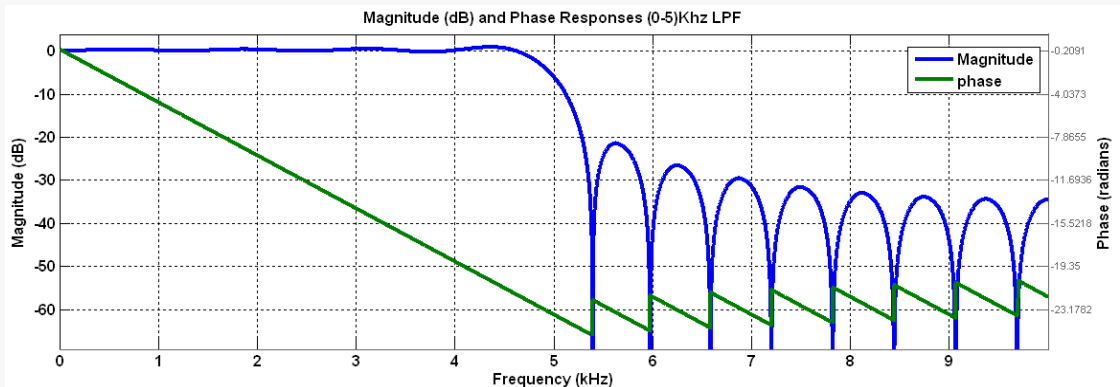


Figure 4.9. Magnitude and phase response of (0-5) kHz low pass filter

(5-10) kHz, FIR high pass filter generates the detailed information at level 2 (d₂). The phase response of this filter and the magnitude has been illustrated through Figure 4.10.

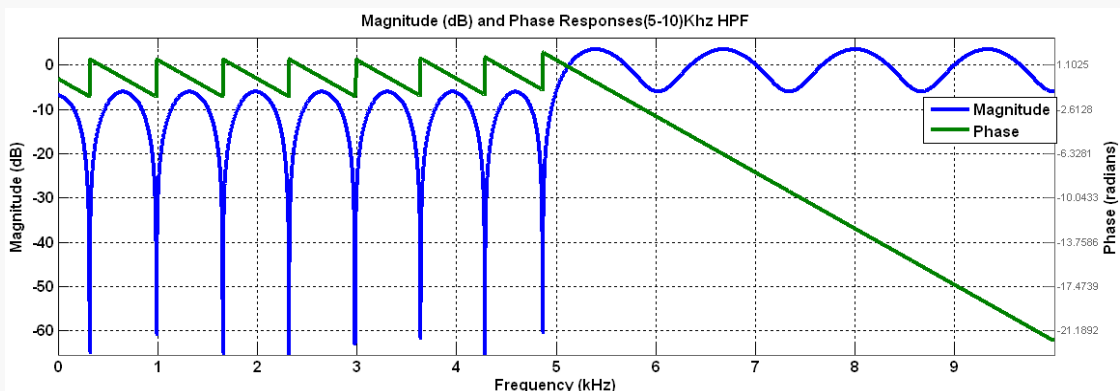


Figure 4.10. Magnitude and phase response of (5-10) kHz high pass filter

(0-2.5) kHz FIR low pass filter yields the approximated information at level 3 (a_3). The phase response of this filter and the magnitude has been illustrated in Figure 4.11

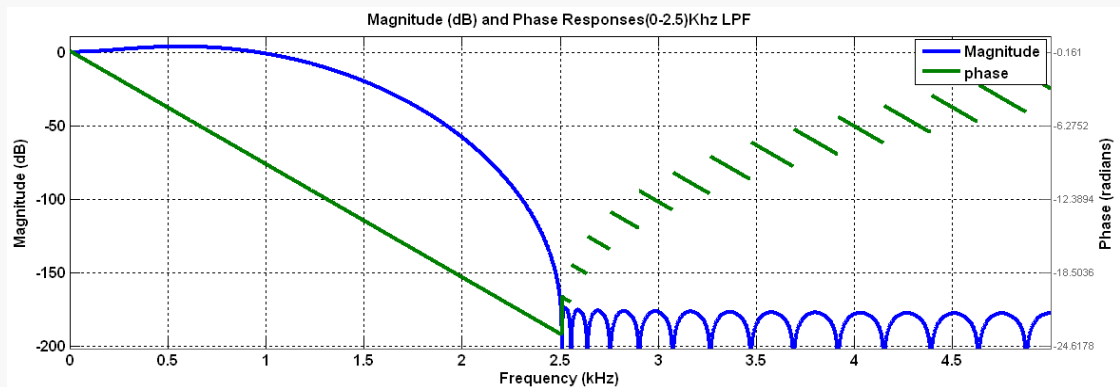


Figure4.11. Magnitude and phase response of (0-2.5) kHz low pass filter

FIR high pass filter with frequency range (2.5-5) kHz generates the detailed information at level 3 (d_3).The phase response of this filter and the magnitude has been illustrated through Figure 4.12

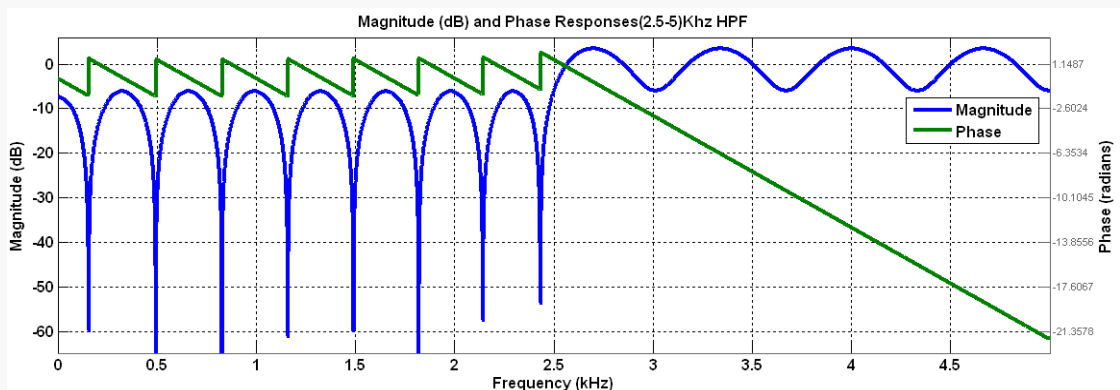


Figure4.12. Magnitude and phase response of (2.5-5) kHz high pass filter

At level 4 (a_4), the approximated information is gathered by FIR finite impulse response with frequency range (0-1.250) kHz, low pass filter. The phase response of this filter and the magnitude has been illustrated through Figure 4.13.

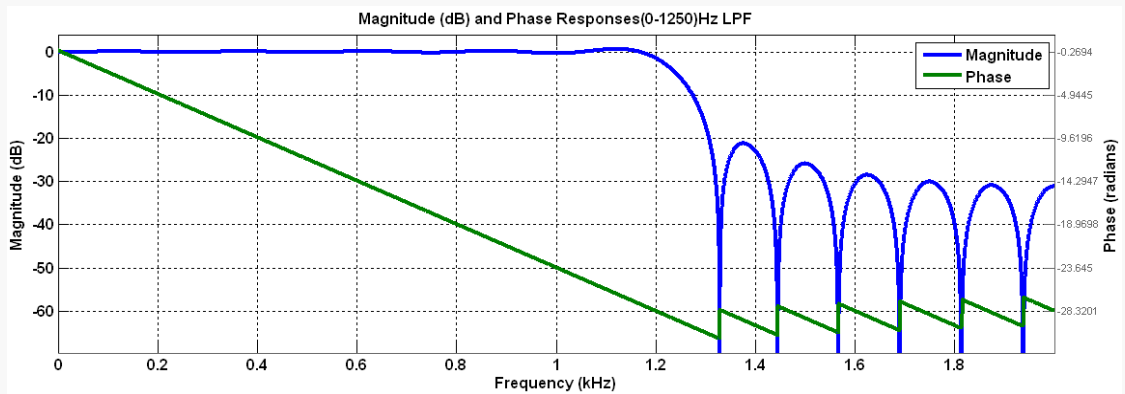


Figure4.13. Magnitude and phase response of (0-1250) Hz low pass filter

FIR HPF with frequency range (1.25-2.5) kHz generates the detailed information at level 4 (d_4). The phase response of this filter and the magnitude has been illustrated through Figure 4.14.

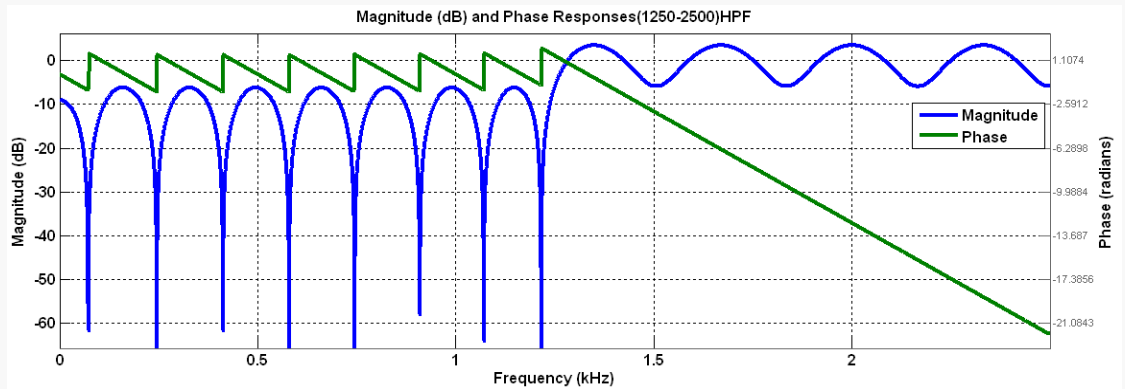


Figure4.14. Magnitude and phase response of 1.25-2.5 kHz high pass filter

FIR LPF with frequency range (0-625) kHz produces the approximated information at level 5 (a_5). The phase response of this filter and the magnitude has been illustrated through Figure 4.15.

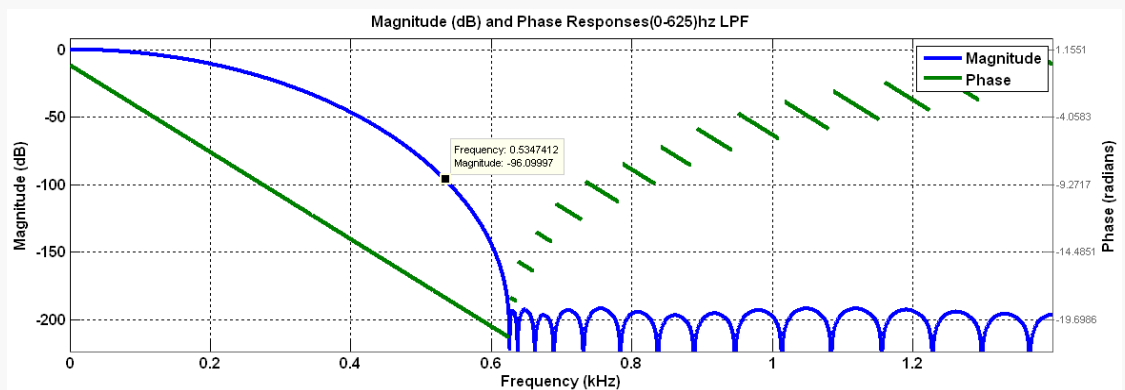


Figure4.15. Magnitude and phase response of (0-625) Hz low pass filter

FIR high pass filter with frequency range (0.625-1.25) kHz yields the detailed information at level 5 (d_5). The phase response of this filter and the magnitude has been illustrated in Figure 4.16.

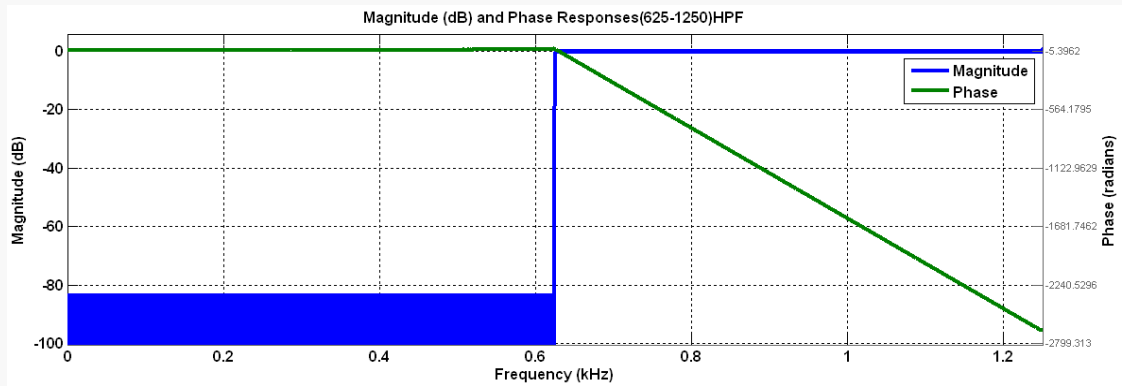


Figure 4.16. Magnitude and phase response of (625-1250) Hz high pass filter

FIR (0-312.5) Hz high low pass filter generates the approximated information at level 6 (a_6). The phase response of this filter and the magnitude has been illustrated in Figure 4.17.

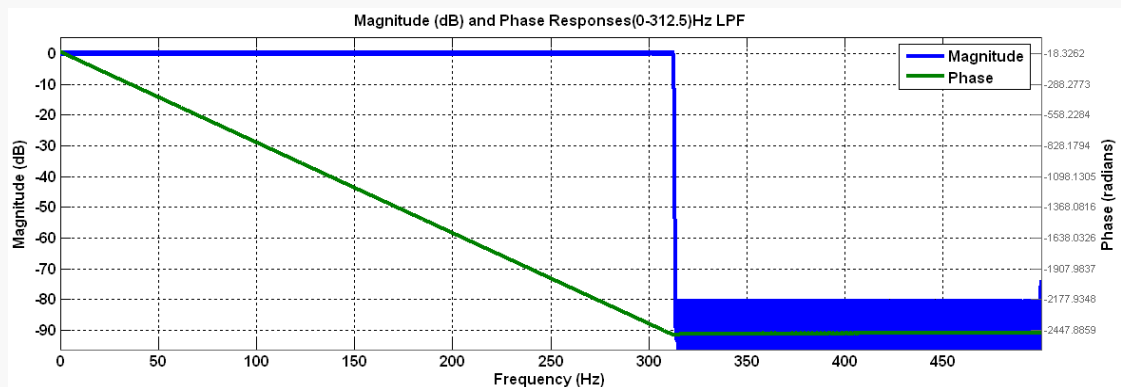


Figure 4.17. Magnitude and phase response of (0-312.5) Hz low pass filter

(312.5-625) Hz FIR high pass filter produces the detailed information at level 6 (d_6). The phase response of this filter and the magnitude has been illustrated through Figure 4.18.

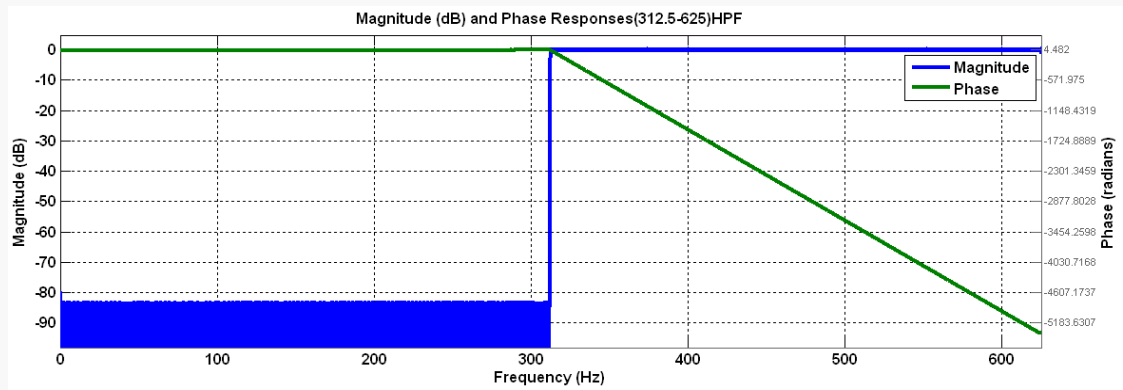


Figure 4.18. Magnitude and phase response of (312.5-625) Hz high pass filter

(0-156.25) Hz FIR low pass filter produces the approximated information at level 7 (a_7). The phase response of this filter and the magnitude has been shown through Figure 4.19.

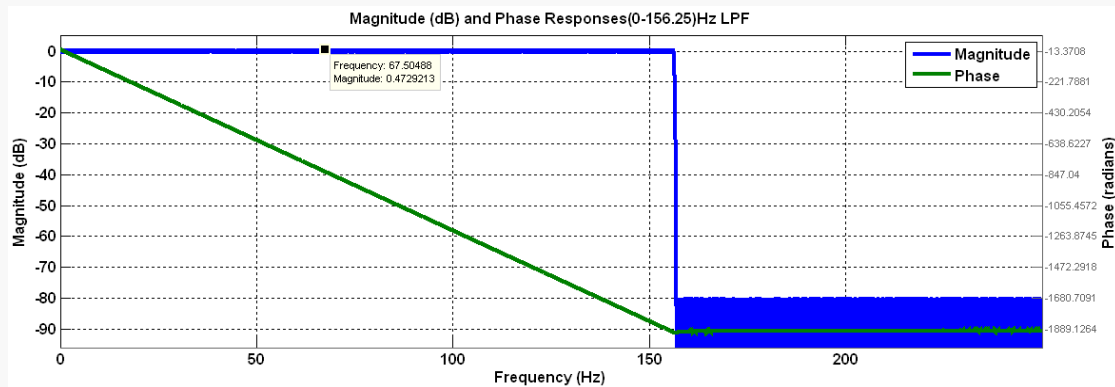


Figure 4.19. Magnitude and phase response of (0-156.25) Hz low pass filter

(156.25 -312.5) Hz FIR high pass filter produces the detailed information at level 7 (d_7). The phase response of this filter and the magnitude has been shown through Figure 4.20.

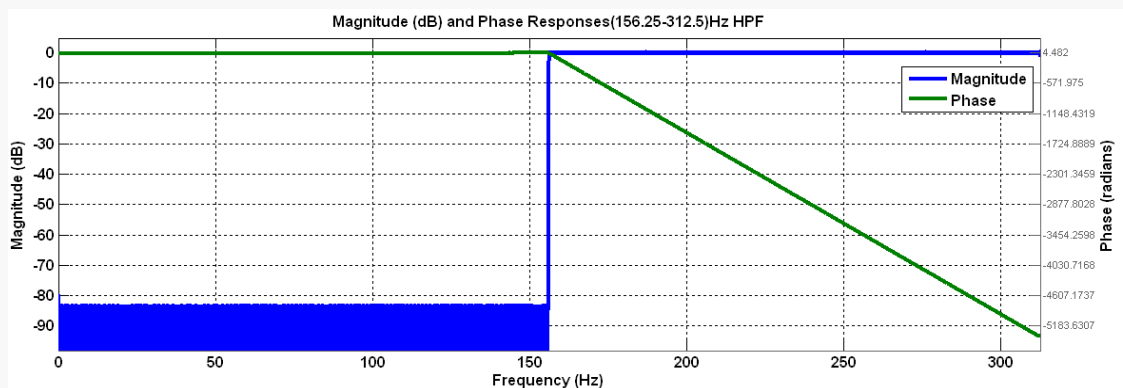


Figure 4.20. Magnitude and phase response of (156.25 -312.5) Hz high pass filter

(0-78.125) Hz FIR low pass filter produces the approximated information at level 8 (a_8). The phase response of this filter and the magnitude has been shown through Figure 4.21.

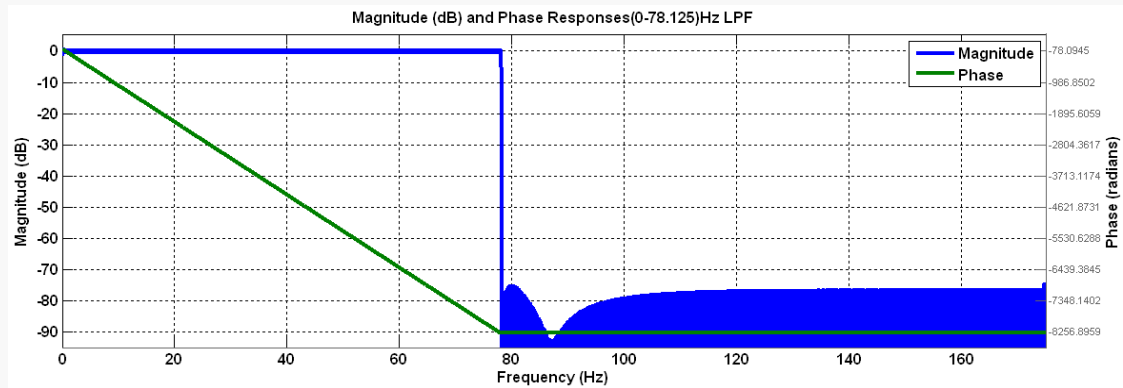


Figure 4.21. Magnitude and phase response of (0-78.125) Hz low pass filter

(78.125-156.5) Hz FIR high pass filter produces the approximated information at level 8 (d_8). The phase response of this filter and the magnitude has been expressed through Figure 4.22.

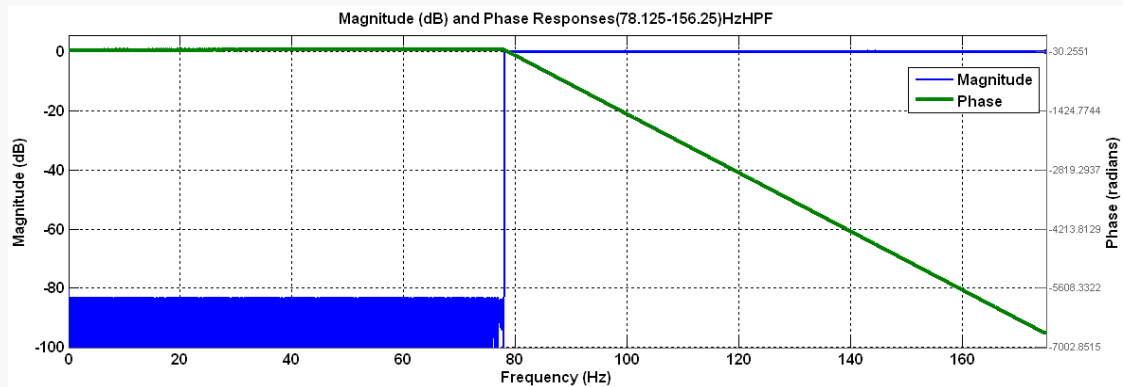


Figure 4.22. Magnitude and phase response of (78.125-156.5) Hz high pass filter

FIR (0-39.0626) Hz low pass filter generates the approximated information at level 9 (a_9). The phase response of this filter and the magnitude has been illustrated in Figure 4.23.

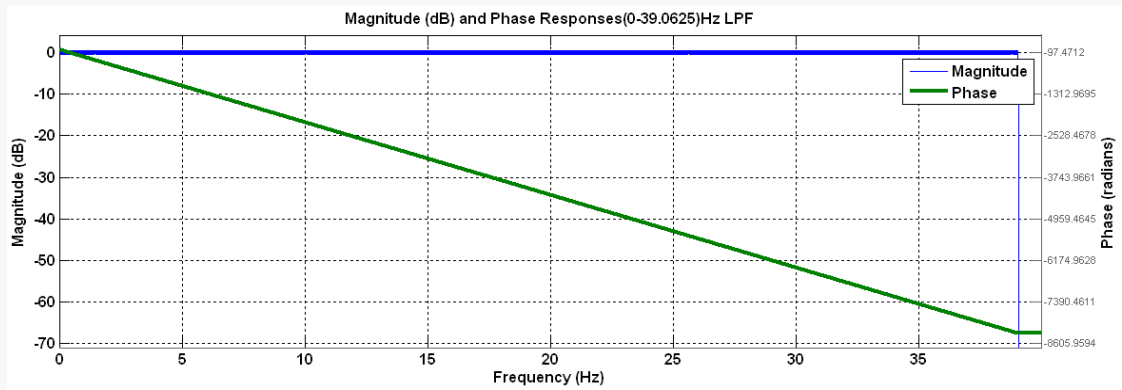


Figure 4.23. Magnitude and phase response of (0-39.0625) Hz low pass filter

FIR (39.0625 -78.125) Hz high pass filter generates the detailed information at level 9 (d₉). The phase response of this filter and the magnitude has been illustrated in Figure 4.24.

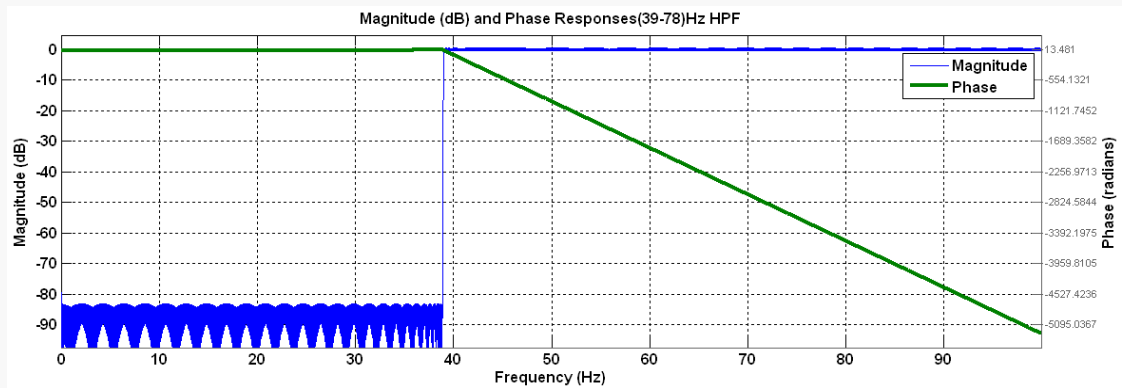


Figure 4.24. Magnitude and phase response of (39.0625 -78.125) Hz high pass filter

(0-19.53) Hz FIR low pass filter produces the approximated information at level 10 (a₁₀). Figure 4.25 illustrates the phase response of the filter and the magnitude.

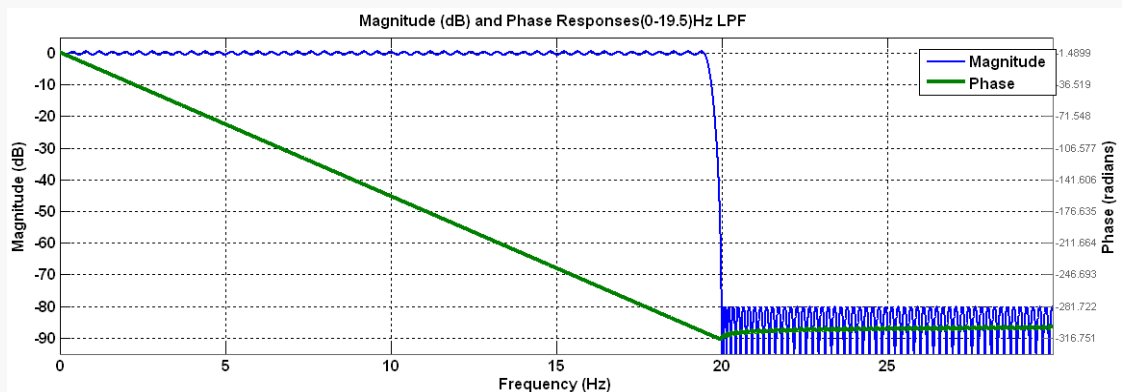


Figure 4.25. Magnitude and phase response of (0-19.5313) Hz low pass filter

The FIR (19.5313 -39.0625) Hz high pass filter produces the detailed information at level 10 (d_{10}). Figure 4.26 shows the magnitude and phase response of this filter.

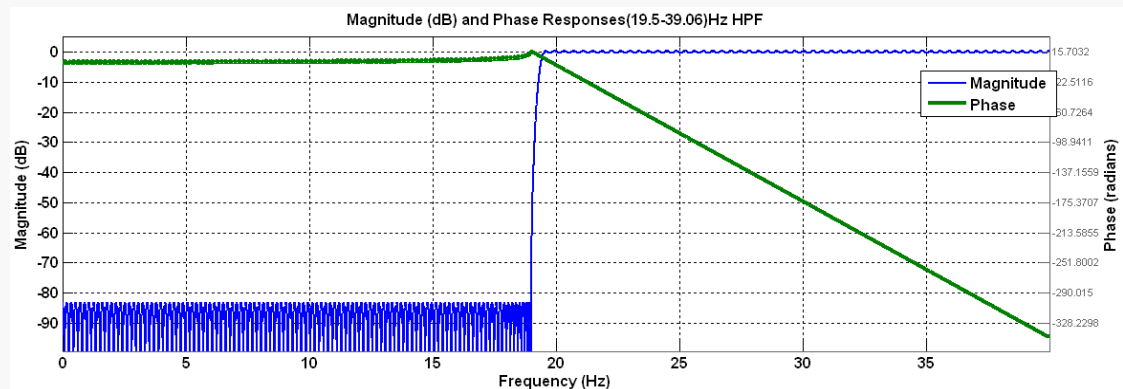


Figure 4.26. Magnitude and phase response of (19.5313 -39.0625) Hz high pass filter (0-9.76) Hz FIR low pass filter generates the approximated information at level 11 (a_{11}). The phase response of the filter and its magnitude can be understood through Figure 4.27.

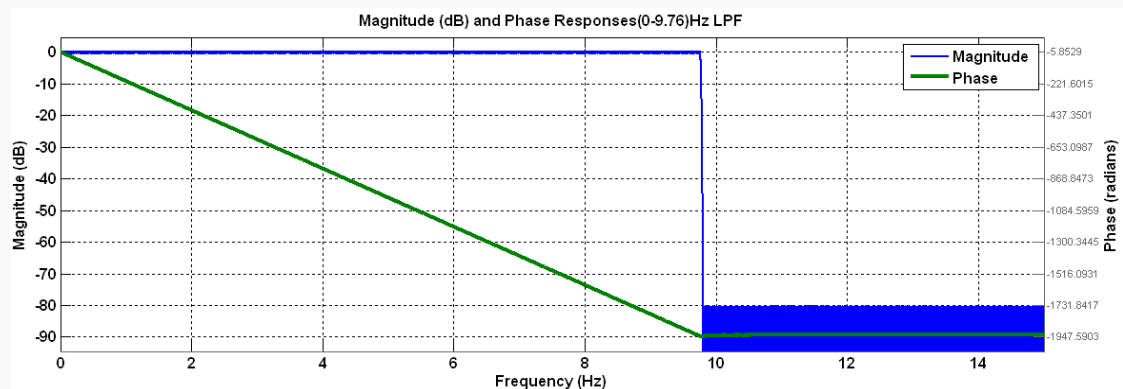


Figure 4.27. Magnitude and phase response of (0-9.76) Hz low pass filter The FIR high pass filter (9.76 -19.5313) Hz produces the detailed information at level 11 (d_{11}). The phase response of the filter and its magnitude are visible in Figure 4.28.

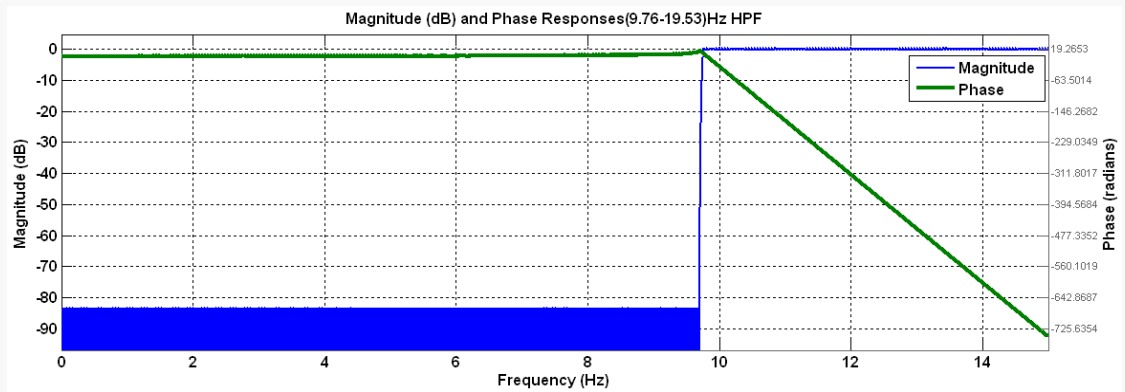


Figure 4.28. Magnitude and phase response of (9.76 -19.53) Hz high pass filter

4.4 Decomposition Levels of the Wavelet

Orthogonal wavelet helps to obtain optimal level; it caters to several decompositions units. The expansion of a signal is possible to expand in various ways. If signal of length L is presented through this equation: $N=2L$. The length of the signal can vary and can reach to the optimum size as it has various ways of expansion. The decomposition value can easily be estimated through an efficient algorithm with respect to a convenient criterion (Mallat S., 1998). The algorithm that has additive cost behavior is a good choice of binary tree structure i.e.

$$E(0) = 0 \quad (4.10)$$

In the signal processing field, the term Entropy is not new. Though it is used in some other fields as well, its significance in this field is imminent. The above mentioned conditions are verified by the Entropy criteria. The relation of Entropy can be expressed through the Equation 4.11 where S = signal, N = the length of signal and E = Entropy:

$$E(s) = -\sum_n^{N-1} S_n^2 \log(S_n^2) \quad (4.11)$$

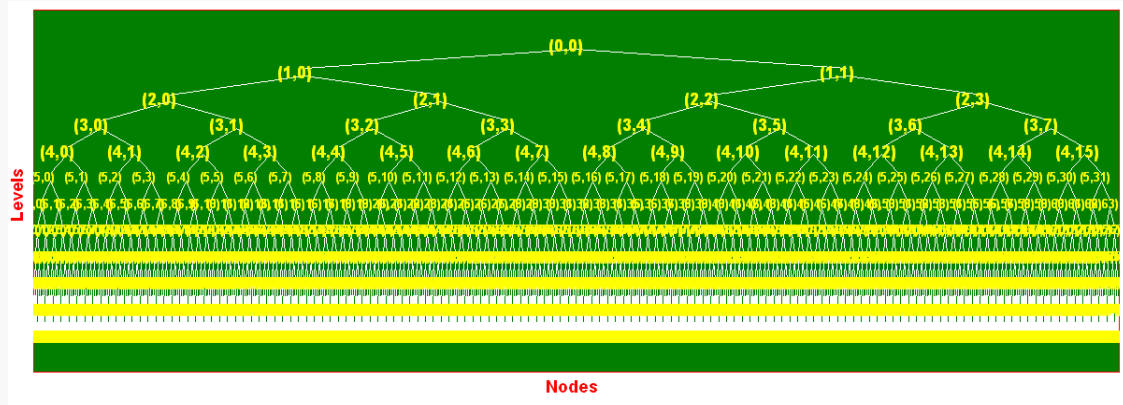


Figure 4.29. Wavelet tree with 11 levels all node response (2047 nodes)

Figure 4.29 and Figure 4.30 express the best tree and levels according to Shannon entropy at level 11 and 8.

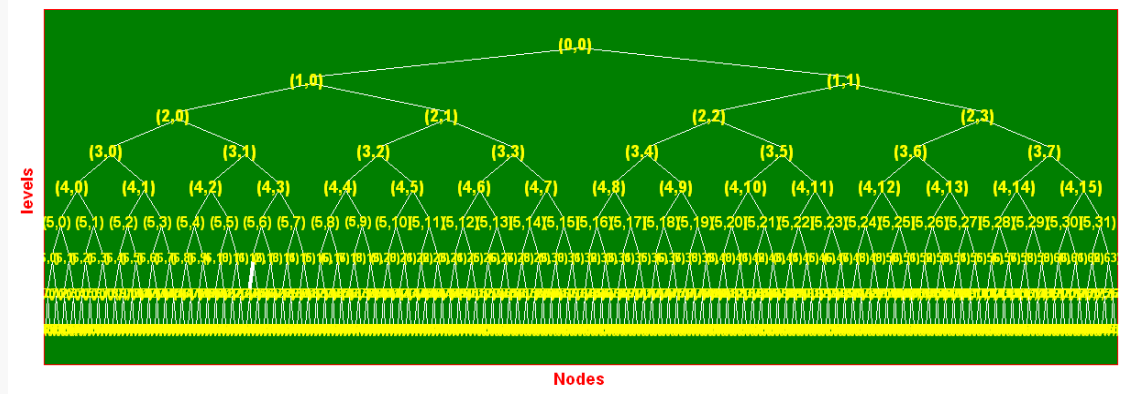


Figure 4.30. Best level wavelet tree with node response (255 nodes)

The optimal levels of decomposition are gauged through the optimum mother wavelet. The Shannon entropy orientates the route in the selection of this optimal level by determining the entropy of each original (parent) subspace of the (DWT) and also views it in comparison to its new (children) subspace (Khan A. , 2010).

The following equation explains the decomposition of the signal. It highlights the fact that if the entropy at level $j-1$ is less than that of the next level j , the level j of the DWT loses its significance. The condition is determined by the above mentioned criterion:

$$E(s)_j \geq E(s)_{j-1} \tag{4.12}$$

The implementation of the decomposition is possible through filtering and down-sampling. It can even be iterated with successive approximation as in (Turkmenoglu, 2010).

The following relationship can help to determine the total decomposition levels (L).

$$L \geq \frac{\log(\frac{f_s}{f})}{\log(2)} + 1 \quad (4.13)$$

If these bands are changed, they can cause complication in the fault detection especially those based on DWT, and create problems in time varying conditions. Thus in order to change these bands it is important to acquire a new acquisition with different sampling frequency (Yasser Gritli, 2011). 11 levels decomposition takes place when Equation 4.13 is implemented at a sampling frequency of 20 kHz. The frequency bands for each wavelet signal have been shown in Table 4.1.

Table 4.1. Frequency bands for the levels of wavelet signals

Approximations «aj»	Frequency bands (Hz)	Details «dj»	Frequency bands (Hz)
a11	[0-9.76]	d11	[9.76-19.52]
a10	[0-19.52]	d10	[19.52-39.04]
a9	[0 - 39.04]	d9	[39.04-78.08]
a8	[0 – 78.08]	d8	[78.08-156.16]
a7	[0- 156.16]	d7	[156.16-312.32]
a6	[0-312.32]	d6	[312.32-624.64]
a5	[0-624.64]	d5	[624.64-1.25e3]
a4	[0-1.25e3]	d4	[1.25e3-2.5e3]
a3	[0-2.5e3]	d3	[2.5e3-5e3]
a2	[0-5e3]	d2	[5e3-10e3]
a1	[0-10e3]	d1	[10e3-20e3]

4.5 Multiresolution Analysis

The multi-resolution analysis (MRA) is used to provide better representation of orthogonal wavelet. It is an algorithm to produce orthogonal wavelet, it also helps to

discrete wavelet transform and filters banks (D.Barnes, 2006). It was introduced by (Mallat S. , 2009) and since then it is being used to reduce the unwanted approximation. It is playing a pivotal role in transferring one dimensional time domain signal into time frequency domains with two dimensions:

$$f(t) = \sum_{-\infty}^{\infty} c_{j_0}(k) \varphi_{j_0,k}(t) + \sum_{j=j_0}^{\infty} \sum_{-\infty}^{\infty} d_j(k) \psi_{j,k}(t) \quad (4.14)$$

First summation gives a coarse approximation of a function $f(t)$ at scale j_0 and the second one for finer resolution at scale j .

where

$$c_{j_0} = \sum_{j_0} f(t) \bar{\phi}_{j_0,k}(t) \quad (4.15)$$

$$d_j = \sum_j f(t) \bar{\psi}_{j,k}(t) \quad (4.16)$$

$\bar{\phi}_{j_0,k}(t)$ & $\bar{\psi}_{j,k}(t)$ are scale function and wavelet conjugates.

The data required in the analysis depends on the sampling frequency and resolution required as in (4.17)

$$D_{required} = f_s / R \quad (4.17)$$

Where

f_s , R are the sampling frequency and resolution respectively.

Figure 4.31 shows the MRA of the above table:

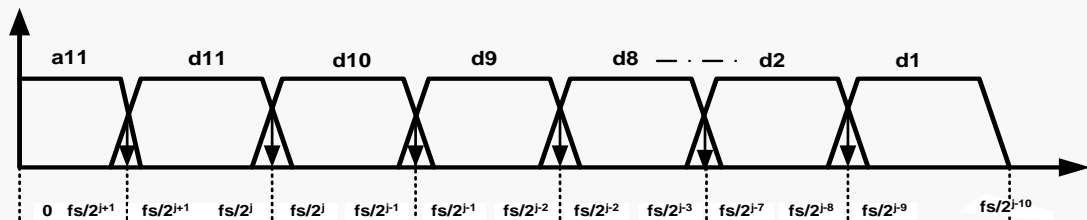


Figure 4.31. Filtering process performed by the DWT

4.6 Wavelet Choosing

The wavelet technology has been found very effective in the fault detection. The usage of this technology helps to prevent machine failures as the fault finding at the early stages prevents heavy losses and give more time and opportunity to fix the problems before embarking upon the real journey. The localized capability, best de-noising and good filtering characteristics are a few features of this technology which helps to detect the fault (Jian Yu Zhang, 2007). An efficient wavelet function is required to be selected for the fault detection as wavelet technology is still at its early stages (R. Rubini, 2001).

The following relationship expresses it quite well:

$$C_{j,k} = \int_{-\infty}^{\infty} f(t)\psi_{j,k}^* dt \quad (4.18)$$

where

$$\psi_{j,k}^* = a_0^{-j/2} \psi(a_0^{-j}t - kb_0) \quad (4.19)$$

The wavelet base function ‘ a_0 & b_0 ’ are scalar and shifting factors respectively.

The function $f(t)$ can be expressed as:

$$f(t) = C \sum_{-\infty}^{\infty} \sum_{-\infty}^{\infty} C_{j,k} \psi_{j,k}(t) \quad (4.20)$$

The quality of wavelet function depends upon better decomposition and reconstruction which eventually saves the loss of energy during the transformation. All these characteristics can be seen in an orthogonal wavelet basic function and a sensible choice to detect and diagnose fault. Basically, every wavelet base function should be based on asymmetry as it helps to minimize the information drift, enhances the filters compression ability, regularity, the compactness characteristic for the real time implementation and keeps a check on zero vanish moment. In this regard the wavelet index is a great help to establish high system reliability and early fault detection. The db 10 has been found to be the best wavelet base as shown in table 4.2.

Table 4.2.The property parameters of wavelet bases (Li Ke, 2007)

Wavelet bases	Regularity	Vanishing moment	Support width (Ws)
db1	discontinuous	1	1
db2	1	2	3
db3	2.75	3	5
db4	5.10	4	7
db5	7.98	5	9
db6	11.33	6	11
db7	15.11	7	13
db8	19.32	8	15
db9	23.95	9	17
db10	29.02	10	19

The selection of ‘db 10’ is the most sensible option as it harmonizes the combination of dbN and SNR. The compactness is reduced by the increasing of dbN ranking which consequently increases SNR and the memory that is required for the high and low pass filters implementation. Thus the MRA of the stator current signal of the proposed fault tolerant control algorithm is effectuated by the wavelet function ‘db 10’. It is equally well suited for both experimental works and the simulation.

4.7 Wavelet Index Construction

The criterion of fault detection of IM fault is one of the most important steps in the whole process. It is implemented right after the construction of DWT. The criterion is directly linked with the relationship between the original stator current (I_a) and maximum detail energy (d_8). Figure 4.32 depicts this relationship.

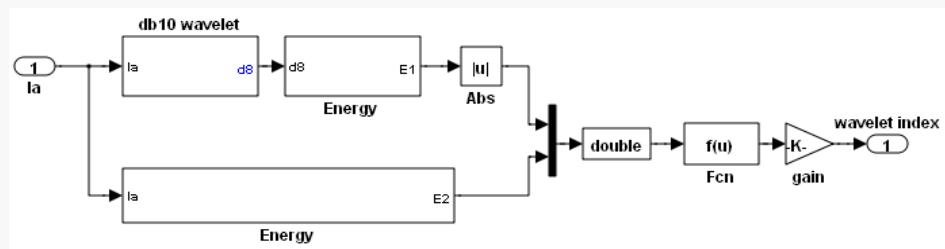


Figure 4.32.Simulink wavelet index (WI) implementation

The energy held by a signal is the most effective tool in detecting the fault of IMs. The addition of the squared coefficients of the details and final approximation which is obtained through wavelet analysis helps to determine the wavelet index for detection of the IM faults. The energy of every detail is computed as wavelet analysis helps to provide both time and frequency information simultaneously (Biju K, 2010). Similarly, this thesis also highlights another important factor, i.e. stator current. It has been used as the input to the DWT. The sudden increases, decreases or transients detected in the magnitude of the current have been termed as ‘the variation’ in the stator current waveform (Mamat Ibrahim, 2004).

The detection of the fault through the wavelet index which is undeniably the best yardstick to check the fault can be shown in this formula:

$$W_{indx} = \frac{abs(energy(d8))}{average(energy(I_a))} \quad (4.21)$$

The energy of both stator current (I_a) and $d8$ coefficient can be calculated according to eq. (4.5).

More details about figure4.32 can be seen in Figure 4.33 to take a decision according to (4.21).

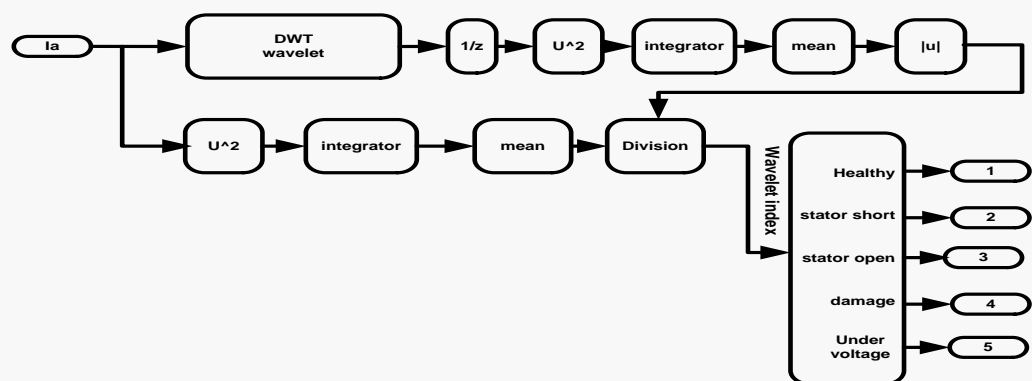


Figure 4.33. Faults detection according to the wavelet index

Thus, the status of a three phase IM can be exposed via wavelet index by using the stator current and the wavelet technology.

Chapter 5: Fault Tolerant Control of IM

5.1 Introduction

The increasing demand of asynchronous AC drive systems has given rise to the need of a reliable and more efficient fault tolerant control system. Thus, fault diagnosis and protection is the need of the time and it is vital in the development of IMs maintenance. It is effective for both small and medium asynchronous AC drive systems in industrial plants (Cristaldi, 2010).

5.2 Definitions

During operation, a system is prone to develop some defects. In order to overcome this stage in a system, FTC has been introduced which is a branch of control theory and it deals with the control of a system.

Figure 5.1 depicts the components of FTC system.

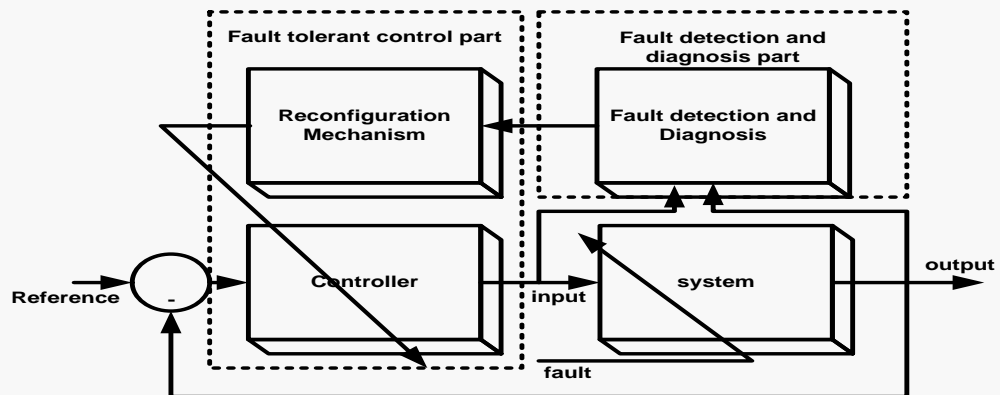


Figure 5.1. Main components of fault tolerant control

The FTC depends upon two methods of analysis:

1. Model free fault detection and isolation (FDI) that does not require any mathematical model of plant dynamics.
2. Model based FDI that needs the quantitative plant model.

The above mentioned methods are further divided into quantitative and qualitative approaches. Figure 5.2 illustrates the fault detection methods. In this thesis, the

approach of data based method-qualitative-frequency and time analysis has been chosen.

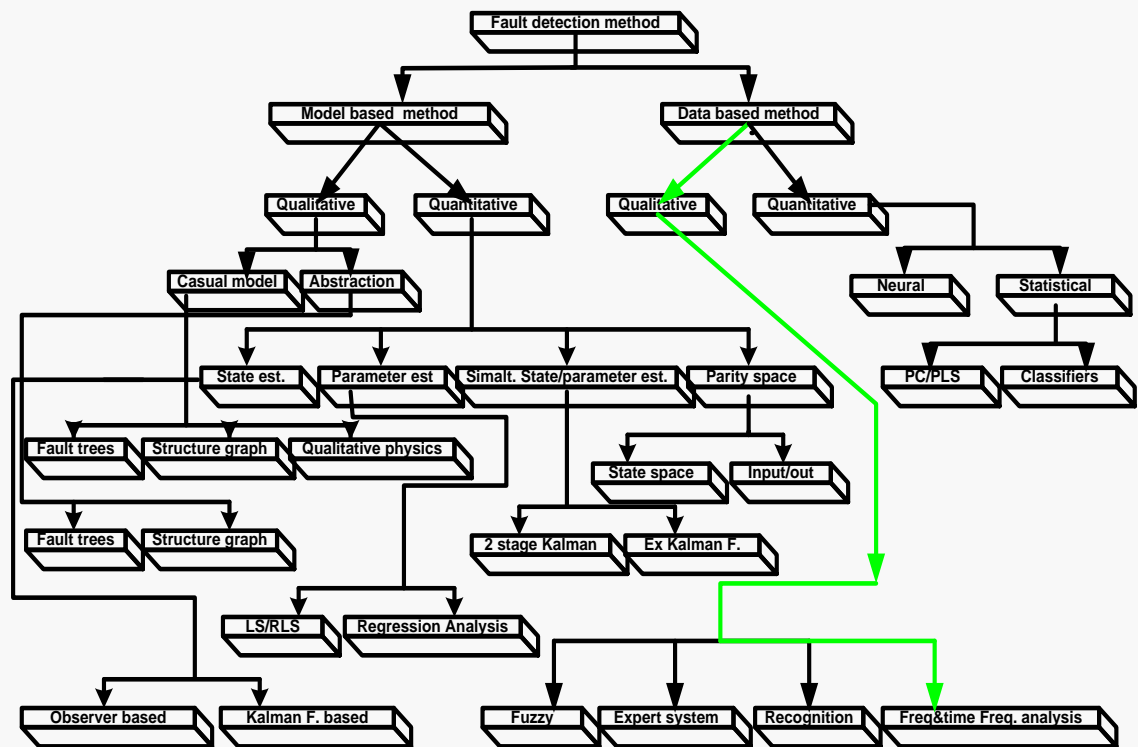


Figure 5.2. Methods of fault detection and isolation part of FTCS

5.3 Features of Fault Tolerant Types

The main features of the above mentioned two categories will be defined as follows.

5.3.1 Passive Fault Tolerant Control

Though passive fault tolerant control is easy to implement, it cannot deal with large number of IM faults. It basically handles the initially defined faults which are the part of the main set up of a controller design. This property owes it the name 'passive' FTC as it tackles with some certain kind of faults. Figure 5.3 indicates the passive FTC.

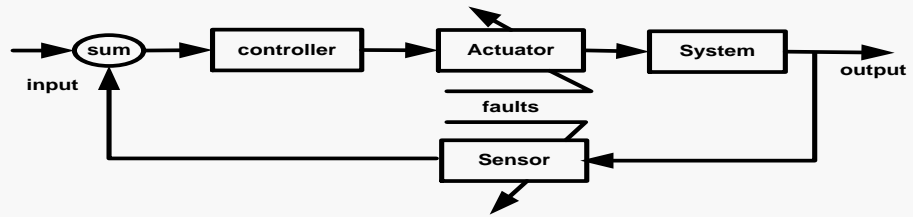


Figure 5.3.Passive FTC

5.3.2 Active Fault Tolerant Control

Unlike passive FTC, it can deal with a large number of IM faults. The ability to handle many unpredictable faults does not prevent it from a major drawback that is it cannot be implemented as easily as the passive FTC and has more complications in implementation. Figure 5.4 indicates the explicit fault detection/diagnosis schemes:

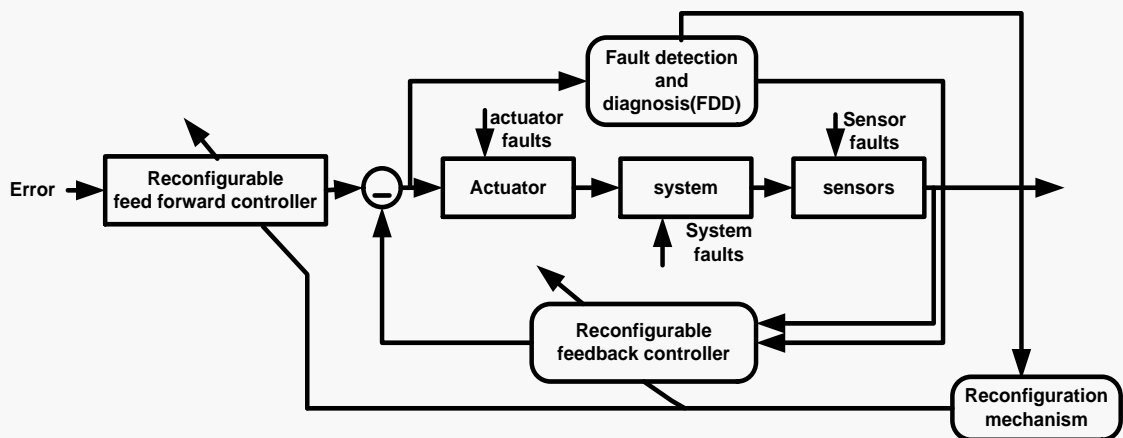


Figure 5.4.Active FTC

The active fault tolerant methods have been categorized into four sections as per the following criteria:

1. Reconfiguration methods
2. The design approach methods
3. The mathematical design tool methods
4. The system being dealt with methods

Figure 5.5 shows the main methods of the active FTC. The reconfiguration method-switching-multiple model has been chosen.

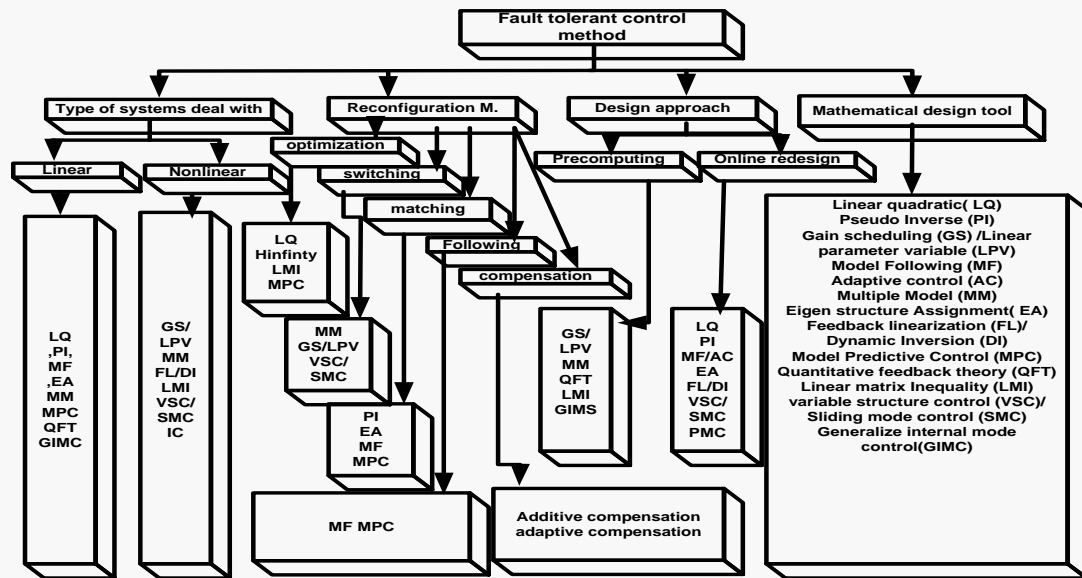


Figure 5.5.Active FTC methods

There are three basic parts of AFTC configuration

1. Control law reconfiguration mechanism
2. Fault detection and diagnosis (FDD) scheme.
3. Reconfigurable controller.

5.3.3 Fault Detection

The identification of a fault is made possible through filter that is a dynamic system specially designed to achieve the target. It notifies the fault detection through signaling.

The input/output data is processed to detect an incipient fault and later on isolate it within exact time and location.

5.3.4 Fault Isolation

The fault isolation is a phenomenon which recommends some method to isolate the components, device or software module for identifying the fault in their functioning. It basically hits the cause of the problem and is also termed as 'fault diagnosis'. This term

may refer to hardware or software but it actually works on the components creating error in the system.

5.3.5 Reconfiguration

The term reconfiguration signifies the change brought into input/output between the controller and plant by changing the structure and parameters of a controller. The performance may be at risk during this operation; however, the main target of original control is achieved through this process.

5.3.6 Fault Tolerant Control Systems

In this thesis, the fault tolerant control system works with some smart strategies by making the best use of IM stator resistance, encoder and the minimum output voltage. Its main purpose is to provide a system with reconfiguration controller. In normal circumstances when no fault has been detected, a sensor vector control is sufficient enough to operate the drive, however, the better result is procured through encoder as it locates the exact information about the location of the rotor. Any one of the following faults can activate closed loop V/F control in the system as will be shown in chapter 6.

1. Stator open winding (will be considered in the experimental results)
2. Stator short winding(will be considered in the experimental results)
3. Max DC voltage
4. Maximum V_1
5. Maximum V_0/V_1
6. Maximum V_2/V_1
7. Maximum line current
8. Maximum I_1
9. Maximum speed

The system switching over to the sensor less vector control with detection of speed sensor fault has been done by (Diallo, 2004). The BMRAS is used by the sensor less vector control to gauge the speed of the motor instead of the encoder.

The open loop V/F control is the fourth control strategy which makes the maintenance of a minimum level of performance possible when any one the following fault occurs:

1. Minimum output voltage V_1 (will be considered in the experiments)
2. Minimum speed
3. Maximum I_2/I_1 current

In case of failure of all of the above mentioned control strategies, the protection circuit comes into action and stops the motor operation. Chapter six will throw light on its mechanism in detail.

The fault in a system is detected in an operation through a circuit termed as the fault detection circuit which produces a binary output. In order to detect different specific faults in an operation, three fault detection and isolation circuits are activated. However, the decision of finalizing the presence of a fault in the IMs is done by the wavelet index. Once the fault is detected, the cause or reason of the fault is investigated through a process called isolation. The output of the isolation and the fault detection is as follows:

1. Trip: it is a binary indication of fault whether it is 0 or 1.
2. Trip status: it determines the type of fault.
3. Trip time: it identifies and verifies the time of fault occurrence.

Figure 5.6 depicts the Simulink implementation of one part of fault detection and isolation unit

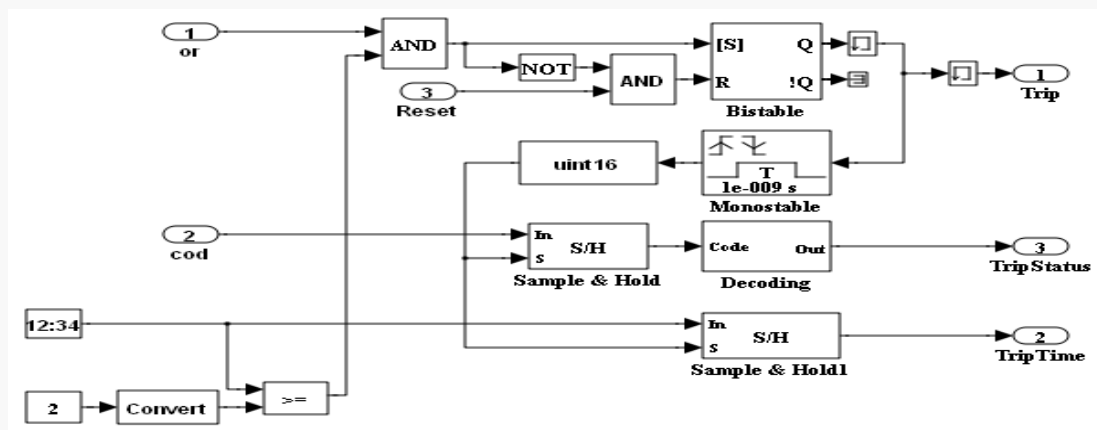


Figure 5.6. Simulink implementation of fault detection and isolation unit

The complete monitoring unit which includes the time, type and the location of the more than 13 faults are shown in Figure 5.7. In this figure, the faults were separated into three different groups according to sensorless vector control, closed loop V/f control and open loop V/f control techniques.

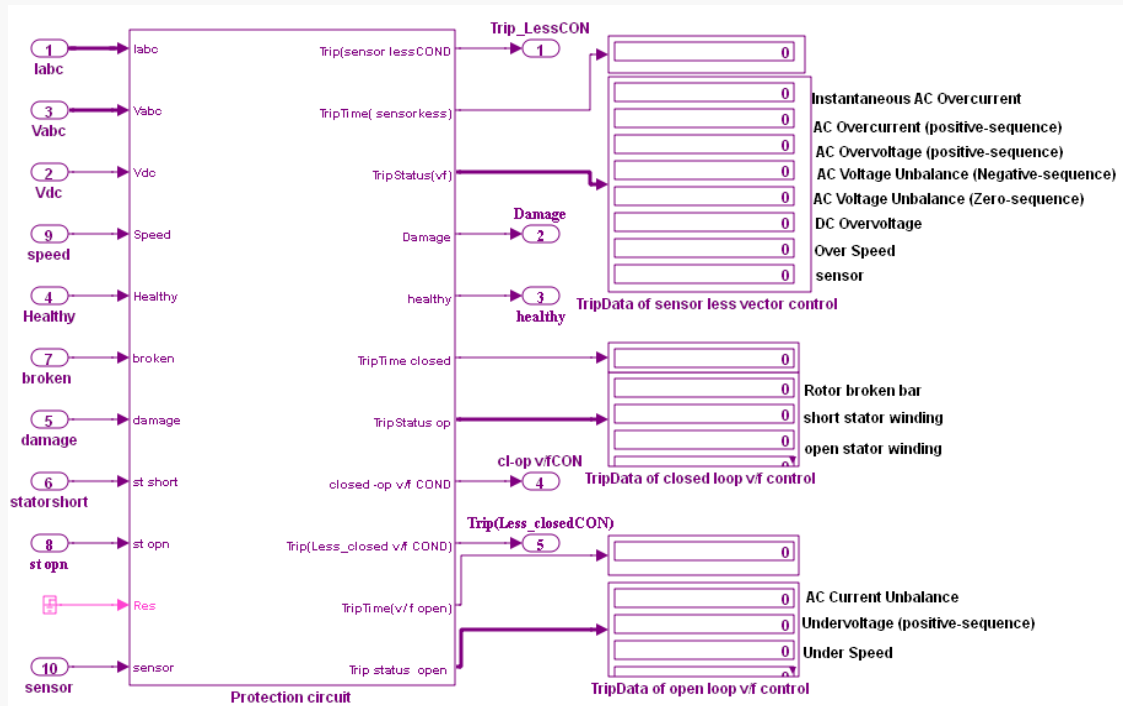


Figure 5.7. Simulink implementation of trip data for the different controllers

5.4 Switching Between the Controllers

The fault tolerant control is operated through a switching mechanism. In order to reach to the target that is finding faults and taking an appropriate action, the switching mechanism is embellished with four main control options namely closed loop V/F control, open loop V/F control, sensor vector control and sensor less vector control. The activation of either of these controls depends upon the level of degradation and the nature, type and reason of the fault. These controls are effectuated in binary version to control a specific switch. So one control strategy is used at one time moment to maintain the pre specified performance.

The controller switch over creates synchronization between the production of SVM signal and the specific controller that is brought about by wavelet index. Figure 5.8 indicates the main parameters and the switching circuit. When the wavelet index is 1.4 which is the threshold of healthy IM, the recognition and action unit make logic 1 and send it as a control to activate the SVM signal generation. The SVM signal is available at any time but it's not active but in the healthy IM.

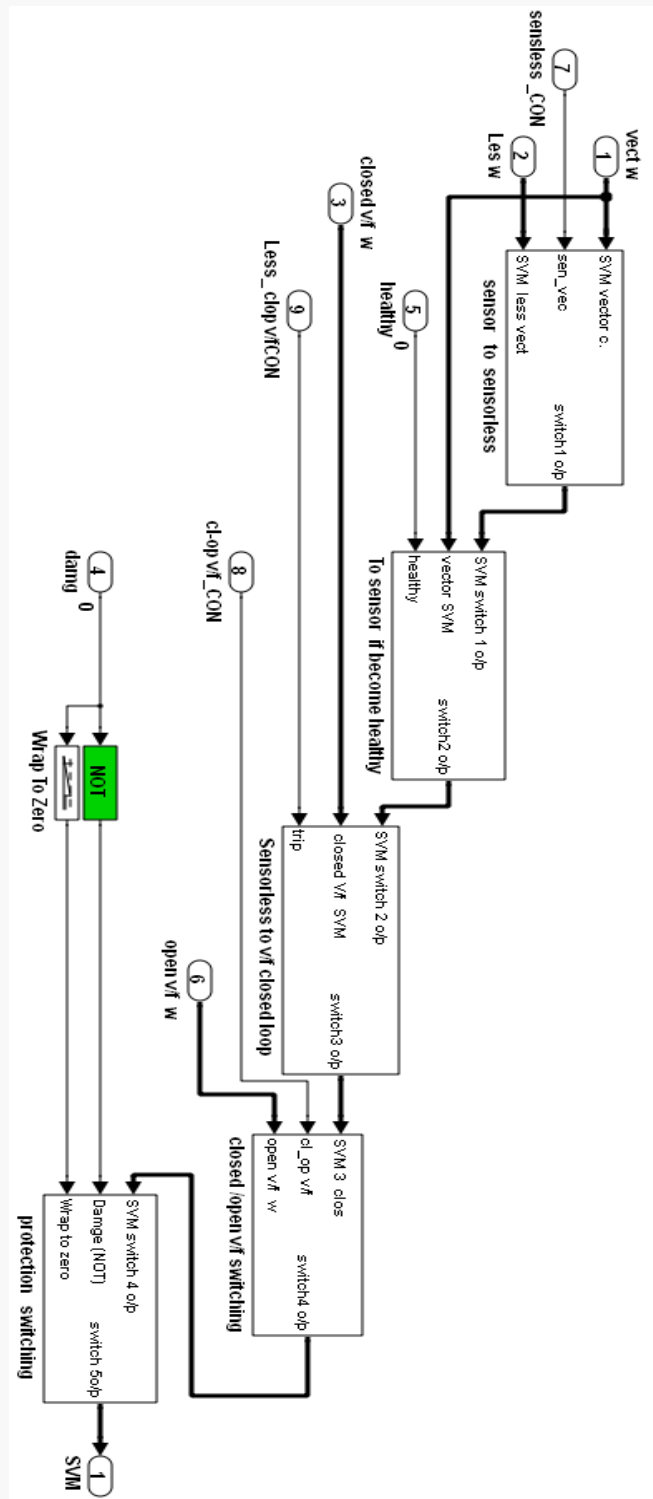


Figure 5.8.Switching mechanism block diagram

Figure5.9 shows how the scaling unit bears the generated parameters of the algorithm.

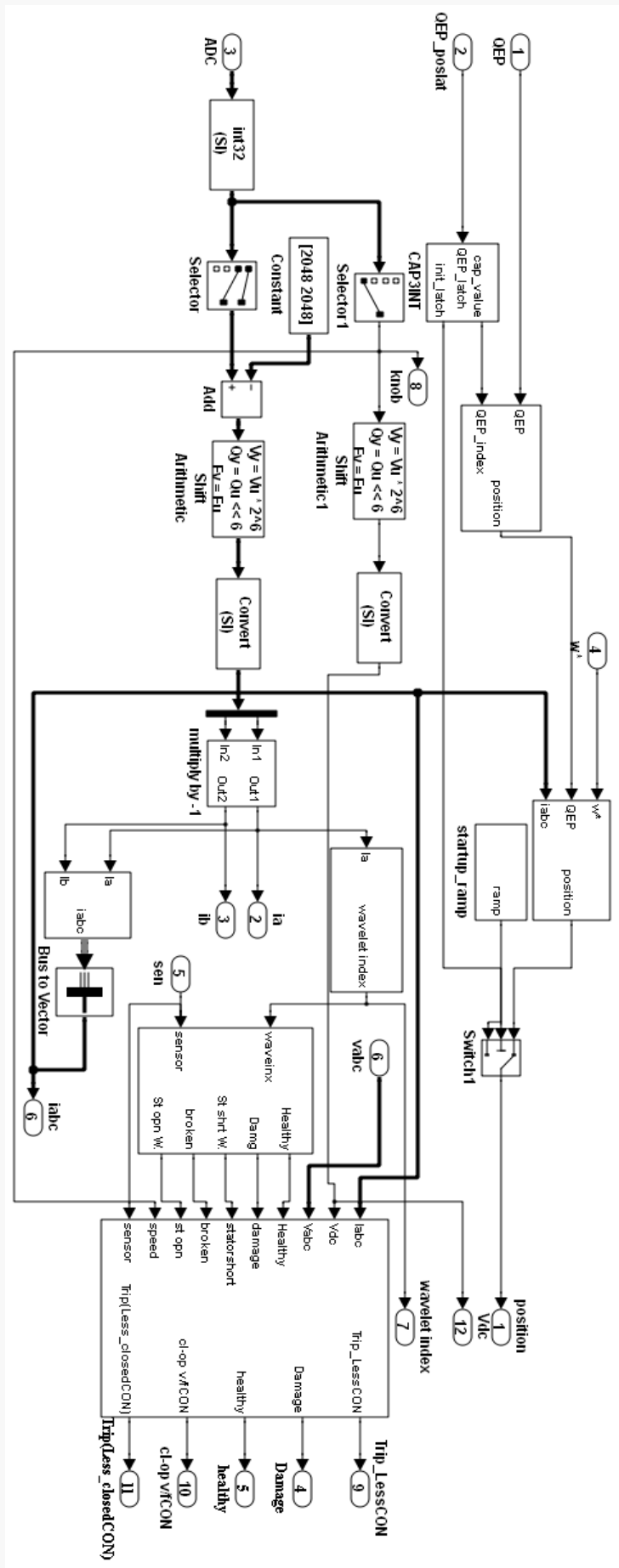


Figure 5.9. Simulink implementation of scaling unit

In case of occurring of any one of the above mentioned faults (first group) the sensor vector control technique switches to sensor less vector control technique. Each ‘switch change’ follows a specific path, the sensor vector control signal only pass through the first input when the threshold of second input satisfies the first one. In case of any variance the sensor less vector will be activated. Figure 5.10 shows this transition

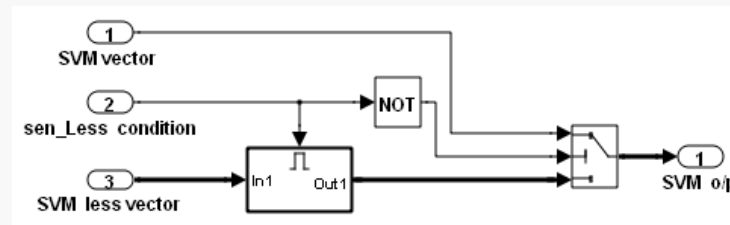


Figure 5.10. Simulink implementation of first block of Figure 5.8

The mechanism follows the same path through different transitory stages. Such as the transition from sensor less vector control technique to closed loop V/F control will be activated when the second group of faults will degrade the system. Similarly, the third group of fault will be the reason of next transition that is from closed loop V/F to open loop V/F and finally when the degradation in the system will reach to the peak point where rest of the above mentioned technique prove ineffective, the protection switching will take place.

Figure 5.11 shows the principle of fault tolerant mechanism as used in this work.

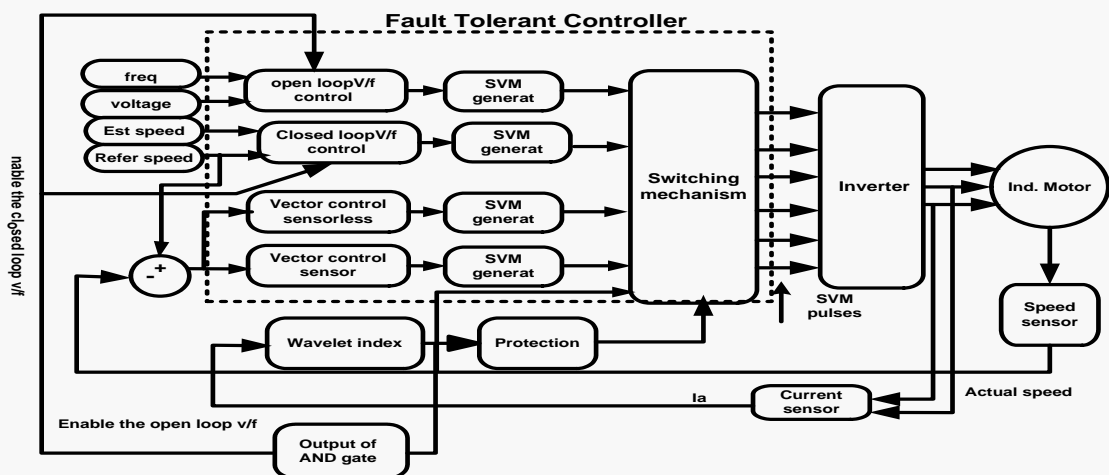


Figure 5.11. Fault tolerant controller with switching mechanism

Table 5.1 summarizes the ratings of the proposed fault tolerant control strategy applied on 0.370 kW squirrel cage IMs.

Table 5.1. IM parameters used in the simulation

Motor spec	Unit	Value
power	kw	0.37
Current	ampere	1.7
Voltage (delta)	volt	230
Rated speed	RPM	2800
No. of pole		2
Moment of inertia	Kgm ²	1.5e-4
Stator resist.	ohm	24.6
Rotor resist.	ohm	16.1
Stator induct.	henry	40e-3
Rotor induct.	henry	40e-3

Figure 5.12 illustrates the proposed fault tolerant control circuit with the monitoring units.

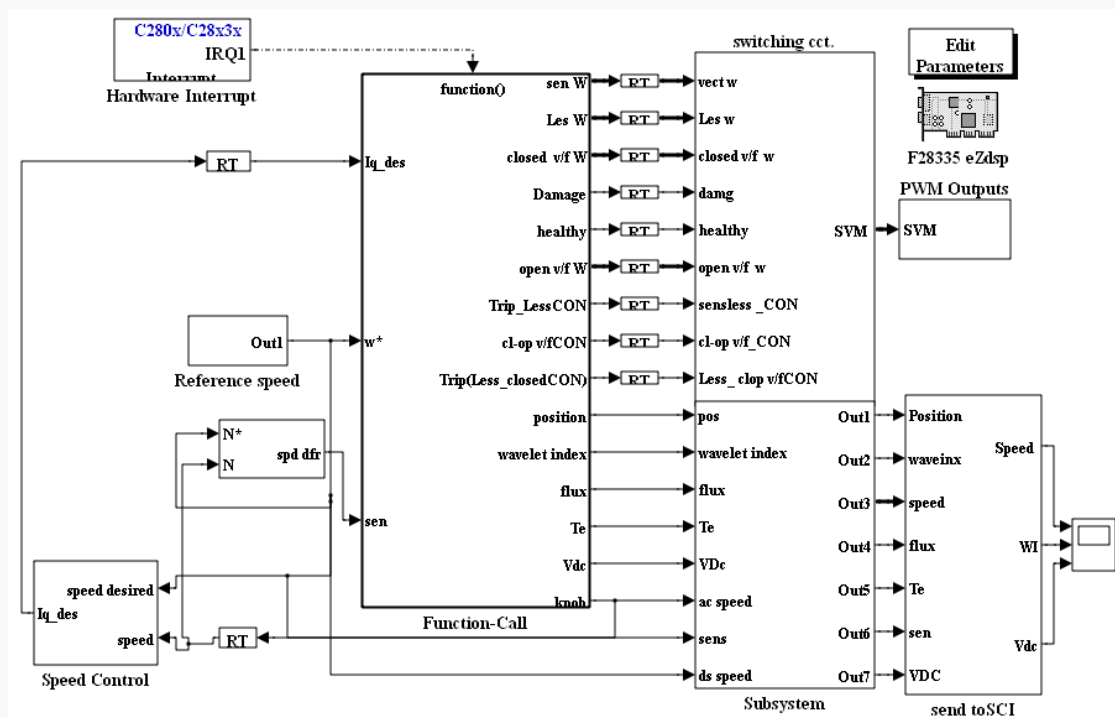


Figure 5.12. Simulink implementation of FTC proposed circuit

5.5 Computer Simulation

The operating features of the proposed scheme are analyzed through computer simulation. Matlab/Simulink is used in this process to get the better results. The system has a small mechanical time constant so the harmonic existing in the shaft torque does help only to some extent.

The developed torque increases its speed within 0.5 seconds due to slip speed; however, its speed starts to diminish when the speed of the motor is intensified.

For a step up in speed command of 2800 RPM, the motor speed increases very rapidly due to the higher value of slip speed at the start.

This simulation investigates three faults. Two are linked to the IM as electrical faults while the third one is related to a sensor fault.

5.5.1 Speed Sensor Fault

The speed difference between the reference speed and the actual speed can determine the speed sensor fault. Figure5.13 shows it.

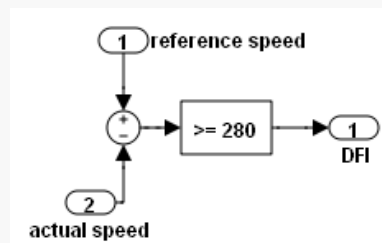


Figure 5.13. Simulink implementation of speed sensor checking

The activation of binary decision 1 depends upon the speed difference, if it is more than 10% or 280 RPM, the sensorless vector control will become activated otherwise the sensor vector control will retain its functioning as per the decision of logic 0. Figure5.14 shows the process.

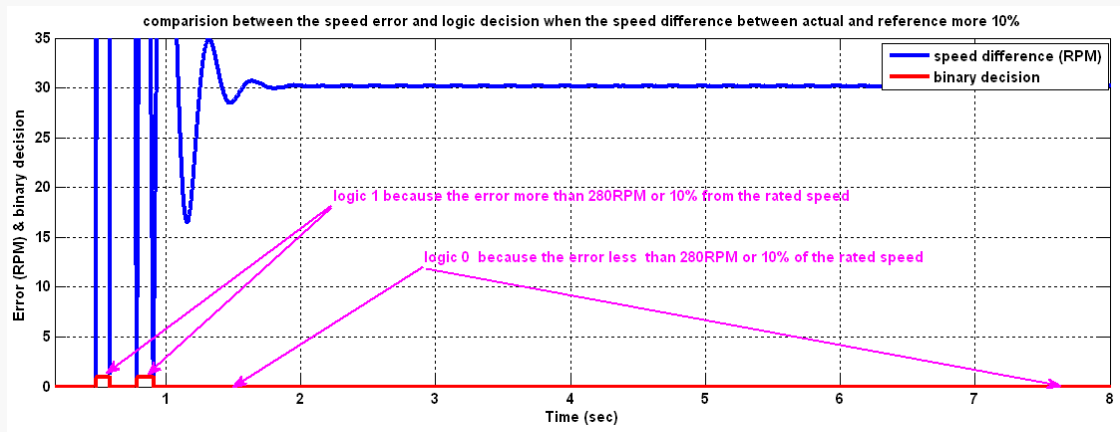


Figure 5.14. Speed error (blue) and error status (red)

The activation of another controller depends upon the difference in the speed and the time duration. If an abrupt fault or sudden change in speed difference has been detected and it retains its state even after the interval of 0.2 seconds, the system will consider it as a fault and the under the track zone of logic 1 the switch will change to another controller to ensure the smooth and uninterrupted performance of the system. This system complies with the fault tolerant control principles.

5.5.2 Stator Shorted Winding

The efficiency of the fault tolerant algorithm to recover the fault is examined by joining it with two control strategies.

The stator resistance is decreased ten times the original value to check the reliability of the fault detecting system. This problem is inserted in the system purposely and retained till 2 seconds. The wavelet index is measured by giving stator current I_a the status of input. Figure 5.15 indicates this process.

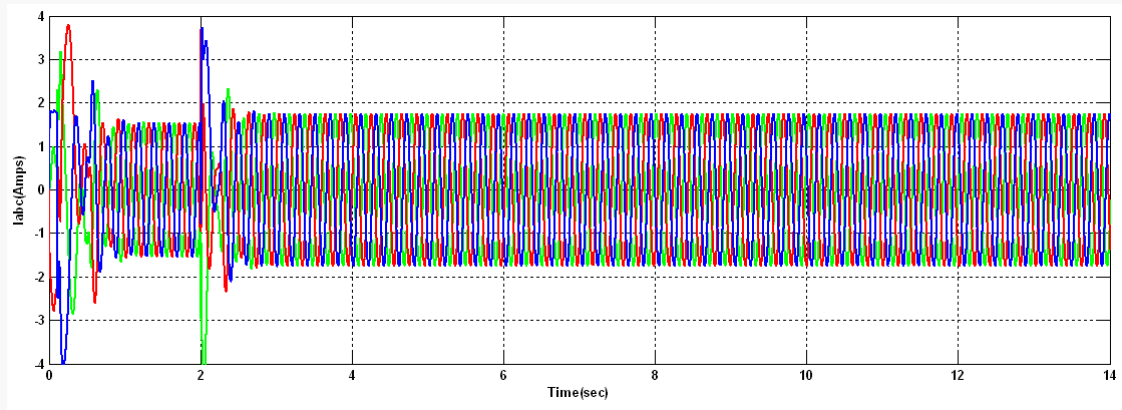


Figure 5.15. Stator current I_{abc} during the operation

Figure 5.16 shows the wavelet decomposition of the stator current. It indicates only 10 levels as the rest of them do not give any significant details about the analyzed signal.

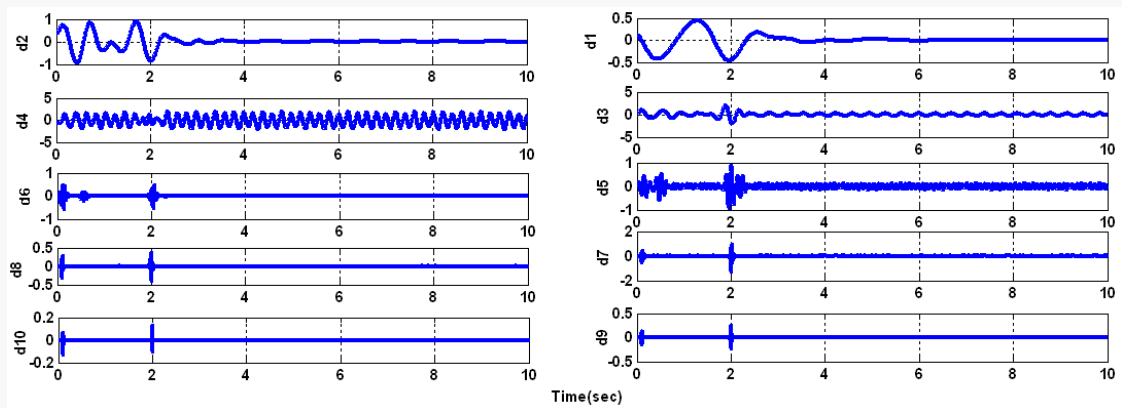


Figure 5.16. Wavelet decomposition for the stator short winding fault case

The value of the wavelet index of healthy IMs is computed as per Equation 4.21. It applies to the 20 kHz sampling frequency.

The speed is the main parameter to determine the activation of switching mechanism from vector control to V/F closed loop control strategy and so on. The transition from one controller to another is put into action when the change in speed is detected for a certain time period and in order to avoid any stoppage and cessation in the system, the wavelet index binary decision becomes activated. Figure 5.17 shows the efficiency of the system.

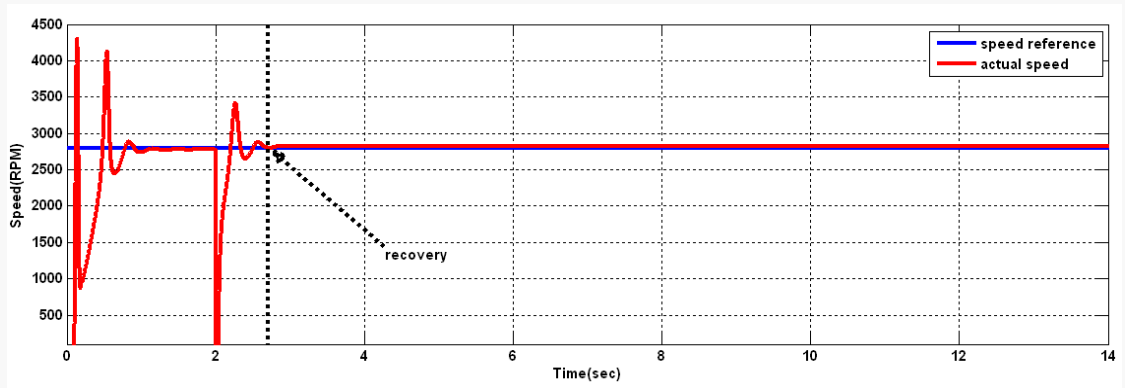


Figure 5.17.Speed response after applying fault tolerant algorithm

In figure 5.17, a transition from transient response within first sec has been happened, the stator short winding fault was injected as 2 sec. This figure shows that the actual speed flows exactly like the reference speed with 2800RPM while the reference speed was 2800RPM after applying FTC technique.

5.5.3 Stator Opened Winding

To check the working of the system, it is put on trial by inserting a fault by increasing the stator resistance which is ten times greater than the original value. This fault is introduced after a steady state of six seconds. Figure.5.18 shows the stator current.

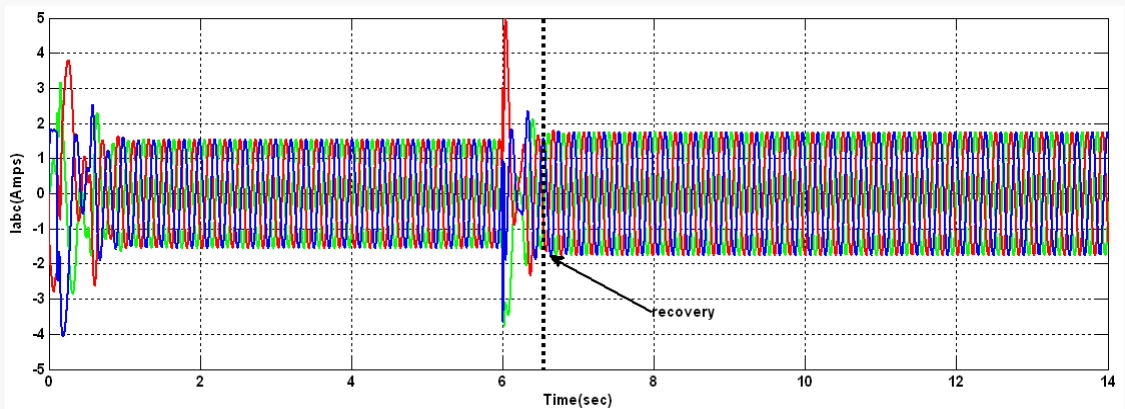


Figure 5.18.Stator currents I_{abc} during the operation

The stator current goes into the wavelet decomposition as shown in Figure 5.19.

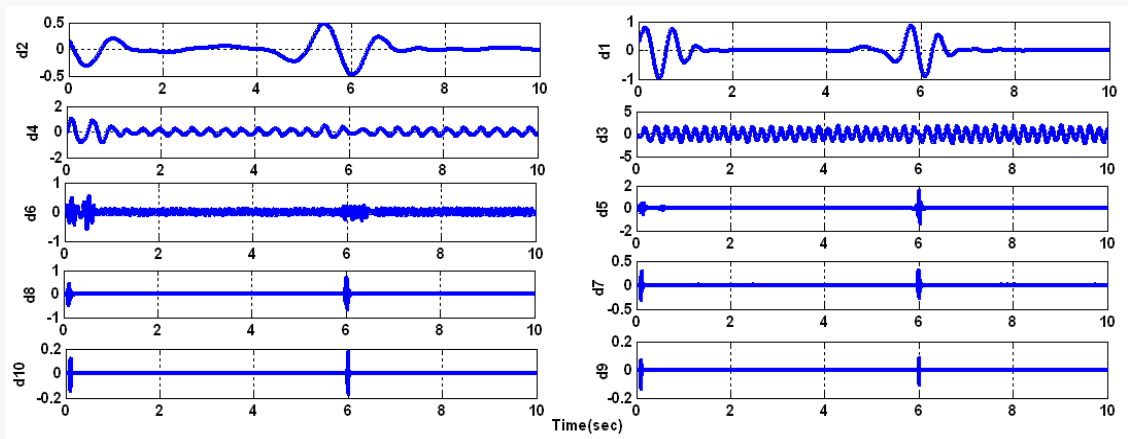


Figure 5.19. Wavelet decomposition for the I_a in the stator open winding fault

The actual speed of the system stabilizes right after receiving an action from the activation of the fault tolerant algorithm; it harmonizes itself with the reference speed to get in momentum with the new control strategy. However, this mechanism is not similar to the stator shorted in time recovery as it required more time for recovery due to uncertainty in the system parameters. Figure 5.20 depicts the speed response during the fault.

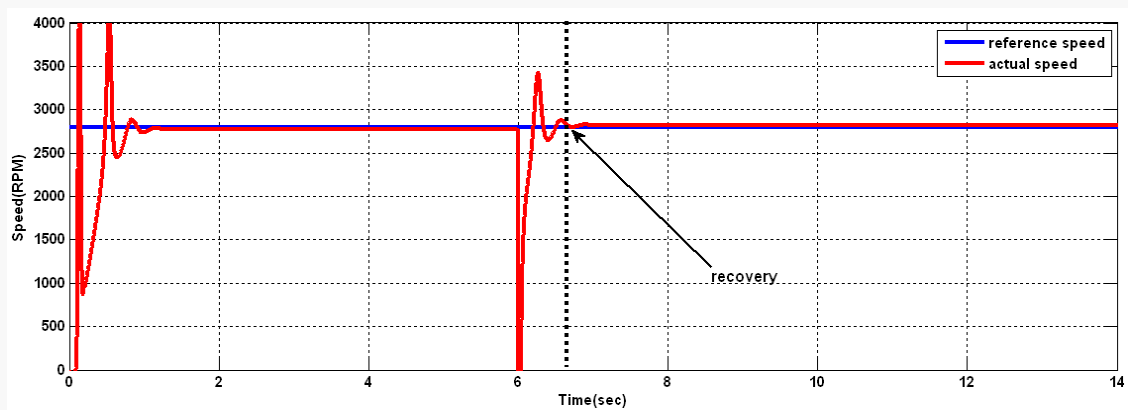


Figure 5.20. Speed response after applying fault tolerant algorithm

Two faults namely stator short and open winding are inserted together in the system at 1.16 sec to examine the flexibility of the fault tolerant control algorithm and its ability to return back to the sensor vector control. The operation of the IM will be stopped when the fault tolerant algorithm switches on the protection unit. However, the process is reversed to its normal state that is the controller transits from control protection to

sensor vector control and vice versa when the artificial fault is alleviated within the time duration of 1.48 seconds. Figure 5.21 illustrates the simulation result.

The wavelet index decides the transition of one control strategy to the other after detecting the fault and activates the corresponding binary decision.

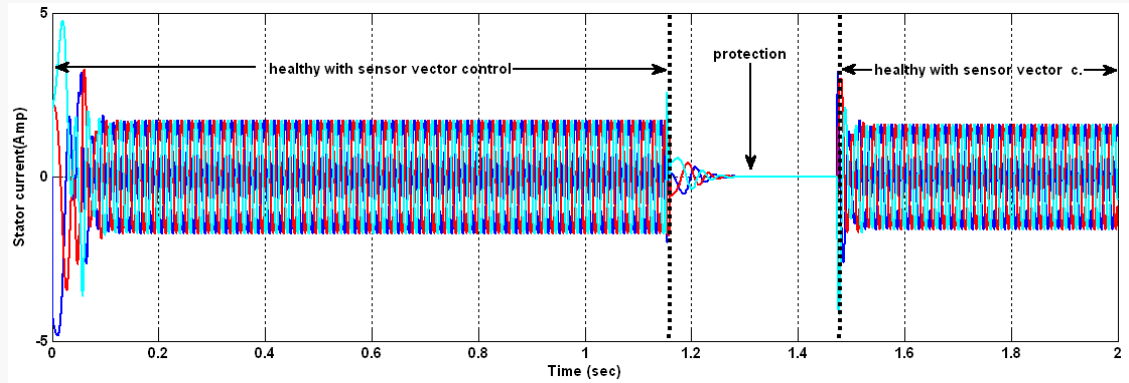


Figure 5.21. I_{abc} response before and after applying fault tolerant algorithm to test the flexibility

The operation of the IM comes to a halt when the fault is introduced between the time duration of 1.16 seconds and 1.48 seconds as the inverter SVM signal with Q13 is brought to the value zero.

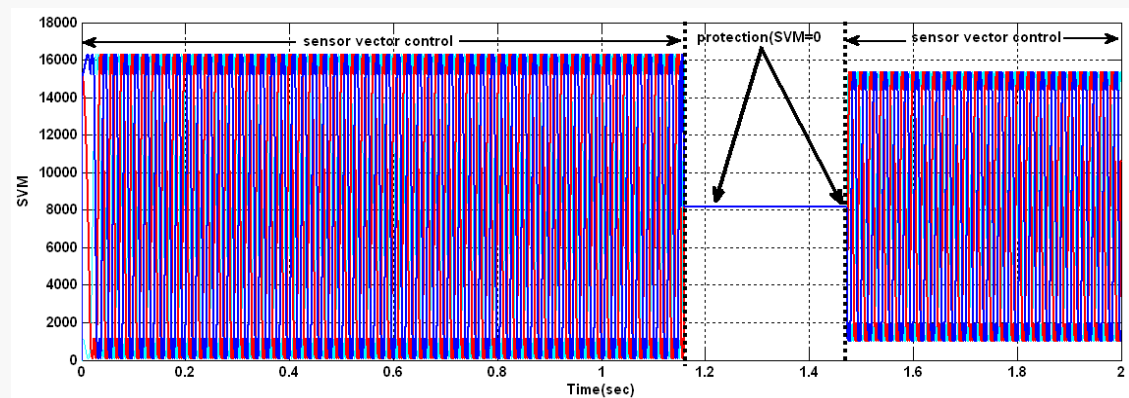


Figure 5.22. SVM inverter signal of the flexibility algorithm test

Figure 5.23 indicates that stator open winding and stator short winding faults are simulated with different times.

When the stator short winding fault was inserted at 1.15 sec, the wavelet index right after detecting the fault sent the binary decision for the transition of sensor vector control to closed loop V/F control technique.

To test the efficiency of the fault tolerant algorithm and the recovery times of both faults, the stator open winding fault was inserted with the time duration of 1.4 sec.

It has been found that the recovery time of the stator short winding is greater than the recovery time of the open stator winding (Figure 5.23).

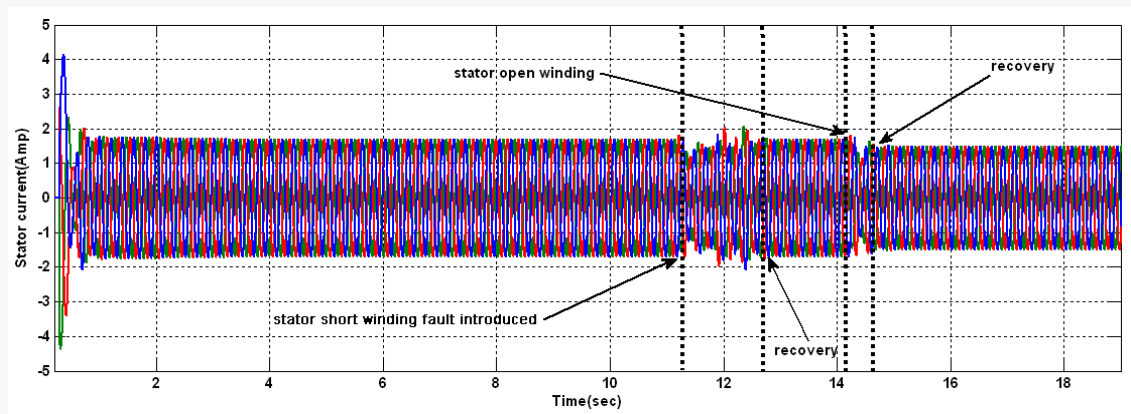


Figure5.23. I_{abc} response before and after applying fault tolerant algorithm to test stator faults

Thus, the above mentioned intrusions of the faults prove that the fault tolerant algorithm helps to bring the operation back to its former performance.

Chapter 6: Condition Monitoring of IM Faults

6.1 Introduction

There are certain limitations in every system and in order to prevent it from any failure or fault some strategies are devised. Condition monitoring (CM) is one of these techniques that help the system to run smoothly and efficiently. It monitors a parameter of condition in the IM and makes sure that the system does not get affected due to any change in the system performance or any parameters that is considered as a machine fault or failure (Mehrijou, 2010). Thus, the irregularities are detected at the earlier stage due to this technique. It is no doubt a very important technique to avoid damages, unscheduled shutdown and unwanted deficits (Jeevanand S, 2008).

The harmonics in the IM current makes the process of the fault detection easy and reliable (Bodkhe, 2009). It makes the use of broken rotor bars, DC short buses and bearing, stator open winding and stator short winding to detect the fault without delay. It carries out its function in cognizance with wavelet.

Different wavelet functions and controllers such as linear discriminated analysis (LDA), quadratic discriminated classifier (QDC) and linear discriminated classifier (LDC) have been proposed by (Basaran, 2011) for the wavelet condition monitoring of the IM. Similarly the condition monitoring in the IM has been introduced by (Georgakopoulos, 2009) with wavelet against the broken rotor bar and end ring faults. (Zhang, 2011), presented a review for medium voltage IM condition monitoring and protection while (Zhu K. Y., 2009) presented a review of wavelet usage in the condition monitoring in the sensor signals. A significant amount of research has been done in this direction and many different techniques for the fault detection have been found which mainly focus on the stator fault due to noninvasive properties.

However, some research and work has been done on the FFT and wavelet by using MCSA method to monitor the fault frequencies. This method has been proposed by

(Mehala, 2009) and it has been found very effective in terms of reliability and noninvasiveness (Thomson, 2001).

Figure 6.1 shows the condition monitoring of induction machine following the sequence

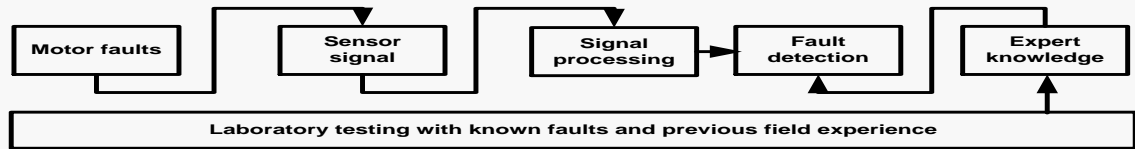


Figure 6.1 .Condition monitoring procedure

6.2 Condition Monitoring

The efficiency of the system can be enhanced by detecting the cause of the fault and the exact fault time occurrences. It not only improves the working of the operation, it also increases the longevity of the function and reduces the cost and maintenance expenses. Different researchers prefer current, flux, voltage, torque and speed as some of the specific signals to examine the faults in the IMs (Erhan Akin, 2011). As the IM is prone to a number of faults, this chapter will discuss at length the monitoring of stator current, DC voltage, speed monitoring and stator voltage that play a vital role in the maintenance of a successful system.

6.2.1 Stator Current

Stator current methodology is given preference over other methods because it can perform physical measurement and provides indication of the IM state quite well. No matter how efficiently the induction machines has been loaded and extracted, a fault can affect the spectrum current signal any time (Menacer A. M., 2004). Figure6.2 explains the standard measurement that defines the fault thresholds. The current measurement is the key note of this circuit which mainly depends upon the negative sequence analysis of stator current per phase.

According to the following relationships, the construction asymmetry, faults transducer gain difference, voltage and load unbalance at the terminals give rise to the generation of the negative sequence current in the system (Zafar, 2010).

$$I_1 = \frac{1}{3}(I_a + \alpha I_b + \alpha^2 I_c) \quad (6.1)$$

$$I_2 = \frac{1}{3}(I_a + \alpha^2 I_b + \alpha I_c) \quad (6.2)$$

$$I_o = \frac{1}{3}(I_a + I_b + I_c) \quad (6.3)$$

$$\alpha = \exp(2\pi / 3) = 1\angle 120 \quad (6.4)$$

α , is the space vector operator.

These faults can be monitored through stator current methodology: (Figure 6.2.)

1. The instantaneous AC over current fault: When the maximum value of stator phase current exceeds 1% of the rated current, this sort of fault is likely to happen. This has been shown in the following relation for 0.5Hp:

$$\max(I_1) > 1.7 * 1.01$$

The result of this action is the activation of decoding unit, thus showing the time and the fault.

2. Max allowable AC current : When the magnitude of stator current increases 10% greater than rated current, this fault takes place as in the following relationship:

$$\text{abs}((I_1) > 1.7 * 1.1$$

The logic 1 will activate the decoding-encoding circuit to indicate the time and the fault.

3. Max AC current unbalance fault: This fault takes place only when the following ratio is satisfied as can be seen in Fig.6.2:

$$I_2 / I_1 > 1.7 * 0.4$$

The fault and the time are shown with the activation of the decoding circuit and it can be observed in the monitoring circuit of the stator current.

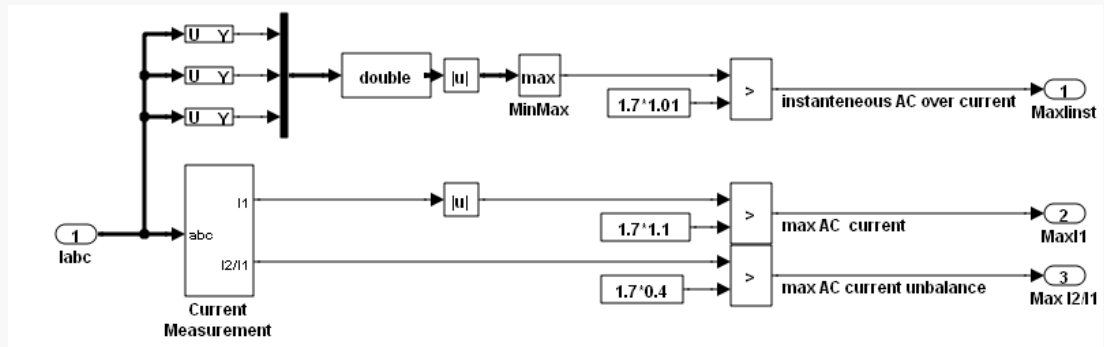


Figure 6.2. Motor current monitoring circuit

6.2.2 Stator Voltage

The IM state receives some observation from the stator phase voltage monitoring. The following measurements are obtained from the monitoring circuit:

$$V_1 = \frac{1}{3}(V_a + \alpha V_b + \alpha^2 V_c) \quad (6.5)$$

$$V_2 = \frac{1}{3}(V_a + \alpha^2 V_b + \alpha V_c) \quad (6.6)$$

$$V_o = \frac{1}{3}(V_a + V_b + V_c) \quad (6.7)$$

α , as in (6.4)

The following faults can be detected by using the above mentioned measurements:

1. AC under voltage (Min V_1): Figure 6.3 shows that this type of fault disturbs the system when V_1 is less than 90% of the nominal stator voltage

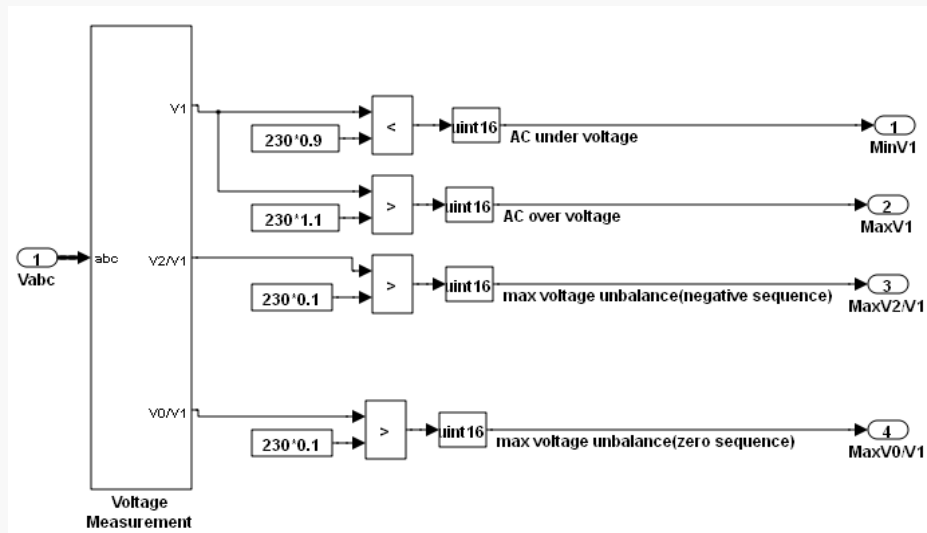


Figure 6.3.Motor voltage monitoring

The time and this fault will be detected with the activation of the decoding circuit.

2. AC over voltage (Max V_1): When V_1 exceeds the nominal stator voltage by 110 %; this sort of fault is likely to happen.
3. Max voltage unbalance or negative sequence (Max (V_2/V_1)): This fault is detected by the activation of the decoding circuit, it also shows the time. This fault takes place when the ratio of V_2/V_1 is 10% more than the stator voltage.
4. Max voltage unbalance (zero sequence): It is the max ratio of the V_0 to the V_1 and more likely to happen when this ratio becomes more than 10% of the stator voltage.

The induction machine needs de-rating when the heating losses at the terminal mounted manifold. It happens when the voltage at the terminal loses the balance. Thus the unbalance is kept under control and the system tries to not exceed it above 5%. Table 6.1 shows this relationship.

Table 6.1.Observation of IM according to IEEE standard

Induction motor faults observation		
Faults	Limits values	Acceptable value
AC over current	2 times rated	1.5 rated
AC current unbalance	Up to 45%	Up to 40%
AC under voltage	5-25%PNDA & PNDI	0.25-20%
AC over voltage	± 10%	± 10%
AC voltage unbalance	1-5% IEEE stand	1-3%
DC over voltage	V_{dc}	V_{dc}
Over speed	+ 25%	+10%
Under speed	-25%	-10%
Rotor broken bar	20% less than 2 m.for 2 pole	20% less than 2 m.for 2 pole
Short stator winding	10% less than 2m for 2p	10% less than 2m for 2p
damage	Not permitted	Not permitted

The 1 kW IM also was used to make sure the algorithm is valid for all motor ratings.

The validity of algorithm for all motor rating is ascertained by using 1 kW IM. It is used for simulation and experimentation and has been explained in chapter 7 with all the details. Table 6.2 has a list of all the specific parameters

Table 6.2.IM parameters

Motor spec	Unit	Value
power	kw	1
Current	ampere	2.5
Voltage (delta)	volt	400
Rated speed	RPM	2780
No. of pole		2
Moment of inertia	Kgm^2	3.5e-4
Stator resist.	ohm	20.9
Rotor resist.	ohm	19.5
Stator induct.	henry	50e-3
Rotor induct.	henry	50e-3

6.2.3 DC Voltage

Figure 6.4 indicates that the maximum DC voltage gets stimulated as soon as the V_{DC} voltage becomes greater than the 400 V.

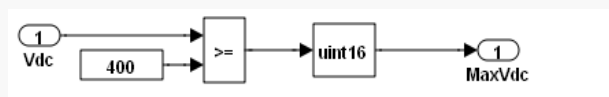


Figure 6.4.DC voltage monitoring circuit

6.2.4 Speed Monitoring

The encoder as input is used to monitor the operating speed of the IM. Since the speed of an IM is the key part of the operating system, its monitoring also needs close observation and careful invigilation (McFate, 2009). The magnetic field around the stator is even affected as the impact of the field is slows down by this speed (Figure 6.5).

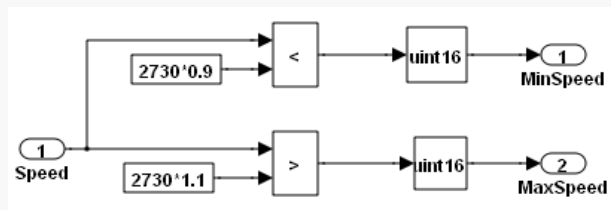


Figure 6.5.Speed monitoring

The limitations of speed are more than 10% of the reference speed of the IM for the over speed and are $0.9 \times 2800\text{RPM}$ for the under speed as per the standards shown in Table6.1

The decoder- encoder combination unit monitors and activates any transition in the system when a fault in speed along with its time is detected. Such as the decoder will remain inactive if the speed is less than 10% of reference speed, however, as soon as the speed crosses this limit the binary decision of logic 1 will get activated by the decoder unit and the transition will start from one control to another. However, there are some limitations in the handling of under and over speed $\mp 10\% * \omega_{reference}$.

There are certain faults which are a threat to the IM such as machine current signature analysis, fast Fourier transform, short time Fourier transform and wavelet transform (Mehdi Arehpanahi, 2005), hence a number of diagnosis techniques have been introduced over time to tackle these faults.

Simulink/ Matlab implementation to highlight and find the faults at its nascent stages along with the source of the fault have been described in this chapter. It shows how it strengthens the monitoring system.

6.3 Proposed Methodology

The main objective of the implication of the technique of fault detection and protection and monitoring in IMs is to achieve these targets: The three phase stator current, three phase voltage and DC voltage fault monitoring and protection. The practicality of the C.M stimulation and this algorithm is ascertained by testing with 0.37 kW for different IM ratings.

The completion of this work has been carried out through the following procedure:

1. The acquisition of the current, voltage, DC voltage signals
2. The negative sequence is used to conclude the over, under or unbalance voltage and the AC voltage to analyze the stator current and voltage
3. The under and over speed is checked through the analysis of the IM speed
4. The trip status and the indication of the fault (0 or 1) is highlighted when output of each stage reaches to the encoding circuit and the OR gate
5. The time of the trip and the trip are shown by the monitoring unit (The output of the OR gate)
6. The encoding output is used to show the trip status being the part of the monitoring unit
7. Wavelet implementation circuit
8. The protection unit is the last resort for the system when the fault of IM reaches to the maximum point.

Figure 6.6 illustrates the proposed detection and monitoring circuit.

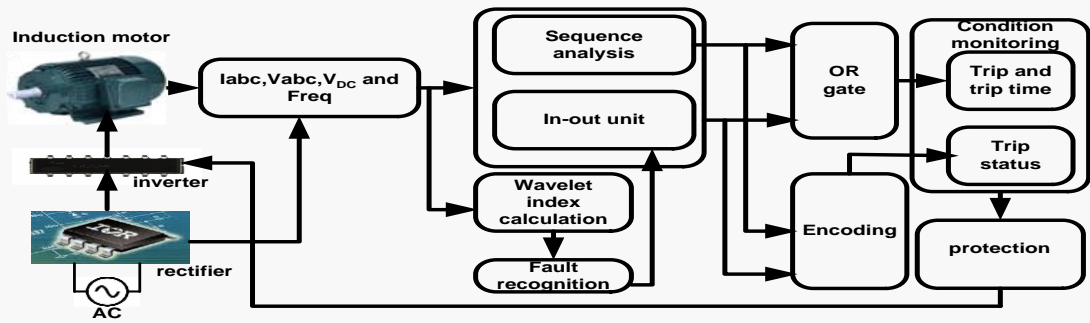


Figure 6.6. Block diagram of proposed monitoring and protection circuit

While Figure 6.6 is the block diagram proposed monitoring and protection circuit. Figure 6.7 indicates the internal connections of both monitoring IM units and detection. In this figure, the faults are divided into three parts as mentioned earlier. Three trip times, three tripe status and three locations can be shown according to that.

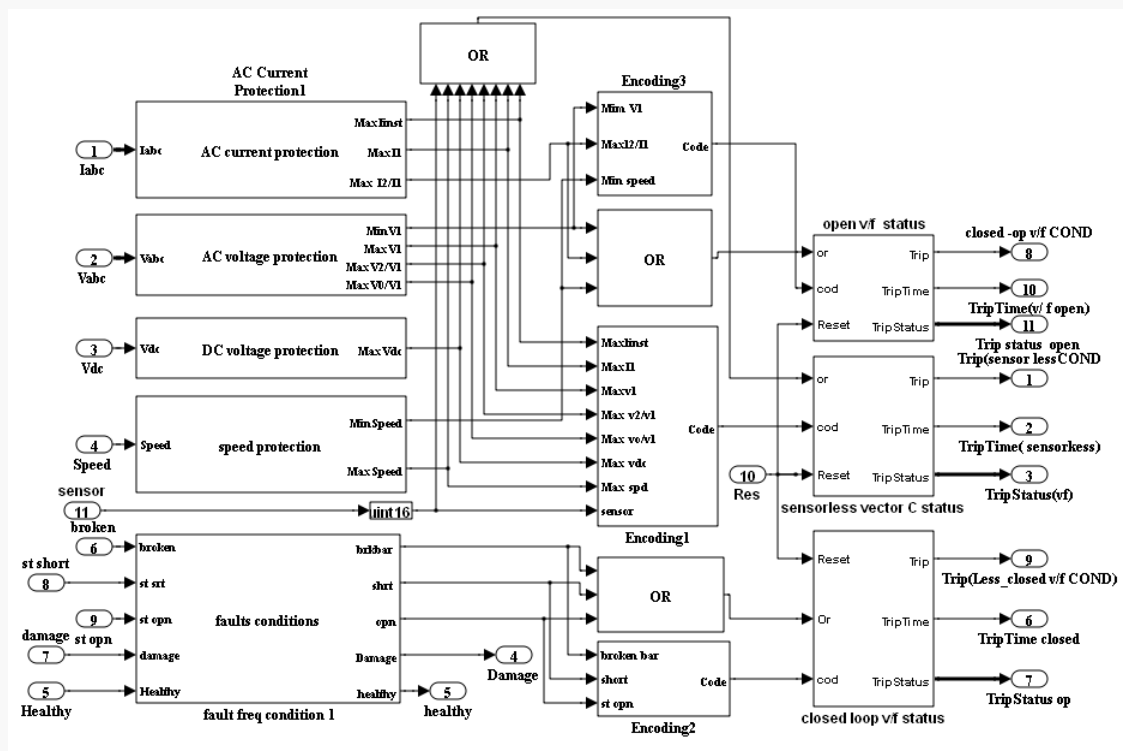


Figure 6.7. Simulink implementation of internal connections of monitoring unit

6.4 Protection

When the fault in IM is extremely grievous another mechanism is brought into action. The SVM pulses are settled at zero to stop the function of the faulty IMs. This

protection circuit works along with the switching mechanism and provides a safeguard to the system. Figure6.8 shows this mechanism.

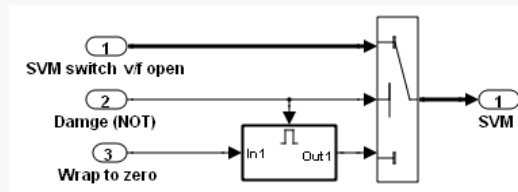


Figure 6.8. Protection unit mechanism

The IM is stopped when a serious fault occurs in the system by activating the switching mechanism to the SVM which is generated by open loop V/F to zero. In normal condition the output of detection unit is logic 0 which turns into 1 as soon as a fault occurs in the system. Three case studies have been modeled against multiple faults to examine the efficacy of the proposed methodology.

6.5 Case Studies

In order to investigate the CM effectiveness to monitor and protect the IM two case studies, healthy and faulty, are considered.

6.5.1 Healthy Case

The monitoring of trip status, SVM, speed and current of the IM are very important. As mentioned in the 0.5 Hp specifications, the stator current should be 1.7Amp; trip status should be zero with uniform SVM generated, the monitoring unit is responsible to record both type of fault with its time as can be seen in the following figures.

Figure6.9 shows the IM in healthy state that is without any fault and under normal operation conditions. The trip status and the space vector values were recorded in this state. The status trip at this moment has been found zero which is clearly visible in figure6.9

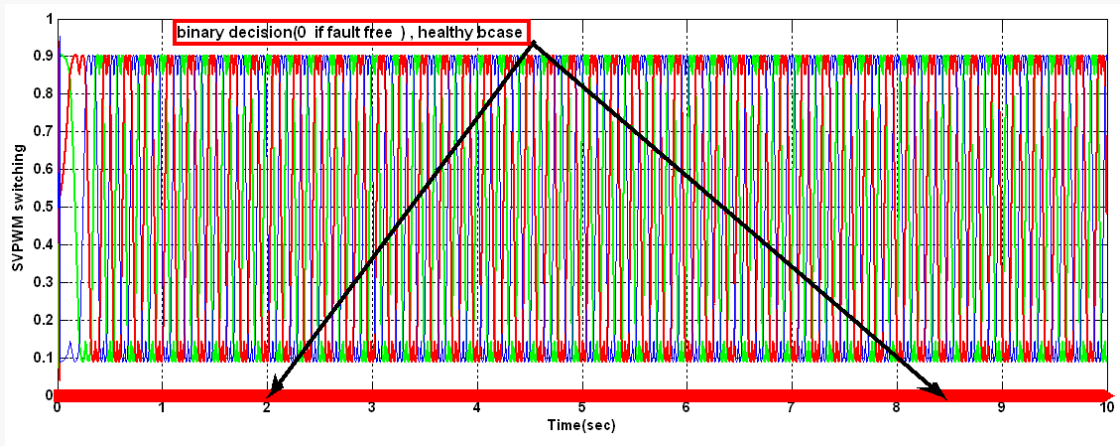


Figure 6.9.SVPWM duty cycle with trip in healthy case

Figure 6.10 indicates the actual speed overlapping the reference speed,

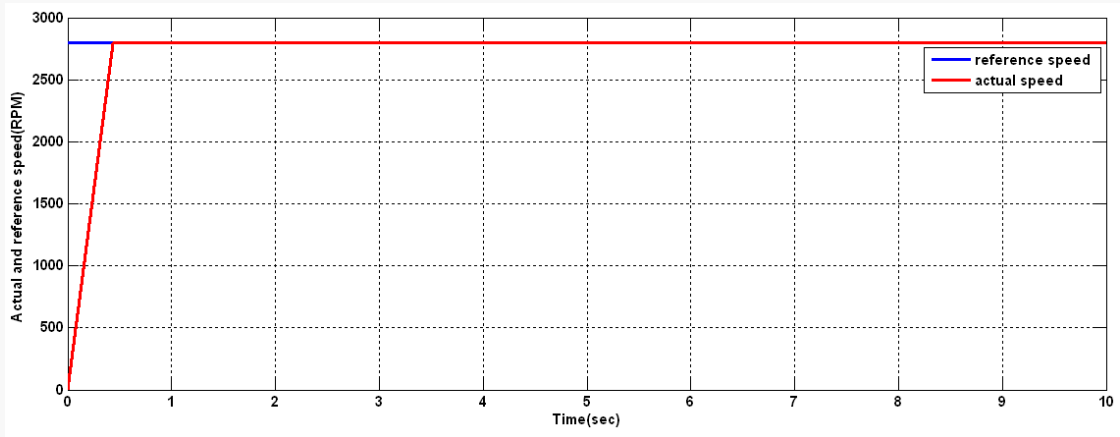


Figure 6.10.Actual and reference speeds in healthy case

Figure 6.11 illustrates the stator currents in the healthy case

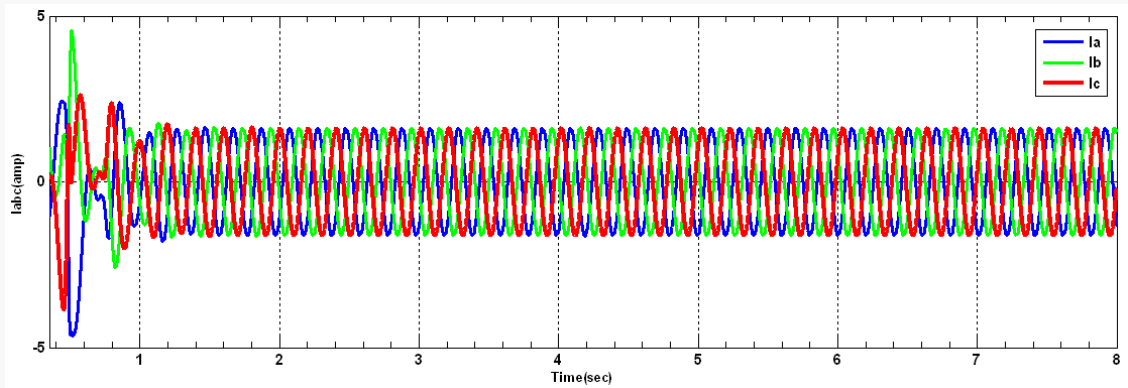


Figure 6.11.Stator currents I_{abc} in healthy case

Figure 6.12 shows the wavelet decompositions of the healthy stator current. The stator current (I_a) exhibits a little extended transient region. It is evident in the decomposition levels ($d_3, d_4, d_5, d_6, d_7, d_8, d_9$).

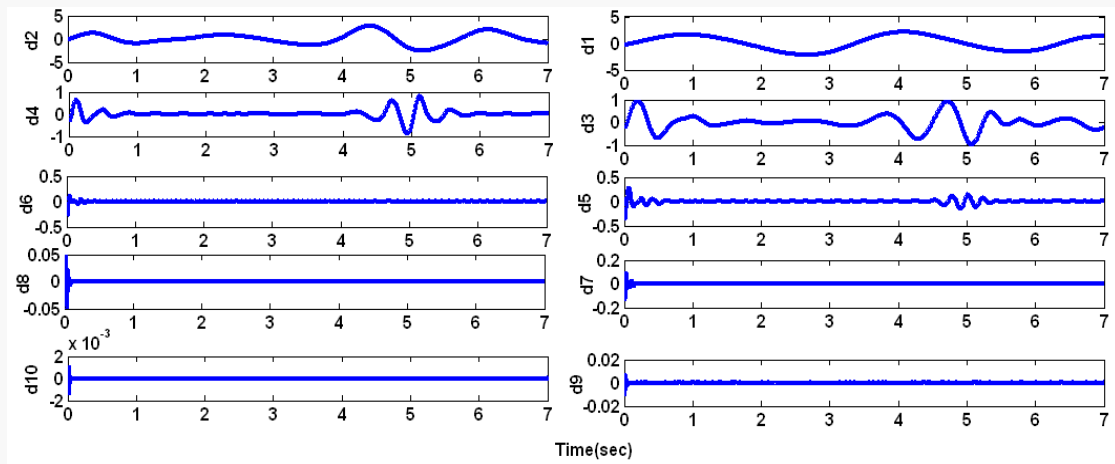


Figure 6.12. Wavelet decomposition of stator current I_a in healthy case

The monitoring circuit shows that there is no fault in the IM as in Figure 6.13.

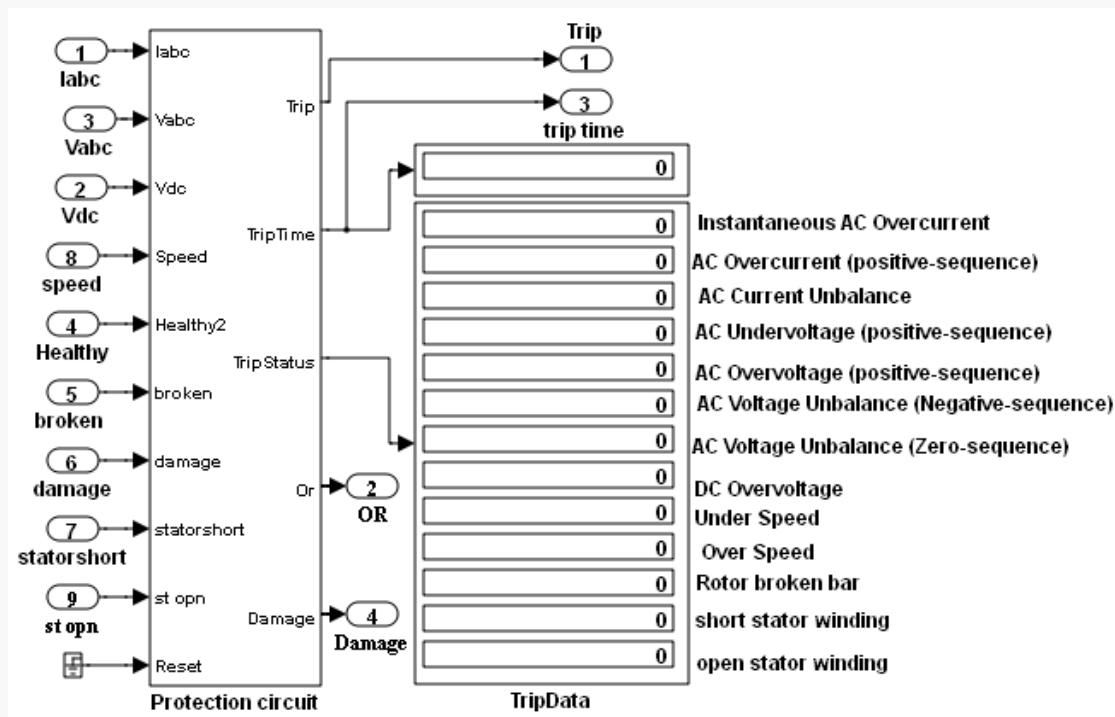


Figure 6.13. Monitoring outputs for the healthy case

6.5.2 Faulty Case

More than 13 trips can be taken as a case study. The following faults and parameters monitoring are included.

6.5.2.1 Voltage and Speed Faults Monitoring

The first case study deals with a fault in the voltage and speed of the IM, the time and the nature of fault is kept under observation during a faulty operation. The time of the first fault and the trip had been shown very efficiently in the monitoring unit. Figure 6.14 depicts the speed response of the proposed FTC based IM drive under fault condition. The performance of the monitoring circuit has been tested by creating the tolerance between actual and reference up to 5%.

However when this difference is extended till 20% (of the reference speed 560 RPM), the operation should come to a halt with the activation of the protection unit. The IMs do not stop completely as the condition in this case is not satisfied. According to the Fig.6.14, the extremes of the IM speed degradations were included to test the ability of V/f control technique to accommodate this fault.

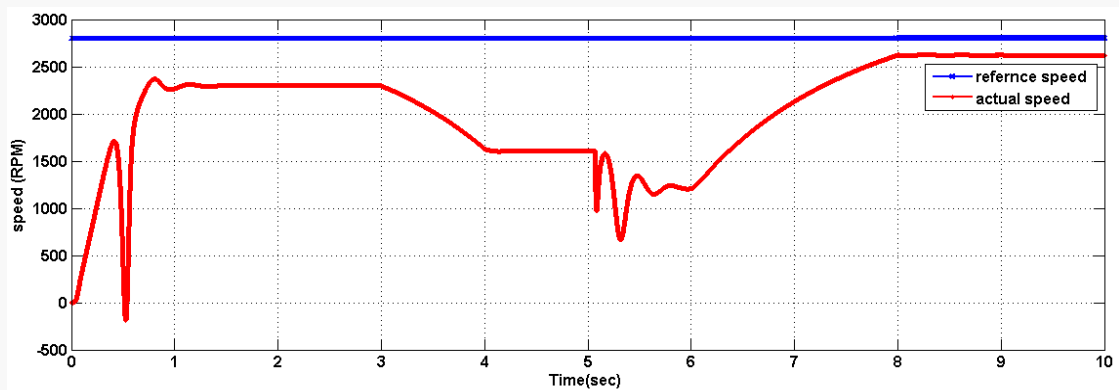


Figure 6.14. Speed response of actual and reference in under speed case

The fault will be presented as a binary decision with logic 1 in case of trip status circuit activation. The fault within the duration of 2 second delay will not be entertained as a

fault and the transition mechanism will not be effectuated in the beginning of operation.

Figure6.15 indicates this state.

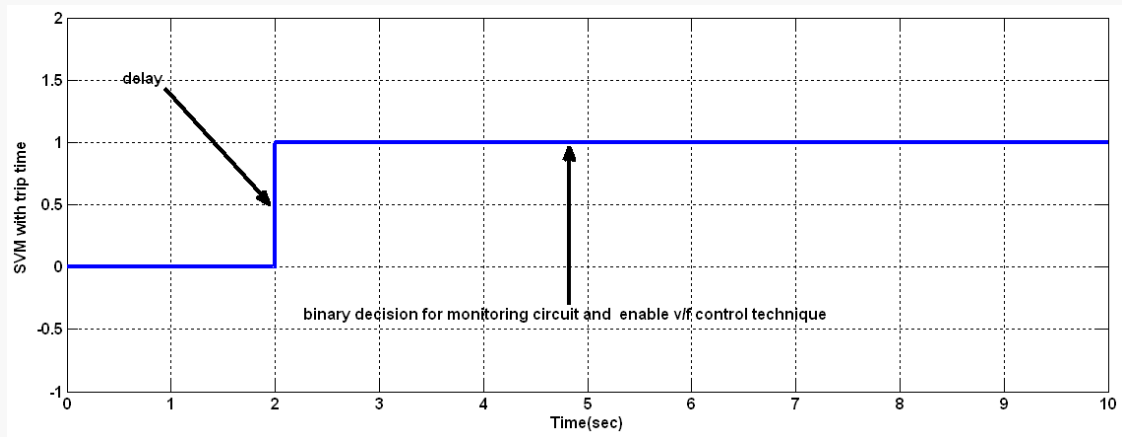


Figure 6.15.Binary decision of fault occurrence

Timing is important in this process which is regularly checked to cover all faults individually.

Figure6.16 shows the monitoring of the above mentioned parameters.

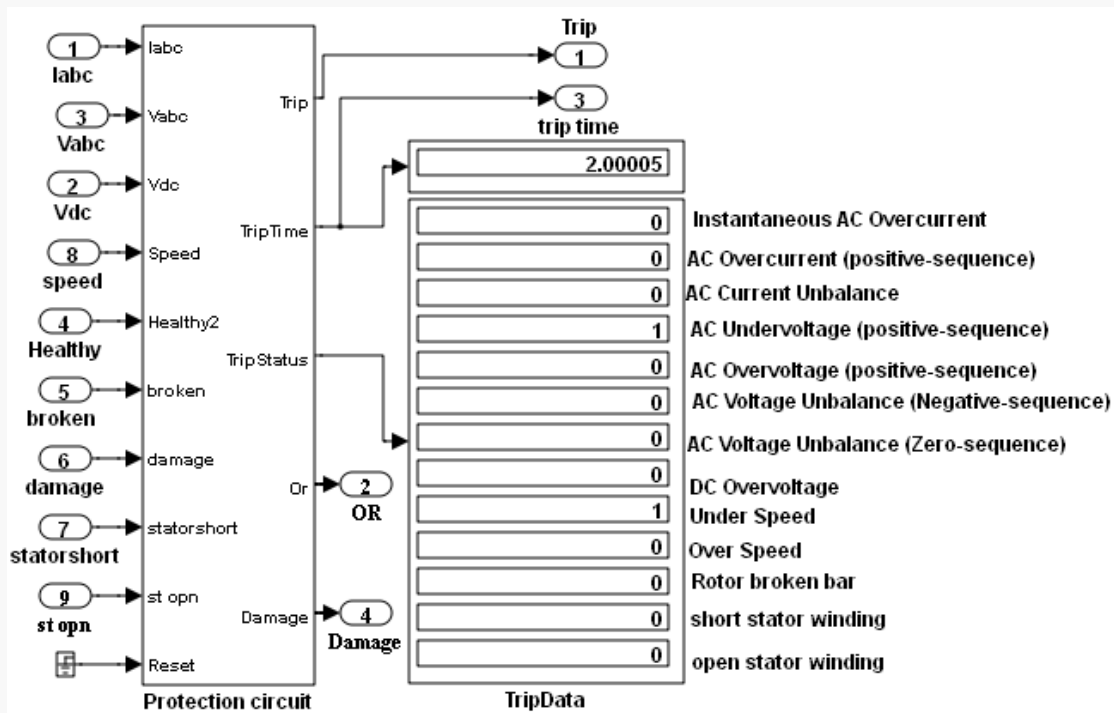


Figure 6.16.Monitoring outputs for the first case study

The validity of the protection circuits is being confirmed by confining it to the main expected stator faults namely the stator short winding, stator open winding monitoring

due to the significance of the aforementioned faults. As the protection circuit has been designed to apply in case of extreme severe condition, the above mentioned faults are more likely to happen and can prove unmanageable by the other controllers.

The fault developed gradually within fraction of seconds as it has been found happening at 0.00265 sec (Figure 6.17) as a signal has been inserted in the very beginning of the operation. In order to control this situation, the binary decision are made responsible to activate the protection circuit that prevents SVM generation ($SVM=0$) to control the inverter and stop the motor.

The same procedure was repeated by increasing the time interval that is, a fault was inserted after a few seconds and the SVM signal was generated right after it. Figure 6.18 shows that the same methods were re-enacted.

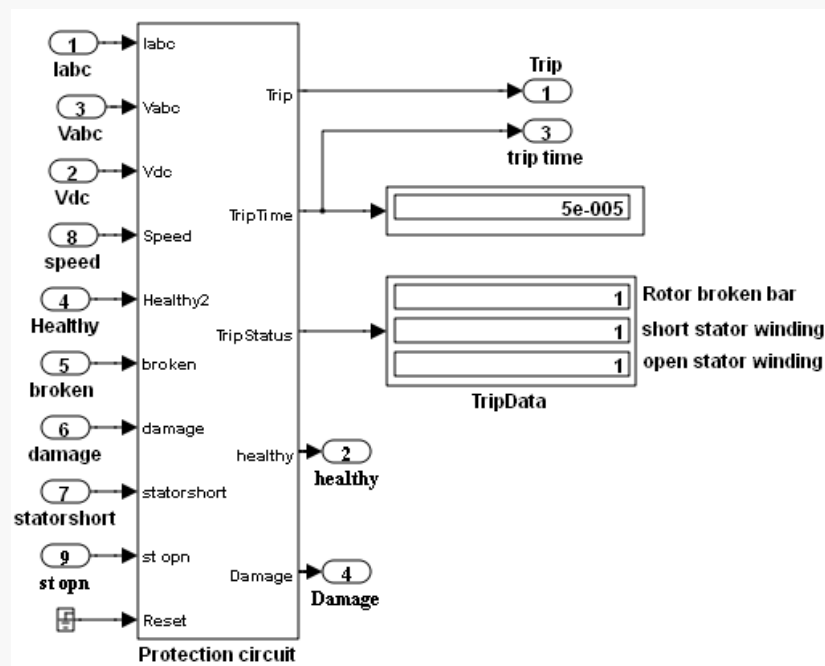


Figure 6.17. Monitoring outputs for three faults case

In another test, the fault was released after a few seconds and then the SVM signal was generated. After that the faults was introduced again as can be shown in Figure 6.18.

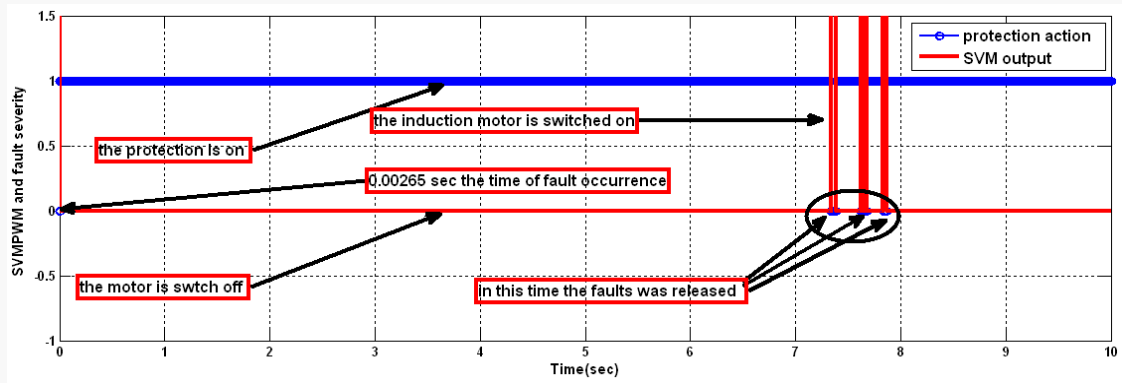


Figure 6.18.SVM (red) with trip binary decision

Finally three different faults were simulated, stator open winding, stator short winding and when the voltage of the supply is less than 200V as mentioned earlier. At the beginning, the IM was healthy, then open and short were introduced in two individual cases at 4sec, after that the voltage reduced to below 200V to simulate the third fault at 5sec, after that both open winding and reduction of volt were introduced together at 7 sec. The vector control was dominant, then after 4 sec switched to closed loop V/F control to compensate the stator open or short winding .This control technique switched to open V/F control to compensate the last fault and maintain the operation of the motor with some perturbation. Protection stage was activated to stop the operation in the compound faults. Figure6.19 shows the smooth transition between the controllers.

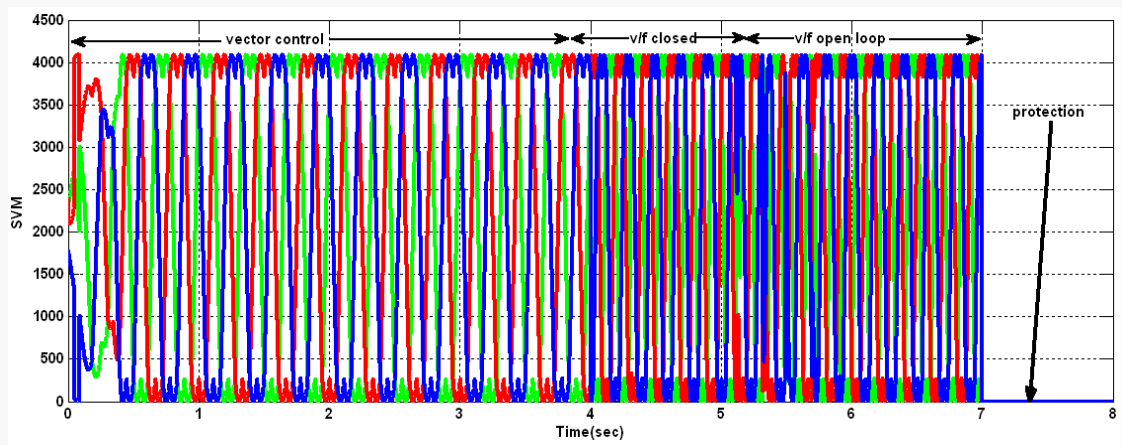


Figure 6.19.SVM signal to control the inverter during different control strategies

In this work, bases of 13 possible trips have been included to prove the importance of this thesis in the field of fault diagnosis. The performance and efficacy of the monitoring and protection unit has been tested for the following electrical faults, stator faults, minimum voltage fault and speed sensor fault and the units have been found quite efficient in dealing with these faults.

6.6 Summary

This chapter has covered up the following finding in detail with respective diagrams and tables.

1. The operating features of the proposed scheme have been assessed by using the computer simulation with Matlab/Simulink.
2. The machine faults have been detected quite successfully with the proposed methods which have been testified by the simulation results.
3. The mechanical and the electrical faults can be monitored quite effectively by applying the condition monitoring with wavelet transform.
4. The protection technique has been found very successful in monitoring and detecting the change of running conditions.

Chapter 7: Experimental Results

7.1 Introduction

Industrial processes or safety critical applications may come across unanticipated halts which result in substantial costs. As such costs are not acceptable, electric drives have been suggested to overcome this problem. In this regard, the availability of information from the system determines detection of fault. A db10 wavelet has been used for fault detection in this study for analysing stator current. The limits of every fault have been checked by using wavelet index.

In the experimental work, the faults mentioned below will be taken into consideration:

1. Speed sensor fault
2. Stator open winding
3. Stator short winding
4. Under voltage fault

All measurements, power electronics, control and motors have been included in the experimental setup of the 1kW IM. Based on a Texas Instrument TMS320F28335 is the platform of eZdspF28335, which provides some measurements and the control.

By using the RS232 cable between the PC and TMS320F28335 DSP, recording of the outputs through serial communication interface (SCI) has been done.

A set-up based on the TMS320F28335 DSP has been utilized for implementing the fault tolerant control algorithm. An ADC with a sampling frequency of 20 kHz has been employed for obtaining the rotor speed and the stator current. The maximum 3V accessibility to the DSP was guaranteed by using the closed loop Hall effect transducer (HX50-p/sp2) as a current transducer that was not inductive with 1.45V/A, the resistive voltage divider and the voltage transducer (LV25-p).

For ensuring the restriction of the encoder signal transmitted to the F28335 DSP to 3V, a signal conditioning circuit was used, which was employed for acquiring the encoder signal in the first place as can be seen in appendix A.

7.2 Serial Communication Interface (SCI)

Two components could be identified with the serial communications interface (SCI):

1. Target side: through SCI to the host, the specific data from the prime Simulink program or the target was delivered by the SCI transmit block, being primarily responsible for this activity and forming this side's main composition.
2. Host side: the SCI setup and SCI receive were the two main identifiable blocks here.

Figure 7.1 shows the serial communication interface linked to the F28335 DSP. The scalar or vector data delivered from here was received by the SCI setup and the SCI receive.

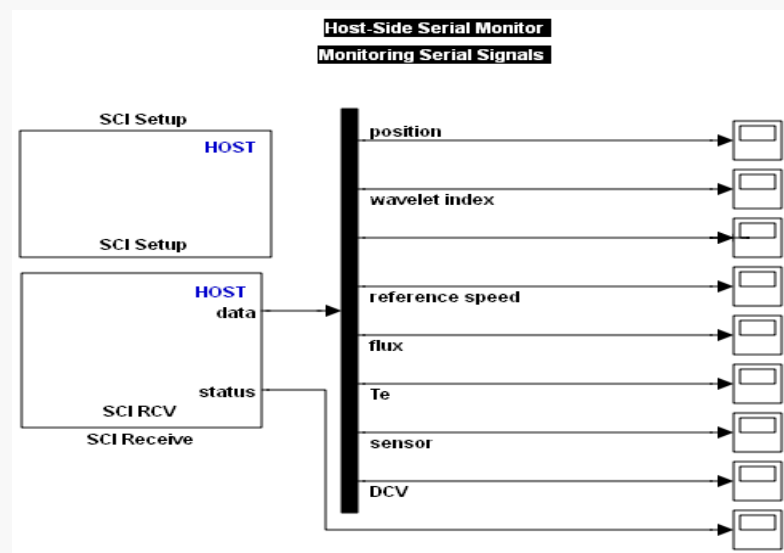


Figure 7.1. Serial communication Interface to show the experimental output

7.3 Experimental Work

The healthy case and the faulty case were the divisions used for dividing the experimental work. The stator's short winding, minimum voltage, open winding and sensor fault were included.

As is evident from the work procedure demonstrated by Fig 7.2, the implementation and the compilation of the fault tolerant control suggested circuit was carried out by the Matlab Simulink and F28335 DSP controller respectively

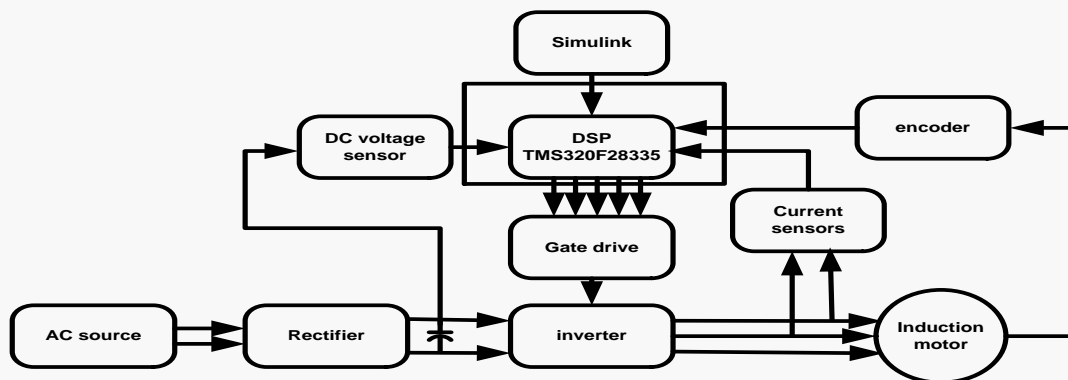


Figure 7.2. Structure of the proposed work

7.4 Prognostic Unit

The analysis method has a crucial part to play in industry, in relation to the investigation of the healthy status of an IM. For detecting fault at the initial stage, one of the many tools of analysis is prognosis. The stator current's signature waveform has been studied extensively in many of the researches carried out in this area (Wesley G. Zanardelli, 2005).

As depicted by Figure7.3, the prognostic has been utilized as an earlier alarm stage in this study.

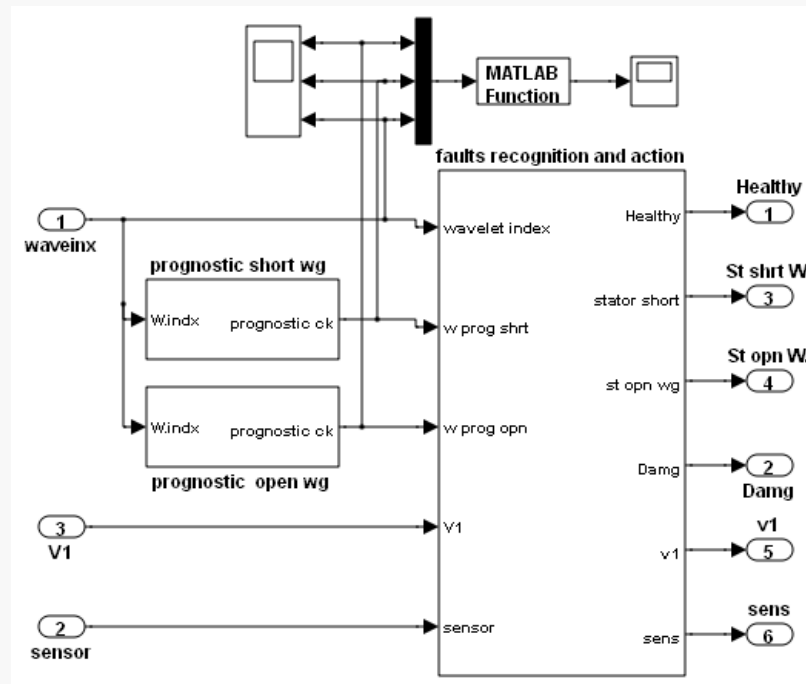


Figure 7.3. Simulink representation of prognostic scheme

After receiving the wavelet index of every case, the unit of fault recognition and action has a significant part to play in taking logical action. Logic 0 or logic 1 can basically be the fault output. For enabling the dominance of the specific controller in action, this logical decision is utilized. Figure 7.4 aptly demonstrates the Simulink representation of the fault recognition and action unit.

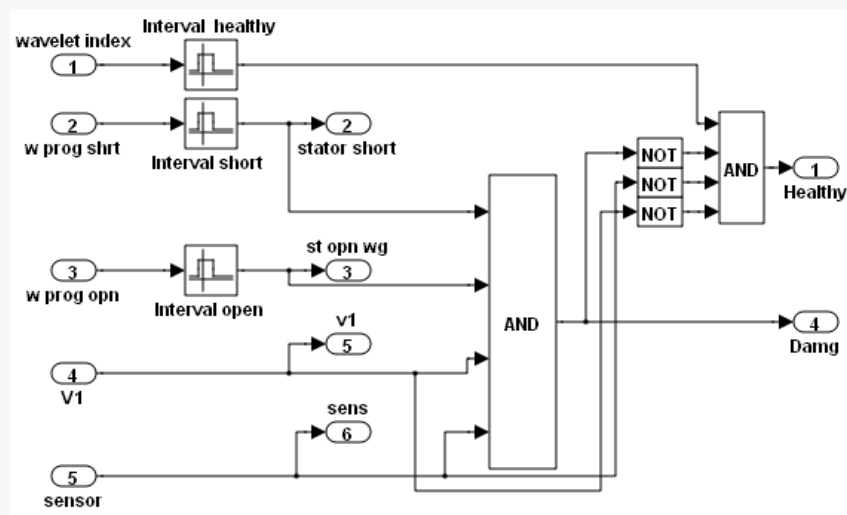


Figure 7.4. Simulink representation of fault recognition and action unit

Figure 7.5 shows the Simulink implementation of the prognostic blocks responsible for receiving the wavelet index.

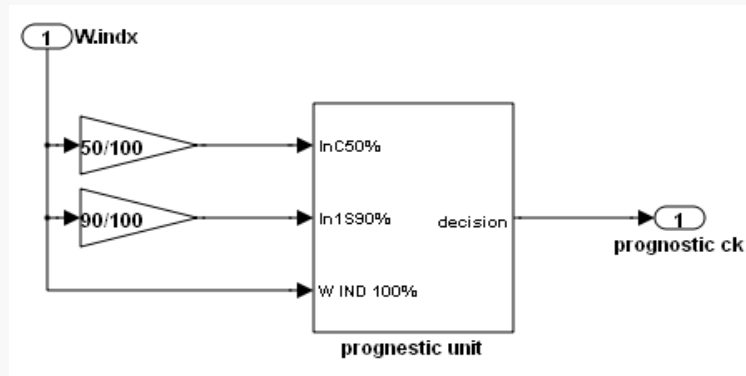


Figure 7.5. Simulink representation of inside prognostic unit of each fault

Figure 7.6 illustrates the Simulink implementation of the prognostic unit block.

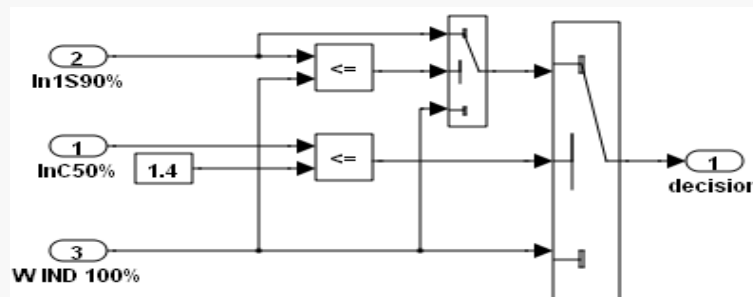


Figure 7.6. Simulink representation of details of the prognostic unit in healthy case

For applications of this sort, wavelet ranks as a suitable option. The value of the wavelet index determines the prognostic. With regards to the stator open winding and stator short winding, the first hint of the variations in parameters is given by a 50% of wavelet index. As the IM's performance would be according to the specifications, this value is just a mere indication. As shown by Figure 7.7, the stator open winding presents the second vital indication, being the 90% of the wavelet index.

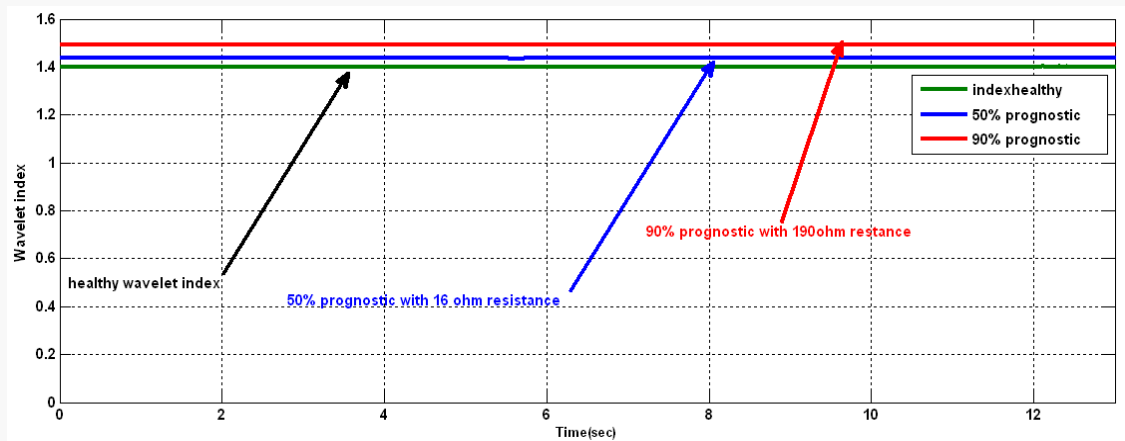
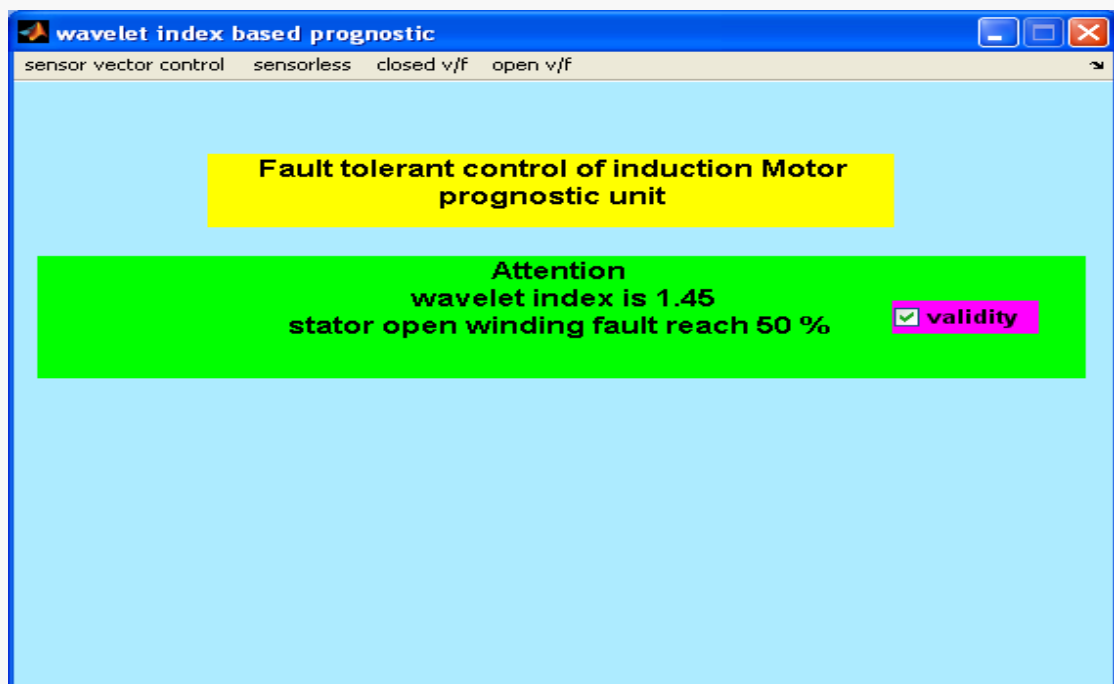


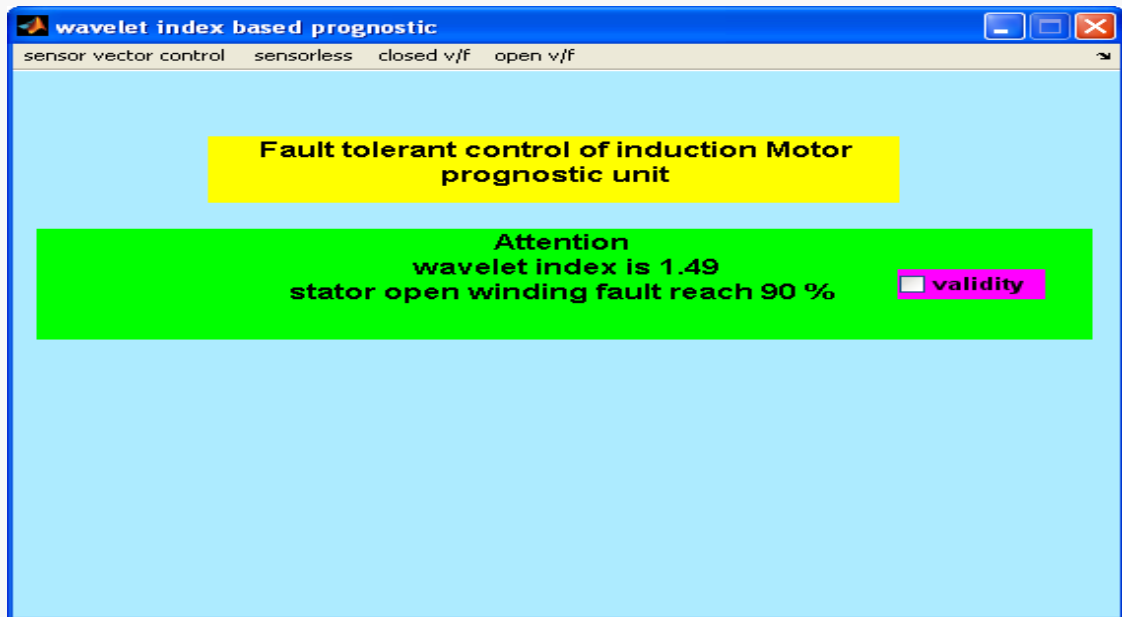
Figure 7.7. Experimental wavelet index for prognostic in the open stator winding

GUI7.1 shows the prognostic circuit's graphical output with 450RPM in the stator open winding. The stator open winding fault experiences an increase till 50% of its complete value as illustrated by the prognostic unit of this GUI.



GUI 7.1. The stator open winding fault reach 50% of its complete value

The GUI7.2 shows the prognostic circuit's graphical output, with 450 RPM in the stator open winding. The stator open winding fault experiences an increase till 90% of its complete value as shown by the prognostic unit in this GUI.



GUI 7.2. The stator open winding fault reach 90% of its complete value

Figure 7.8 shows the extremities of the wavelet indices with 900RPM in the short stator winding.

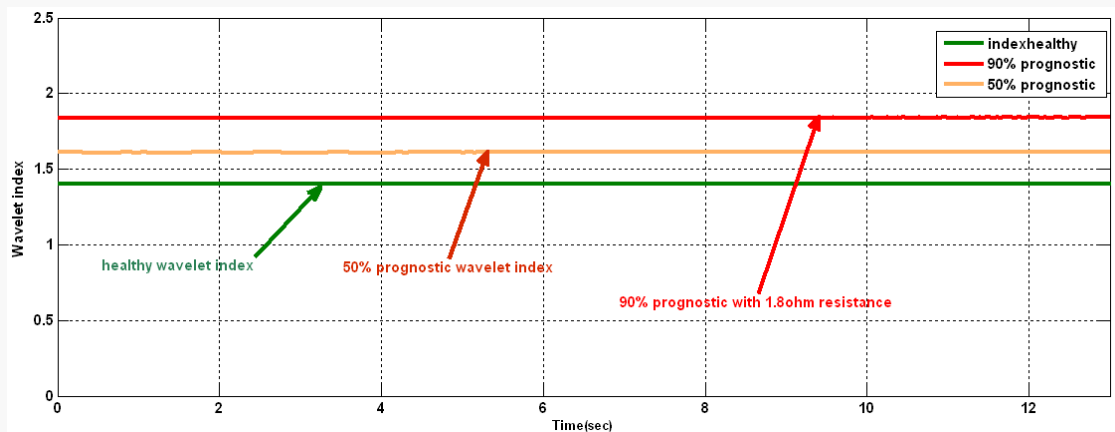
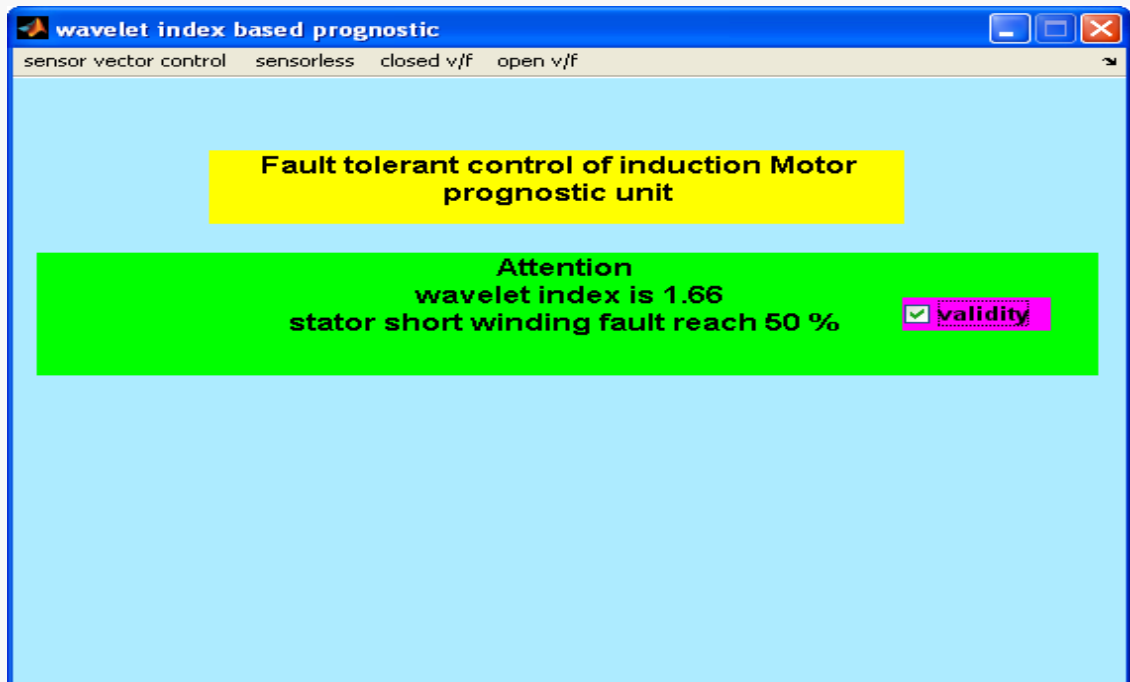


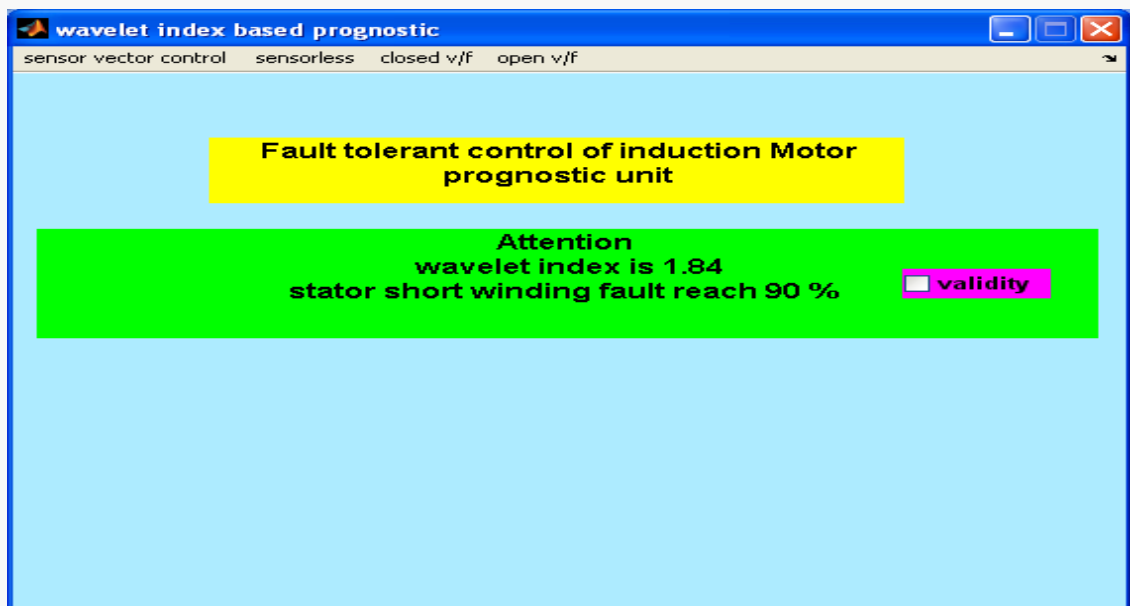
Figure 7.8. Experimental wavelet index for prognostic in the short stator winding

GUI 7.3 shows the prognostic circuit's graphical output, with 900RPM in the stator short winding. The stator short winding fault experiences an increase till 50% of its complete value (0.8 Ω) as shown by the prognostic unit in this GUI.



GUI 7.3. The stator short winding fault reach 50% of its complete value

GUI 7.4 shows the prognostic circuit's graphical output with 900RPM in the stator short winding. The stator short winding experiences an increase till 90% of its complete value as demonstrated by the prognostic unit in this GUI.



GUI 7.4. The stator short winding fault reach 90% of its complete value

The faults can be divided into the following in accordance with the impact on performance of the system:

1. Additive faults
2. Multiplicative faults
3. Abrupt faults
4. Incipient faults

The slow variation makes incipient fault more risky (Wenjun Li, 2006). The inability to differentiate between this fault and parameters variation is its principal difficulty. Simulation was utilized for determining the healthy wavelet index threshold in order to overcome such a misunderstanding. Figure7.9 shows 1.4 WI as the practical result, employed for the same reason as above as well as the simulation wavelet index in same conditions.

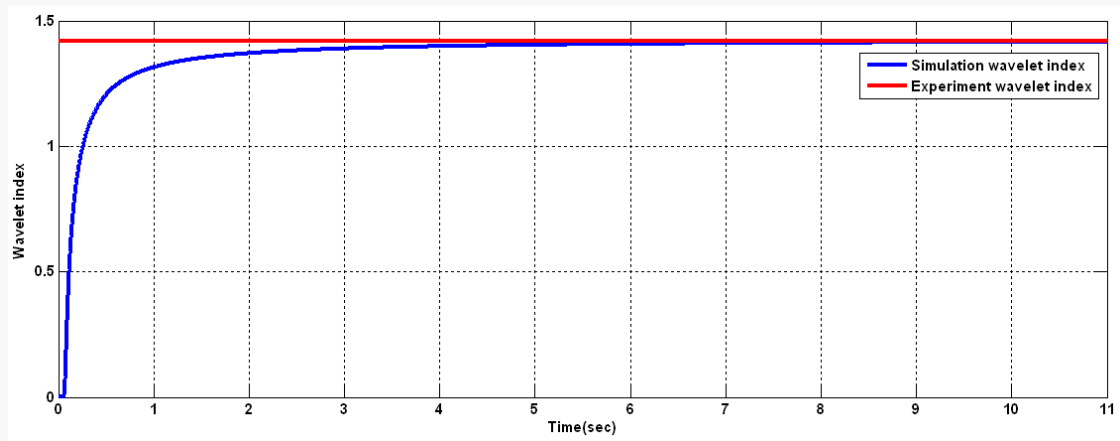


Figure 7.9. Experimental and simulation wavelet index in the healthy case

7.5 Healthy Case

The wavelet index recorded through SCI Simulink block with RS232 is linked to the PC in the healthy IM. The results were nearly matching each other according to the calculations done at various speeds (450RPM, 900 RPM and 1600RPM) for the experimental wavelet index.

Figure7.9 shows how the healthy motor wavelet index will be accounted for.

Figure7.10 shows the ARX modeling of experimental I.M healthy wavelet index

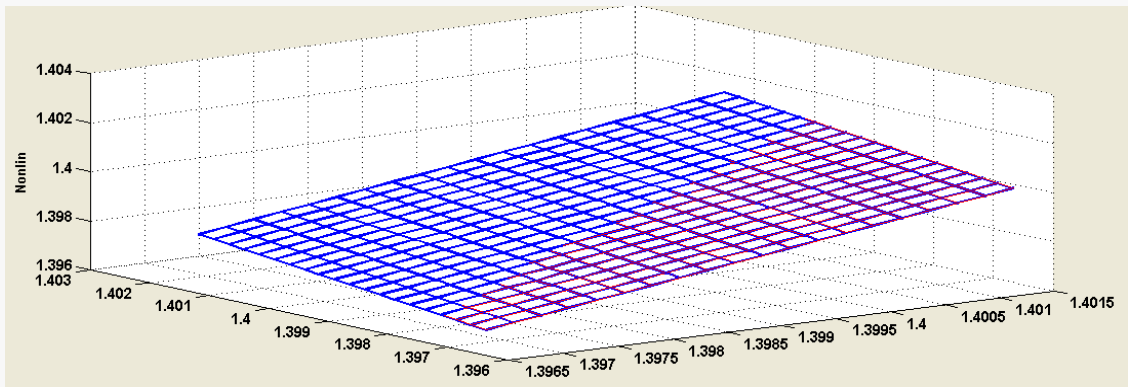


Figure 7.10. ARX modeling of healthy IM wavelet index

A good indication of the frequency and time localization is provided by the domain construction and frequency domain of the stator current signal due to the wavelet decomposition. Any frequency of the signal experiencing any change or variation was detected by this decomposition.

As shown by Figure 7.11, for all levels of decomposition, the stator current sinusoidal waveform was not distorted from the main signal in the healthy IM.

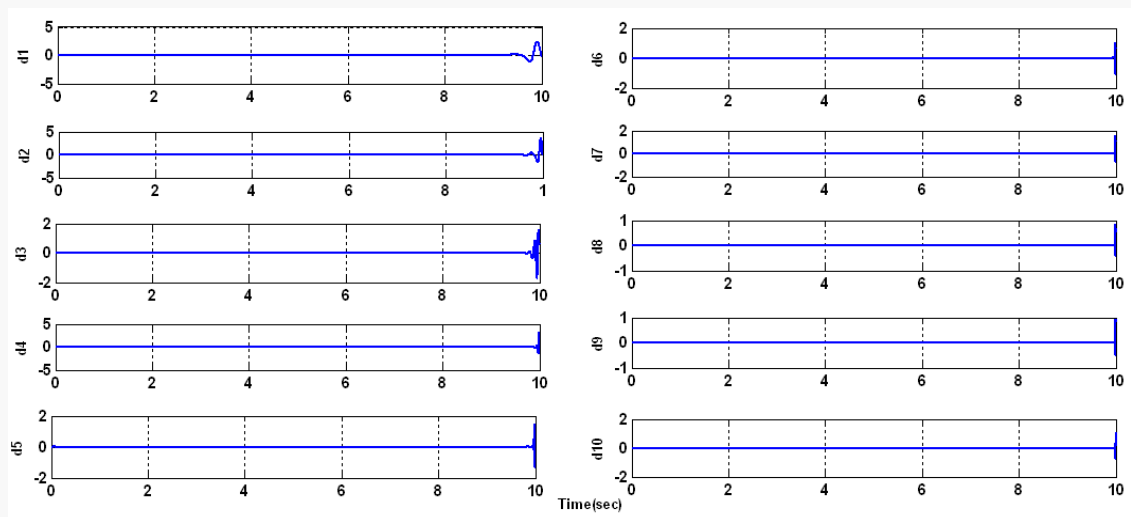


Figure 7.11. Stator current wavelet decomposition in healthy motor

7.6 Faulty Case

Consideration will be given to the stator short winding fault, stator open winding fault, speed sensor fault and the minimum voltage.

7.6.1 Shorted Stator Winding

As demonstrated in Fig 2.7, the stator resistance of the IM is linked to the parallel variable resistance for the stator short circuit winding fault.

The shunt resistance was increased in steps 0.1Ω for the purpose of performing the reduction of 20Ω stator winding resistances. As shown in Eq. 7.1, this was done till the total shunts combination became 2Ω .

$$R_{sh} = 0.1R_{org} \quad (7.1)$$

From lower short circuit current to a higher level, most of the induction winding failures gradually proceed, finally breaking in the end (Dimas Anton A, 2010).

Recording of the wavelet index was done at every step, followed by the plotting of its major value.

Every step witnessed the stator current's wavelet decomposition. Figure 7.12 illustrates the final decomposition.

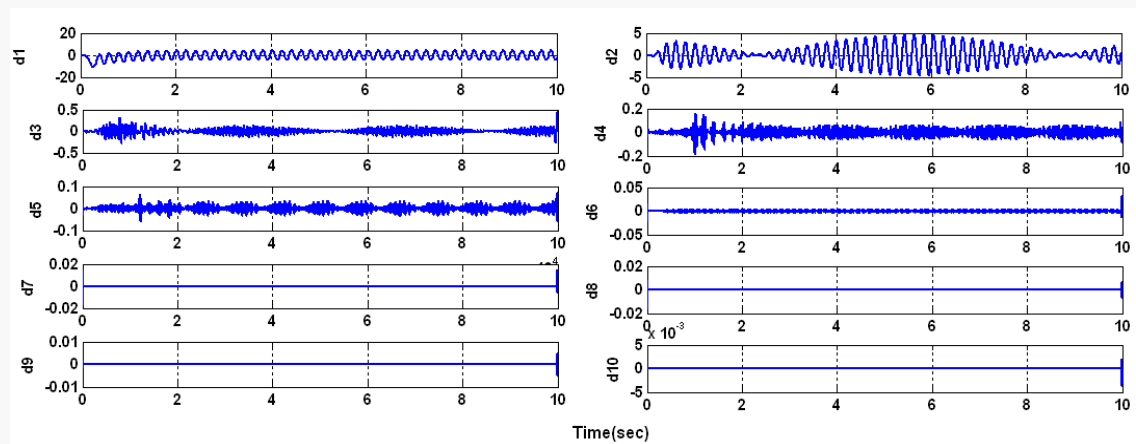


Figure 7.12. Wavelet decomposition of stator current in the short winding fault

This figure shows the detailed decompositions, the output of the high pass filter implemented previously. The stator current wave form is not included as it is nearly the same as the wavelet decomposition at d_1 . The signal will be categorized as a sound indication of the original signal in $[d_2-d_6]$. For the wavelet index measurements, the first stage of extracting information can be $[d_7-d_{10}]$; for calculating the wavelet, d_8 is the best

level for utilization. The approximation levels were recorded but have no effect in this stage so it is not included.

To assess the IM, the wavelet index has been utilized for various levels of speed. As is evident for the following results, comparison with the simulation results has also been carried out.

7.6.1.1 At 450 RPM

Figure 7.13 shows the experimental test of speed response in the healthy IM.

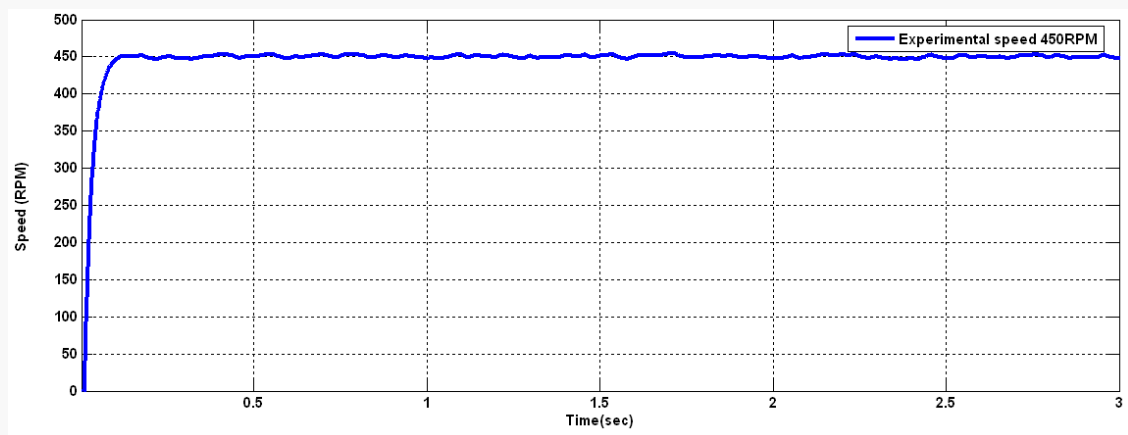


Figure 7.13. Experimental speed response of the proposed FTC at command speed of 450RPM

Figure 7.14 shows the mean value of the wavelet index for simulation and experiment due to the influence of shunt resistance. The phase resistance at 450RPM was also added.

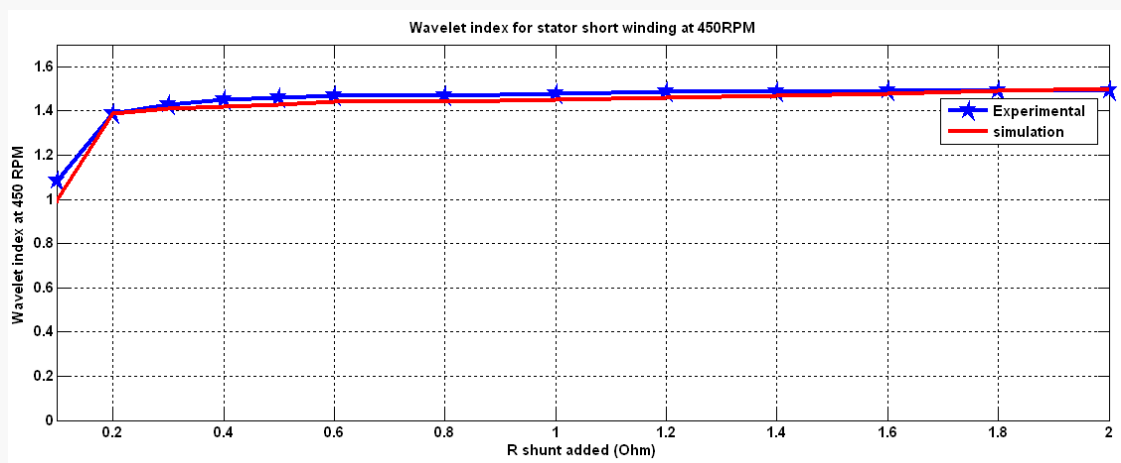


Figure 7.14. Simulation and experimental wavelet index at 450RPM

After the addition of the shunt resistance, table7.1 illustrates the value of the stator resistance with the wavelet index at 450RPM.

Table7.1 Wavelet index at 450RPM

$R_{sh}(\Omega)$	$R_s R_{sh}(\Omega)$	Wavelet index
0.1	0.0995	1.1
0.2	0.1980	1.4
0.4	0.3922	1.43
0.8	0.7692	1.43
1.6	1.4815	1.5
1.8	1.6514	1.5
2	1.8182	1.5

7.6.1.2 At 900 RPM

Figure 7.15 shows the speed response in the healthy IM.

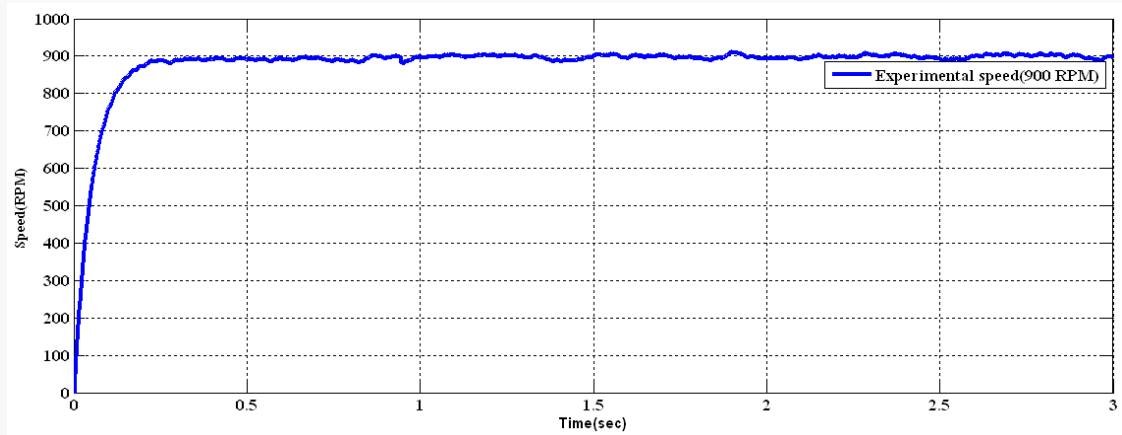


Figure 7.15. Experimental speed response of the proposed FTC at command speed of 900RPM

Figure7.16 shows the mean value for experimental and simulation results alike due to the influence of shunt resistance. Phase resistance at 900 RPM was also added.

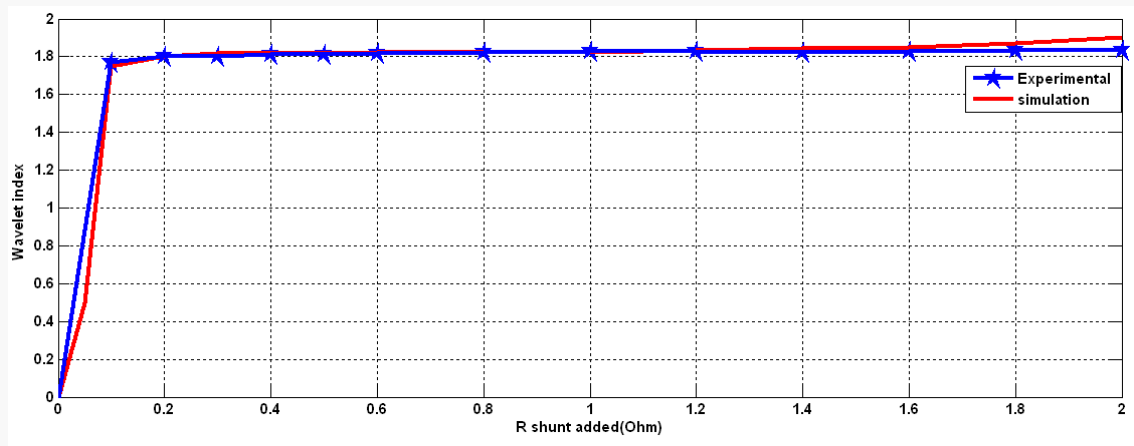


Figure 7.16. Experimental and simulation wavelet index at 900RPM

After the addition of the shunt resistance with the wavelet index, table 7.2 illustrates the value of the stator resistance.

Table 7.2. Wavelet index due phase resistance and shunt resistance at 900PM

$R_{sh}(\Omega)$	$R_s R_{sh}(\Omega)$	Wavelet index
0.1	0.0995	1.78
0.2	0.1980	1.8
0.4	0.3922	1.8
0.8	0.7692	1.82
1.6	1.4815	1.84
1.8	1.6514	1.84
2	1.8182	1.84

7.6.1.3 At 1600 RPM

With the full addition of the shunt resistance, Figure 7.17 shows the speed response in the healthy IM.

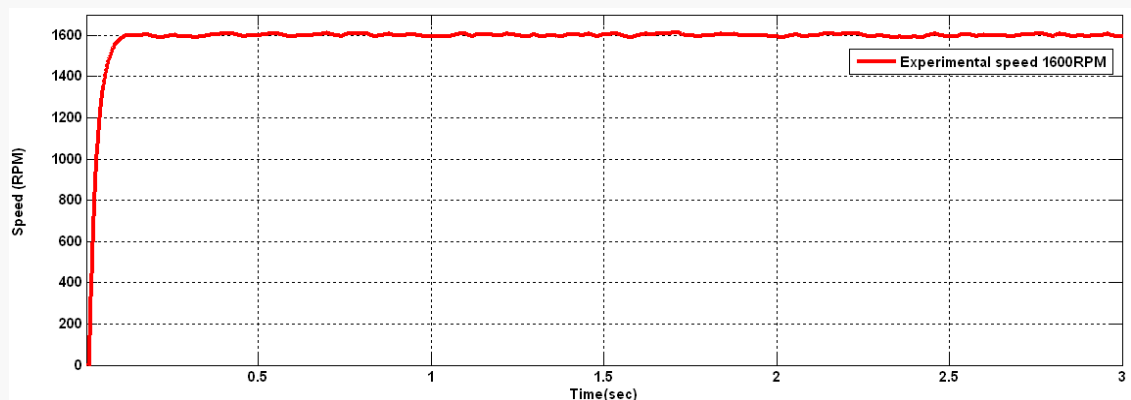


Figure 7.17. Experimental speed response of the proposed FTC at command speed of 1600RPM

Figure7.18 shows the mean value of the wavelet index for simulation and experimental work alike due to the impact of shunt resistance. At 1600 RPM, the phase resistance was also added.

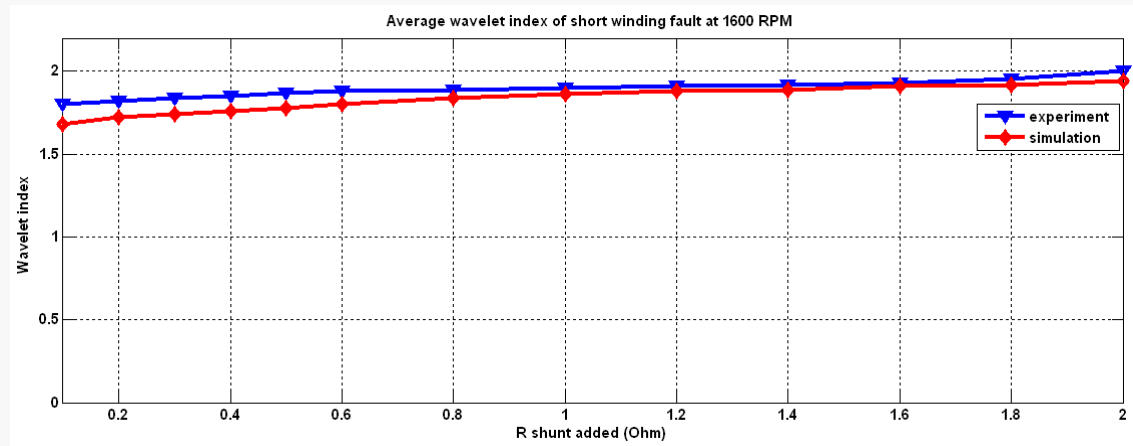


Figure7.18. Experimental and simulation wavelet index at 1600RPM

Table7.3 illustrates the value of the stator resistance after the addition of the shunt resistance with the wavelet index at 1600 RPM.

Table 7.3 Wavelet index due phase resistance and shunt resistance at 1600RPM

$R_{sh}(\Omega)$	$R_{st} R_{sh}(\Omega)$	Wavelet index
0.1	0.0995	1.8
0.2	0.1980	1.81
0.4	0.3922	1.85
0.8	0.7692	1.9
1.6	1.4815	1.92
1.8	1.6514	1.95
2	1.8182	2

Figure7.19 shows the comparison done between three experimental wavelet index levels of all speeds in the stator short winding.

Controllers have been given important information by this figure i.e. to activate the specific controller linked to the faults. The amplitude of the stator current is proportional to fault level and induction's rotation speed.

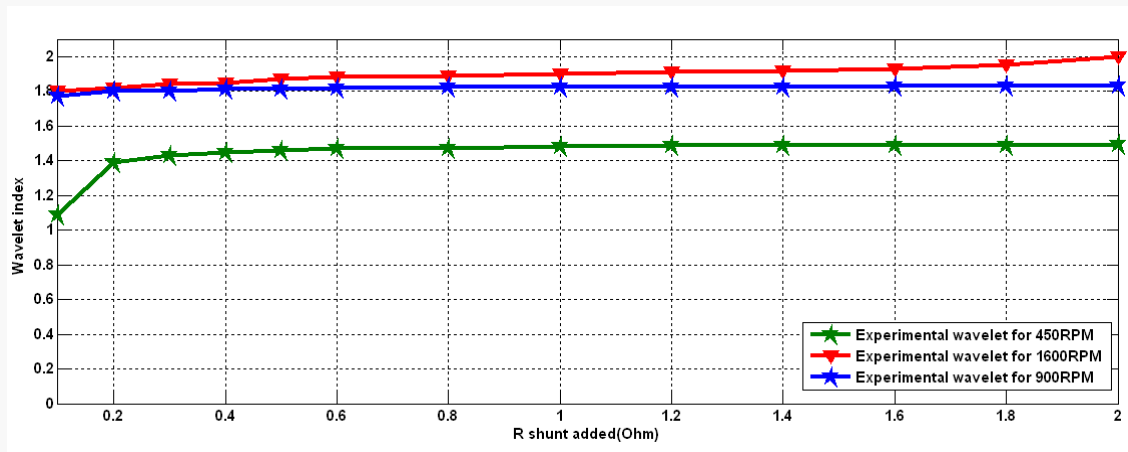
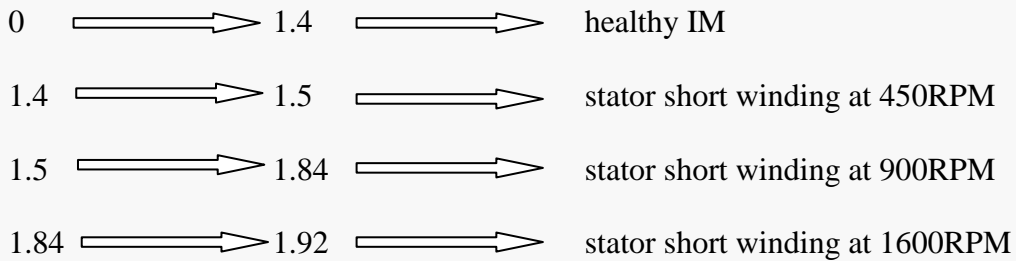


Figure 7.19. Experimental wavelet indices for different speed in stator short winding

In this figure the wavelet indices as follows:



The following will present the wavelet indices of this figure:

The suggested criteria for the wavelet index is well representative of the IM condition as is evident from the levels of the wavelet indices. For the evolution of controllers, it can also be termed as very efficacious.

Determining the mathematical relation between total impact of the stator resistance and the wavelet index is another supporting mechanism for the wavelet index intervals. No mismatching of the FTC algorithm with switching mechanism should exist due to any situation, and this equation should ensure that.

The following equations will represent the obtainable stator short winding wavelet index:

Stator short winding wavelet index can be obtained as in the following equations:

1. The wavelet index equation at 1600 RPM with linear curve fitting is:

$$W_{ind} = 0.0217 * R_{shunteffect} + 1.796 \quad (7.2)$$

And the norm of the residual which is the length of a residual vector expressed as the square root of the sum of the square of its components =0.0365.

2. The 900 RPM wavelet index equation with linear curve fitting is:

$$W_{ind} = 0.0843 * R_{shunteffect} + 1.7822 \quad (7.3)$$

And the norm of the residual =0.0456

3. The 450 RPM wavelet index equation with linear curve fitting is:

$$W_{ind} = 0.0986 * R_{shunteffect} + 1.146 \quad (7.4)$$

And the norm of the residual=0.3119

For progressing to the design stage of formulating mitigating strategies for faults of such types, a thorough understanding of the impacts of these faults on the performance of machines is mandatory, according to this investigator. A smooth transition existed between the observers and the sensor output, with no observable spikes or oscillations during the switching modes.

The FTC algorithm was tested by utilizing one fault from each group of faults described earlier on in chapter 5. For the first group, encoder fault was selected as the sample, while for the second and the third group, the selection was stator short winding, stator open winding and minimum output voltage together with compound fault respectively, for ensuring the timely introduction of the protection circuit.

Introduction of the speed sensor fault was given at the commencement of operation. The complimentary controller of the sensor vector control was the sensorless vector control. After the 1 sec of operation, stator short winding was introduced. As demonstrated by Figure7.20, a short smooth speed transition with a little speed reduction was experienced by the suggested switching strategy in reconfiguring the control from sensorless vector control to closed loop V/F control.

The minimum output voltage fault was introduced at 1.7 seconds. In place of closed loop V/F control, the corresponding open loop V/F controller was switched on with a short speed transition.

For testing the protection unit, compound fault from the above two faults was introduced. As illustrated by Figure7.20, zero SVM signals were transmitted to the inverter for halting the operation of the IM.

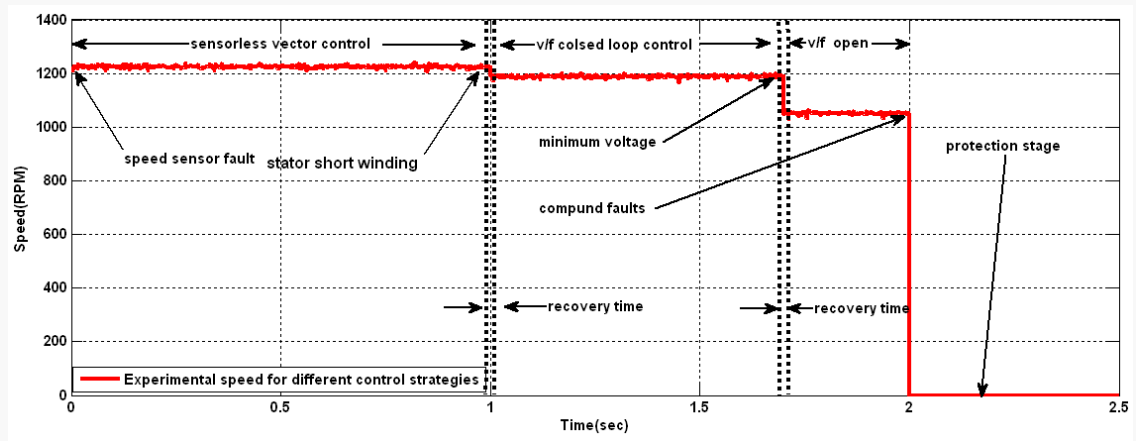


Figure7.20. Experimental speed transition for different controllers at 1200RPM

Figure7.21 shows the experimental setup for measuring the wavelet index in the short stator winding. As mentioned previously, a shunt resistance was linked to one of the stator phase resistance in this figure.

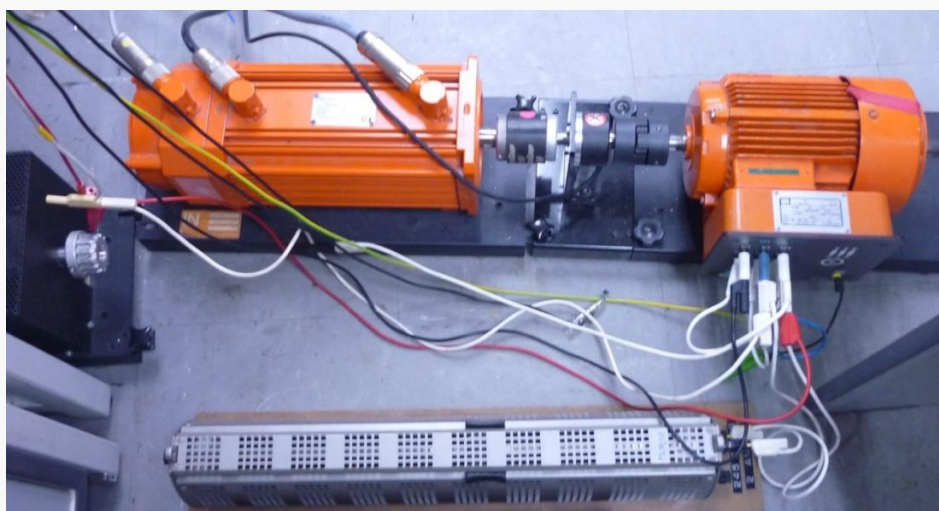


Figure7.21. Experimental setup to measure the wavelet index in the short stator winding fault

7.6.2 Stator Opening Winding

The stator phase resistance of the IM was linked in series with variable resistance for the stator open winding fault.

The series resistance was increased in steps 1Ω for executing the increase of the original stator phase winding resistances. This was done till the series combination of the two series resistances exceeded by ten times of the original stator resistance ($20\ \Omega$).

$$R_{series} = 10R_{org} \quad (7.5)$$

Each step was subjected to the wavelet decomposition of the stator current in the open winding. Figure 7.22 shows the final decomposition.

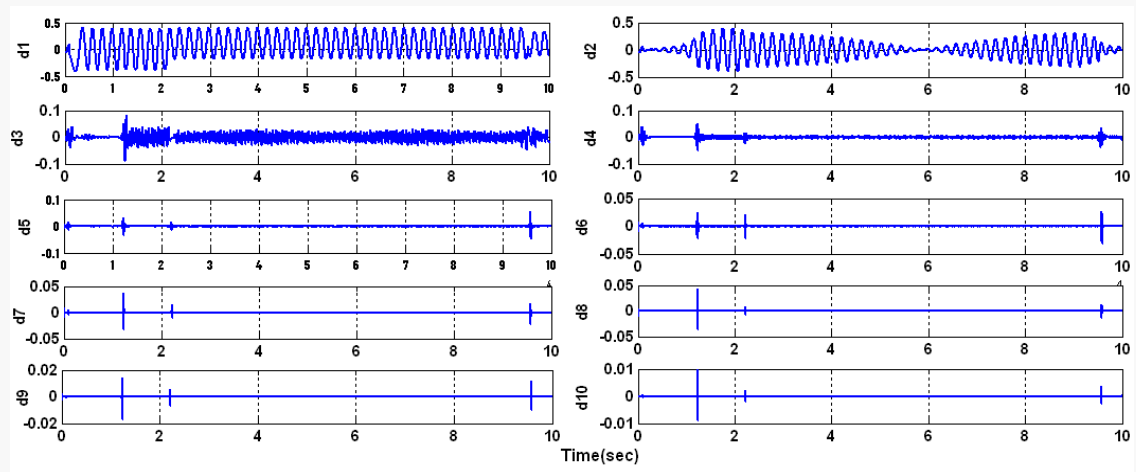


Figure 7.22. Wavelet decomposition of the stator current in the open winding fault

For the stator open winding, a procedure similar to the previous one will be performed.

7.6.2.1 At 450RPM

Figure 7.23 presents the mean value of the wavelet index for experimental and simulation work alike, as a result of the efficacious series resistance. At 450 RPM, this was added with the phase resistance.

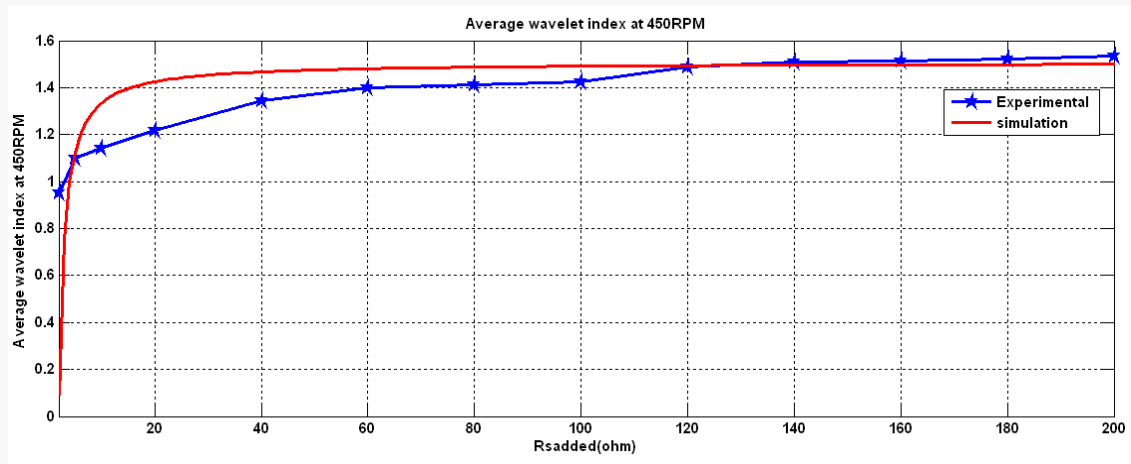


Figure 7.23. Experimental and simulation Wavelet index at 450RPM

After the addition of series resistance with the wavelet index, table 7.4 illustrates the value of the stator resistance at 450 RPM.

Table 7.4 .Wavelet index due to the combination of the two series resistance at 450RPM

$R_{ser}(\Omega)$	$R_{st} + R_{ser}(\Omega)$	Wavelet index
1	21	0.95
20	40	1.21
40	60	1.38
60	80	1.40
100	120	1.42
160	180	1.60
200	220	1.75

7.6.2.2 At 900 RPM

Figure 7.24 shows the value after adding the efficacious series resistance with the phase resistance at 900 RPM for the average wavelet index in relation to both experimental and simulation work.

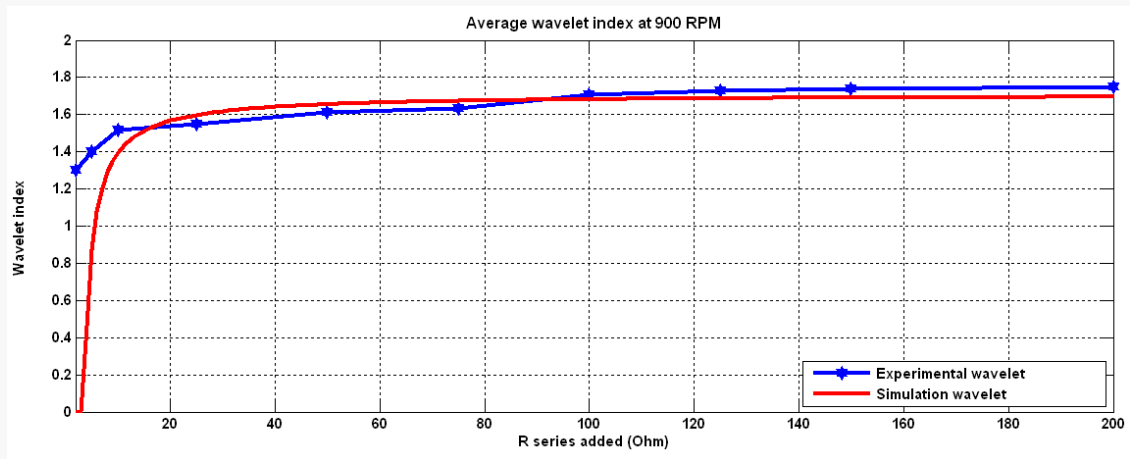


Figure 7.24. Experimental and simulation wavelet index for open winding at 900RPM

After adding the series resistance to the wavelet index at 900RPM, table 7.5 presents the value obtained for the stator resistance.

Table 7.5. Wavelet index and series resistance at 900RPM

$R_{ser}(\Omega)$	$R_{st} + R_{ser}(\Omega)$	Wavelet index
1	21	0.17
20	40	0.39
40	60	0.9
60	80	1.25
100	120	1.58
160	180	1.6
200	220	1.6

7.6.2.3 At 1600 RPM

Figure 7.25 shows the value after adding the efficacious series resistance to the phase resistance at 1600 RPM for the average wavelet index in relation to both experimental and simulation work.

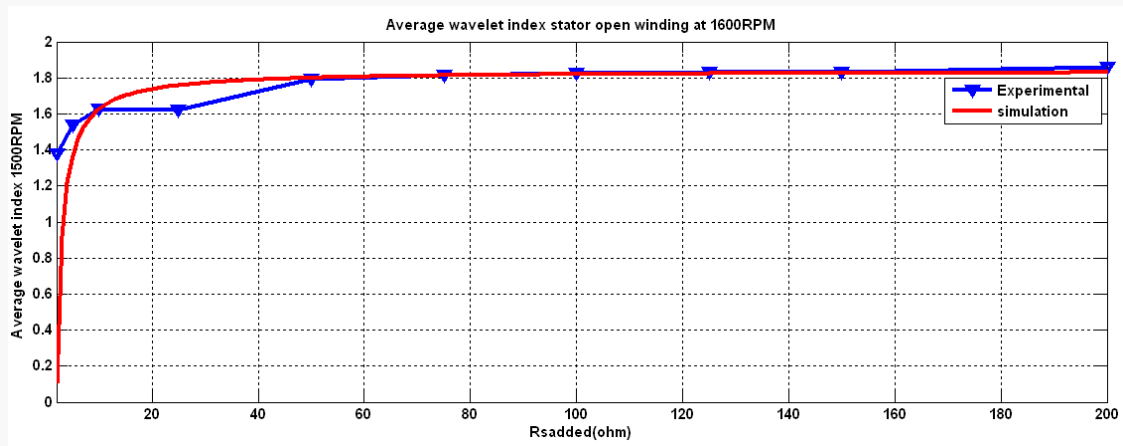


Figure7.25. Experimental and simulation wavelet index for open winding at1600RPM

The value of the stator resistance after adds the series resistance with the wavelet index at 1600 RPM can be illustrated as in the table7.6

Table7.6. Wavelet index and series resitance at 1600 RPM

$R_{ser}(\Omega)$	$R_{st} + R_{ser}(\Omega)$	Wavelet index
1	21	1.4
20	40	1.62
40	60	1.72
60	80	1.82
100	120	1.83
160	180	1.84
200	220	1.88

Figure7.26 illustrates the experimental wavelet index of all speeds in the open winding case.

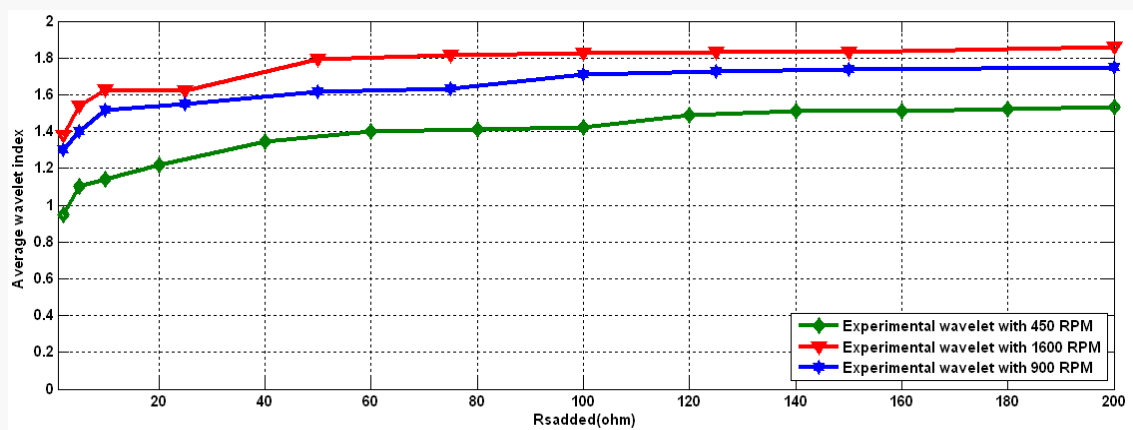


Figure7.26. Wavelet indices for different speeds in stator open winding

The following equations are the ones obtained for every stator open winding wavelet index.

The wavelet index equation at 1600RPM with linear curve fitting in the stator open winding is:

$$W_{ind} = 0.00919 * R_{serieseffect} + 1.369 \quad (7.6)$$

And the norm of the residual=0.287

The 900 RPM wavelet index equation with linear curve fitting in the stator open winding is:

$$W_{ind} = 0.0084 * R_{serieseffect} + 1.257 \quad (7.7)$$

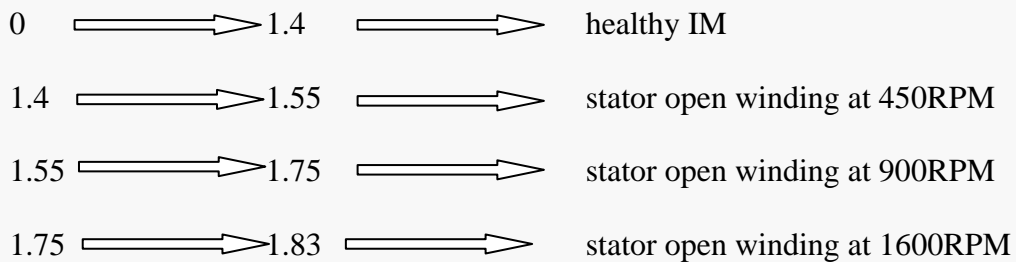
And the norm of the residual =0.932

The 450 RPM wavelet index equation with linear curve fitting in the stator open winding is:

$$W_{ind} = 0.0024 * R_{serieseffect} + 0.943 \quad (7.8)$$

And the norm of the residual=0.30084

In this figure the wavelet indices as follows:



The faults given below are dealt with by the second case study:

1. Encoder fault
2. For testing the incorporation of the protection circuit, open stator winding together with compound fault.

Due to operation in healthy case, the IM commenced with sensor vector control. The sensorless vector control was the complimentary controller of the sensor.

Vector control as the speed sensor fault was introduced at 0.95 sec. At the 1.7 sec of operation, the stator open winding fault was introduced. With a short smooth speed transition but little speed reduction, the suggested switching strategy reconfigured the control from the sensorless vector control to closed loop V/F.

For testing the protection unit, compound fault from the two faults mentioned above were introduced at 2.5 seconds. As shown by Figure7.27, the zero signals were transmitted to the inverter in this scenario and the operation of the IM was halted.

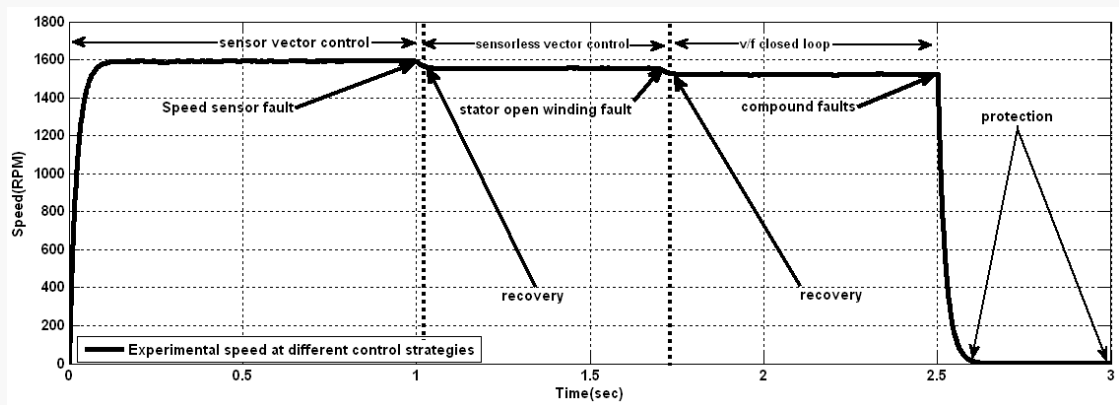


Figure7.27. Experimental speed transition for different controllers with filtering

The activation of the transition controller in sensorless vector control can be illustrated as in Figure7.28. The sensor vector control is available during all transition regions but it will be activated in the starting of operation and when there is no fault in the IM.

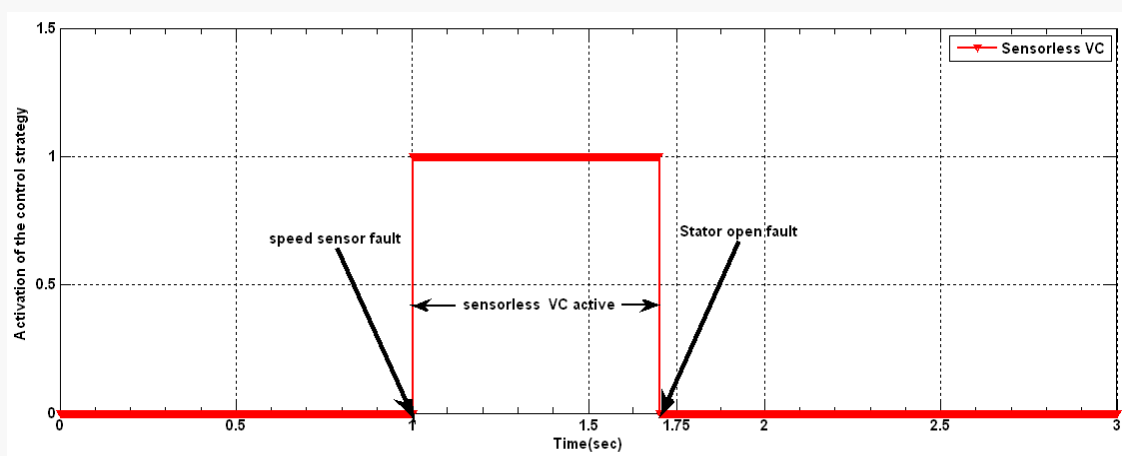


Figure7.28. Experimental logical sensorless and sensor vector control activation

Figure 29 shows the effectiveness of sensorless vector control against the speed sensor fault and its recovery time.

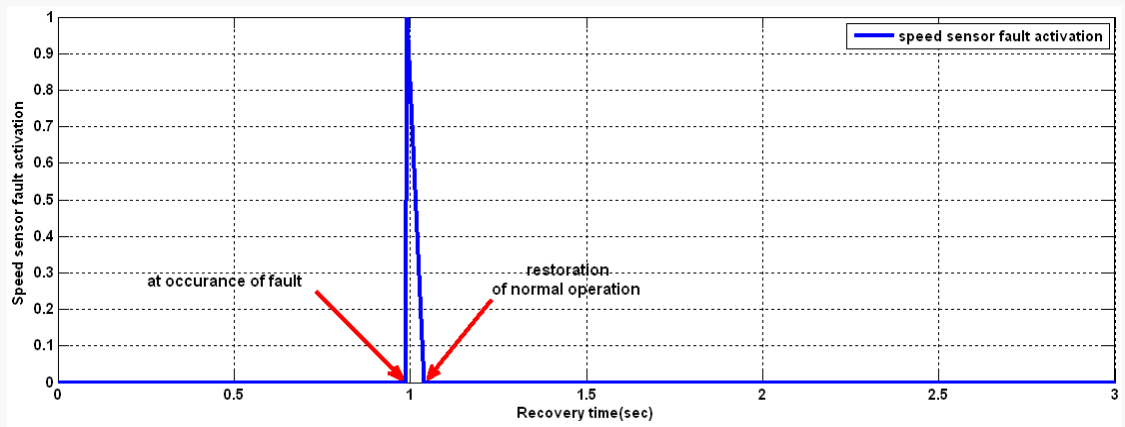


Figure7.29. Speed sensor fault recovery due to activation of sensorless vector control

Figure7.30 shows the experimental closed loop V/F activation in the open stator winding. As previously mentioned, a series resistance was linked to one of the stator phase resistance

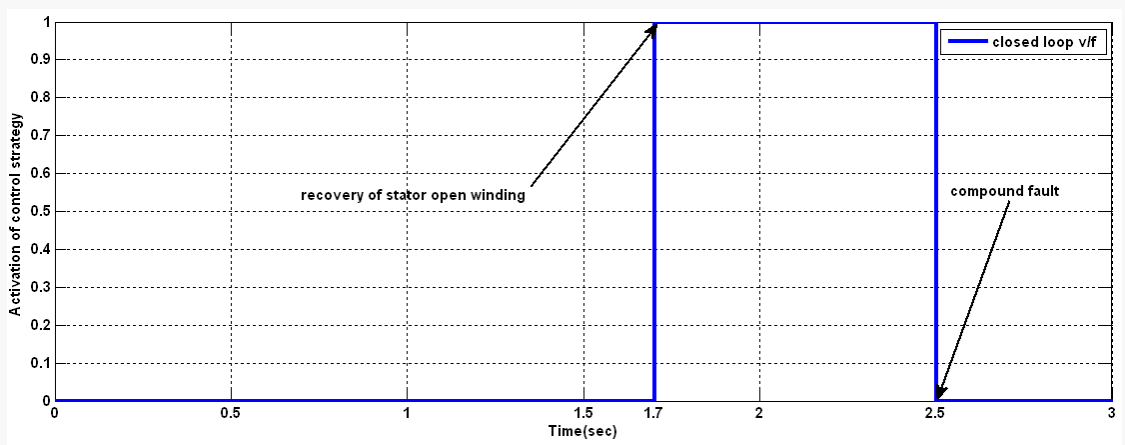


Figure7.30. Experimental logical closed loop V/F control activation

Figure 7.31 shows the effectiveness of closed loop V/F control against the stator open winding fault and its recovery time

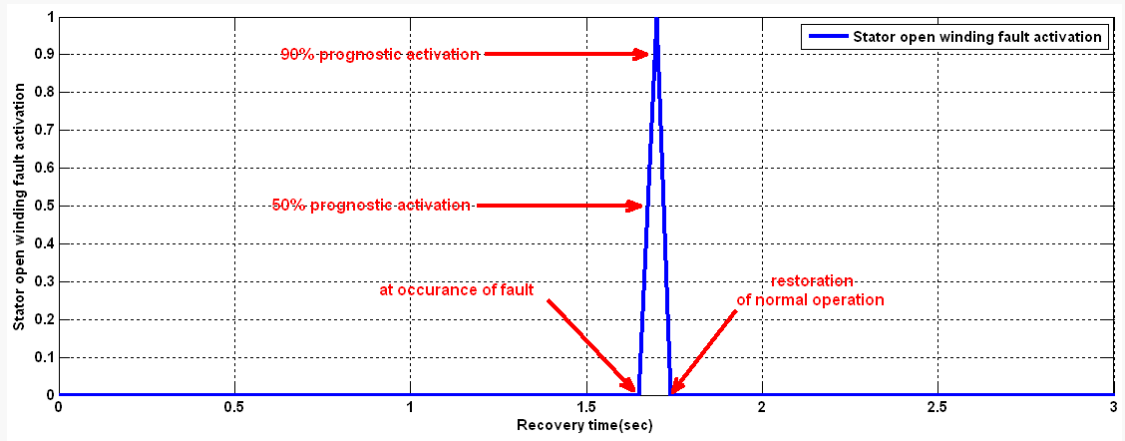


Figure7.31. Stator open fault recovery due to activation of closed loop V/F

Figure7.32 shows the experimental of protection activation stage when the open stator winding with the voltage reduction up to (0.9* rated voltage) as previously mentioned.

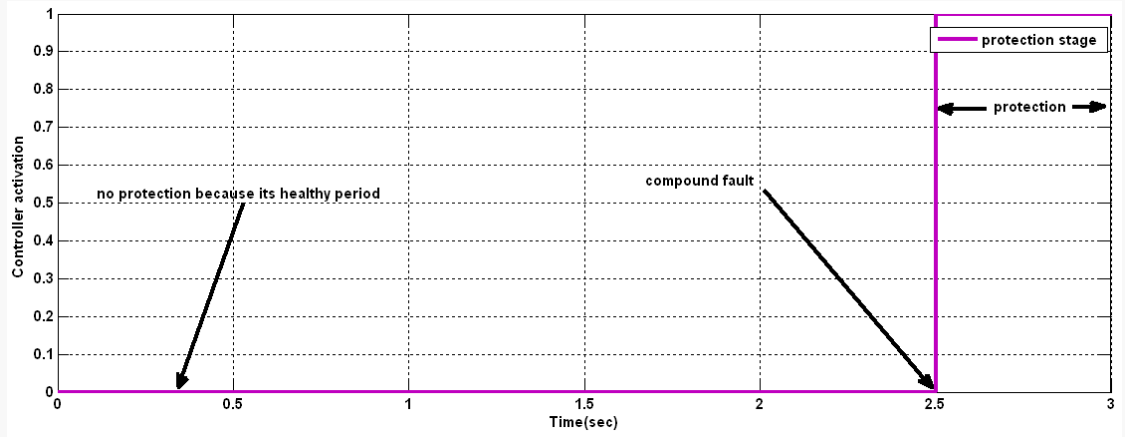


Figure7.32. Experimental logical protection stage activation

The Experimental setup to measure the wavelet index in the open stator winding can be shown in Figure 7.33. In this Figure a series resistance is connected with one of the stator phase resistance as mentioned earlier.

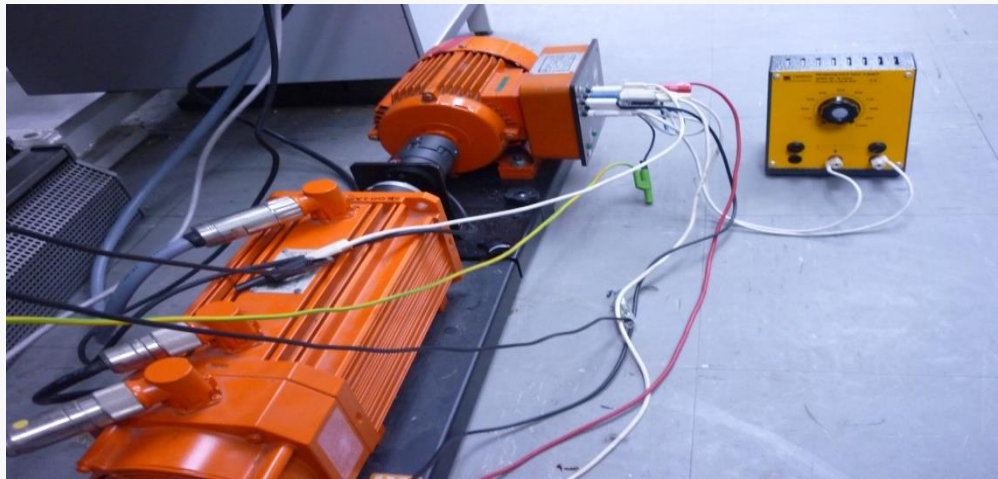


Figure7.33. Experimental setup for stator open winding fault WI measurement

7.6.3 Speed Sensor Fault

In this study, two kinds of speed sensor (encoder) failure are explained:

1. Complete speed sensor failure.

The cables of the encoder channels A, B and index I are disconnected for introducing complete speed sensor failure. Figure7.34 shows the estimation of the sensorless rotor position and the encoder's real output.

As a complimentary to the encoder position measurement, the estimations of the rotor angular position through the BMRAS were utilized. The transition from the sensor control to the sensorless one was facilitated by the calculated speed difference.

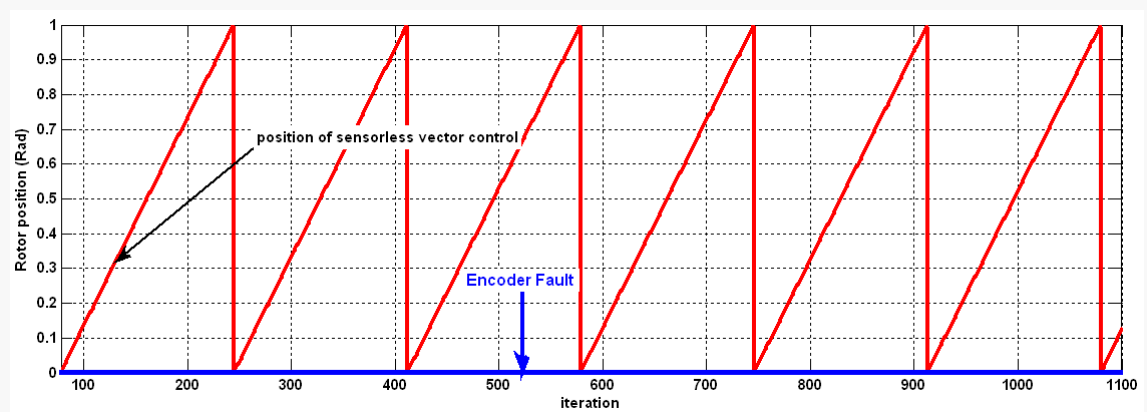


Figure7.34 .Experimental output of BMRAS estimated and encoder failure rotor position

2. Reading speed sensor error in the position. A noise was made in the encoder

LED for introducing this fault.

For a transition from the sensor control to the sensorless one, the measured difference between the angles for estimated rotor position through BMRAS technique and rotor position measured by encoder is utilized. The difference should ideally be zero or render a value close to zero. Figure7.35 demonstrates the BMRAS and the encoder output.

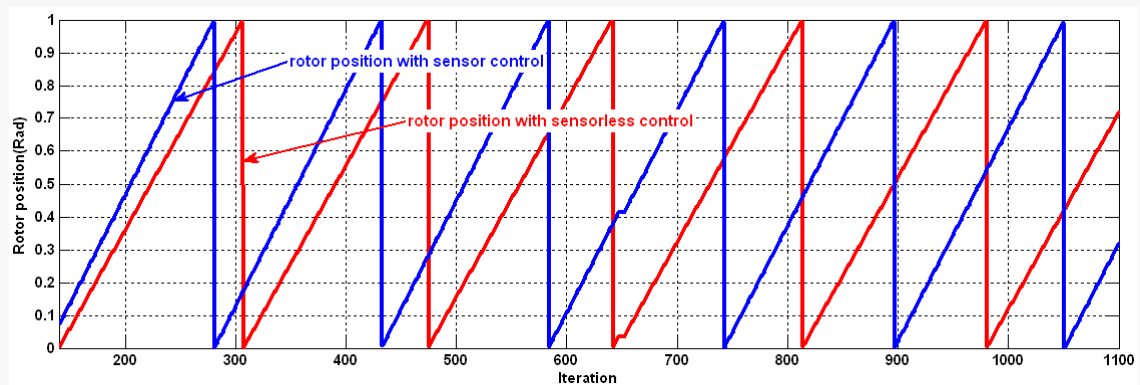


Figure7.35. Experimental output of BMRAS estimated and fault of encoder rotor position

In the beginning of the IM's operation, encoder fault was introduced for testing the flexibility of the fault tolerant control algorithm and its capability of returning back to the sensor vector control. At the beginning of the operation period, sensorless vector control was the complimentary controller. The controller transition from the sensorless vector control and back to the sensor vector control is demonstrated by an experimental result (Figure7.36). Pulses were missed at the beginning of operation when the encoder was disconnected. After 0.6sec, the encoder was connected once again.

By connecting the parallel variable resistance with full scale, stator short winding fault was introduced at 2 seconds. Hence, instead of the sensorless vector control, the fault tolerant control algorithm was switched on for reconfiguring the normal operation. Fig 7.36 shows this.

Minimum voltage fault was introduced at 3 seconds. This marked the switching ON of the last stage of control strategies, for maintaining the accepted operational

performance.

The wavelet index determines all fault detections and consequently the binary decisions for switching from one control strategy to the other.

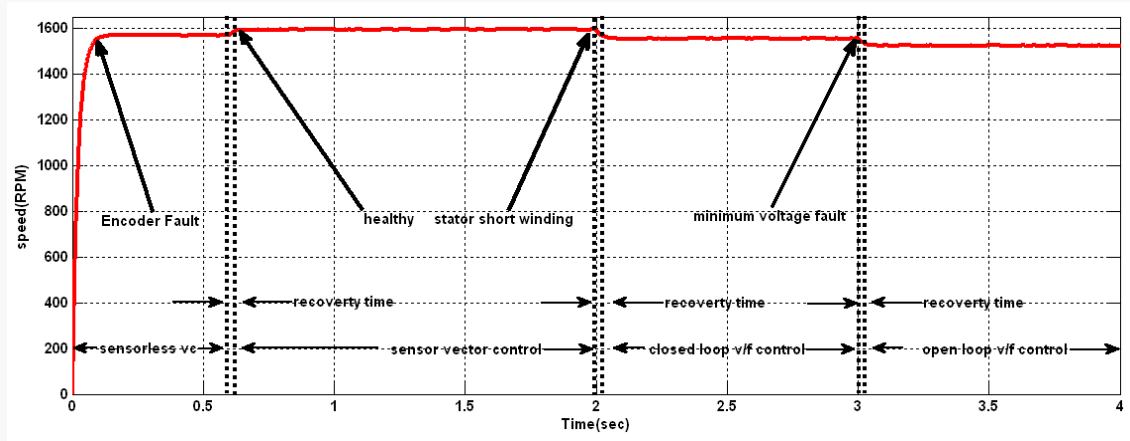


Figure 7.36. Experimental speed transition for different controller for flexibility test

Figure 7.37 shows the effectiveness of closed loop V/F control against the stator short winding fault and its recovery time.

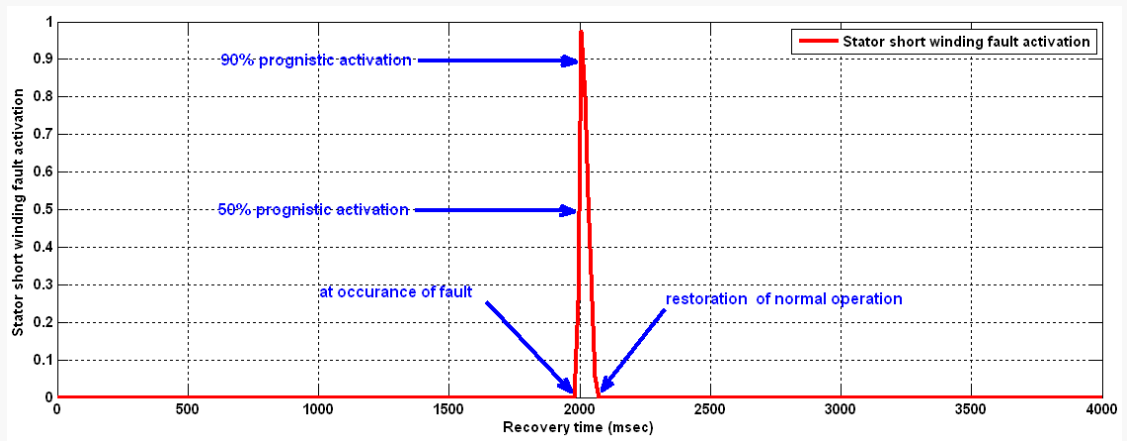


Figure 7.37. Stator short fault recovery due to activation of closed loop V/F

Figure 7.38 shows the effectiveness of open loop V/F control against the under voltage fault and its recovery time.

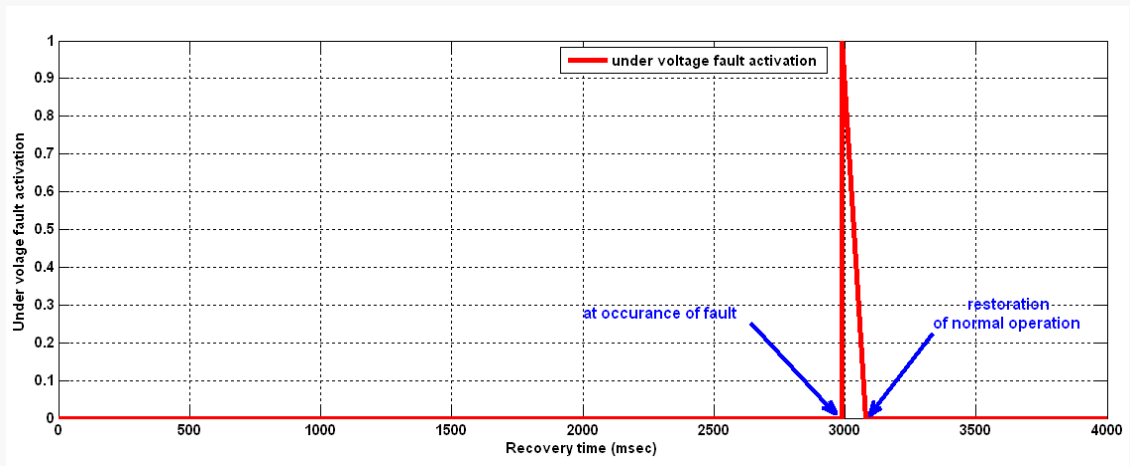


Figure7.38. Under voltage fault recovery due to activation of open loop V/F

Figure7.39 shows speed transition between sensor vector control to sensorless vector control in the event of speed sensor fault at 3 sec and from sensorless to closed loop V/F at 9.3 sec when the stator open winding fault occur.

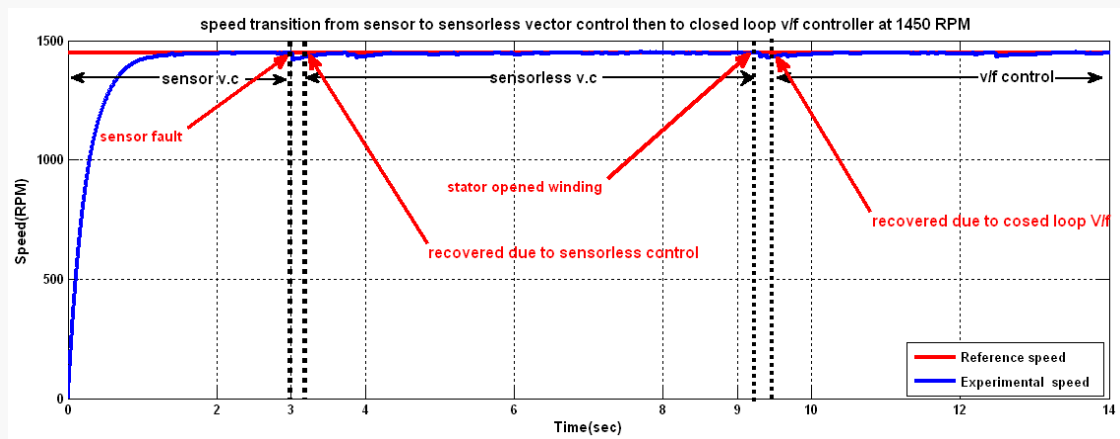


Figure7.39. Speed transitions at 1450RPM

One of the suggested solutions was the fault tolerant strategy for IM faults based on a wavelet topology and control. The main target was to overcome the falling motor performance. This was kept in mind while formulating this strategy which consequently extended the life of a motor drive system for a span of time prior to the need for maintenance. Figure7.40 illustrates the block diagram of multisensory control system.

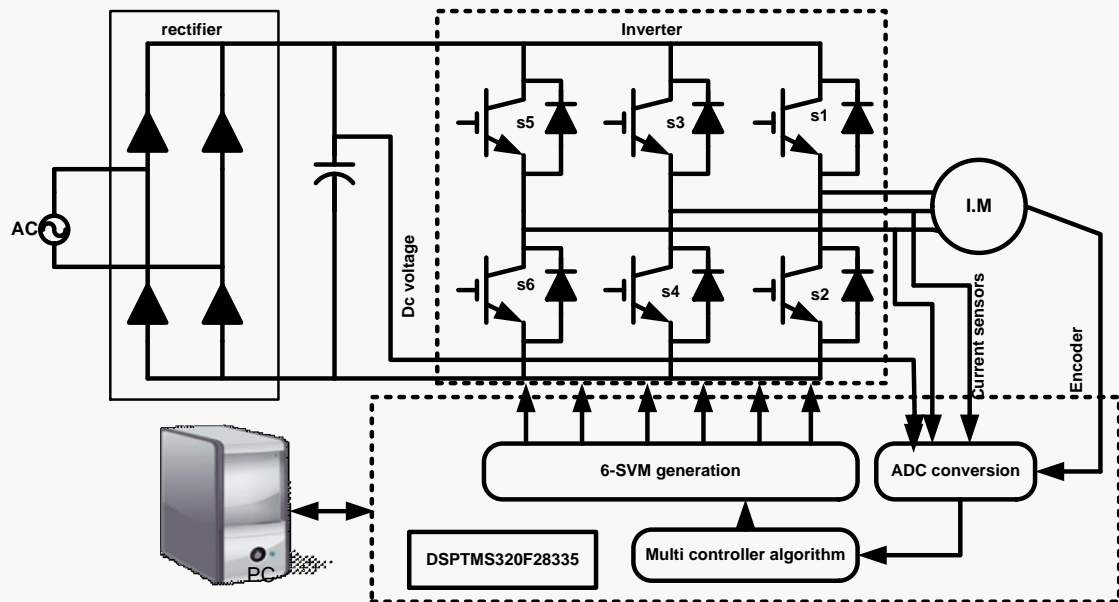


Figure7.40. Block diagram of multisensory control system

For low speed and high speed motor applications, the above mentioned fault tolerant control algorithm stands as an appropriate choice.

The flow chart of the whole work can be seen in Figure 7.41

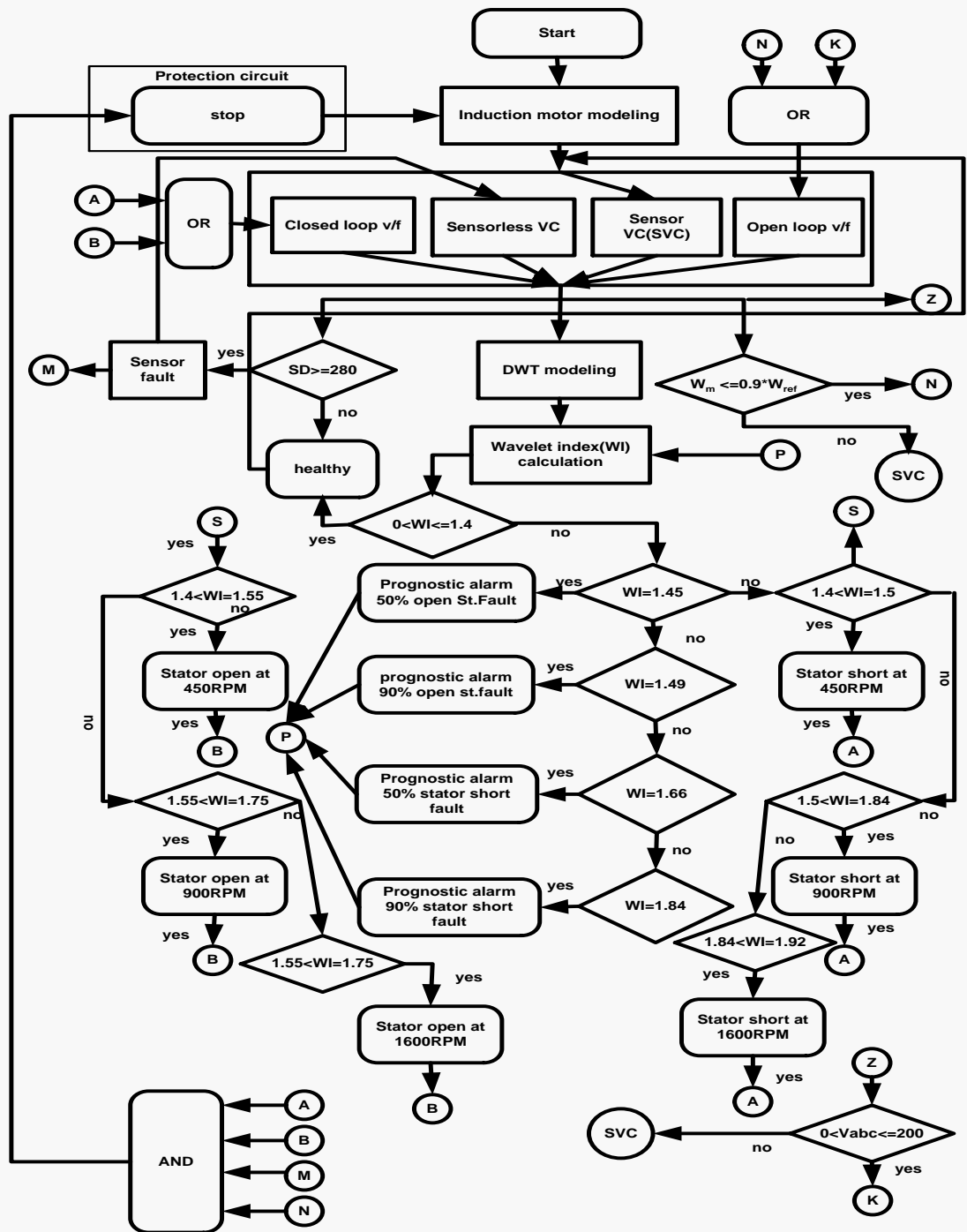


Figure 7.41. Flow chart of the control algorithm of the proposed FTC based IM drive

In the Fig.7.41 the wavelet indices of prognostic for both stator open winding and stator short winding are calculated experimentally. The experimental work was carried out with 450RPM, 900 RPM and 1600RPM because one of the most important features of

fault tolerant control is dealing with large faults but not need to check full potential of the system.

Chapter 8: Conclusions and Suggestions for Future Work

8.1 Introduction

Contributions of this thesis and accomplishments of this work are discussed in this chapter. Recommendations and suggested future works are presented following from here.

- The background of this work has been provide a achievements of this thesis described in chapter 1, with particular emphasis placed on the thesis goals, the principal contributions, core definitions of the fault diagnosis and fault tolerant control and lastly the summary of this work.
- A literature survey of the principal methods of diagnosing faults, faults in the IM without employing the wavelets for fault detection and similar faults with using wavelets and inverter faults were covered in chapter 2. Other researchers have worked on the principal works and the fault control definition in this survey. Multiple controllers with wavelets are an area on which no prior work has been carried out. For inserting specific controller and exact time impact, the wavelet index operates as a fault indicator. For preventing IM damage by halting the operation, fault protection is used which is a part of the fault tolerant algorithm based wavelet.

For developing the wavelet fault tolerant control solutions for sensor and sensorless IMs, these new remedial strategies will pave the way for the author to carry on research in this area for the future.

- IMs are presented in chapter 3. Introduction of control strategies, sensor vector control, open loop V/F control, closed loop V/F control, sensorless vector control together with all Simulink implementation of each controller is also given. For evaluating the stability and response of the controllers in relation to the strategies mentioned above, implementation of the PI controller performance

was also done. Control techniques were classified next. The speed in the speed sensor faults was estimated by the new MRAS estimator.

- Wavelet techniques in the diagnosis of faults were described in chapter 4. Normally, fault prognostic with a pre fault warning stage for 50% and 90% of faults occur.
- For performing as a warning indicator, the prognostic unit relies on wavelet index. Decomposition is influenced by structure and meanings of the wavelets with low and high pass construction for 20 kHz, principal parameters and decomposition levels. The major subjects of this chapter are multilevel resolution and selecting the criteria for constructing the wavelet and wavelet index.
- The fault tolerant control was studied in chapter 5. The following were also included: introduction of the IM's fault tolerant control, kinds of fault tolerant control like active or passive together with reconfiguration, definitions of the most well known words in fault tolerant, switching mechanism between the controllers and computer simulation with 0.5 Hp IM for checking the legitimacy of the algorithm for maintaining the operation in the presence of faults and lastly, fault detection and isolation.
- For utilization in simulation, the 0.5hp IM parameters were obtained from the short circuit test, DC test and locked experimental tests in this chapter.

Results of the simulation exercise were obtained for the healthy IM. Introduction of the investigation pertaining to stator short winding and stator open winding is also given, done at different time intervals. In order to maintain operations, the algorithm was found to perform soundly under every scenario. Moreover, for achieving integrity of every stage of fault tolerant commencing from detection till the protection, the protection unit was tested. Verification of the authentication of simulation implementation conducted in chapters 3 and 4

previously was the prime objective of this chapter. A sound fault tolerant algorithm was indicated by the simulation results.

- Investigation of condition monitoring was focused upon in chapter 6. For the continuation of any industrial process, stator voltage, stator current, speed monitoring and DC voltage, an important part is played by condition monitoring.
- Simulink implementation of monitoring more than 13 trips for rendering the location and time of fault was introduced in this chapter as well. A 0.5hp IM was used for performing the simulation as well as for authenticating this unit.

Simulation of the AC voltage unbalance with low speed and broken rotor bar case studies was also done. For stopping the operation of the motor, this was clearly indicative of the fact that testing was carried out for location of both time and kinds of faults. Avoidance of any IM damage is highly dependent on this unit.

- Indication of the excess of minimum speed and maximum output from the normal was given by experimental test outcomes of the fault tolerant strategy under the stator open winding fault, stator short winding fault, reduction of rated voltage below 0.9* rated voltage and speed sensor in chapter 7. Both healthy and faulty cases are presented in relation to the wavelet decomposition outputs of stator current. Recording of the wavelet index for three speeds namely 450RPM, 900RPM and 1600RPM was also done. The efficaciousness of the algorithm was acknowledged by the selected output speed response. In order to ensure conformity with speed response, the controller activation at every operational stage was also checked.

For utilization in simulation and comparison with the experimental results, the 1kW motor parameters were obtained from the DC test, locked experimental tests and short circuit test.

In order to categorize the fault tolerant operation as a commercial project, minimum hardware components are essential. In comparison with the perplexing fault tolerant algorithms, this implies a cost reduction.

The efficaciousness and authenticity of the fault tolerant approach for industry employment has been demonstrated by the results of the simulation and experimental tests.

- This algorithm can be applicable to many types of motors such as PMSM motor with little bit modification. Normally the IM position can be obtained by integration of summing both electrical and mechanical speeds. In PMSM motor it just has mechanical speed.

8.2. Conclusions

Usefulness in relation to maintaining a minimum level of performance can be identified with scalar control of IM drives, despite its drawbacks like difficult operation at every point of the speed torque curve, torque ripple, slow response and low performance.

The above mentioned problems have been known to get resolved by vector control. A sound choice for implementing the fault tolerant control can be obtained by combining multi controllers.

For maintaining performance of the system at an acceptable level, FTC in the IM is quite vital. The efficaciousness of the algorithm has been acknowledged with its success with all faults.

The following are some of the derived conclusions:

1. In detecting faults and diagnosing IMs, the wavelet is thought of as a very powerful tool.
2. For detecting the presence of a fault in the system, the expert wavelet index is a sound sensing parameter.

3. For obtaining high diagnostic and detection efficaciousness, the enhancement of fault detection and diagnosis can exploit the properties of the wavelet.
4. In order to ensure the best selection of mother wavelet, theories of wavelet need to be studied more vigorously.
5. For estimating the speed of the sensorless and V/F in an efficient manner, the new model of MRAS observer has been studied.
6. The switching mechanism was found to switch efficiently between the controllers.
7. An IM was used as the test application for proving the efficaciousness of the fault tolerant control approach.
8. For verifying the algorithm and ensuring its validity for all motors, more than one IM is used.
9. As new fault tolerant control algorithm both prognostic and protection units were added to this algorithm to ensure better detection, isolation, reconfiguration and protection.

8.3. Suggestions for future works

1. Inverter fault diagnosis can be considered in greater depth.
2. Plug in controllers like direct torque control can be inserted in this scheme during the period of transition.
3. The impact of harmonics can be tested.
4. In place of switching mechanism, utilization of look up table.
5. Studying the impact of switching on the inverter's stability
6. Completion of the prognostic stage with all faults.
7. Intelligent control such as fuzzy, neural, genetic or any combination of the can be used in the future.

8. Implementation of the digital motor control (DMC) blocks according to the equations of the vector control and v/f control techniques.

8.4 Publications

1. Khalaf Salloum Gaeid, Hew Wooi Ping, Haider A.F. Mohamed, (2010). Diagnosis and Fault Tolerant Control of the Induction Motors Techniques a Review. Australian Journal of Basic and Applied Sciences (ISI), 4(2), pp 227-246.
2. Khalaf Salloum Gaeid and Hew Wooi Ping (2010). Induction Motor Fault Detection and Isolation through Unknown Input Observer. Scientific Research and Essays journal (ISI).5(20):3152-3159.
3. Khalaf Salloum Gaeid, Hew Wooi Ping (2011). Wavelet Fault Tolerant Control Review of Induction Motor. IJPS (ISI) journal, 6(3):358-376.
4. Khalaf Salloum Gaeid, Hew Wooi Ping (2011). Fault Tolerant vector Control of Induction Motor Drive. Modern Applied Science journal (Scopus), Canadian Center of Science and Education, 5(4):83-94.
5. Khalaf Salloum Gaeid, Hew Wooi Ping (2011). Condition Monitoring and Protection of Induction Motor using Wavelet Indicator. International journal of Electrical Engineering, 4(7):787-806.
6. Khalaf Salloum Gaeid, Hew Wooi Ping, Mustafa Khalid, Atheer L. Salih (2011). Fault Diagnosis of Induction Motor Using MCSA and FFT. Electrical and Electronic Engineering journal, 1(2): 85-92.
7. Khalaf Salloum Gaeid, Hew Wooi Ping (2011). Wavelet Fault Diagnosis of Induction Motor. MATLAB for Engineers - Applications in Control, Electrical Engineering, IT and Robotics .book chapter, Intech publisher
8. Khalaf Salloum Gaeid, Hew Wooi Ping, Mustafa Khalid, Saad M. Herdan (2012). Fault Tolerant Control of Induction Motor through Observer Techniques II. Scientific Research and Essays journal (ISI), 7(6), pp. 679-692
9. Gaeid, K.S. Hew Wooi Ping; Mohamed, H.A.F (2009). Indirect Vector Control of a Variable Frequency Induction Motor Drive (VCIMD), IEEE conference, ICICIBME, pp36-40.
10. Gaeid, K.S. Hew Wooi Ping; Mohamed, H.A.F (2009). Simulink Representation of Induction Motor Reference Frames, IEEE conference, TECHPOS, pp1-4
11. Khalaf Salloum Gaeid, Haider A.F. Mohamed, Hew Wooi Ping, Lokman H Hassan (2009). NNPID Controller for Induction Motors with Faults, 2nd International conf. on control, Instrumentation & Mechatronic (CIM2009). pp548-552
12. Khalaf Salloum Gaeid, Hew Wooi Ping, Mustafa Khalid (2011). Induction Motor Fault Tolerant Control with Wavelet Indicator. IEEE conference, TMEE2011, pp1512-1516.

13. Khalaf Salloum Gaeid, Hew Wooi Ping, Mustafa Khalid (2012). Wavelet techniques for Induction Machines with Reconfigurable fault Tolerant Controller, International Electrical, Electronic and Control Technology conference (MCEECT 2012), UMP, Malaysia, pp1-5.
14. Khalaf Salloum Gaeid, Hew Wooi Ping, Mustafa Khalid, Ammar Masaoud (2012) .Sensor and Sensorless Fault Tolerant Control for Induction Motor using Wavelet Index ,Sensors,12(4),pp.4031-4050.

References

- Abdesselam, L.(2007). Diagnosis of induction machine by time frequency representation and hidden Markov modelling. *IEEE International Symposium on Diagnostics for Electric Machines, Power Electronics and Drives, SDEMPED*, (pp. 272 - 276).
- Afef Fekih, F. N. (2006). A Robust Fault Tolerant Control Strategy for a Class of Nonlinear Uncertain Systems. *Proceedings of American Control Conference*, (pp. 5474-5480).
- Ahmad Akrad, M. H. (2011). Design of a Fault Tolerant Controller Based on Observers for a PMSM Drive. *IEEE Transactions on Industrial Electronics* , 58 (4), 1416-1427.
- Ahmed Sayed Ahmed, B. M. (2011). A fault-tolerant technique for Delta-connected vector-control AC motor-drives. *Twenty-Sixth Annual IEEE Applied Power Electronics Conference and Exposition (APEC)*, (pp. 1034 - 1041).
- Ahmed Sayed Ahmed, B. M. (2011). Fault-Tolerant Technique for Δ -Connected AC-Motor Drives. *IEEE Transactions on Energy Conversion* , 26 (2), 646 - 653 .
- Anderzej M., T. (2001). *Control of Induction Motors*. Academic Press.
- Andrew K.S. Jardine, D. L. (2006). A review on machinery diagnostics and prognostics implementing condition-based maintenance. *Mechanical Systems and Signal Processing* , 20 (7), 1483–1510.
- Andriamalala, R. R. (2006). A Model of Dual Stator Winding Induction Machine in case of Stator and Rotor Faults for Diagnosis Purpose. *IEEE Industry Applications Conference, 41st IAS Annual Meeting*, 5, (pp. 2340 - 2345).
- Anjali P. Deshpandea, S. C. (2009). Intelligent state estimation for fault tolerant nonlinear predictive control. *Journal of Process Control* , 19 (2), 187-204.
- Anjaneyulu, N.(2007). Adaptive Vector Control of Induction Motor Drives. *International Journal of Electrical and Engineering* , 1 (2), 239-245.
- Antonino, J. R.F. (2005). Validation of a new method for the diagnosis of rotor barfailures via wavelet transformation in industrial inductionmachines. *5th IEEE International Symposium on Diagnostics for Electric Machines, Power Electronics and Drives, SDEMPED, DEMPED*, (pp. 1-6).
- Antonino Daviu, J. R.G. (2006). Validation of a new method for the diagnosis of rotor. *IEEE Transactions on Industry Applications* , 42 (4), 990 –996.

- Ayaz, E. O. (2006). Continuous Wavelet Transform for Bearing Damage Detection in Electric Motors. *IEEE Electrotechnical Conference, MELECON. Mediterranean*, (pp. 1130 –1133).
- Ayhan, B. T. (2008). On the Use of a Lower Sampling Rate for Broken Rotor Bar Detection With DTFT and AR-Based Spectrum Methods. *IEEE Transactions on Industrial Electronics* , 55 (3), 1421 - 1434.
- Babaa, F. K. (2007). Condition monitoring of stator faults in induction motors: Part I— Analytical investigation on the effect of the negative voltage sequence. *International Aegean Conference on Electrical Machines and Power Electronics, ACEMP*, (pp. 205 - 210).
- Banerjee, T. C. (2010). Off-line optimization of PI and PID controller for a vector controlled induction motor drive using PSO. *International Conference on Electrical and Computer Engineering ,ICECE*, (pp. 74 - 77).
- Bangura, J. P. (2003). Diagnostics of Eccentricities and Bar/End-Ring Connector Breakages in Poly phase Induction Motors Through a Combination of Time-Series Data Mining and Time-Stepping Coupled FE–State-Space Techniques. *IEEE Transactions on Industry Applications* , 39 (4), 1005 - 1013.
- Barakat, Y. A. (2011). Modeling and Diagnostic of Stator Faults in Induction Machines Using Permeance Network Method. *PIERS Proceedings, Marrakesh, MOROCCO*, (pp. 1550-1559).
- Basaran, D. G. (2011). Condition monitoring of speed controlled induction motors using wavelet packets and discriminant analysis. *Expert Systems with Applications* , 38 (7), 8079-8086.
- Bech, M. B. (2000). Random modulation techniques with fixed switching frequency for three-phase power converters. *IEEE Transactions on Power Electronics* , 15 (4), 753 - 761.
- Bekheira Tabbache, M. B.-M. (2011). DSP-Based Sensor Fault-Tolerant Control. *IEEE International Symposium on Industrial Electronics (ISIE)*, (pp. 2085 - 2090).
- Biju K, J. G. (2010). Fault Detection of Induction Motor using Energy and Wavelets. *International Conference on Control, Communication and Power Engineering*, (pp. 210-214).
- Blodt, M. R. (2009). Distinguishing Load Torque Oscillations and Eccentricity Faults in Induction Motors Using Stator Current Wigner Distributions. *IEEE conference, 41st IAS Annual Meeting ,Industry Applications Conference, 2006.*, (pp. 1549 - 1556).
- Bodkhe, S. B. (2009). Speed-sensorless, adjustable-speed induction motor drive based on dc link measurement. *International Journal of Physical Sciences* , 4 (4), 221–232.

- Bose, B. K. (2002). *Modern Power Electronics and AC drives*". Prentice-Hall.
- Bossio, G. D. (2006). Application of an Additional Excitation in Inverter-Fed Induction Motors for Air-Gap Eccentricity Diagnosis. *IEEE Transactions on Energy Conversion* , 21 (4), 839 - 847.
- C. BatlleA, D. C. (2006). Simltaneous Interconnection and Damping Assignment T Passivity Based Control: Two PracticalL Examples. *3rd IFAC Workshop on Lagrangian and Hamiltonian Methods for Nonlinear Control*, (pp. 93-98).
- C.U. Ogbuka, a. M. (2009). A Modified Closed Loop V/F Controlled Induction Motor Drive. *The Pacific Journal of Science and Technology* , 10 (1), 52-58.
- Cabal Yopez, E. O.R.T.H.G. (2009). FPGA-Based Online Induction Motor Multiple-Fault Detection with Fused FFT andWavelet Analysis. *International Conference on Reconfigurable Computing and FPGAs*, (pp. 101 –106).
- Cao Zhitong, C. H. (2001). Rotor fault diagnosis of induction motor based on wavelet reconstruction. *Proceedings of the Fifth International Conf. on Electrical Machines and Systems, ICEMS*, (pp. 374 –377).
- Chandorkar, B. M. (2010). Feedback Linearization Control of Induction Machines: EFFECT . *National Power Electronics Conference*, (pp. 1-9).
- Chen, C. M.(1998). Electric fault detection for vector-controlled induction motors using the discrete wavelet transform. *Proceedings of the American Control Conference*, (pp. 3297 –3301).
- Chetwani, S. H. (2005). Online Condition Monitoring of Induction Motors through Signal Processing. *Proceedings of the Eighth International Conference on Electrical Machines and Systems, ICEMS*, (pp. 2175-2179).
- Chia Chou, Y. G. (2007). A Reconfigurable Motor for Experimental Emulation of Stator Winding Inter-Turn and Broken Bar Faults in poly phase Induction Machines. *IEEE Electric Machines & Drives Conference ,IEM DC*, (pp. 1413-1419).
- Chinmaya Kar, A. M. (2006). Monitoring gear vibrations through motor current signature analysis and wavelet transform. *Mechanical Systems and Signal Processing* , 20 (1), 158-187.
- Choi, J. (2006). *Model Based Diagnostics of Motor and Pumps*. Doctor of Philosophy thesis . University of Texas ,Austin.
- Chua, Y. L. (2009). Numerical and Experimental Investigations of Flexural Vibrations of a Rotor System with Transverse or Slant Crack. *Journal of Sound and Vibration* , 324 (1-2), 107-125.

- Claudio Bonivento, A. I. (2004). Implicit fault-tolerant control: application to induction motors. *Automatica* , 40 (3), 355-371.
- Cristaldi, L. F. (2010). Rotor fault detection in field oriented controlled induction machines. *International Symposium on Power Electronics Electrical Drives Automation and Motion, SPEEDAM*, (pp. 529 - 534).
- Cross, A. (1999). DC link current in PWM inverters with unbalanced and nonlinear loads. *IEE Proc.Electr.Pow.Appl* , 143 (6), 620-626.
- Cui, B. (2007). Simulation of Inverter with Switch Open Faults Based on Switching Function. *IEEE International Conference on Automation and Logistics*, (pp. 2774 - 2778).
- Cusido, J. J. (2006). Wavelet and PSD as a Fault Detection Techniques. *processing of the IEEE Conf. On Instrumentation and Measurement Technology,IMTC*, (pp. 1397-1400).
- Cusido, J. L. (2008). Fault Detection in Induction Machines Using Power Spectral Density in Wavelet Decomposition. *IEEE Transactions on Industrial Electronics*, 55 (2), 633-643.
- Cusido, J. R. (2006). Induction Motor Fault Detection by using Wavelet decomposition on dq0 components. *IEEE International Symposium on Industrial Electronics*, (pp. 2406 -2411).
- Cusido, J. R. (2007). On-Line System for Fault Detection in Induction Machines based on Wavelet Convolution. *IEEE Conf.On Power Electronics Specialists, PESC*, (pp. 927-932).
- Cusido, J. R. (2007). On-Line System for Fault Detection in Induction Machines Based on Wavelet Convolution. *IEEE Instrumentation and Measurement Technology Conference Proceedings, IMTC*, (pp. 1-5).
- D.Barnes, J. (2006). *Multiscale Anomaly Detection and Image Registration Algorithms for Airborne Landmine Detection* . Master Thesis .Electrical Engineering,University of Missouri–Rolla.
- D.U. Campos Delgado, D. E. (2008). Fault-tolerant control in variable speed drives:a survey. *IET Electric Power Applications* , 2 (2), 121–134.
- Da Silva, A. P. (2008). Induction Machine Broken Bar and Stator Short-Circuit Fault Diagnostics Based on Three-Phase Stator Current Envelopes. *IEEE Transactions on Industrial Electronics* , 55 (3), 1310 - 1318.

- Diallo, D. B. (2004). A fault-tolerant control architecture for induction motor drives in automotive applications. *IEEE Transactions on Vehicular Technology* , 53 (6), 1847 - 1855.
- Dimas Anton A, S. D. (2010). Characterization of Temporary Short Circuit in Induction Motor Winding using Wavelet Analysis. *Proceedings of the International Conference on Modelling, Identification and Control*, (pp. 477 -482).
- Dongmo, J. K. (2007). Variable Structure Design of a Fault Tolerant Control System for Induction Motors. *IEEE Electric Ship Technologies Symposium, ESTS*, (pp. 531 - 535).
- Douglas, H. P. (2003). Detection of broken rotor bars in induction motors using wavelet analysis. *International IEEE Conf. On Electric Machines and Drive, IEMDC'03*, (pp. 923 – 928).
- Drif, M. C. (2006). Airgap eccentricity fault diagnosis, in three-phase induction motors, by the complex apparent power signature analysis. *International Symposium on Power Electronics, Electrical Drives, Automation and Motion*, (pp. 61 - 65).
- Drif, M. M. (2008). Airgap eccentricity fault diagnosis, in three-phase induction motors, using the instantaneous power factor signature analysis. *4th IET Conference on Power Electronics, Machines and Drives*, (pp. 587 - 591).
- Egorov, V. V. (2011). Discontinuous Space Vector Modulation Technique for Motor Supply . *IEEE International Conference on Computer as a Tool ,EUROCON*, (pp. 1-4).
- El Khil, S. S.B.D. (2006). A Fault Tolerant Operating System in a Doubly Fed Induction Machine Under Inverter Short-circuit Faults. *32nd Annual IEEE Industrial Electronics, IECON*, (pp. 1125 - 1130).
- El Menzhi, L.(2007). Induction motor fault diagnosis using voltage spectrum of an auxiliary winding. *International Conference on Electrical Machines and Systems, ICEMS*, (pp. 1028 - 1032).
- Eltabach, M. C. (2004). A comparison of external and internal methods of signal spectral analysis for broken rotor bars detection in induction motors. *IEEE Transactions on Industrial Electronics* , 51 (1), 107 - 121 .
- Emil Levi(2008). Multiphase Electric Machines for Variable-Speed Applications. *IEEE Transactions on Industrial Electronics*, 55(5),1893-1909.
- Eren, L. D. (2004). Bearing damage detection via wavelet packet. *IEEE Transactions on Instrumentation and Measurement* , 53 (2), 431 - 436.
- Erhan Akin, I. A. (2011). FPGA Based Intelligent Condition Monitoring of Induction Motors: Detection, Diagnosis, and Prognosis. *IEEE International Conference on Industrial Technology (ICIT)*, (pp. 373 - 378).

- F. C. Trutt, J. S. (2002). Online condition monitoring of induction motors. *IEEE Trans. Industry Applications* , 38 (6), 1627-1632.
- Faiz, J. E. (2007). A criterion function for broken bar fault diagnosis in induction motor under load variation using wavelet transform. *International Conf. on Electrical Machines and Systems, ICEMS*, (pp. 1249 –1254).
- Faiz, J. E. (2008). Finite-Element Transient Analysis of Induction Motors under Mixed Eccentricity Fault. *IEEE Transactions on Magnetics* , 44 (1,part 1), 66-74.
- Figoli, Z. Y. (1998). *AC Induction Motor Control Using Constant V/Hz Principle and Space Vector PWM Technique with TMS320C240*. Texas Instruments.
- G. B. Kliman, W. J. (1996). A new approach to on-line turn fault detection in AC motors. *international Conf. Rec. IEEE IAS*, (pp. 687-693).
- G.K. Singh, S. A. (2009). (2009). Isolation and identification of dry bearing faults in induction machine using wavelet transform. *Tribology International* , 42 (6), 849–861.
- Gadoue, S. G. (2010). MRAS Sensorless Vector Control of an Induction Motor Using New Sliding-Mode and Fuzzy-Logic Adaptation Mechanisms. *IEEE Transactions on Energy Conversion* , 25 (2), 394 - 402.
- Gaetan Didier, E. T. (2006). Fault Detection of Broken RotorBars in Induction rotor Using a Global Fault Index. *IEEE transaction on Industry applications* , 42 (1), 79-88.
- Gamal Mahmoud, M. M.A. (2007). Inverter Faults In Variable Voltage Variable Frequency Induction Motor Drive. *Compatibility in Power Electronics, CPE* , (pp. 1-6).
- Gan, W.(2003). Design and analysis of a plug-in robust compensator: an application to indirect-field-oriented-control induction machine drives. *IEEE Transactions on Industrial Electronics* , 50 (2), 272 - 282.
- Georgakopoulos, I. E. (2009). Condition monitoring of an inverter-driven induction motor using Wavelets. *8th International Symposium on Advanced Electromechanical Motion Systems & Electric Drives Joint Symposium, ELECTROMOTION*, (pp. 1-5).
- Ghada Boukettaya, L. K. (2010). A comparative study of three different sensorless vector control strategies for a Flywheel Energy Storage System. *Energy* , 35 (1), 132-139.
- Gojko M. Joksimovic, J. P. (2000). The Detection of Inter-Turn Short Circuits in the Stator Windings of Operating Motors. *IEEE Transactions on Industrial Electronics* , 47 (5), 1078-1085.
- Gordi Armaki, M.(2010). A new approach for fault detection of broken rotor bars in induction motor based on support vector machine. *18th Iranian Conference on Electrical Engineering (ICEE)*, (pp. 732 - 738).

- Grieger, J. S. (2006). Estimation of Static Eccentricity Severity in Induction Motors for On-Line Condition Monitoring. *IEEE Conference on Industry Applications, 24th IAS Annual Meeting*, 5, (pp. 2312 - 2319).
- Grieger, J. S. (2007). Induction Motor Static Eccentricity Severity Estimation Using Evidence Theory. *IEEE International Electric Machines & Drives Conference, IEMDC*, 1, (pp. 190 - 195).
- Guan, Y. S. (2007). Mean Current Vector Based Online Real-Time Fault Diagnosis for Voltage Source Inverter fed Induction Motor Drives. *IEEE, Electric Machines & Drives Conference, IEMDC*, (pp. 1114-1118).
- Habetler, T. R. (2002). Complete current-based induction motor condition monitoring: stator, rotor, bearings, and load. *IEEE International Power Electronics Congress, Technical Proceedings. CIEP*, (pp. 3-8).
- Hakan Calis, A. C. (2007). Rotor bar fault diagnosis in three phase induction motors by monitoring fluctuations of motor current zero crossing instants. *Electric Power Systems Research*, 77 (5-6), 385-392.
- Halim Alwi, C. E. (2008). Fault tolerant control using sliding modes with online control allocation. *Automatica*, 44 (7), 859-1866.
- Hamidi, H. N. (2004). Detection and isolation of mixed eccentricity in three phase induction motor via wavelet packet decomposition. *5th Asian Control Conference*, 2, (pp. 1371 -1376).
- Hengli Quan, Z. G. (2011). study of novel modulation techniques based on Space vector PWM. *International Conference on Computer Distributed Control and Intelligent Environmental Monitoring*, (pp. 295-299).
- Hsu, J. S. (1995). Monitoring of defects in induction motors through air gap torque. *IEEE Trans. Industry Applications*, 31 (5), 1061-1021.
- Huang, X. H. (2007). Detection of Rotor Eccentricity Faults in a Closed-Loop Drive-Connected Induction Motor Using an Artificial Neural Network. *IEEE Transactions on Power Electronics*, 22 (4), 1552-1559.
- Huang, X. H. (2007). Using a Surge Tester to Detect Rotor Eccentricity Faults in Induction Motors. *IEEE Transactions on Industry Applications*, 43 (5), 1183-1190.
- Huang, X., Habetler, T., & Harley, R. (2007). Detection of Rotor Eccentricity Faults in a Closed-Loop Drive-Connected Induction Motor Using an Artificial Neural Network. *IEEE Transactions on Power Electronics*, 22 (4), 1552-1559.

Huaxing Tang, C. L.T. (2007). Improving Performance of Effect-Cause Diagnosis with Minimal Memory Overhead. *Proceedings of the 16th Asian Test Symposium ,ATS* (pp. 1-7). IEEE Computer Society.

Inseok Hwang, S. K. (2010). A Survey of Fault Detection, Isolation, and Reconfiguration Methods. *IEEE Transactions on Control Systems Technology* , 18 (3), 636-653.

Intesar Ahmed , Manzar Ahmed , Kashif Imran , M. Shuja Khan ,S. Junaid Akhtar(2011). Detection of Eccentricity Faults in Machine Using Frequency Spectrum Technique. *International Journal of Computer and Electrical Engineering*,3(1), 1793-8163.

Instrument, T. (1998). *Field Orientated Control of 3-Phase AC-Motors*.

Isermann, R. (2011). *Terminology in fault detection and diagnosis*. Springer eBook.

Izzet, Y. N. (2006). Detection of Bearing Defects in Three-Phase Induction Motors Using Park's Transform and Radial Basis Function Neural Networks. *Sadhana* , 31 (3), 235-244.

J. Amarnath, M. H. (2009). Control induction motor drive without shaft encoder using model referencing adaptive system avoid torque jerks in transition at starting. *International Journal of Applied Engineering Research* , 4 (6), 921–929.

J. Antonino Daviu, M. R. (2006). Application and optimization of the discrete wavelet transform for the detection of broken rotor bars in induction machines. *Applied and Computational Harmonic Analysis* , 21 (2), 268–279.

J. Antonino Daviu, P. J. (2009). Transient detection of eccentricity-related components in induction motors through the Hilbert–Huang Transform. *Energy Conversion and Management* , 50 (7), 1810–1820.

J. Chen, R. P. (1999). Active fault tolerant flight control systems design using the linear matrix inequality method. *Transactions of the Institute of Measurement Control* , 21 (2-3), 77-84.

J. Antonino Daviu, P. M. (2009). Detection of combined faults in induction machines with stator parallel branches through the DWT of the startup current. *Mechanical Systems and Signal Processing* , 23 (7), 2336–2351.

Jafar Zarei, J. P. (2007). Bearing fault detection using wavelet packet transform of induction motor stator current. *Tribology International* , 40 (5), 763–769.

Jannati, M.(2010). Modeling and vector control of unbalanced induction motors faulty three phase or single phase induction motors. *1st Power Electronic & Drive Systems & Technologies Conference ,PEDSTC*, (pp. 208 - 211).

Jawad Ahmed Farooq, T. R. (2008). Modelling and simulation of stator winding inter-turn faults in permanent magnet synchronous motors. *The International Journal for*

Computation and Mathematics in Electrical and Electronic Engineering , 27 (4), 887-896.

Jawad Faiz, M. O. (2009). Different indexes for eccentricity faults diagnosis in three-phase squirrel-cage induction motors: A review. *Mechatronics* , 19 (1), 2-13.

Jeevanand S, A. T. (2008). Condition Monitoring of Induction Motors Using Wavelet Based Analysis of Vibration Signals. *Second International Conference on Future Generation Communication and Networking Symposia*, (pp. 75-80).

Jian Yu Zhang, L. L.X. (2007). Research on the Selection of Wavelet Function for the Feature Extraction of Shock Fault in Bearing Diagnosis . *International Conference on Wavelet Analysis and Pattern Recognition*, (pp. 1630-1634).

Jian, M. (2009). Texture Image Classification Using Visual Perceptual Texture Features and Gabor Wavelet Features. *Journal of Computers* , 4 (8), 763-770.

Joachin Holtz, J. Q. (2000). Sensorless vector control at very low speed using a nonlinear inverter model and parameter identification. *IEEE transactions on industry applications* , 38 (4), 1087-1095.

Jose A. Antonino Daviu, M. R. (2006). Validation of a New Method for the Diagnosis of Rotor Bar Failures via Wavelet Transform in Industrial Induction Machines. *IEEE transaction on industry application* , 42 (4), 990-996.

Jose M . Machorro Lopez, D. E. (2009). Identification of Damaged Shafts using Active Sensing Simulation and Experimentation. *Journal of Sound and Vibration* , 327 (3-5), 368-390.

K.Bose, B. (2006). *Power lectronics and motor drives* . Accademic press.

K.Vinoth Kumar, S. S. (2010). Soft Computing Based Fault Diagnosis. *Second International conference on Computing, Communication and Networking Technologies*, (pp. 1-7).

Kanev, S.(2004). *Robust Fault-Tolerant Control*. Ph.D. Thesis . University of Twente,Netherlands.

Karanayil, B. R. (2007). Online Stator and Rotor Resistance Estimation Scheme Using Artificial Neural Networks for Vector Controlled Speed Sensorless Induction Motor Drive. *IEEE Transactions on Industrial Electronics* , 54 (1), 167 - 176.

Kawady, A. I. (1999). ANN-Based Novel FaultT Detector for Generator Windings Protection. *IEEE Transactions on Power Delivery* , 14 (3), 824-830.

Keyhani, A. (N/A). *Pulse-Width Modulation (PWM) Techniques*. The Ohio State University: Department of Electrical and Computer Engineering.

- Khalaf Salloum Gaeid, H. W. (2010). Diagnosis and Fault Tolerant Control of the Induction Motors Techniques: A review. *Australian Journal of Basic and Applied Sciences* , 4 (2), 227-246.
- Khan, A. (2010). *A Wavelet Based Speed Controller for Interior Permanent Magnet Motor Drives*. PhD thesis in Electrical Engineering, Memorial University of Newfoundland.
- Khan, M.(2006). Discrete Wavelet Transform Based Detection of Disturbances in Induction Motors. *Electrical and Computer Engineering, ICECE*, (pp. 462 –465).
- Kia, S. H. (2009). Diagnosis of Broken-Bar Fault in Induction Machines Using Discrete Wavelet Transform without Slip Estimation. *EEE Transactions on Industry Applications* , 45 (4), 1395 –1404.
- Kim, D. H. (2007). GA–PSO based vector control of indirect three phase induction motor. *Applied Soft Computing* , 7 (2), 601–61.
- King, G. J. (2010). *Induction motor fault detection using the fast orthogonal search algorithm*. Msc thesis in Electrical Engineering, Royal Military College of Canada.
- Kumar, R. G. (2007). Indirect vector controlled induction motor drive with fuzzy logic based intelligent controller. *IET-UK International Conference on Information and Communication Technology in Electrical Sciences ,CTES* , (pp. 368-373).
- Lai, C. P. (2010). Vector control of induction motor based on online identification and ant colony optimization. *2nd International Conference on Industrial and Information Systems (IIS)*, 2, (pp. 206 - 209).
- Lee, S. H. (2007). A study on the motor fault diagnosis using a digital protective relay system. *International Conference on Electrical Machines and Systems, ICEMS*, (pp. 1071 - 1075).
- Lee, Y. (2007). *A Stator Turn Fault Detection Method and a Fault Tolerant Operation Strategy For Interior PM Synchronous Motor Drives in Safety Critical Application* . Ph.d thesis ,School of Electrical and Computer Engineering, Georgia Institute of Technology.
- Leite, D. H. (2007). Real-Time Model-Based Fault Detection and Diagnosis for Alternators and Induction Motors. *IEEE ,Electric Machines & Drives Conference, IEMDC.*, (pp. 202-207).
- Li Ke, Q. D. (2007). The Correlation between the Wavelet Base Properties and Image Compression . *International Conference on Computational Intelligence and Security Workshops*, (pp. 429-432).
- Li, X. S. (2000). Real Time Tool Condition Monitoring Using Wavelet. *IEEE Ttransactions on Systems, Man, and Cybernetics—Part C: Applications and Reviews* , 30 (2), 352-357.

- Li, X., Wu, Q., & Nandi, S. (2007). Performance Analysis of a Three-Phase Induction Machine With Inclined Static Eccentricity. *IEEE Transactions on Industry Applications* , 43 (2), 531 - 541.
- Liang Tang, G. J. (2008). Prognostics-enhanced Automated Contingency Management for Advanced Autonomous systems. *International Conference on Prognostics and Health Management, PHM.* , (pp. 1 - 9).
- Liu, H. L. (2008). Adaptive fault tolerant control for a class of inherent nonlinear systems. *Control and Decision Conference, CCDC*, (pp. 541 - 545).
- Longa, P. (2006). *An Optimized Architecture for 2D Discrete Wavelet Transform on FPGAs using Distributed Arithmetic*. Faculty of Engineering , University of Ottawa.
- Lorand SZABO, J. D. (2005). Discrete Wavelet Transform Based Rotor Faults Detection Method for Induction Machines. In W. M. Elmenreich, *ntelligent Systems at the Service of Mankind, vol2* (pp. 63-74). Augsburg (Germany).
- Lu, B.(2008). Induction motor rotor fault diagnosis using wavelet analysis of one-cycle average power. *Twenty-Third Annual IEEE Applied Power Electronics Conference and Exposition, APEC*, (pp. 1113 - 1118).
- M. A. Cash, T. G. (1998). Insulation failure prediction in AC machines using line-neutral voltages. *IEEE Trans. Industry Applications* , 34 (6), 1234-1239.
- M. A. Rodriguez, A. C. (2008). A Strategy to Replace the Damaged Element for Fault-Tolerant Induction Motor Drive. *International Conference on Electrical Engineering, Computing Science and Automatic Control (CCE)*, (pp. 51-55).
- M. Mena, O. T. (2008). Sensorless direct vector control of an induction motor. *Control Engineering Practice* , 16 (1), 67–77.
- M. Riera Guaspa, J. A. (2009). Diagnosis of rotor asymmetries in induction motors based on the transient extraction of fault components using filtering techniques. *Electric Power Systems Research* , 79 (8), 1181–1191.
- M. Sabarimalai Manikandan, a. S. (2007). Wavelet energy based diagnostic distortion measure for ECG. *Biomedical Signal Processing and Control* , 2 (2), 80-96.
- M. Sushama, G. T. (2009). Detection OF High-Impedance Faults in Transmission. *ARPN Journal of Engineering and Applied Sciences* , 4 (3), 6-12.
- Ma, H. L. (2007). Vibration research on winding faults of induction motor based on experiment modal analysis method. *International Power Engineering Conference, IPEC*, (pp. 366 - 370).
- Mahmoud, G. M.A. (2007). Inverter Faults in Variable Voltage Variable Frequency Induction Motor Drive. *Compatibility in Power Electronics, CPE*, (pp. 1-6).

- Makarand S. Ballal, Z. J. (2007). Adaptive Neural Fuzzy Inference System for the Detection of Inter-Turn Insulation and Bearing Wear Faults in Induction Motor. *IEEE transaction on industrial electronics* , 54 (1), 250-259.
- Mallat, S. (1998). *A wavelet tour of signal processing*. Academic press.
- Mallat, S. (2009). *A Wavelet Tour of Signal processing*. San Diego: Academic Press.
- Mamat Ibrahim, M. M. (2004). Condition monitoring algorithm for induction motor drive. *IEEE Region 10 Conference, TENCON*, (pp. 9- 12).
- Masoud Hajiaghajan, H. A. (2004). Advanced Fault Diagnosis of a DC Motor. *IEEE Transactions on Energy Conversion* , 19 (1), 60-65.
- Matic, D. B. (2010). Minimal configuration PI fuzzy gain scheduling speed controller in indirect vector controls scheme. *5th IET International Conference on Power Electronics, Machines and Drives ,PEMD*, (pp. 1-6).
- Matthew O.T. Cole, P. S. (2004). Towards fault tolerant active control of rotor magnetic bearing systems. *Control Engineering Practice* , 12 (4), 491-501.
- Mc Fate, D. (2009). Induction Motor Testing and Evaluation. (pp. 1-11). Clevelan, Ohio: IOtech.
- Mehala, N. (2009). Rotor Faults Detection in Induction Motor by Wavelet Analysis. *International Journal of Engineering Science and Technology* , 1 (3), 90-99.
- Mehdi Arehpanahi, S. (2005). Broken Rotor Bar Detection in Induction Motor via Stator Current Derivative. *Proceedings of the Eighth International Conference on Electrical Machines and Systems, ICEMS*, (pp. 2202-2206).
- Mehrjou, M. R. (2010). Evaluation of Fourier and wavelet analysis for efficient recognition of broken rotor bar in squirrel- cage induction machine. *IEEE International Conference on Power and Energy ,PECon*, (pp. 740-743).
- Menacer, A. M. (2006). Effect of the Position and the Number of Broken Bars on Asynchronous Motor Stator Current Spectrum. *12th International Power Electronics and Motion Control Conference,EPE-PEMC*, (pp. 973 - 978).
- Menacer, A. M. (2004). Stator Current Analysis of Incipient fault Into Asynchronous Motor Bars using Fourier Fast Transform. *Journal of Electrical Engineering* , 55 (5-6), 122-130.
- Meshgin Kelk, H. M. (2004). Interbar currents and axial fluxes in healthy and faulty induction motors. *IEEE Transactions on Industry Applications* , 40 (1), 128 - 134.
- Mirafzal, B.(2006). On innovative methods of induction motor interturn and broken-bar fault diagnostics. *IEEE Transactions on Industry Applications* , 42 (2), 405 - 414.

Mogens Blanke, M. K. (2006). *Diagnosis and Fault Tolerant Control*. 2nd Edition, Verlag Berlin Heidelberg, Springer.

Mohamadi, H. M. (2008). Vibration Condition Monitoring Techniques for Fault Diagnosis of Electromotor with 1.5kw power. *Journal of Applied Science* , 8 (7), 1268-1273.

Mohamed El Hachemi Benbouzid, D. D. (2007). Advanced Fault-Tolerant Control of Induction-Motor Drives for EV/HEV Traction Applications: From Conventional to Modern and Intelligent Control Techniques. *IEEE Transactions on Vehicular Technology* , 56 (2), 519-527.

Mohamed, H. Y. (2008). Sliding mode sensor fault tolerant control structure for induction motor. *SICE Annual Conference*, (pp. 2630 - 2635).

Mohammed, O. A. (2006). Modelling and Characterization of Induction Motor Internal Faults Using Finite-Element and Discrete Wavelet Transforms. *IEEE Transactions on Magnetism* , 42 (10), 3434 –3436.

Mohanty, A. (2006). Multiresolution Fourier transform of ripple voltage and current signals for fault detection in a gearbox. *IEEE International Conference on Industrial Technology, ICIT* , (pp. 1367 - 1373).

Mohanty, A. (2006). Fault Detection in a Multistage Gearbox by Demodulation of Motor Current Waveform. *IEEE Transactions on Industrial Electronics* , 53 (4), 1285 - 1297.

Nademi, H. T. (2008). Fault tolerant IPMS motor drive based on adaptive backstepping observer with unknown stator resistance. *3rd IEEE Conference on Industrial Electronics and Applications, ICIEA*, (pp. 1785 - 1790).

Nakamura, H. Y. (2007). Diagnosis of short circuit fault of induction motor based on hidden markov model. *Conference on Electrical Insulation and Dielectric Phenomena*, (pp. 61 - 64).

Neacsu, D. O. (2001). Space Vector Modulation –An Introduction. *The 27th Annual Conference of the IEEE Industrial Electronics Society*, (pp. 1583-1592).

Nemec, M. D. (2010). Detection of Broken Bars in Induction Motor Through the Analysis of Supply Voltage Modulation. *IEEE Transactions on Industrial Electronics* , 57 (8), 2879 - 2888 .

Nikranjbar, A. M. (2009). Model-Based Fault Diagnosis of Induction Motor Eccentricity using Particle Swarm Optimization. *Proceedings of the Institution of Mechanical Engineers, Part C: Journal of Mechanical Engineering Science* , 223 (3), 607-615.

Nirmesh Yadav, S. S. (2007). From wavelets to filter banks. In P. Roberts, *Wavelet analysis and applications* (pp. 97-117).

- Okuda, T. K. (2009). Diagnosis of Multi-Phase Turn Faults of Induction Motor Stator Windings. *International Conference on Power Electronics and Drive Systems, PEDS* , (pp. 144 - 149).
- Onel, I. (2008). Induction Motor Bearing Failure Detection and Diagnosis: Park and Concordia Transform Approaches Comparative Study. *IEEE/ASME Transactions on Mechatronics* , 13 (2), 257 - 262 .
- Ordaz Moreno, A.(2008). Automatic Online Diagnosis Algorithm for Broken-Bar Detection on Induction Motors Based on Discrete Wavelet Transform for FPGA Implementation. *IEEE Transactions on Industrial Electronics* , 55 (5), 2193 –2202.
- Ouma amar, M. K. (2007). Neutral Voltage Analysis for Broken Rotor Bars Detection in Induction Motors Using Hilbert Transform Phase. *IEEE Industry Applications Conference, 42nd IAS Annual Meeting*, (pp. 1940 - 1947).
- P. C. Krause, O. W. (2002). *Analysis of Electric Machinery and Drive Systems*. 2nd ed., New York, Wiley.
- P. H. Mellor, T. J. (2003). Faulted behavior of permanent magnet electric vehicle traction drives. *international Conf. Rec. of IEEE, IEMDC*, (pp. 554-558).
- Paoli, A. (2003). *Fault Detection and Fault Tolerant Control for Distributed Systems. A General Framework*. Ph.D thesis . University of Bologna.
- Parekh, R. (2005). *V/F Control of 3-Phase Induction Motor Using Space Vector Modulation*. Microchip, AN955.
- Parekh, R. (2003). *VF Control of 3-Phase Induction Motors Using PIC16F7X7 Microcontrollers*. Microchip.
- Patton, R. J. (1997). *Fault -Tolerant Control Systems: The 1997 Situation*. University of Hull, School of Engineering, Hull HU6 7RX, UK.
- Pedra, J. C. (2009). Modelling of squirrel-cage induction motors for electromagnetic transient programs. *IET Electric Power Applications* , 3 (2), 111 - 122.
- Pedrayes, F.R.(2007). Application of a Dynamic Model based on a Network of Magnetically Coupled Reluctances to Rotor Fault Diagnosis in Induction Motors. *IEEE International Symposium on Diagnostics for Electric Machines, Power Electronics and Drive*, (pp. 241-246).
- Pietilainen, K. (2005). *Voltage Sag Ride-Through of AC Drives: Control and Analysis*. Ph.d thesis, department of Electrical systems, Royal Institute of Technology.
- Ponci, F. C. (2007). Innovative Approach To Early Fault Detection For Induction Motors. *IEEE International Symposium on Diagnostics for Electric Machines, Power Electronics and Drives, SDEMPED*, (pp. 283 - 288).

- Pons Linares, J. A.D.G.S.A. (2009). Induction motor fault diagnosis based on analytic wavelet transform via Frequency B-Splines. *IEEE International Symposium on Diagnostics for Electric Machines, Power Electronics and Drives, SDEMPED*, (pp. 1-7).
- Poyhonen,S.(2004). *Support Vector MachineE Based Classification in Condition Monitoring of Induction Motors* . Ph.d thesis in Technology ,Helsinki University of Technology.
- Q.T. An, L. S. (2010). Low-cost diagnostic method for open-switch faults in inverters. *Electronics Letters* , 46 (14), 1-2.
- Qian Cheng, L. Y. (2011). *Vector Control of an Induction Motor based on a DSP*. thesis project ,Department of Energy and Environment,Charmers University off Technology.
- Qiao Hua, Z. H. (2007). Fault diagnosis of rotating machinery based on improved waveletpackage transform and SVMs ensemble. *Mechanical Systems and Signal Processing* , 21 (2), 688–705.
- R. Rajeswari, N. K. (2007). Diagnosis of Inter Turn Fault in the Stator of Synchronous Generator Using Wavelet Based ANFIS. *World Academy of Science, Engineering and Technology* , 36, 203-209.
- R. Rubini, U. M. (2001). Application of the envelope and wavelet transform analysis for the diagnosis of incipient faults in ball bearings. *Mechanical systems and signal processing* , 15 (2), 287-302.
- R. Salehi Arashloo, A. J. (2010). Design, Implementation and Comparison of Two Wavelet Based Methods for the Detectionof Broken Rotor Bars in Three Phase Induction Motors. *1st Power Electronic & Drive Systems & Technologies Conference,PEDSTC*, (pp. 345 –350).
- R.B. Sepe, J. C. (2003). Fault Tolerant Operation of Induction Motor Drives with Automatic Controller Reconfiguration. *Practical Failure Analysis* , 3 (1), 64-70.
- Ramirez, F. A. (2009). A Space-Vector PWM Voltage-Source Inverter for a Three-Phase Induction Motor Based on the dsPIC30F3011. *Electronics, Robotics and Automotive Mechanics Conference, CERMA '09*, (pp. 429 - 434).
- Reney, D. (2011). Modeling and Simulation of PWM Inverter. *International Conference on Devices and Communications (ICDeCom)*, (pp. 1-4).
- Report, A. A. (2006). *Sensor Field Oriented Control (IFOC) of Three-Phase AC Induction Motors Using ST10F276*. STMicroelectronics.
- Riera Guasp, M. A. (2008). A General Approach for the Transient Detection of Slip-Dependent Fault Components Based on the Discrete Wavelet Transform. *IEEE Transactions on Industrial Electronics* , 55 (12), 4167 –4180.

- Roberto Cardena, R. P. (2008). MRAS Observers for Sensorless Control of Doubly-Fed Induction Generators. *IEEE Transactions on Power Electronics* , 23 (3), 1075-1084.
- Romero, M. S. (2010). Sensor fault-tolerant vector control of induction motors. *IET Control Theory & Applications* , 4 (9), 1707 - 1724.
- Rui Zhou, W. B. (2010). Second generation wavelet packet transform Mechanical equipment fault diagnosis based on redundant. *Digital Signal processing* , 20 (1), 276–288.
- S. Abbasiona, A. R. (2007). Rolling element bearings multi-fault classification based on the wavelet de-noising and support vector machine. *Mechanical Systems and Signal Processing* , 21 (7), 2933–2945.
- S. Radhika, G. S. (2010). Precise wavelet for current signature in 3 ϕ IM. *Expert Systems with applications* , 37 (1), 450–455.
- Saleh, A. S. (2007). Fault Tolerant Field Oriented Control of Induction Motor for Loss of One Inverter Phase with Re-starting Capability. *IEEE International Symposium on Industrial Electronics, ISIE*, (pp. 1340 - 1345).
- Saleh, S. K. (2005). Application of a wavelet-based MRA for diagnosing disturbances in a three phase induction motor. *5th IEEE Conf. on Diagnostics for Electric Machines, Power Electronics and Drives, SDEMPED*, (pp. 1-6).
- Samsi, R. R. (2006). Wavelet-based symbolic analysis for detection of broken rotor bars in inverter-fed induction motors. *IEEE Conf. on Control, ThB07.3*, (pp. 3032-3037).
- Sepe, R. J. (2001). Fault tolerant operation of induction motor drives with automatic controller reconfiguration. *IEEE International ,Electric Machines and Drives Conference, IEMDC*, (pp. 156-162).
- Serhat Seker, E. A. (2003). Feature extraction related to bearing damage in electric motors by wavelet analysis. *Journal of the Franklin Institute* , 340 (2), 125–134.
- Serna, E. (2006). Detection of Rotor Faults in Field Oriented Controlled Induction Machines. *IEEE Industry Applications Conference, 41st IAS Annual Meeting*, (pp. 2326 - 2332).
- Seydi Vakkas Ustun, M. D. (2009). Modeling and control of V/F controlled induction motor using genetic-ANFIS algorithm. *Energy Conversion and Management* , 50 (3), 786–791.
- Siddique, A. G. (2005). A Review of Stator Fault Monitoring techniques of induction motors. *IEEE transaction on energy conversion* , 20 (1), 106-114.
- Silva, A. M. (2006). *Induction Motor Fault Diagnostic and Monitoring Methods*. Thesis Master of Electrical and Computer Engineering . Milwaukee, Wisconsin.

Simaan, L. U. (1997). A Passivity-Based Method for Induction Motor Control. *IEEE Transactions on Industrial Electronics* , 44 (5), 688-695.

Sulowicz, M.(2007). Application of Fuzzy Inference System for Cage Induction Motors Rotor Eccentricity Diagnostic. *IEEE International Symposium on Diagnostics for Electric Machines, Power Electronics and Drives*, (pp. 101-105).

Supangat, R. N. (2006). Detection of Broken Rotor Bars in Induction Motor Using Starting-Current Analysis and Effects of Loading. *IEE Proceedings. The Institution of Engineering and Technology*, (pp. 848- 855).

Teotrakool, K. D. (2009). Adjustable-Speed Drive Bearing-Fault Detection via Wavelet Packet Decomposition. *IEEE Transactions on Instrumentation and Measurement* , 58 (8), 2747 –2754.

Teresa Orłowska Kowalska, M. D. (2010). Rotor Fault Analysis in the Sensorless Field Oriented Controlled Induction Motor Drive. *AUTOMATIKA* , 51 (2), 149-156.

Thomson, W. (2001). Current signature analysis to detect induction motor faults. *IEEE Industry Applications Magazine* , 7 (2), 26-34.

Tsoumas, I. M. (2005). Induction motor mixedfault diagnosis based on wavelet analysis of the current space vector. *Proceedings of the Eighth International Conference on Electrical Machines and Systems, ICEMS,3*, (pp. 2186 –2191).

Tsuji, M. C. (2008). A novel V/F control of induction motors for wide and precise speed operation. *International Symposium on Power Electronics, Electrical Drives, Automation and Motion, SPEEDAM*, (pp. 1130 - 1135).

Turkmenoglu, M. A. (2010). Wavelet-based switching faults detection in direct torque control induction motor drives. *IET Science, Measurement and Technology* , 4 (6), 303–310.

Tze Fun Chan, K. S. (2011). *Applied Intelligent Control of Induction Motor Drives*. 1st edition, John wiley and sons.

Uddin, M. N. (2000). Performance of Current Controllers for VSI-Fed IPMSM Drive. *IEEE Transactions on Industry Applications* , 36 (6), 1531-1538.

Wei Chen, D. X. (2009). A Novel Stator Voltage Oriented V/F Control Method Capable of High Output Torque at Low Speed. *International Conference on Power Electronics and Drive Systems, PEDS*, (pp. 228 - 233).

Wenjun Li, Y. L. (2006). A Method of Abrupt Sensor Fault Diagnosis. *IEEE proceedings of the Sixth International Conference on Intelligent Systems Design and Applications*, (pp. 856-861).

- Wesley G. Zanardelli, E. G. (2005). Wavelet-based methods for the prognosis of mechanical and electrical failures in electric motors. *Mechanical Systems and Signal Processing*, 19 (2), 411–426.
- Wolbank, T. (2007). Adjustment, measurement and on-line detection of air gap asymmetry in ac machines. *European Conference on Power Electronics and Applications*, (pp. 1-8).
- Xu hong, W. Y.g. (2007). Fuzzy Neural Network based On-line Stator Winding Turn Fault Detection for Induction Motors. *2nd IEEE Conference on Industrial Electronics and Applications, ICIEA*, (pp. 2461 - 2464).
- Xuhong, W. Y. (2007). Diagonal recurrent neural network based on-line stator winding turn fault detection for induction motors. *Proceedings of the Eighth International Conference on Electrical Machines and Systems, ICEMS*, (pp. 2266 - 2269).
- Yang, C. C. (2007). Fault Diagnosis for Induction Motors Using the Wavelet Ridge. *Second International Conf. on Bio-Inspired Computing: Theories and Applications, BIC-TA*, (pp. 231 –235).
- Yang, D. (2007). Induction Motor Bearing Fault Detection with Non-stationary Signal Analysis. *4th IEEE International Conference on Mechatronics, ICM2007*, (pp. 1-6).
- Yang, Q. S. (2004). *Diagnosis Methods with Applications to Process Monitoring*. Case Western Reserve University.
- Yasser Gritli, A. S. (2011). Experimental validation of doubly fed induction machine electrical faults diagnosis under time-varying conditions. *Electric Power Systems Research*, 81 (3), 751-766.
- Ye, Z. B. (2001). Signature analysis of induction motor mechanical faults by wavelet packet decomposition. *Sixteenth Annual IEEE Conference on Applied Power Electronics and Exposition, APEC*, 2, (pp. 1022-1029).
- Yeh, C. (2007). Fault Tolerant Operations in Adjustable-Speed Drives and Soft Starters for Induction Motors. *IEEE Power Electronics Specialists Conference, PESC*, (pp. 1942 - 1949).
- Yeh, C. C. (2008). *"Fault tolerant operations of induction motor-drive systems"*. PH.D Dissertation submitted to the Faculty of the Graduate School, Marquette University.
- Ying, X. (2009). Characteristic Performance Analysis of Squirrel Cage Induction Motor With Broken Bars. *IEEE Transactions on Magnetics*, 45 (2), 759 - 766.
- Yixiang Huang, C. L. (2010). A lean model for performance assessment of machinery using second generation wavelet packet transform and Fisher criterion. *Expert Systems with Applications*, 37 (5), 3815-3822.

- Youmin Zhang, J. J. (2008). Bibliographical review on reconfigurable fault tolerant control systems. *Annual Reviews in Control* , 32 (2), 229-252.
- Youssef, B. (2007). On Line Parametric Faults Detection in Induction Motors Based on Graphical Signature Tool. *The 33rd Annual Conference of the IEEE Industrial Electronics Society (IECON)*, (pp. 138-1143).
- Yusof, Y. (2003). Simulation and modeling of stator flux estimator for induction motor using artificial neural network technique. *National Power Engineering Conference, PECon*, (pp. 11-15).
- Yuttana Kumsuwan, S. P. (2008). Modified direct torque control method for induction motor drives based on amplitude and angle control of stator flux. *Electric Power Systems Research* , 78 (10), 1712–1718.
- Zafar, J.(2010). CUSUM based Fault Detection of Stator Winding Short Circuits in Doubly-Fed Induction Generator based Wind Energy Conversion Systems. *International Conference on Renewable Energies and Power Quality*, (pp. 1-4).
- Zanardelli, W.G.(2005). Failure Prognosis for Permanent Magnet AC Drives Based on Wavelet Analysis. *IEEE International Conference on Electric Machines and Drives*,(pp. 64- 70).
- Zarei, J. (2006). An Advanced Park's Vectors Approach for Bearing Fault Detection. *IEEE International Conference on Industrial Technology, ICIT*, (pp. 1472 - 1479).
- Zelechowski, M. (2005). *Space Vector Modulated – Direct Torque Controlled (DTC – SVM) Inverter – Fed Induction Motor Drive*. Ph.D. Thesis,Electrical Engineering,Warsaw University of Technology.
- Zelechowski, M. (2005). *Space Vector Modulated – Direct Torque Controlled (DTC – SVM) Inverter – Fed Induction Motor Drive*. Ph.D. Thesis, Faculty of Electrical Engineering, Institute of Control and Industrial Electronics, Warsaw University of Technology, Poland.
- Zhang Jian wen, Z. N.h. (2007). A Fault Diagnosis Approach for Broken Rotor Bars Based on EMD and Envelope Analysis. *Journal China University Mining & Technolgy* , 17 (2), 205-209.
- Zhang Ren, W. W. (2011). New robust fault tolerant controller for self repairing flight. *Journal of Systems Engineering and Electronics* , 22 (1), 77–82.
- Zhang, P. Y. (2011). A Survey of Condition Monitoring and Protection. *IEEE Transaction on Industrial application* , 47 (1), 34-46.

Zhou, W. L. (2009). Incipient Bearing Fault Detection via Motor Stator Current Noise Cancellation Using Wiener Filter. *IEEE Transactions on Industry Applications* , 45 (4), 1309 - 1317.

Zhu, J. (2008). *Modeling, Simulation and Implementation of a Fault Tolerant Permanent Magnet AC Motor Drive with Redundancy* . Ph.d thesis ,School of Electrical and Electronics Engineering, University of Adelaide.

Zhu, K. Y. (2009). Wavelet analysis of sensor signals for tool condition monitoring: A review and some new results. *International Journal of Machine Tools and Manufacture* , 48 (7-8), 537-553.

Zidani, F. D. (2007). Diagnosis of Speed Sensor Failure in Induction Motor Drive. *IEEE International Electric Machines & Drives Conference, IEMDC*, (pp. 1680-1684).

Appendix A: Specifications and Design of Hardware

A1. Introduction

In this appendix, detailed designs and specifications of the hardware of the fault tolerant control and power electronics equipments, like the inverter, rectifier and the gate drive. Complete listing of the specifications of each of the hardware components used in the implementation of the system, as well as the design schematics and circuit wiring diagrams of the power topologies and their associated signal conditioning circuits and gate drives.

A2. Descriptions of the system

A2.1. Digital Photo of the Overall System Topology

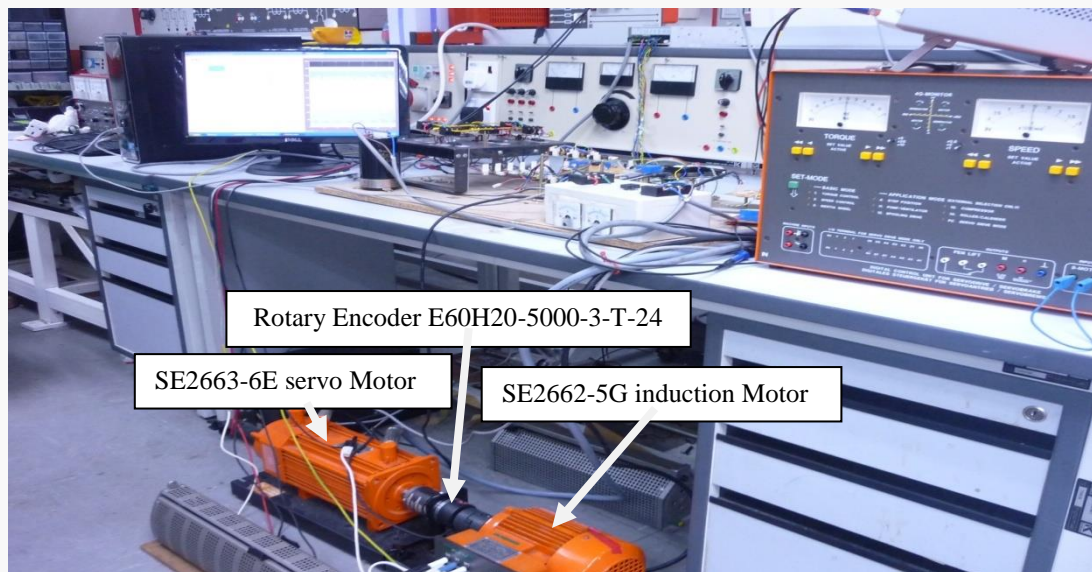


Figure A2.1a. Complete setup of the work

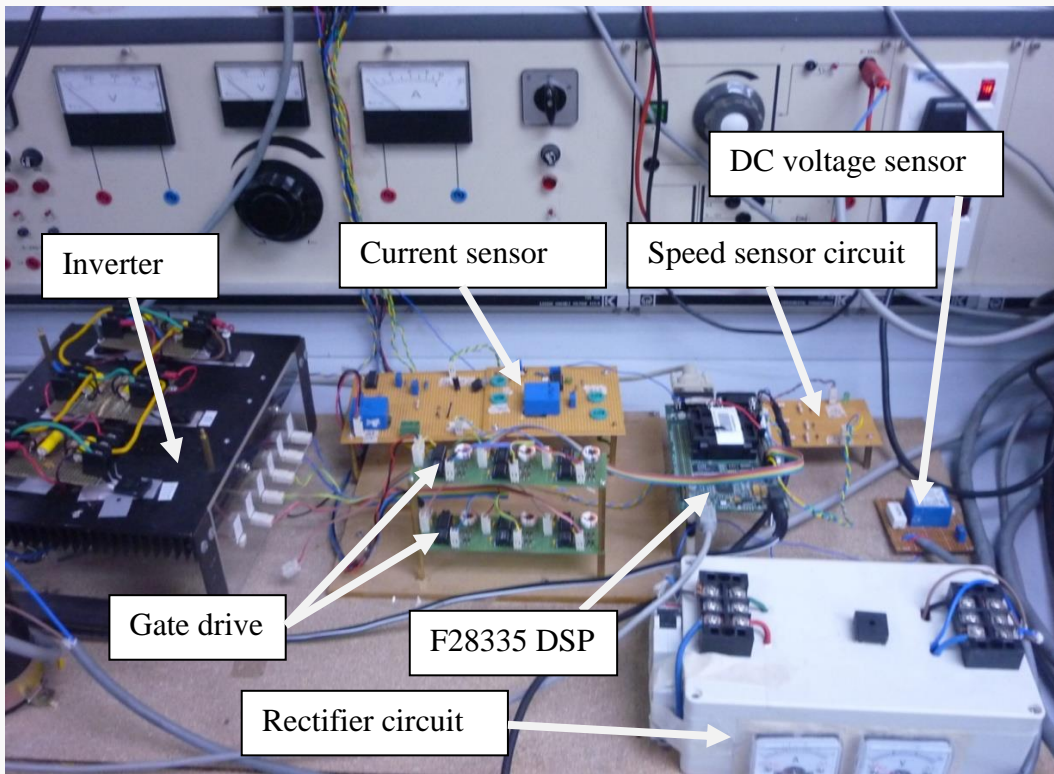


Figure A2.1b. Close snap of complete setup of the work

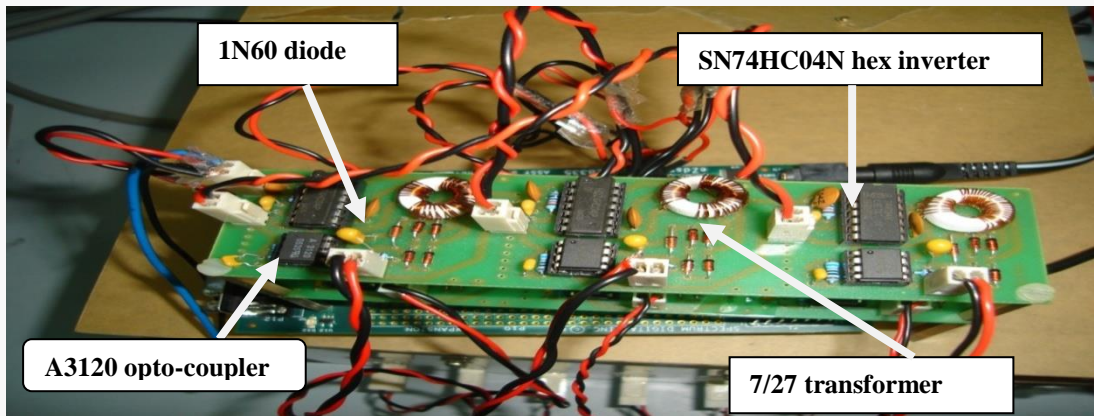


Figure A2.1c. Gate drive circuit

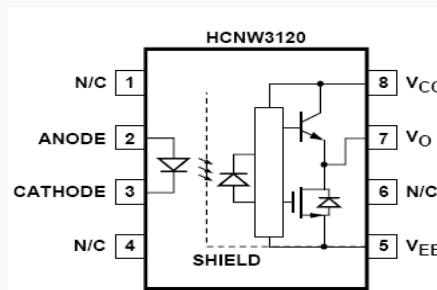


Figure A2.1d. A3120 opto-coupler used in the gate drive circuit

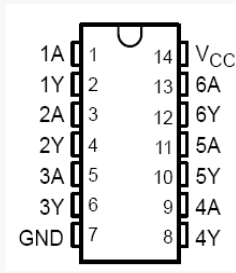


Figure A2.1e. SN74HC04N hex inverter used in the gate drive circuit

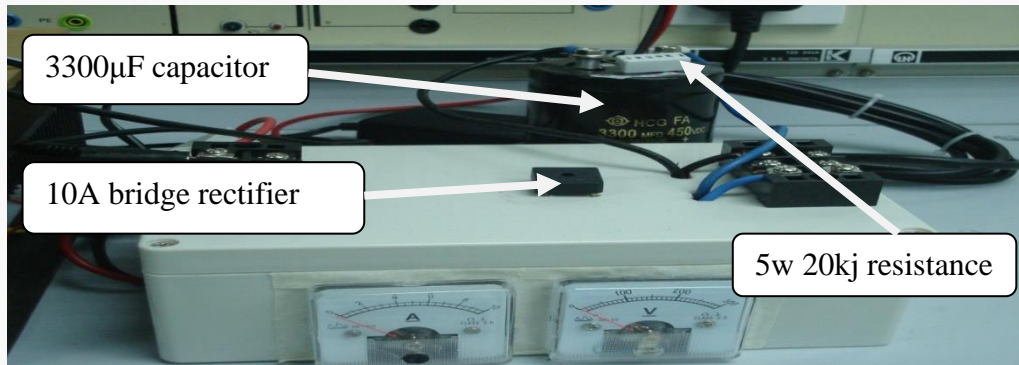


Figure A2.1f. Rectifier circuit

A2.2 DSP Controller Board

A digital photo of the Texas Instruments (TI) DSP board is shown in Figure A2.2

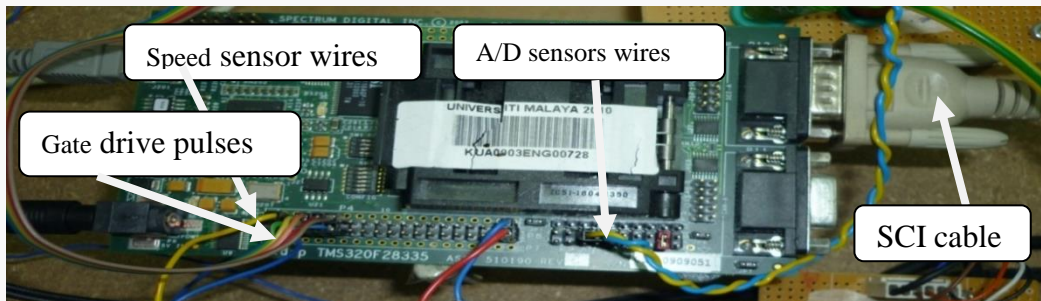


Figure A2.2. TMS320F28335 DSP

The TMS320F28335 DSP performance specifications are listed in the table A2.2a.

Table A2.2a TMS320F28335 DSP performance specification

Generation	TMS320F28335
CPU	C28x, 32-bit, floating-point
Frequency	150MHz
PWM	16 channel
ADC	16 channels at 12-bit each
ADC Conversion Time	80 ns
10 Supply / Core Supply	3.3 V / 1.9 V
Flash	512KB
Timers	3 of 32-bit General-Purpose Timers

A2.3 Signal Conditioning Circuits

The conditioning circuits of the Current sensor, DC voltage sensor circuit and Encoder conditioning signal circuit are illustrated before.

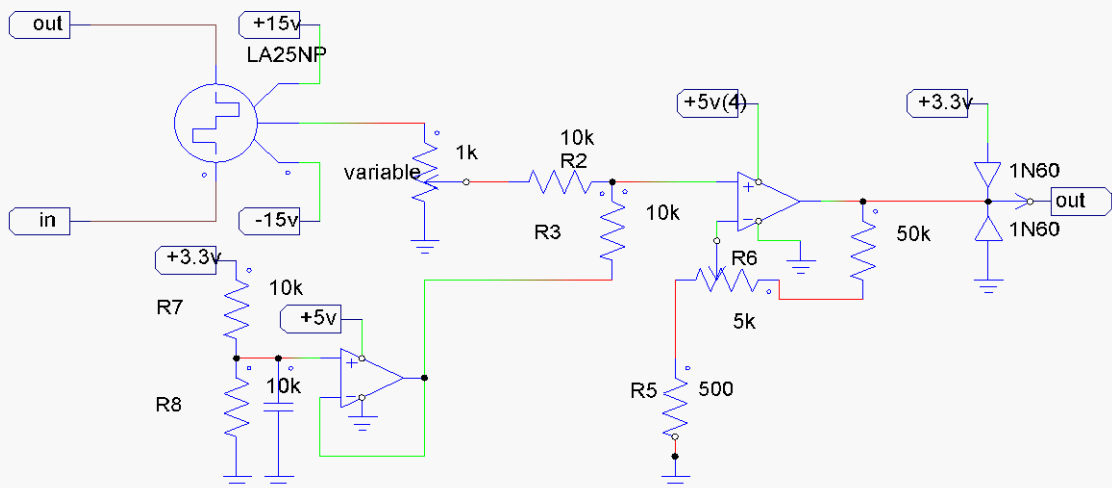


Figure A2.3a. Current sensor circuit

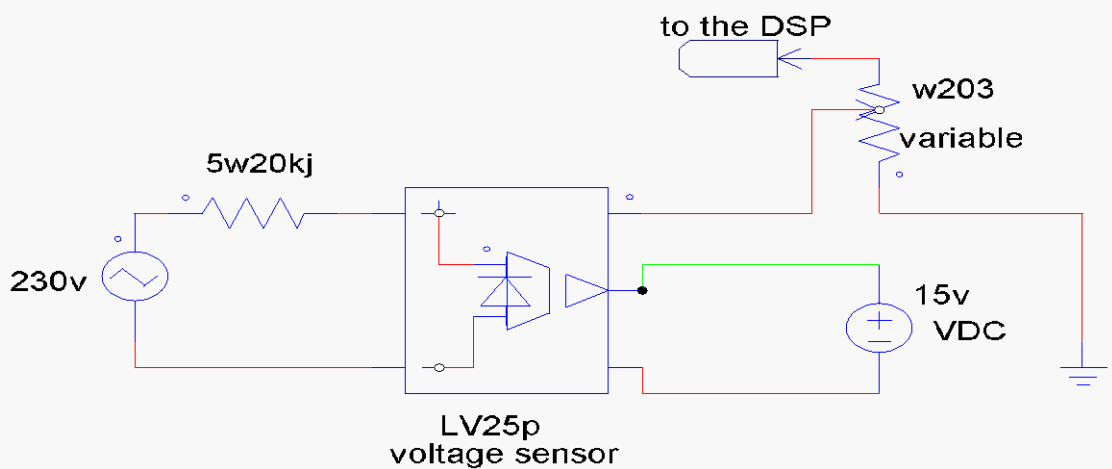


Figure A2.3b. DC voltage sensor circuit

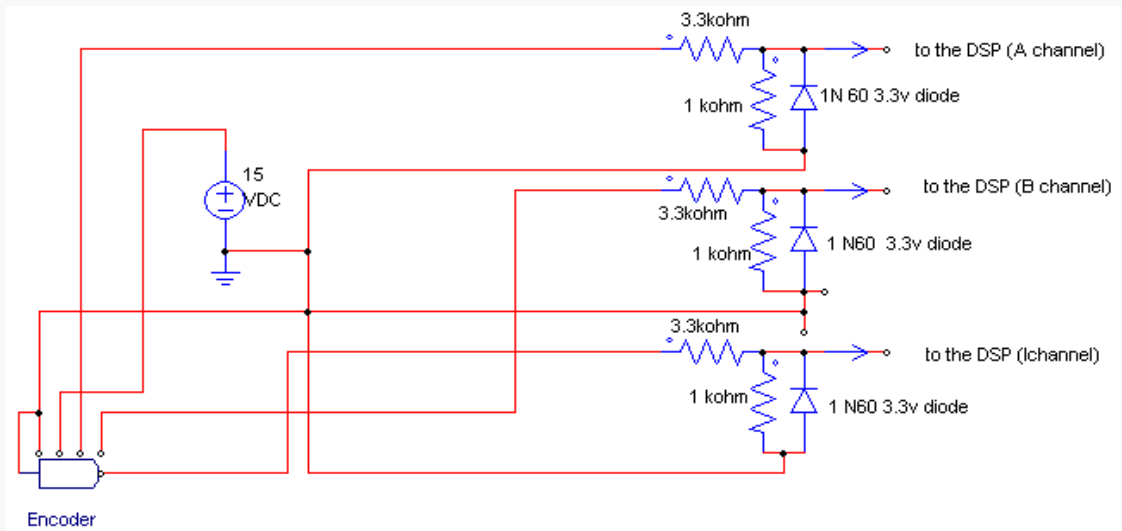


Figure A2.3c. Encoder conditioning signal circuit